UNIVERSIDAD DE LA RIOJA

TESIS DOCTORAL

Título
Aplicación de plasma atmosférico frío para la descontaminación de superficies
Autor/es
Ana Sainz García
Director/es
Yolanda Sáenz Domínguez y Ana González Marcos
Facultad
Escuela Técnica Superior de Ingeniería Industrial
Titulación
Departamento
Ingeniería Mecánica
Curso Académico
2023-2024

Tesis presentada como compendio de publicaciones. La edición en abierto de la misma NO incluye las partes afectadas por cesión de derechos

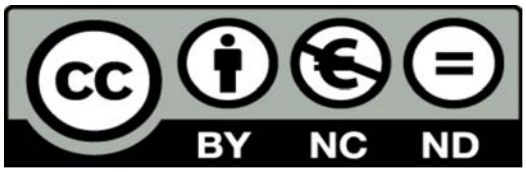

publicaciones.unirioja.es
E-mail: publicaciones@unirioja.es

TESIS DOCTORAL

2024

Programa de Doctorado en *CIENCIAS BIOMÉDICAS Y BIOTECNOLÓGICAS POR LA UNIVERSIDAD DE LA RIOJA Y LA UNIVERSIDAD DE ZARAGOZA*

APLICACIÓN DE PLASMA ATMOSFÉRICO FRÍO PARA LA DESCONTAMINACIÓN DE SUPERFICIES

Ana Sainz García

Directora: Yolanda Sáenz Domínguez

Directora: Ana González Marcos

UNIVERSIDAD DE LA RIOJA

Universidad Zaragoza
1542

Dra. **YOLANDA SÁENZ DOMÍNGUEZ**, Investigadora Principal del Área de Microbiología Molecular del Centro de Investigación Biomédica de La Rioja (CIBIR)

Dra. **ANA GONZÁLEZ MARCOS**, Profesora Titular de Universidad del Departamento de Ingeniería Mecánica de la Universidad de La Rioja

Por la presente declaran que,

La memoria titulada «**Aplicación de plasma atmosférico frío para la descontaminación de superficies**», que presenta Dña. ANA SAINZ GARCÍA, Graduada en Ciencia y Tecnología de los Alimentos, ha sido realizada en el Área de Microbiología Molecular del Centro de Investigación Biomédica de La Rioja y en el Área de Proyectos de Ingeniería de la Universidad de La Rioja, bajo su dirección, y reúne las condiciones exigidas para optar al título de Doctor.

Lo que hacen constar en Logroño, a 9 de mayo de 2024.

Fdo.: Dra. Yolanda Sáenz Domínguez

Fdo.: Dra. Ana González Marcos

TESIS PRESENTADA EN MODALIDAD DE COMPENDIO DE PUBLICACIONES

Esta Tesis Doctoral se presenta en formato de tesis por compendio de publicaciones constituida por el compendio de cuatro trabajos de investigación publicados en revistas científicas de carácter internacional. Asimismo, se incluye el factor de Impacto de cada revista que hace referencia al del año de publicación o al último disponible. Todos los parámetros se han obtenido del Journal Citation Reports® disponible en la página web de FECYT perteneciente al Ministerio de Ciencia, Innovación y Universidades del Gobierno de España. Además, se incluye la justificación de la contribución del doctorando en cada trabajo.

- Publicación I: Sainz-García, A., Toledano, P., Muro-Fraguas, I., Álvarez-Erviti, L., Múgica-Vidal, R., López, M., Sainz-García, E., Rojo-Bezares, B., Sáenz, Y., Alba-Elías, F. 2022. Mask disinfection using atmospheric pressure cold plasma. *International Journal of Infectious Diseases*, 123, 145-156. https://doi.org/10.1016/j.ijid.2022.08.012.

  Revista: International Journal of Infectious Diseases
  Año: 2022
  Área temática: Infectious diseases
  Factor de impacto: 8.4 (Q1, posición 13/96)
  Contribución doctorando: Conceptualización, metodología, validación, realización de ensayos, investigación, procesado de datos, escritura del texto original.

- Publicación II: Sainz-García, A., González-Marcos, A., Múgica-Vidal, R., Muro-Fraguas, I., Escribano-Viana, R., González-Arenzana, L., López-Alfaro, I., Alba-Elías, F., Sainz-García, E. 2021. Application of atmospheric pressure cold plasma to sanitize oak wine barrels. *LWT - Food Science and Technology,* 139, 110509. https://doi.org/10.1016/j.lwt.2020.110509.

  Revista: LWT - Food Science and Technology
  Año JCR: 2021
  Área temática: Food Science and Technology
  Factor de impacto: 6.056 (Q1, posición 29/144)
  Contribución doctorando: Conceptualización, metodología, validación, realización de ensayos, investigación, procesado de datos, escritura del texto original.

- Publicación III: Sainz-García, A., González-Marcos, A., Muro-Fraguas, I., Múgica-Vidal, R., Gallarta-González, f., González-Arenzana, L., López-Alfaro, I., Santamaría, P., Escribano-Viana, R., Alba-Elías, F., Sainz-García, E. 2024. Plasma Activated water for wine barrels disinfection. *LWT - Food Science and Technology* 189, 116024. https://doi.org/10.1016/j.lwt.2024.116024.

  Revista: LWT - Food Science and Technology
  Año JCR: 2022
  Área temática: Food Science and Technology
  Factor de impacto: 6 (Q1, posición 24/142)
  Contribución doctorando: Conceptualización, metodología, validación, realización de ensayos, investigación, procesado de datos, escritura del texto original.

- Publicación IV: Sainz-García, A., González-Marcos, A., Múgica-Vidal, R., Muro-Fraguas, I., Gallarta-González, F., González-Arenzana, L., López-Alfaro, I., Santamaría, P., Escribano-Viana, R., Sainz-García, E., Alba-Elías, F. 2023. Wine corks decontamination using plasma activated water. *Current Research in Food Science*, 7, 100639. https://doi.org/10.1016/j.crfs.2023.100639.

Revista: Current Research in Food Science
Año JCR: 2022
Área temática: Food Science and Technology
Factor de impacto: 6.3 (Q1, posición 21/142)
Contribución doctorando: Conceptualización, metodología, validación, realización de ensayos, investigación, procesado de datos, escritura del texto original.

La siguiente publicación ha sido elaborada por la doctoranda durante el periodo de estancia de investigación realizado en la Università di Bologna y se incluye en el Anexo I:

- Publicación V: Maccaferri, C., Sainz-García, A., Capelli, Filippo., Gherardi, M., Alba-Elías, F., Laurita, R. 2023. Evaluation of the Antimicrobial Efficacy of a Large-Area Surface Dielectric Discharge on Food Contact Surfaces. *Plasma Chemistry and Plasma Processing*, 43, 1773,1790. https://doi.org/10.1007/s11090-023-10410-2.

  Revista: Plasma Chemistry and Plasma Processing
  Año JCR: 2022
  Área temática: Physics, Fluids and Plasmas
  Factor de impacto: 3.6 (Q1, posición 7/34)
  Contribución doctorando: Metodología, validación, realización de ensayos, investigación, procesado de datos, escritura del texto original.

La presente Tesis Doctoral se ha llevado a cabo en el laboratorio del grupo de Microbiología Molecular del Centro de Investigación Biomédica de La Rioja (CIBIR) y en las instalaciones del grupo *Projects, Plasma and Machine Learning* (P2ML) de la Universidad de La Rioja, ambos situados en Logroño, La Rioja.

La realización de dicha Tesis Doctoral ha sido posible gracias a la **"Ayuda para contratos predoctorales para la formación de doctores/as 2020"** contemplada en el Subprograma Estatal de Formación, del Programa Estatal de Promoción del Talento y su Empleabilidad, en el marco del Plan Estatal de Investigación Científica y Técnica e Innovación 2017-2020. Esta ayuda está asociada al proyecto PID2019-105367RB-**C21 titulado: "Optimización de la tecnología del plasma atmosférico f**río **(apcp) para reducir los microorganismos causantes del deterioro del vino en contacto con la madera de roble"** convocatoria de «Proyectos de I+D+i» de los Programas Estatales de Generación de Conocimiento y Fortalecimiento Científico y Tecnológico del Sistema de I+D+i y de I+D+i Orientada a los Retos de la Sociedad, en el marco del Plan Estatal de Investigación Científica y Técnica y de Innovación 2017 -2020.

AGRADECIMIENTOS

En primer lugar, me gustaría agradecer a mis directoras de tesis Yolanda Sáenz Dominguez y Ana González Marcos por guiarme, aconsejarme y apoyarme durante esta etapa. También quiero expresar mi agradecimiento a Fernando Alba Elías por sus consejos.

Gracias a mis compañeros del laboratorio de ingeniería, Ignacio y Rodolfo, pues han sido muy importantes en el día a día y en especial gracias a Elisa, por ayudarme siempre y confiar en mi desde el primer día.

Asimismo, gracias a las chicas del CIBIR, María Bea, Gabriela, Paula, María López y Beatriz, el laboratorio de micro no hubiera sido lo mismo sin vosotras.

Por último, quiero expresar mi gratitud hacia mi familia y amigos, en especial a mis padres y a mis hermanas Elisa y Teresa, por animarme, apoyarme y tranquilizarme durante este camino. Me habéis enseñado la importancia del esfuerzo para perseguir mis objetivos.

Ana Sainz García

ÍNDICE

RESUMEN

Las contaminaciones microbianas son un grave problema cada vez más extendido no solo en el ámbito médico, sino también en la industria alimentaria. Se requiere la búsqueda de nuevas tecnologías capaces de acabar con dichos microorganismos, pero sin producir daños en los productos tratados, como es el caso de alimentos y materiales termosensibles. Por ello, una tecnología con una elevada temperatura o que modifique las propiedades nutricionales o sensoriales de los productos alimentarios no es adecuada. En este sentido, esta tesis doctoral estudia la aplicación de Plasma Atmosférico Frío (PAF) tanto para la inactivación de microorganismos del ámbito médico y alimentario como para la descomposición de moléculas químicas procedentes de la industria enológica. Por un lado, se ha investigado el poder antimicrobiano de la aplicación directa de PAF sobre mascarillas y barricas de vino. Por otro, se ha analizado el Agua Activada por Plasma (PAW) como método indirecto de aplicación de PAF frente a microorganismos y moléculas químicas, todos ellos procedentes del sector alimentario y, más concretamente, relacionados con el vino. Las mascarillas son un aliado fundamental a la hora de prevenir la propagación de enfermedades y evitar contraer infecciones. Su utilización se incrementó tras la pandemia de la COVID-19 y, como consecuencia, las reacciones cutáneas como enrojecimiento, picor o maskné (mask + acné) se intensificaron. Debe tenerse en cuenta que las condiciones de temperatura humedad o CO_2 que se dan en la atmósfera entre la mascarilla y la piel son ideales para la proliferación bacteriana. Así, en el primer artículo de esta tesis se ha estudiado la efectividad del PAF en la inactivación de bacterias patógenas inoculadas en mascarillas KN95 y FFP2 con el fin de permitir su reutilización segura y evitar la contaminación ambiental a la hora de su desechado. Los resultados sugirieron que el gas utilizado, la potencia o el tiempo de tratamiento deben ser considerados para determinar el grado de inactivación bacteriana. Así, a mayores tiempos y potencias de tratamiento se obtuvieron mayores inactivaciones. En cuanto al mejor proceso, el uso de plasma de nitrógeno, 300 W de potencia y 1,5 min de tratamiento fueron los parámetros de plasma óptimos para la inactivación total de las bacterias. Además, el estudio térmico confirmó que tanto *P. aeruginosa* PAO1 como *E. coli* ATCC25922 fueron inactivadas principalmente mediante el efecto térmico. Por el contrario, las especies reactivas de oxígeno y nitrógeno (RONS) generadas en el plasma fueron la principal causa de inactivación de *Staphylococcus* spp. En concreto, el radical NO• pareció ser el más biocida. Por último, tanto las pruebas de respirabilidad y capacidad de filtración como los análisis SEM y visuales, después de uno y cinco ciclos de tratamiento con plasma, mostraron que los tratamientos de PAF no afectaron negativamente ni la morfología ni la capacidad funcional de las mascarillas.

Posteriormente, se aplicó PAF directamente en duelas de madera pertenecientes a barricas de vino para inactivar bacterias y levaduras presentes. Las barricas se utilizan en la etapa de envejecimiento del vino ya que aportan los característicos olores y sabores, enriqueciendo el producto final y aportando estabilidad física y química. El PAF directo se aplicó sobre microorganismos causantes del deterioro del vino (*Pediococcus pentosaceus, Acetobacter pasteurianus* y *Brettanomyces bruxellensis*). Se estudiaron varias potencias (90 W y 500 W) y gases de plasma (aire, nitrógeno y argón). Con los tratamientos de aire y nitrógeno se logró una inactivación total de la levadura. Asimismo, se sugirió que las RONS generadas durante el proceso de generación de plasma parecían desempeñar un papel principal en la inactivación microbiana. Por último, no se identificaron modificaciones morfológicas en la superficie de la madera tras los tratamientos con PAF. Los resultados de esta investigación fueron publicados en el segundo artículo de esta tesis.

En relación al tercer artículo, se trataron duelas de madera naturalmente contaminadas con *B. bruxellensis* utilizando PAW, esto es, aplicando PAF de forma indirecta. Fragmentos de duelas de madera se sumergieron durante 3 h en cuatro PAW con tiempos de generación distintos (1,5 min; 5 min; 15 min y 30 min). Se realizaron ensayos de Cromatografía Líquida de Alto Rendimiento (HPLC) demostrando la existencia de radicales secundarios como OH•, NO• y NO_2•. Además, se sugirió que estas especies reactivas juegan un papel crucial en la inactivación microbiana. Por último, se eligió la PAW generada durante 5 min como la mejor en términos económicos y de consumo de tiempo, logrando una reducción de 3,49 ± 0,83 unidades logarítmicas en la población de *B. bruxellensis*.

Por último, en el ámbito de la industria enológica, el corcho con el que se cierran las botellas tiene un papel fundamental en la etapa final de maduración del vino. Sin embargo, en ocasiones, el corcho aporta olores desagradables y modifica negativamente la composición del vino siendo una de las principales causas por las que se produce el descarte de vinos embotellados. El 2,4,6-Tricloroanisol (TCA) es la molécula más conocida responsable de este problema. En la cuarta publicación presentada en esta tesis doctoral, tapones de corcho contaminados artificialmente con haloanisoles se

sumergieron en cuatro PAW (tiempos de generación: 1,5 min; 5 min; 15 min y 30 min) durante 3 h. Se eligió la PAW generada durante 5 min como la mejor alcanzando más del 72% de TCA descompuesto. Además, tras observar los productos de OH•, NO• y NO_2• con fenol mediante HPLC se sugirió el OH• como la principal especie reactiva que descomponía el TCA. Por último, se examinaron otras moléculas de cloroanisol y clorofenol tras los tratamientos con PAW mostrando reducciones satisfactorias en casi todas las moléculas.

La investigación llevada a cabo permite concluir que el tratamiento con PAF utilizado en esta tesis tiene efectos antimicrobianos frente a microorganismos de origen clínico y alimentario. Asimismo, se ha comprobado su capacidad para descomponer moléculas químicas. De este modo, la tecnología del PAF podría ser una alternativa innovadora y sostenible frente a microorganismos patógenos o alterantes de alimentos y moléculas químicas tanto en el ámbito clínico como en la industria alimentaria.

ABSTRACT

Microbial contaminations are a widespread problem not only in medical area but also in food industries. New technologies capable of killing those microorganisms are needed, and so is avoiding the damage of the treated products, for instance, food or thermosensitive materials. Therefore, technologies that reach high temperatures or modify food nutritional and sensorial properties are not suitable. For that reason, this doctoral thesis studies the Atmospheric Pressure Cold Plasma (PAF) to inactivate microorganisms from the medical and food field and to decompose chemical molecules. On the one hand, the antimicrobial effect of PAF directly applied over face masks and wine barrels was investigated. On the other hand, Plasma Activated Water (PAW), as an indirect method of PAF, was applied against microorganisms and molecules from the food field, specifically, the wine industry.

Face masks are essential to prevent the spreading of diseases and to avoid microbiological infections. Moreover, their use increased during the COVID-19 pandemic and consequently, skin reactions such as itching, stinging or maskne (mask+acne) were intensified. Specific temperature, humidity or CO_2 conditions, created between the mask and the skin, favour the proliferation of bacteria. Then, the first paper studied the effectiveness of PAF to inactivate pathogenic bacteria inoculated on KN95 and FFP2 masks to safely reuse them and to avoid an environmental contamination when they are discarded. Results suggested that the gas, power and treatment time of PAF were required to determinate the bacterial inactivation degree. Then, the longer the treatment time and power, the higher the inactivation rate. Regarding the best PAF treatment, nitrogen, 300 W and 1.5 min were the optimal plasma parameters to totally inactivate bacteria. The thermal study also confirmed the inactivation of *P. aeruginosa* PAO1 and *E. coli* ATCC25922 by temperature effect. On the other hand, the reactive oxygen and nitrogen species (RONS) generated during plasma treatment were involved in *Staphylococcus* spp. inactivation. NO• seemed to be the most biocidal reactive specie. Finally, neither breathing and filtration capacity tests nor SEM and visual analysis showed modifications in the morphology or functional capacity of masks.

PAF was applied directly in wood staves of wine barrels to inactivate bacteria and yeasts. The barrels are employed during the wine aging step, and transfer characteristic odours and flavours to wines. The final product is enriched by giving physical and chemical stability. Direct PAF was executed against wine spoilage microorganisms (*Pediococcus pentosaceus*, *Acetobacter pasteurianus* and *Brettanomyces bruxellensis*). Different powers and gasses were considered (90 W and 500 W; air, nitrogen and argon). A total inactivation of the yeast was achieved after air and nitrogen plasma treatments, and RONS generated during plasma process was proposed as the main cause of microbial inactivation. No morphological modifications were shown in wood surfaces after PAF practices.

Regarding the third article, naturally contaminated wood staves were subjected to PAW treatment to eliminate *B. bruxellensis*. The wood staves were immersed in four different PAW (generation times: 1.5 min; 5 min; 15 min and 30 min) during 3 h. High Performance Liquid Chromatography (HPLC) analyses were performed confirming the presence of secondary radicals such as OH•, NO• and NO_2•. Furthermore, a crucial role of these reactive species to microbial inactivation was suggested. Finally, the PAW generated during 5 min was selected as the best one by economic and time cost consuming concepts, and reached 3,49 ± 0,83 log reduction of *B. bruxellensis*.

In the oenological industry, corks that close the wine bottles play an important role during the last stage of wine processes. Nevertheless, corks could transfer undesirable odours and flavours modifying chemical wine composition, which involves the discarded bottled wines. 2,4,6-Trichloroanisole (TCA) is the most known molecule responsible for this problem. In this fourth published article, artificially contaminated cork stoppers with haloanisoles were immersed in four PAW (generation times: 1.5 min; 5 min; 15 min and 30 min) during 3 h. PAW generated during 5 min was the optimal since it achieved more than 72% of TCA decomposed. Subproducts of OH•, NO• and NO_2• were observed with phenol by HPLC analysis, and OH• was suggested to be the main reactive specie to decompose TCA. Then, other chloroanisole and chlorophenol molecules were examined after PAW treatments, and satisfactory decreases in the concentration of almost all molecules were observed.

The performed investigation concludes that PAF treatment used throughout this project has antimicrobial effect against clinical and food microorganisms, and the capacity to decompose chemicals was also confirmed. Thereby, PAF could be an innovative and sustainable alternative against pathogenic and food spoilage microorganisms, and chemicals in the medical area and food industries.

ABREVIATURAS

ADN	Ácido desoxirribonucleico
AP	Agua Purificada
APPJ	Jet de Plasma Atmosférico Frío (del inglés “Atmospheric Pressure Plasma Jet”)
ATCC	Colección de Cultivos Tipo Americana (del inglés “American Type Culture Collection”)
BAC	Bacterias Ácido Acéticas
BAL	Bacterias Ácido Lácticas
BHI	Infusión Cerebro Corazón (del inglés “Brain Heart Infusion”)
CD	Descarga de Corono (del inglés “Corona Discharge”)
CECT	Colección Española de Cultivos Tipo
CF	Capacidad de filtración
CIBIR	Centro de Investigación Biomédica de La Rioja
COVID-19	Enfermedad de Coronavirus 2019 (del inglés “Coronavirus Disease 2019”)
CLSI	Instituto de Normas Clínicas y de Laboratorio (del inglés “Clinical and Laboratory Standards Institute”)
DBD	Descarga Dieléctrica de Barrera (del inglés “Dielectric Barrier Discharge”)
EC	Conductividad Eléctrica (del inglés “Electric Conductivity”)
EPS	Exopolisacáridos
FNS	Primer Sistema Negativo (del inglés “First Negative System”)
GFP	Proteína Verde Fluorescente (del inglés “Green Fluorescent Protein”)
GYP	Glucosa Levadura Peptona (del inglés “Glucose Yeast Peptone”)
HPLC	Cromatografía Líquida de Alta Resolución (del inglés “High Performance Liquid Chromatography”)
Maskné	Mascarilla (del inglés “Mask”) y Acné
MD	Descarga por Microondas (del inglés “Microwave Discharge”)
MH	Mueller Hinton
MRS	Medio “Man, Rogosa y Sharpe”
NaCl	Cloruro de sodio
OES	Optical Emission Spectroscopy
ORP	Potencial de Óxido Reducción (del inglés “Oxygen Reduction Potential”)
PAC	Plasma Atmosférico Caliente
PAF	Plasma Atmosférico Frío
PAW	Agua Activada por Plasma (del inglés “Plasma Activated Water”)
PBS	Solución Salina tamponada con fosfato (del inglés “Phosphate Buffer Saline”)
PCR	Reacción en Cadena de la Polimerasa (del inglés “Polymerase Chain Reaction”)

qPCR	Reacción en cadena cuantitativa de la polimerasa (del inglés “quantitative Polymerase Chain Reaction”)
RNS	Especies Reactivas de Nitrógeno (del inglés “Reactive Nitrogen Species”)
ROS	Especies Reactivas de Oxígeno (del inglés “Reactive Oxygen Species”)
RONS	Especies Reactivas de Oxígeno y Nitrógeno (del inglés “Reactive Oxygen and Nitrogen Species”)
SEM	Microscopía Electrónica de Barrido (del inglés “Scanning Electron Microscopy”)
slm	Litros Estándar por Minuto (del inglés “Standard Liter per Minute”)
SO_2	Dióxido de Sulfuro
SPS	Segundo Sistema Positivo (del inglés “Second Positive System”)
TCA	2,4,6-Tricloroanisol
TCP	2,4,6-Triclorofenol
TSB	Caldo de Tripticaseína de Soja (del inglés “Trypticasein Soy Broth”)
UFC	Unidades Formadoras de Colonias
UV-vis	Ultravioleta visible

LISTA DE FIGURAS

LISTA DE TABLAS

1. INTRODUCCIÓN

1.1. ANTECEDENTES

Los microorganismos son protagonistas de la emergencia sanitaria en todo el mundo al ser responsables de enfermedades infecciosas en animales y en el ser humano en particular; así como por causar contaminaciones microbiológicas en alimentación. La incidencia se ha reducido con los años gracias al saneamiento ambiental, el control sanitario de los alimentos, la correcta higiene personal, la implantación de vacunas y el uso de antimicrobianos y desinfectantes. Sin embargo, existen casos en los que el control y erradicación microbiana presenta grandes dificultades, como en las infecciones causadas por bacterias multirresistentes a los antibióticos.

Por otra parte, también existen alteraciones y defectos en los alimentos causadas por microorganismos o moléculas químicas que no suponen un alto riesgo para la salud de los consumidores. Sin embargo, influyen de forma negativa en el producto, aportando malos olores y sabores, reduciendo su vida útil, alterando sus propiedades físico-químicas y, en resumen, haciéndolos inadecuados para su consumo.

Por todo ello, se buscan nuevas soluciones y tecnologías con actividades antimicrobianas que eviten la infección, la contaminación, el deterioro y la propagación de los distintos microorganismos con aplicación en salud humana, salud animal y en la industria alimentaria.

El interés de esta tesis es la búsqueda de una tecnología con capacidad desinfectante frente a bacterias implicadas en infecciones de piel que, junto con las infecciones de las vías respiratorias, son las infecciones más frecuentes en clínica humana. Así mismo, dicha tecnología debe poder aplicarse en los procesos de elaboración y conservación de los vinos para evitar la contaminación microbiana o química de superficies.

1.2. INFECCIONES BACTERIANAS ASOCIADAS AL USO DE MASCARILLAS

El uso de mascarillas faciales se ha visto incrementado durante los últimos años y promovido por la pandemia de la COVID-19 [1]. Sin embargo, un uso inadecuado de éstas ha provocado la aparición de enfermedades cutáneas como enrojecimiento o sequedad del cutis o incluso el acné asociado a la mascarilla, conocido como maskné (mask + acné). Esta última se ve incrementada por cambios en los niveles de CO_2 o la humedad de la piel; factores que favorecen la proliferación de bacterias cutáneas específicas pudiendo causar problemas respiratorios u otras enfermedades [2–4]. Estas infecciones cutáneas pueden estar producidas por una amplia variedad de microorganismos que forman parte de la microbiota de la piel y de las mucosas, e incluso proceden del medio ambiente. Concretamente, algunas especies como *Cutibacterium acnes*, *Staphylococcus epidermis*, *Staphylococcus aureus* y *Escherichia coli* pueden desencadenar enfermedades como el maskné. El uso prolongado y la incorrecta reutilización de las mascarillas, como causa de la escasez de las mismas durante la pandemia de la COVID-19, agravó los problemas anteriormente mencionados. Por otro lado, en relación con el medioambiente, no solo una correcta reutilización de mascarillas conlleva la reducción de los recursos necesarios para la fabricación y transporte de materiales, si no que su desinfección facilita el manejo de residuos biológicos evitando la propagación de enfermedades de origen bacteriano [5,6].

En las heridas agudas como en las crónicas, tradicionalmente se consideran potencialmente patógenos a *Staphylococcus aureus, Enterococcus* spp., estreptococos beta-hemolíticos*, Bacillus anthracis, Pseudomonas aeruginosa* y otros bacilos Gram-negativos como las *Enterobacteriaceae*. En esta tesis se han estudiado especies bacterianas cutáneas y nasofaríngeas,

es decir aquellas bacterias comensales y patógenas que pueden estar presentes en la piel y las secreciones nasales y causar enfermedad al individuo:

Escherichia coli es una bacteria Gram-negativa perteneciente al grupo *Enterobacteriaceae*. Es un agente comensal, cuyo hábitat más común es el tracto gastrointestinal de animales y humanos; sin embargo, también es uno de los patógenos humanos y animales más frecuente y responsable de un amplio espectro de enfermedades. Durante los últimos años, se ha visto un incremento mundial de *E. coli* multirresistentes a antimicrobianos. Este hecho complica el tratamiento de diversas infecciones causadas por dicha bacteria, particularmente en hospitales [7,8].

P. aeruginosa es un bacilo Gram-negativo con una gran versatilidad metabólica y extraordinaria habilidad para crecer en variados ambientes (como suelos, aguas, artículos de limpieza, combustible, alimentos, fomites, etc.) desde los que son fácilmente transmisibles de forma cruzada. Es un patógeno oportunista causante de graves infecciones de elevada morbi-mortalidad a nivel mundial. La trascendencia de *P. aeruginosa* viene marcada por su gran resistencia a antimicrobianos y antisépticos y a la presencia de factores de virulencia. En los últimos años, se ha visto incrementada la resistencia de esta bacteria a antimicrobianos [8,9].

Staphylococcus spp. son bacterias Gram-positivas comensales de la piel y mucosas de humanos y animales sanos, pero también pueden actuar como patógenos oportunistas, causando infecciones de diversa severidad. Las especies *S. aureus* y *S. epidermidis* están ampliamente implicadas en infecciones desde leves a graves y son cada vez más difíciles de tratar, asociándose con infecciones crónicas [10]. Un problema importante es la creciente aparición de cepas altamente virulentas y multirresistentes.

En cuanto a las tecnologías empleadas con el fin de desinfectar mascarillas, las más estudiadas son: radiación ultravioleta, radiación microondas, etanol o vapor de peróxido de hidrógeno. Sin embargo, se observó que la mascarilla perdía su capacidad funcional e incluso se encontraron residuos del propio tratamiento en mascarillas tras todos los tratamientos anteriores [11–14].

1.3. ALTERACIONES DEL VINO Y SUS CAUSAS

El número de consumidores que demandan vinos de alta calidad ha aumentado durante los últimos años. Como consecuencia, la industria enológica ha visto incrementada su competitividad lo que le ha hecho mejorar tanto las condiciones de manufactura como las de calidad y seguridad alimentaria, sin perder el carácter tradicional que hace que cada vino sea especial.

Entre las causas físicas, químicas y microbiológicas que afectan a la producción de vinos, esta tesis pretende dar soluciones para reducir la presencia de bacterias y levaduras; así como de haloanisoles y halofenoles alterantes de los vinos.

- Causas biológicas: Microorganismos alterantes

El envejecimiento en barrica es una etapa en la elaboración del vino que juega un papel fundamental, pues aporta atributos organolépticos característicos al producto final. Durante este proceso se producen intercambios entre la madera y el vino consiguiendo enriquecer este último con aromas y sabores. Además, se produce una microoxigenación que provoca estabilidad física y química y deriva en la complejidad y el balance de aromas tan buscados por los consumidores. En este proceso, la diferenciación entre el uso de barricas nuevas y barricas ya utilizadas es muy importante. Las primeras ayudan a impulsar la fermentación maloláctica, los taninos o los polisacáridos; sin embargo, las reusadas desarrollan la acidez volátil de los vinos [15]. Además, en términos económicos, en muchas ocasiones se hace necesario el uso de barricas viejas ya que la inversión para la compra de nuevas es inasumible.

En relación a la reutilización de barricas, la correcta limpieza y desinfección de las mismas es de total importancia. La estructura de la madera es muy porosa por lo que facilita la penetración de microorganismos hasta los 8 mm de profundidad, provocando contaminaciones biológicas en grietas y hendiduras de la superficie. Algunas de las bacterias y levaduras más comunes son las bacterias acido lácticas (BAL), las bacterias acido acéticas (BAC) y la levadura *Brettanomyces bruxellensis* (*B. bruxellensis*) [16–18].

En particular, la etapa de envejecimiento en barrica se ha identificado como la etapa más propensa a la contaminación por *B. bruxellensis* [19–21]. Así, ésta se ha descrito como la principal levadura alterante en vinos habiendo aumentado el número de

vinos contaminados como consecuencia de cambios en el proceso de los vinos, como por ejemplo un aumento del contenido de azúcar o la eliminación del filtrado [22,23].

En esta tesis se han realizado ensayos frente a bacterias y levaduras pertenecientes a los tres grupos más comunes que provocan contaminaciones en barricas:

Las levaduras son las encargadas de la fermentación alcohólica en la elaboración de los vinos, que consiste en convertir el azúcar en etanol. Durante los últimos años, *B. bruxellensis* ha sido foco de estudio debido a su papel en diferentes aplicaciones industriales. Sin embargo, esta levadura también puede contribuir negativamente en las características del vino siendo asociada con la producción de compuestos volátiles y aportando aromas indeseables (carácter "Brett"). Su resistencia a las condiciones enológicas de pH y oxígeno bajos y altas concentraciones de etanol y su capacidad para generar compuestos indeseados, representan un desafío para los expertos de la industria del vino. La adición de dióxido de azufre (SO_2) es el método más común utilizado en la industria enológica para la eliminación de microorganismos. Sin embargo, algunas cepas de *B. bruxellensis* están desarrollando resistencia a este agente antiséptico [24].

Pediococcus es un género de las BAL Gram-positivas de la familia Lactobacillaceae. Este género puede mejorar o deteriorar la calidad de muchas bebidas. Así, la bacteria estudiada en esta tesis, *Pediococcus pentosaceus*, contribuye a la maduración de los vinos aportando características de sabores particulares. Sin embargo, una población elevada de este microorganismo reduce la calidad de los vinos ya que provoca una formación excesiva de diacetilo, exopolisacáridos (EPS), aminas y sabores amargos, entre otros [25].

Acetobacter pasteurianus pertenece a las BAC. Estas bacterias afectan a la calidad del vino al influir en la composición del mosto y alterar el crecimiento de levaduras y bacterias del ácido láctico durante la fermentación. Además, el principal componente de la acidez volátil de vinos y mostos es el ácido acético. Éste puede formarse como subproducto de la fermentación alcohólica o como producto del metabolismo de las bacterias del ácido acético y del ácido láctico pues metabolizan el etanol y los azúcares [26].

Entre los métodos empleados para la eliminación de bacterias y levaduras en barricas de vino el mechado de sulfuroso es el más extendido. Este método tiene múltiples desventajas como la generación de compuestos no deseables en el vino, las reacciones alérgicas tanto para trabajadores como para consumidores o los problemas de residuos de sulfitos que se detectan en los productos finales. Por ello, la Comisión Europea propuso su prohibición; aunque aún no es ilegal su uso [27]. Por estos motivos, la industria enológica se encuentra en la búsqueda de alternativas, algunas de ellas son: agentes oxidantes, peróxido de hidrógeno, ozono, agua caliente (80-90 ºC), vapor de agua (105 ºC) o ultrasonidos [28]. Pese a que todos estos métodos son ampliamente utilizados en bodegas, presentan inconvenientes como: a) alteración de la composición de la madera, b) largos tiempos de tratamiento debido al bajo coeficiente de conductividad térmica de la madera, c) elevados costes económicos, d) productos finales tóxicos para los consumidores o e) baja efectividad del tratamiento debido al carácter superficial del mismo.

- Causas químicas: presencia de TCA en corchos

En relación al embotellado, última etapa de la producción de vinos, los tapones de corcho son muy efectivos para la conservación del vino ya que permiten su desarrollo y envejecimiento a lo largo del tiempo. Sin embargo, estos corchos pueden sufrir contaminaciones tanto químicas como biológicas desencadenando la formación de haloanisoles, siendo el 2,4,6-tricloroanisol (TCA) el más conocido. Esta molécula produce la denominada "enfermedad del corcho", aportando olor a moho al vino y modificando negativamente su composición final [29,30]. El límite de detección de esta molécula es muy bajo (1-2 ng/L) por lo que una pequeña cantidad puede afectar a las propiedades sensoriales del vino final. Es conocido que entre el 1 y el 7% de los vinos embotellados son descartados como consecuencia de esta molécula [29,31,32].

En relación con el origen del TCA, existen publicaciones en las que se describen algunos como la biosíntesis de compuestos clorofenólicos en los bosques o tras la recolección del corcho. No obstante, la única vía de formación científicamente probada es la síntesis de TCA debido a la biometilación del 2,4,6-triclorofenol (TCP) [33]. Cuando el TCP se encuentra en los troncos de los árboles o ya en los corchos, microorganismos de su microbiota como *Penicillium* spp., *Aspergillus* spp., *Actinomyces*

spp. y *Streptomyces* spp., entre otros, transforman el TCP en TCA mediante la enzima clorofenol O-metiltransferasa a través de un proceso de metilación [34].

Por lo anterior, la industria del corcho está tratando de prevenir, controlar y erradicar el TCA. Sin embargo, la mayoría de los tratamientos se centran en la prevención de estos defectos más que en la eliminación de los mismos. Algunas de las técnicas utilizadas son: aplicación de flujos de etanol y agua, utilización de fluidos supercríticos, vapor sobrecalentado o empleo de métodos electroquímicos [32,35–40]. El problema de estas tecnologías radica en su falta de efectividad y su alto coste económico.

1.4. PLASMA ATMOSFÉRICO FRÍO

En el contexto anteriormente descrito, resulta imprescindible la búsqueda de nuevas tecnologías que eviten la contaminación microbiana o química de superficies, para a su vez, evitar la alteración de los vinos y la propagación de los distintos microorganismos en los diferentes nichos estudiados. Dichas tecnologías no deben afectar negativamente al producto objeto de estudio: no deben modificar las propiedades nutricionales o sensoriales de los productos alimenticios, ni deben alterar las propiedades termosensibles, de filtración o respirabilidad del producto estudiado. La tecnología del plasma atmosférico frío (PAF) se presenta en esta tesis como una nueva alternativa para inactivar microorganismos y descomponer moléculas químicas.

El plasma es conocido como el cuarto estado de la materia (precedido por sólido, líquido y gas), siendo el más energético de todos ellos [41]. El estado de plasma se alcanza tras aplicar energía a un gas consiguiendo la reorganización de átomos y moléculas con el objetivo de excitar iones y otras especies que se encuentran en el gas activado. Generalmente, el plasma se divide en dos tipos: plasma atmosférico caliente (PAC) y PAF. En el primero, la temperatura puede alcanzar los 1000 ºC debido a que los electrones están a temperaturas cercanas a las de partículas más pesadas como son iones, moléculas neutras y átomos. Por otro lado, el PAF se genera cuando la mayor parte de la energía es transmitida a los electrones, quedando las moléculas neutras e iones con una cantidad de energía insignificante, por lo que las temperaturas máximas alcanzadas están cercanas a los 100 ºC [42]. Esta particular característica hace que materiales termosensibles (como plásticos o la piel humana) puedan ser tratados mediante la tecnología de PAF y, por ello, es la tecnología que se ha utilizado para esta tesis.

El PAF es descrito como un gas ionizado generado a presión atmosférica. Durante el proceso, radicales y electrones libres, iones positivos y negativos y radiación ultravioleta y visible colisionan y se combinan entre sí dando como resultado especies reactivas de oxígeno y de nitrógeno (*Reactive Oxygen and Nitrogen Species*, RONS) causantes de la química del plasma [42,43].

Como su denominación indica, los equipos que generan este plasma trabajan a presión atmosférica lo que reduce costes y simplifica el proceso. Son muy variados los equipos de PAF que se han diseñado desde que en el siglo XIX se construyera el primero [44]. Los más comunes son descarga de barrera dieléctrica, descarga de corona y chorro de plasma.

- a) Descarga de barrera dieléctrica (*Dielectric Barrier Discharge*, DBD): este equipo se caracteriza por tener dos electrodos de metal en paralelo separados por una distancia de escasos milímetros y al menos uno está recubierto con una capa de material dieléctrico. Este sistema se ha utilizado para el tratamiento de diferentes materiales, así como la deposición de polímeros, entre otros. Sin embargo, debido a la poca uniformidad del plasma generado, su uso se limita a casos en los que no sea necesario una superficie lisa [45].
- b) Descarga de corona (*Corona discharge*, CD): esta configuración se caracteriza por la posición perpendicular de los electrodos ya que normalmente la descarga ocurre cerca de la punta de éstos, por lo que se le conoce a esa zona como región de ionización. En la práctica se utiliza la configuración con múltiples electrodos (*multi-electrodes corona*), lo que aumenta la eficacia de producción de especies reactivas ya que, en el sistema con dos electrodos, la zona tan restrictiva en la que se produce el plasma conlleva limitaciones. La configuración de descarga de corona ha sido utilizada para descontaminación biológica, tratamiento de superficies y procesado en la industria alimentaria [46].
- c) Chorro de plasma (*Atmospheric Pressure Plasma Jet*, APPJ): en este caso, el gas de plasma fluye entre dos electrodos coaxiales separados por un material dieléctrico y transporta las especies reactivas generadas hacia un

espacio abierto lo que provoca una interacción directa entre el plasma y la superficie del objeto a tratar. Una de las grandes ventajas de este equipo de plasma es la capacidad de trabajar con objetos de diversos tamaños y formas [45].

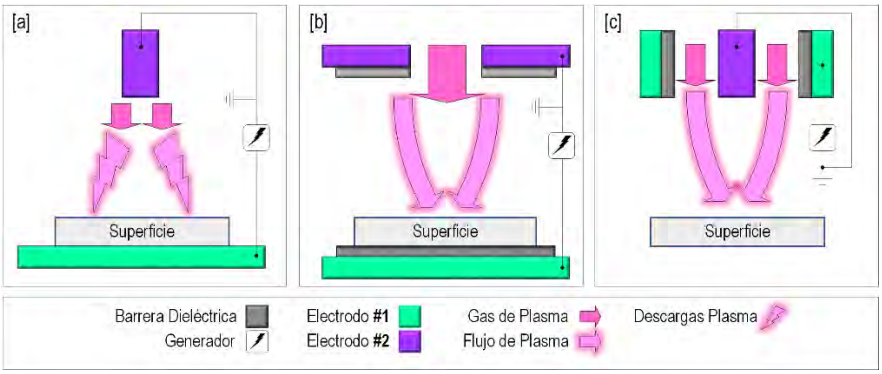

Fig. 1. Esquema de los tres equipos de plasma descritos: [a] Descarga de barrera dieléctrica; [b] Descarga de corona y [c] Chorro de plasma.

En esta tesis se ha utilizado un equipo de plasma tipo Jet, es decir, chorro de plasma. El tratamiento con PAF se puede realizar aplicando el chorro de plasma directamente sobre la superficie a estudiar o indirectamente, a través de un líquido, que en esta tesis ha sido agua purificada (AP) tratada con plasma (PAW, del inglés "Plasma Activated Water"). En el primer caso, el gas ionizado es dirigido hacia la superficie de estudio como se observa en la Fig. 2a. En relación con la generación de PAW, el plasma es conducido hasta el recipiente que contiene el agua a tratar (Fig. 2b).

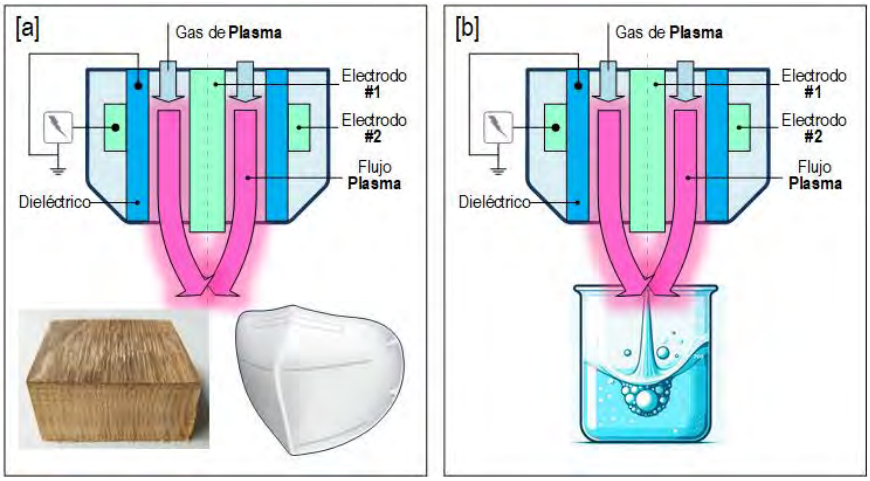

Fig. 2. Métodos de aplicación de PAF: [a] directo y [b] PAW.

Es importante mencionar que las especies reactivas de oxígeno y nitrógeno (RONS) formadas durante la ionización dependen de diferentes parámetros tales como el tipo y flujo de gas utilizado, el voltaje y tiempo de tratamiento o la distancia (gap) desde la salida del plasma (conocido como noozle) hasta el área de tratamiento. Es también importante recalcar que caracterizar las RONS en cualquiera de las zonas de interacción (fase gaseosa, interfase gas-líquido y fase acuosa) es una tarea complicada. Si bien es cierto que la composición y riqueza de las especies reactivas depende en gran medida del tipo de equipo de plasma utilizado, las más comunes encontradas en la fase gaseosa son: O_2, N_2, O, $^1O_2$, O_2^-, O_3, NO•, H_2O_2, OH•, H_2O^+ [42]. Una vez estas partículas activadas interaccionan con la atmósfera que les rodea y/o con el agua, se desencadenan reacciones bioquímicas provocando un aumento en la concentración de las RONS ya descritas y generando la aparición de nuevas especies reactivas.

En relación a la PAW, estas especies reactivas penetran y se disuelven en el líquido para iniciar nuevos procesos [47]. Todas estas especies reactivas son dependientes de las propiedades físico-químicas de cada PAW y a su vez éstas de las RONS formadas. Entre las propiedades más estudiadas destacan el pH, la conductividad eléctrica (EC, del inglés "Electric conductivity") y el potencial de óxido-reducción (ORP, del inglés "Oxygen Reduction Potential"). El pH se caracteriza con el fin

de conocer la acidez o alcalinidad del líquido. Durante la generación de PAW, las reacciones químicas que tienen lugar promueven la acidificación del medio y producen una drástica reducción de pH, siendo mayor cuanto más largo es el tiempo de tratamiento [48–51] . En este sentido, algunos autores indican que la acidificación de la PAW favorece la formación de especies reactivas como el ácido nítrico (HNO_3) [49]. Cabe destacar que, dependiendo del gas utilizado para generar plasma, la disminución en los valores de este parámetro puede variar [52]. En cuanto a la EC, ésta es una medida de la capacidad de la PAW para conducir electricidad a través de los iones disueltos. En este caso, se produce un aumento de la misma tras generar PAW por la presencia de iones en el agua [53]. Se ha observado que cuando se utiliza aire como gas de plasma, el incremento de EC es atribuido a la formación de peroxinitrito, sin embargo, si el gas utilizado es nitrógeno, se debe a iones H_3O^+, pues no se ha encontrado la presencia de óxidos de nitrógeno [54]. Por último, el ORP sigue la misma tendencia al alza que la EC. En este contexto, el ORP indica la capacidad para oxidar o reducir sustancias. Así, a mayor tiempo de tratamiento, mayor capacidad de oxidación-reducción, por lo que los valores de este parámetro se incrementan [55].

A continuación, se explica la formación de RONS en la PAW, así como el motivo por el que los efectos antibacterianos y de descomposición química de la misma persisten en el tiempo. En primer lugar, es importante mencionar que no todas las RONS se forman durante la generación del plasma, es decir, hay efectos sinérgicos de estos procesos, así como reacciones posteriores a la finalización del tratamiento en el interior de la PAW. Las reacciones [a-j] indican las vías por las que se forman las especies reactivas durante la generación de plasma.

$$O_{3gas} \rightarrow O_{3líq} \quad [a]$$

$$NO_2^- + H_2O_2 + H^+ \rightarrow O{=}N{-}OO^- + H_3O^+ \quad [b]$$

$$OH\bullet + NO_2 \rightarrow O{=}N{-}OO^- + H^+ \quad [c]$$

$$O_2^{\bullet-} + NO\bullet \rightarrow O{=}N{-}OO^- \quad [d]$$

$$H_2O_{2gas} \rightarrow H_2O_{2líq} \quad [e]$$

$$OH^-_{gas} + OH^-_{gas} \rightarrow H_2O_{2líq} \quad [f]$$

$$O_{3gas} + H_2O + OH^- \rightarrow OH\bullet + HO_2\bullet + O_2 \quad [g]$$

$$O_{3gas} + H_2O_2 + OH^- \rightarrow OH\bullet + HO_2\bullet + O_2 + OH^- \quad [h]$$

$$OH\bullet_{gas} \rightarrow OH\bullet_{líq} \quad [i]$$

$$e + O_2 \rightarrow {}^1O_2\bullet + e \quad [j]$$

Además, de estas reacciones, la existencia de radiación UV da lugar a otros procesos, denominados procesos fotoquímicos (reacciones [k-t]) [56].

$$O_3 + h\nu \rightarrow O_2 + O(^1D) \quad [k]$$

$$O(^1D) + 2O \rightarrow 2OH\bullet \quad [l]$$

$$H_2O_2 + h\nu \rightarrow 2OH\bullet \quad [m]$$

$$OH\bullet + H_2O_2 \rightarrow H_2O + HO_2\bullet \quad [n]$$

$$HO_2 + H_2O_2 \rightarrow O_2 + H_2O + OH\bullet \quad [ñ]$$

$$NO_2^- + h\nu \rightarrow NO\bullet + O\bullet^- \quad [o]$$

$$NO_3^- + h\nu \rightarrow NO_2\bullet + O\bullet^- \quad [p]$$

$$NO_3^- + h\nu \rightarrow NO_2^- + O \quad [q]$$

$$O + H_2O \rightarrow 2OH\bullet \quad [r]$$

$$O\bullet^- + H_2O \rightarrow OH\bullet + OH^- \quad [s]$$

$$2NO_2^- + H_2O_2 \rightarrow NO_2^- + NO_3^- + 2H^+ \quad [t]$$

Según la literatura las especies reactivas que poseen las capacidades más elevadas de descontaminación biológica y química tienen una vida muy corta (micro o nanosegundos), es decir, el tiempo que transcurre entre que se forman y que reaccionan con otras especies es muy corto [47,57,58]. Sin embargo, se ha comprobado que la PAW tiene actividad bactericida o de descomposición de químicos durante un tiempo prolongado, llegando a ser activa tras varios meses [59]. Es por ello, que es importante mencionar las reacciones secundarias por las que se forman estas RONS, ya que existen reacciones cíclicas en constante generación (reacciones [u-ag]).

$$NO_2^- + H^+ \rightarrow HNO_2 \quad [u]$$

$$2HNO_2 \rightarrow NO\bullet + NO_2\bullet + H_2O \quad [v]$$

$$HNO_2 + H^+ \rightarrow H_2NO_2^+ \rightarrow NO^+ + H_2O \quad [w]$$

$$2NO_2\bullet + H_2O \rightarrow NO_3^- + NO_2^- + 2H^+ \quad [x]$$

$$4NO\bullet + O_2 + 2H_2O \rightarrow 4NO_2^- + 4H^+ \quad [y]$$

$$4NO_2^- + O_2 + 2H_2O \rightarrow 4NO_3^- + 4H^+ \quad [z]$$

$$O{=}NOOH + H_2O_2 \rightarrow O_2NOOH + H_2O \quad [aa]$$

$$O_2NOOH \rightarrow O_2NOO^- \quad [ab]$$

$$O_2NOO^- \rightarrow {}^1O_2 + NO_2^- \quad [ac]$$

$$O_2NOO^- \rightarrow NO_2{*} + O_2^{-}\bullet \quad [ad]$$

$$2O_2^{-}\bullet + 2\,H \rightarrow {}^1O_2 + H_2O_2 \quad [af]$$

$$O_2^{\bullet-} + NO\bullet \leftrightarrow O{=}NOO^- \leftrightarrow O{=}NOOH \leftrightarrow OH\bullet + NO_2\bullet \quad [ag]$$

Destacan las reacciones [u-z] ya que son conocidas como nitritos ácidos (*acidified nitrites*) y tienen lugar a pH menores de 3,5.

Por último, la Fig. 3 indica las RONS más conocidas e identificadas tanto en la fase gas y líquida como en la interfase gas-líquido.

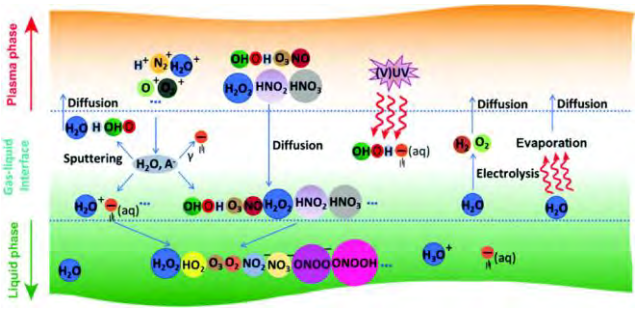

Fig. 3. Especies reactivas identificadas en la fase gas, la interfase gas-líquido y la fase líquida. Fuente: [47].

La tecnología del PAF se emplea para numerosas aplicaciones en diferentes áreas. Por ejemplo, dentro del ámbito médico, se utiliza para reducir melanomas y atacar directamente a células tumorales debido a su especificidad, así como desinfectar equipos y utensilios de laboratorios. Por otro lado, el plasma ayuda a desinfectar y cicatrizar heridas, así como limpiar y desinfectar encías o canales bucales. Además, en el campo de la industria alimentaria se emplea para incrementar la vida útil de los productos (sin afectar negativamente a sus propiedades físico-químicas), desinfectar materiales y superficies, incrementar la germinación de semillas y el crecimiento de plantas, entre otras muchas aplicaciones [60,61].

1.5. JUSTIFICACIÓN DE LA UNIDAD TEMÁTICA

La tecnología del PAF abre un mundo de posibilidades como alternativa para evitar la contaminación microbiana o química de superficies, pero requiere un mejor conocimiento de sus mecanismos de actuación y sus efectos sobre las superficies tratadas. Por ello, con esta tesis, se pretende contribuir al conocimiento y comprensión de: a) el efecto antimicrobiano del PAF sobre microorganismos de interés clínico y alimentario, b) el impacto de esta tecnología en la descomposición de moléculas químicas relevantes en el sector vitivinícola y c) la influencia de PAF en las características de las superficies tratadas.

En esta tesis, la primera publicación se encuentra dentro del ámbito clínico y pretende reducir problemas cutáneos, como el maskné, derivados de largas exposiciones a mascarillas faciales. Para ello, se ha investigado la aplicación directa de la tecnología de PAF para la inactivación de bacterias comensales y patógenas de la piel preservando las propiedades físicas y morfológicas de las mascarillas.

Las tres siguientes publicaciones se centran en el sector vitivinícola. Dos de ellas ponen el foco en la etapa de envejecimiento en barrica de los vinos, en las que se ha analizado el efecto del uso directo de la tecnología de PAF y de PAW en la eliminación de bacterias y levaduras con el objetivo de poder limpiar y reutilizar las barricas. El último artículo se dirige hacia las etapas finales del embotellado y almacenamiento del vino. Mediante el empleo de PAW, se persigue descomponer moléculas químicas indeseables de los corchos, como los haloanisoles, causantes de olores y sabores desagradables en el vino.

2. OBJETIVOS/OBJECTIVES

2.1. OBJETIVOS

- Objetivo general

El objetivo general de esta tesis es buscar nuevos tratamientos, basados en el plasma atmosférico frío, con actividad antimicrobiana frente a microorganismos de interés clínico y alimentario y con capacidad de descomposición de moléculas químicas alterantes de alimentos.

- Objetivos específicos

1. Analizar el efecto antimicrobiano del tratamiento del plasma atmosférico frío sobre microorganismos de interés clínico y alimentario.
2. Estudiar el efecto de descomposición del tratamiento del plasma atmosférico frío sobre moléculas químicas de interés alimentario, en concreto de la industria enológica.
3. Determinar las características morfológicas y funcionales de las superficies tras el tratamiento con PAF.
4. Analizar las características físico-químicas del PAF en cada tratamiento.

2.2. OBJECTIVES

- Main objective

The general objective of this work is to search for new treatments, based on atmospheric cold plasma, with antimicrobial activity against clinical and food microorganisms, and with decomposition activity of chemical molecules involved in food areas.

- Specific objectives

1. To analyze the antimicrobial effect of atmospheric cold plasma treatment in microorganisms of clinical and food interest.
2. To study the decomposition effect of atmospheric cold plasma treatment against chemical molecules within the food field, specifically in the wine industry.
3. To determine the morphological and nutritional characteristics on the studied surfaces after atmospheric cold plasma treatment.
4. To analyze the PAF physical-chemical characteristics in each treatment.

3. METODOLOGÍA

3.1. MEDIOS DE CULTIVO Y OTROS COMPUESTOS UTILIZADOS

En esta tesis se han empleado diferentes medios de cultivo según el microorganismo objeto de estudio. A continuación, se indican los ingredientes de cada uno de ellos.

- Solución salina tamponada con fosfato (PBS, del inglés "Phosphate Buffer Saline") (Gibco): cloruro sódico, fosfato sódico, cloruro de potasio y fosfato de potasio.
- Medio MRS agar (desarrollado por Man, Rogosa y Sharpe) (MRS broth: Scharlau y agar: Panreac Applichem): agar bacteriológico, peptona, dextrosa, extracto de carne, extracto de levadura, fosfato dipotásico, sulfato magnésico, sulfato de manganeso, acetato de sodio, Tween 80, citrato amónico.
- Medio GYP agar (del inglés "Glucose Yeast Peptone"): peptona 20 g/L, peptona 5 g/L, extracto de levadura 5 g/L, agar 20 g/L.
- Caldo TSB (del inglés "Trypticasein Soy Broth") (CondaLab, Madrid, España): glucosa monohidratado, cloruro sódico, hidrogenofosfato dipotásico, digerido pancreático de caseína, digerido papaico de soja.
- Caldo Mueller Hinton (MH) (CondaLab): infusión de carne, hidrolizado de caseína y almidón.
- Medio Mann agar: manitol 25 g/L, peptona 3 g/L, extracto de levadura 5 g/L, agar 20 g/L.
- Medio BHI agar (del inglés "Brain Heart Infusion Agar") (CondaLab): agar, extracto de cerebro y corazón, digerido péptico de tejido animal, digerido pancreático de caseína, glucosa, fosfato disódico de hidrógeno y cloruro de sodio.
- Solución Ringer (Oxoid): cloruro sódico, bicarbonato sódico, cloruro potásico, cloruro cálcico dihidrato.

Por otro lado, para el estudio de desinfección de duelas de madera mediante plasma directo, se utilizó vino sintético cuyos ingredientes son: 4 g/L extracto de levadura, 2 g/L glicerol, 6 g/L DL-Malic, 100 mL/L etanol.

3.2. MICROORGANISMOS ESTUDIADOS

La Tabla 1 muestra las bacterias y levaduras empleadas en esta tesis y el trabajo en el que se han incluido. Además, se indican los medios de cultivo y las condiciones de crecimiento de cada microorganismo.

Las cepas *S. epidermidis* W213, *S. epidermidis* W232, *S. aureus* W1570 y *S. aureus* W1623 presentaron un fenotipo de multirresistencia antimicrobiana (resistentes a al menos tres familias de antibióticos). Específicamente, *S. epidermidis* W213 fue resistente a beta-lactámicos, oxazolidinonas, aminoglucósidos y fenicoles; *S. epidermidis* W232 fue resistente a beta-lactámicos, oxazolidinonas, lincosamidas y aminoglucósidos; *S. aureus* W1570 fue resistente a beta-lactámicos, macrólidos, lincosamidas, aminoglucósidos y fluoroquinolonas, y *S. aureus* W1623 fue resistente a beta-lactámicos, aminoglucósidos y fluoroquinolonas. El resto de cepas estudiadas presentaron un fenotipo de sensibilidad a todos los antibióticos testados según CLSI [62].

Tabla 1. Lista de los microorganismos, medios de cultivo y condiciones de crecimiento estudiados en esta tesis doctoral.

Microorganismos	Publicaciones científicas			
	Sainz-García, A., et al. (2022)	Sainz-García, A., et al. (2021)	Sainz-García, A., et al. (2024)	Medios de cultivo y condiciones de crecimiento
E. coli ATCC25922	✓	-	-	BHI agar 37 ºC/24 h
P. aeruginosa PAO1	✓	-	-	BHI agar 37 ºC/24 h
P. aeruginosa ATCC15692GFP	✓	-	-	BHI agar suplementado con 300 mg/L de ampicilina 37 ºC/24 h
Staphylococcus aureus ATCC29213	✓	-	-	BHI agar 37 ºC/24 h
Staphylococcus hominis W220	✓	-	-	BHI agar 37 ºC/24 h
Staphylococcus haemolyticus W1493	✓	-	-	BHI agar 37 ºC/24 h
Staphylococcus saprophyticus W1498	✓	-	-	BHI agar 37 ºC/24 h
Staphylococcus epidermidis W213	✓	-	-	BHI agar 37 ºC/24 h
Staphylococcus epidermidis W232	✓	-	-	BHI agar 37 ºC/24 h
Staphylococcus epidermidis W1346	✓	-	-	BHI agar 37 ºC/24 h
Staphylococcus aureus W1623	✓	-	-	BHI agar 37 ºC/24 h
Staphylococcus aureus W1570	✓	-	-	BHI agar 37 ºC/24 h
Pediococcus pentosaceus CECT 923	-	✓	-	MRS agar 28 ºC/48 h
Acetobacter pasteurianus CECT 824	-	✓	-	Mann agar 25 ºC/48 h
Brettanomyces bruxellensis CECT 11045	-	✓	-	GYP agar 28 ºC/48 h
Brettanomyces spp.	-	-	✓	GYP agar 28 ºC/48 h

3.3. MOLÉCULAS QUÍMICAS ESTUDIADAS

Para el artículo Sainz-García, A., et al. (2023) se han utilizado diferentes moléculas químicas pertenecientes al grupo de los haloanisoles (Tabla 2).

Tabla 2. Lista de moléculas químicas utilizadas en esta tesis doctoral (CPAChem).

Cloroanisoles	Clorofenoles
2,4,6-Tricloroanisol (TCA)	2,4,6-Triclorofenol (TCP)
2,4,5-Tricloroanisol	2,3,4-Triclorofenol
2,3,4,5-Tetracloroanisol	2,3,4,5-Tetraclorofenol
2,3,4,6-Tetracloroanisol	2,3,4,6-Tetraclorofenol
2,3,5,6-Tetracloroanisol	2,3,5,6-Tetraclorofenol
Pentacloroanisol	

3.4. SUPERFICIES ESTUDIADAS Y CONTAMINACIÓN DE LAS MISMAS

3.4.1. MASCARILLAS

Se estudiaron mascarillas KN95 (Chinese standard: GB/T 32610-2016) y FFP2 (EN 149:2001; Certificate: 20/3212/00/0161; CE-0161FFP2). Las primeras fueron utilizadas tanto en discos (26 y 10 mm de diámetro) como completas para análisis microbiológicos. En cambio, como consecuencia de la prohibición de las mascarillas KN95 en España desde enero de 2021, las mascarillas FFP2 se usaron para los análisis de filtración y respirabilidad. Los estudios se realizaron en triplicado.

Los discos de mascarillas se inocularon con 10 µl de una solución 10^8 UFC/mL de bacteria en PBS (Gibco) de *E. coli* ATCC25922, *P. aeruginosa* PAO1, *S. aureus* ATCC29213, *S. hominis* W220, *S. haemolyticus* W1493, *S. saprophyticus* W1498, *S. epidermidis* W213, *S. epidermidis* W232, *S. epidermidis* W1346, *S. aureus* W1623 y *S. aureus* W1570. Para cada tratamiento, tres bacterias fueron inoculadas en cada disco, como se muestra en la Fig. 4. Como control positivo de crecimiento bacteriano, se utilizaron discos inoculados a los que no se les aplicó tratamiento de plasma y como control negativo, discos sin inocular y sin aplicar plasma con el fin de evaluar posibles contaminaciones.

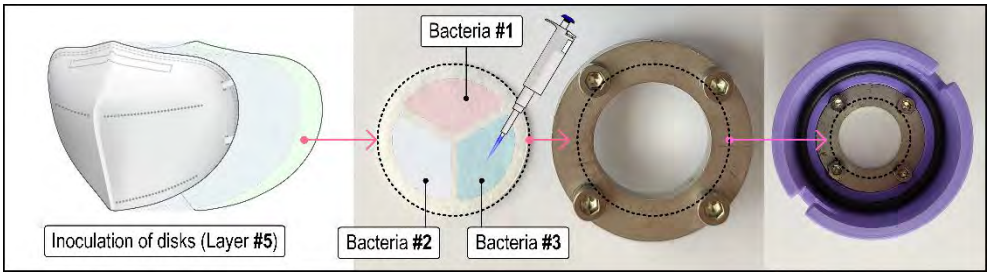

Fig. 4. Esquema de la inoculación de bacterias sobre los discos de mascarilla.

La inoculación bacteriana de las mascarillas KN95 se realizó en cinco puntos de la parte interior de cada mascarilla (Nariz, Boca, Mentón, Pómulos). Se inocularon en cada punto 10 µl de una suspensión 10^8 UFC/mL de bacteria en PBS (Gibco). Tres bacterias (*E. coli* ATCC25922, *P. aeruginosa* PAO1 y *S. aureus* ATCC29213) se inocularon por mascarilla para cada tratamiento. Además, las mascarillas sin tratar, pero inoculadas con bacteria, fueron utilizadas como controles de crecimiento positivo. Una vez secas las gotas bajo condiciones estériles se aplicó el tratamiento de plasma.

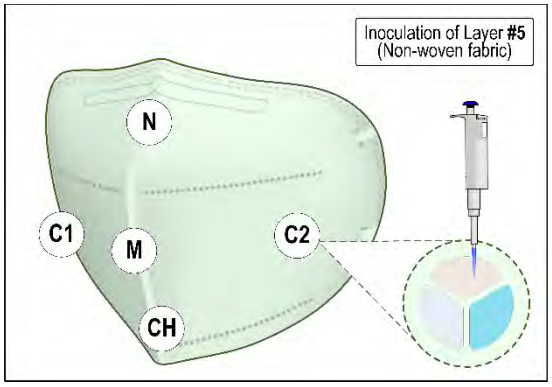

Fig. 5. Esquema de la inoculación de bacterias sobre las mascarillas.

3.4.2. DUELAS DE BARRICAS DE VINO

En esta tesis se han realizado dos publicaciones en las que el objeto de estudio fueron duelas de madera.

En la segunda publicación (Sainz-García, A., et al. 2024), las duelas empleadas se obtuvieron de barricas de madera de roble empleadas en la producción de vino envejecido que estaban contaminadas de forma natural con *B. bruxellensis*. Las muestras consistían en porciones de 5x5 cm cortadas de las duelas. Para determinar el nivel de población viable de *B. bruxellensis* en la madera, se analizó una muestra compuesta por tres porciones de duelas.

3.4.3. CORCHOS DE BOTELLAS DE VINO

Corchos naturales de alcornoque (Ø24×45 mm) con garantía de estar libres de cloroanisoles y clorofenoles fueron adquiridos en Lafitte Cork Portugal (Paços de Brandão, Portugal).

Para su contaminación artificial se utilizó una solución stock (CPA Chem Ltd., Stara Zagora, Bulgaria) preparada en etanol (96% de pureza, Labbox Labware S.L., Premià de Dalt, Barcelona, España) que contenía 400 ppt de cada molécula de cloroanisoles y clorofenoles (Tabla 2). Esta solución se diluyó hasta los 400 ng/L en agua purificada para contaminar los corchos.

El procedimiento de contaminación fue el siguiente: cada corcho fue introducido en un bote (Ø44×94,8 mm) y sumergido en 80 mL de solución 400 ng/L de cloroanisoles y clorofenoles rotando a 50 rpm (Multi Bio RS-24, Biosan, Riga, Letonia). Tras 4 h, los corchos se secaron a temperatura ambiente durante 24 h.

3.5. TRATAMIENTOS CON PAF

Todos los trabajos que se incluyen en esta tesis han utilizado el mismo equipo de plasma, PlasmaSpot500 (MPG, Luxemburg). Éste consiste en un electrodo externo conectado a una fuente de alto voltaje, un electrodo interno conectado a tierra y un tubo dieléctrico de óxido de aluminio entre ambos electrodos como se muestra en la Fig. 6.

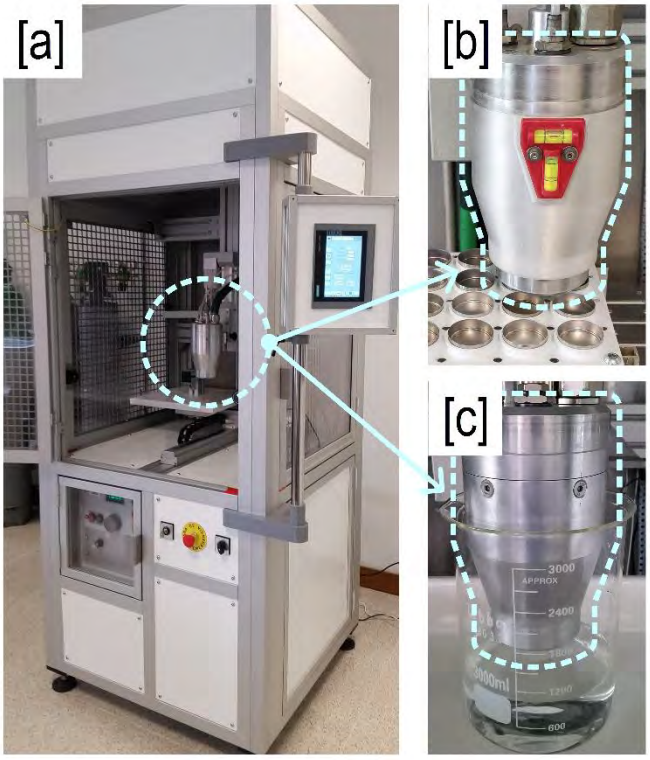

Fig. 6. [a] Equipo de generación de plasma; [b] Equipo de plasma aplicando tratamiento directo y [c] Equipo de plasma generando PAW.

A continuación, se explican los tratamientos de plasma directo e indirecto que se han llevado a cabo para cada una de las publicaciones en las que se ha utilizado esta tecnología.

3.5.1. TRATAMIENTOS DE PLASMA DIRECTO

3.5.1.1. MASCARILLAS

La Tabla 3 muestra los tratamientos realizados a las mascarillas. Para el estudio microbiológico en discos de mascarillas se utilizaron nitrógeno, aire y argón como gases de plasma a 80 y 60 slm durante tiempos diferentes de tratamiento. En cuanto al análisis de inactivación en mascarillas enteras, se utilizó el tratamiento N2, consistente en nitrógeno a 80 slm, 300 W durante 1,5 minutos.

La aplicación de los tratamientos de plasma se realizó una vez secas las gotas de solución bacteriana depositadas en las mascarillas (bien en los discos, Fig. 7, bien en las mascarillas completas, Fig. 8).

Tabla 3. Tratamientos de plasma directo aplicados sobre las mascarillas.

Tratamiento	Gas de plasma	Flujo de gas (slm)	Gas de cooling	Potencia de plasma (W)	Tiempo de tratamiento

CT	-	-	-	-	-
N1	Nitrógeno	80	Aire	300	45 s
N2	Nitrógeno	80	Aire	300	1,5 min
N3	Nitrógeno	80	Aire	300	2,5 min
N4	Nitrógeno	80	Aire	220	5 min
A1	Aire	80	Aire	300	45 s
A2	Aire	80	Aire	300	1,5 min
Ar1	Argón	60	Aire	90	1,5 min
Ar2	Argón	60	Aire	60	5 min

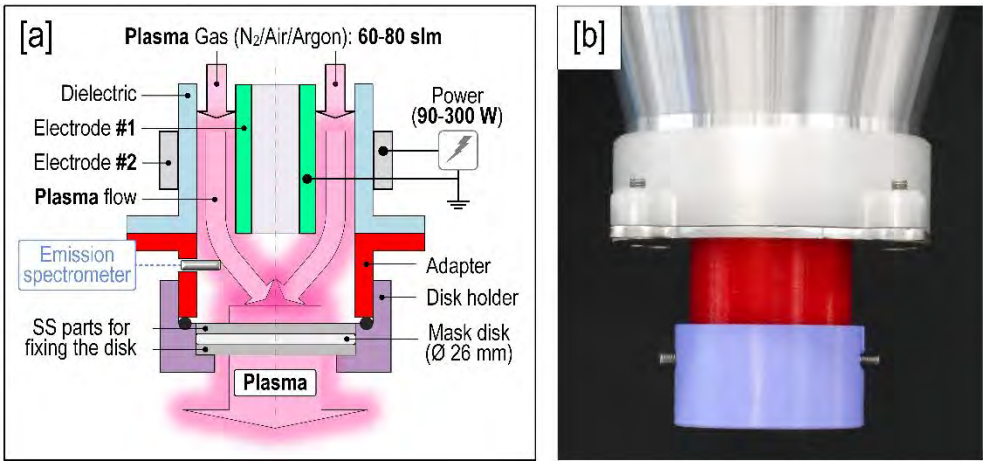

Fig. 7. [a] Equipo de plasma y [b] Equipo de plasma tratando discos de mascarilla.

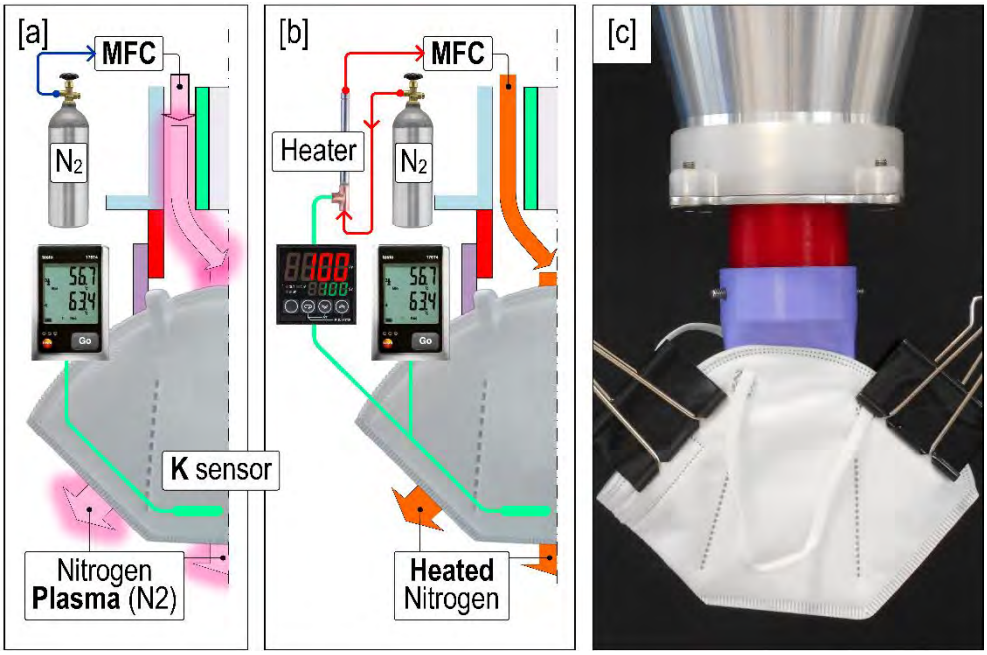

Fig. 8. [a-c] Esquema del tratamiento de plasma y el tratamiento térmico de las mascarillas y [e] Equipo de plasma tratando mascarillas.

3.5.2. TRATAMIENTOS DE PLASMA INDIRECTO (PAW)

Los tratamientos con PAW se estudiaron en dos de las cuatro publicaciones incluidas en esta tesis (Sainz-García, A., et al. 2023 y 2024).

La PAW se generó exponiendo 2000 mL de agua purificada (AP) a la pistola de plasma con un gap de 30 mm durante 1,5; 5; 15 y 30 min (Fig. 9). El gas de plasma utilizado para ambos estudios fue aire con un flujo de 60 slm y una potencia de 500 W. Dependiendo del tiempo de exposición del AP, se consiguieron 4 PAW diferentes; es decir, PAW-1,5, PAW-5; PAW-15 y PAW-30.

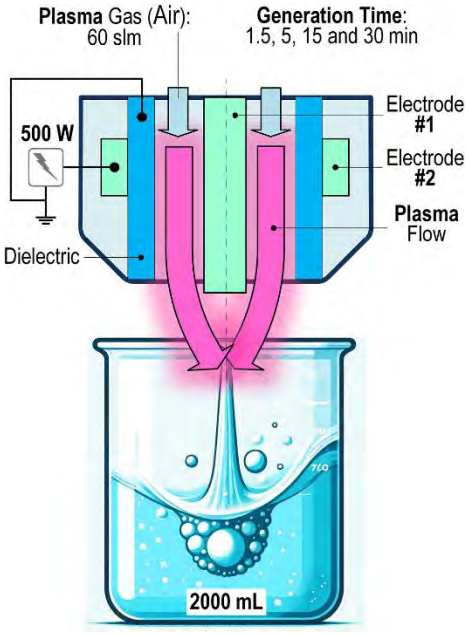

Fig. 9. Sistema de plasma generando PAW.

En relación al estudio de las duelas de madera, para cada tratamiento de PAW o AP, tres muestras de madera contaminadas se sumergieron en 450 mL de PAW o AP. En cuanto al tratamiento con dióxido de sulfuro (SO_2), tres duelas contaminadas se introdujeron en jarras de 4000 mL y 5 g de una pastilla de SO_2 fueron quemados en el interior durante 30 minutos. El AP y el SO_2 se utilizaron como controles.

En el caso de los corchos, éstos se introdujeron en 80 mL de PAW o AP durante 3 h. Seguido se mantuvieron a temperatura ambiente 24 h para su secado. El AP fue empleado como control.

3.6. CARACTERIZACIÓN DEL TRATAMIENTO DE PAF

Las características físico-químicas de los tratamientos con PAF y PAW se analizaron empleando diferentes equipos y tecnologías, como se indican a continuación:

3.6.1. CARACTERIZACIÓN DEL PAF DIRECTO

3.6.1.1. OES

Con el fin de caracterizar la fase gas de los tratamientos de PAF se empleó la espectrometría de emisión óptica (OES del inglés “Optical Emission Spectrometry”).

Esta técnica consiste en el análisis de un espectro de luz separado por longitudes de onda. Así, el OES identifica las RONS producidas por cada plasma en la fase gas. El equipo utilizado fue un espectrómetro HR4PRO-XR-ES (Ocean Insight, Orlando, Florida, EE.UU.) conectado a una fibra óptica (QP600- 2SR-Ocean Optics) con una lente que recolecta la información de cada flujo de plasma (Fig. 10). Los datos fueron procesados con el software SpectraWiz (StellarNet, Tampa, Florida, EE.UU.).

Fig. 10. Equipo de OES y fibra óptica.

3.6.2. CARACTERIZACIÓN DE LAS PAW

3.6.2.1. MULTÍMETRO PORTABLE

Un multímetro portable sensION MM150 DL con una sonda 50 48 (Hach Company, EE.UU.) se utilizó para medir los parámetros descritos a continuación:

- pH: indica el grado de acidez o alcalinidad.
- ORP: indica el potencial de óxido reducción.
- EC: indica la capacidad para dejar pasar la corriente eléctrica.
- Tª: indica el grado de frío o calor.

Fig. 11. Equipo multímetro portable.

3.6.2.2. MEDIDOR DE IONES PORTÁTIL

Para la cuantificación de NO_3^- se utilizó un equipo denominado Imacimus® MultiIon analyser (NTsensors S.L., España) con electrodo selectivo. Estos dispositivos detectan y miden concentraciones específicas de iones en diversas soluciones. A través de una membrana selectiva generan un potencial eléctrico que es directamente proporcional a la concentración de nitratos basándose en la ecuación de Nernst.

$$E = E^0 - \frac{RT}{nF}\ln(Q)$$

Donde E es el potencial corregido del electrodo, E^0 el potencial en condiciones estándar, R la constante de gases, T la temperatura (K), n la cantidad de moles, F la constante de Faraday (~ 96500 Coulomb/mol) y Q:

$$Q = \frac{[C]^c[D]^d}{[A]^a[B]^b}$$

Donde [C] y [D] son las presiones parciales y/o concentraciones molares de los iones disueltos y [A] y [B] para los reactivos. Además, los exponentes son los coeficientes estequiométricos de la reacción.

Fig. 12. Equipo medidor de iones portátil.

3.6.2.3. ESPECTROFOTOMETRÍA

Este ensayo fue utilizado para el análisis de NO_2^- y H_2O_2. Se usó un espectrofotómetro Onda V-11 SCAN (Giorgio Bormac s.r.l., Italia).

El método colorimétrico de Griess fue empleado para la determinación de NO_2^- en cada PAW. Mediante este procedimiento, los nitritos son detectados por la reacción de la muestra con ácido sulfanílico bajo condiciones ácidas para formar el ion diazonio. Éste se enlaza con α-naftilamina para formar un compuesto de color magenta que es cuantificado espectrofotométricamente a 548 nm [63].

Por otro lado, para cuantificar el H_2O_2, fue necesaria la determinación de la absorbancia del peróxido de titanio a 407 nm. Este método se basa en la reacción del sulfato de titanilo para formar sulfato de peroxititanilo de color amarillento.

El reactivo de Griess y el oxisulfato de Titanio (IV) fueron adquiridos en Sigma Aldrich (EE.UU.).

Fig. 13. Equipo de espectrofotometría UV-vis.

3.6.2.4. CROMATOGRAFÍA LÍQUIDA DE ALTA RESOLUCIÓN (HPLC)

Esta técnica permite separar sustancias de una mezcla compleja para identificarlas y cuantificarlas.

En esta tesis, se empleó un HPLC con detección UV (Agilent 1100 Series, Agilent Technologies, España) para detectar RONS secundarias con un método basado en la reacción entre el fenol (C_6H_5-OH) y los radicales OH•, NO• y NO_2• [57]. Se detectó la presencia del fenol y los productos primarios de su degradación (benzoquinona (fenol + OH•), 4-nitrosofenol (fenol + NO•) and 2-nitrofenol (fenol + NO_2•)).

A continuación, se detallan las características del ensayo:

Se utilizó una columna Supelcosil C-18 de fase inversa de 5 µm (25 cm × 2,4 mm; Supelco Inc. EE.UU.). El límite de detección para el análisis por HPLC fue de 0,01-0,1 µM (dependiendo del compuesto y de la detección utilizada). Se preparó una solución de $2 \cdot 10^{-2}$ M de fenol (Monplet & Esteban S.A., España) en agua; 5,0 mL de esta solución se mezclaron con 95 mL de PAW y se incubaron a 50 ºC durante 24 h. A continuación, la solución se filtró (0,45 µm) y se midió mediante análisis HPLC utilizando una elución en gradiente (Tabla 5) y las siguientes condiciones: volumen de inyección de 20 µL, caudal a 1,0 mL/min de fase móvil; tiempo total 16 min; P: ≈90 bar a 90-100, ≈60 bar a 60-40; y un detector a 260 nm (referencia: 699 nm). Los tiempos de retención fueron los siguientes: benzoquinona 5,0 min, 4-nitrosofenol 5,4 min, fenol 8,2 min y 2-nitrofenol 11,2 min. Para cuantificar los subproductos de la degradación, se prepararon diferentes curvas de calibración con soluciones de concentración conocida de benzoquinona (Sigma Aldrich, EE.UU.) ($1{,}35 \cdot 10^{-5}$ M), 4-nitrosofenol (TCI Chemicals, Japón) ($2{,}54 \cdot 10^{-4}$ M) y 2-nitrofenol (Sigma Aldrich, EE.UU.) ($2{,}54 \cdot 10^{-4}$ M) (Tabla 4).

Fig. 14. Equipo HPLC con detección UV.

Tabla 4. Curvas de calibración de los subproductos del fenol.

Subproducto de degradación	Curva de calibración	R^2
Benzoquinona	A (mAU) = 0,09 + 6,99 x 10^5 c (M)	0,9996
2-nitrofenol	A (mAU) = -0,24 + 1,50 x 10^5 c (M)	0,9997
4-nitrosofenol	A (mAU) = -1,00 + 3,78 x 10^5 c (M)	0,9997

Tabla 5. Gradientes de elución para el análisis HPLC.

t (min)	Ácido acético: 1% (V/V)	Acetonitrilo
0	90	10
7	60	40
13	90	10

3.7. OTROS ESTUDIOS Y ENSAYOS REALIZADOS

3.7.1. ESTUDIO TÉRMICO

En el estudio relacionado con la inactivación bacteriana en mascarillas (Sainz-García, A. et al., 2022) se realizó a su vez una caracterización térmica con el fin de evaluar si se producía la muerte microbiana debido al efecto térmico o del tratamiento de plasma. Para ello se controló la temperatura durante los tratamientos de plasma. La superficie exterior de la mascarilla fue caracterizada mediante el uso de una cámara de imagen térmica (TESTO 871) (Testo SE & Co. KGaA, Alemania). Las imágenes obtenidas se analizaron con el software IRSoft (versión 4.3). Por otro lado, la temperatura de la parte interior de la mascarilla también fue determinada con una sonda de teflón tipo-K conectada a un data logger (Testo 167T4).

Una vez conocida la temperatura máxima del tratamiento de plasma, se sometió a las mascarillas a esa misma temperatura, únicamente mediante tratamiento de calor y se evaluó la actividad antimicrobiana de este tratamiento térmico.

Fig. 15. Cámara termográfica.

También se realizó estudio térmico para la caracterización de las duelas de madera en Sainz-García, A., et al. (2021) para comprobar la temperatura máxima alcanzada utilizando la sonda tipo-K conectada al data logger (Testo 167T4).

3.7.2. MICROSCOPIO DE FLUORESCENCIA

Esta técnica se empleó en la publicación Sainz-García, A., et al. (2022) relacionada con la inactivación bacteriana en mascarillas de la cepa de *P. aeruginosa* ATCC15692GFP. El equipo utilizado fue un microscopio de fluorescencia (Nikon) (Fig. 16) con el software ImageJ para la recogida de fotografías.

La bacteria *P. aeruginosa* ATCC15692GFP posee un vector multicopia que codifica para la proteína verde fluorescente GFPmut3. El objetivo de este ensayo fue conocer si la intensidad de la fluorescencia de la proteína GFP se veía afectada tras la aplicación de PAF.

Fig. 16. Microscopio de fluorescencia.

3.8. DETERMINACIÓN DE LA CAPACIDAD ANTIMICROBIANA DEL TRATAMIENTO CON PAF Y PAW

3.8.1. MASCARILLAS

En la publicación Sainz-García, A., et al. (2022) relacionada con mascarillas, una vez aplicado el tratamiento de plasma a cada disco, cada área inoculada se recortó y se lavaron independientemente en tubos Eppendorf con 300 µl de caldo MH durante 24 h. A continuación, se realizaron diluciones seriadas que se cultivaron en BHI agar a 37 °C durante toda la noche para determinar las UFC/mL. En cuanto a las mascarillas completas el procedimiento fue el mismo una vez cortados los puntos en los que se habían inoculado las bacterias. En ambos estudios se incluyeron discos y mascarillas completas inoculadas, pero sin tratamiento con PAF, como controles positivos de crecimiento.

3.8.2. DUELAS DE BARRICAS DE VINO

En la publicación Sainz-García, A., et al. (2024), las duelas de madera tratadas con PAW, AP y SO_2 se cepillaron hasta alcanzar una profundidad de 1 cm. Se pesaron las virutas en bolsas de plástico estériles, se añadieron 600 mL de medio TSB y las bolsas selladas se incubaron a 28 ºC en un agitador orbital a 100 rpm durante 24 h. La suspensión se centrifugó (10000 rpm; 30 min; 4 ºC) y el pellet obtenido se resuspendió en una solución de Ringer hasta un volumen de 15 mL en tubos de plástico estériles. Las muestras se enviaron a un laboratorio externo (Excell Ibérica S.L., Logroño, La Rioja) allí fueron tratadas con monoazida de propidio (PMATM, Biotium, Fremont, CA) y sometidas a un protocolo de extracción de ADN, para posteriormente cuantificar la población viable de *Brettanomyes* spp. presente en la madera mediante una PCR cuantitativa (qPCR) usando Eva Green®.

3.9. DETERMINACIÓN DEL GRADO DE DESCOMPOSICIÓN QUÍMICA TRAS TRATAMIENTO CON PAW

En la publicación Sainz-García, A., et al. (2023) se determinó la capacidad del tratamiento con PAW para descomponer las moléculas de haloanisoles y halofenoles contaminantes de los corchos de botellas de vino. Para ello se siguieron dos métodos químicos.

- Método OIV-MA-AS315-16. Determinación de 2,4,6-Tricloroanisol en vino procedente de tapones de corcho; Resolución OIV/OENO 296/2009 [64]
- Método OIV-MA-AS315-17. Determinación de policlorofenoles y policloroanisoles en vinos, tapones de corcho, madera y bentonitas utilizadas como adsorbentes de esos compuestos en la atmósfera; Resolución OIV/ OENO 374/2009 [64].

Estos métodos simulan la migración de 2,4,6-Tricloroanisol, 2,4,6-Triclorofenol, 2,3,4,6-Tetracloroanisol, 2,3,4,6-Tetraclorofenol, pentacloroanisol y pentaclorofenol susceptibles de producirse entre el vino embotellado y los tapones de corcho.

En primer lugar, se realizó una extracción alcohólica con un sistema de microextracción en fase sólida (SPME Fibras ARROW: 50/30µm DVB/CAR/PDMS) con un "liner" (SPME Injection Sleeve 0,75 mmID). A continuación, las muestras se analizaron por cromatografía de gases (AGILENT TECHNOLOGIES. Modelo 8890; Inyector: Agilent Technologies. PAL-System Modelo PAL III Series 2) con detección por espectrómetro de masas (Agilent Technologies. Modelo 7000C).

3.10. CARACTERIZACIÓN DE LAS MUESTRAS ESTUDIADAS (MASCARILLAS, DUELAS Y CORCHOS)

3.10.1. ANÁLISIS DE FILTRACIÓN DE MASCARILLAS

El estudio relativo a las mascarillas incluye análisis de filtración de las mismas con el fin de comprobar si el tratamiento con plasma afectó negativamente a dicho parámetro. Según su eficacia de filtración pueden clasificarse en: FFP1, FFP2 y FFP3 siendo las FFP3 las que mayor poder de filtración poseen y las FFP1 las que menor.

La prueba de filtración se realizó por penetración del filtro con aceite de parafina siguiendo la norma EN 149:20 01 + A1:20 09. La incertidumbre expandida fue de ±10% del valor medido para una probabilidad de cobertura del 95%. La Tabla 6 indica el porcentaje máximo de penetración de aceite de parafina del material filtrante según la clasificación de mascarilla.

Tabla 6. Porcentaje máximo de penetración de aceite de parafina del material filtrante.

Clasificación	95 L/min (Porcentaje máx.)
FFP1	20
FFP2	6
FFP3	1

3.10.2. ANÁLISIS DE RESPIRABILIDAD DE MASCARILLAS

La prueba de resistencia a la respiración se llevó a cabo siguiendo la norma EN 149:20 01 + A1:20 09 así como los requisitos según la RfU PPE-R/02.075.02. En este caso, la incertidumbre expandida fue de ±18% del valor medido para una probabilidad de cobertura del 95%. Cada análisis se realizó cinco veces.

Tabla 7. Valores de máxima resistencia permitida según la norma indicada.

Clasificación	Inhalación 30 L/min	Inhalación 95 L/min	Exhalación 160 L/min
FFP2	0,7	2,4	3,0
FFP3	1,0	3,0	3,0

3.10.3. MICROSCOPÍA ELECTRÓNICA DE BARRIDO (SEM)

Esta técnica se ha utilizado en tres de los cuatro estudios incluidos en esta tesis.

Para los trabajos Sainz-García, A., et al. (2021) y Sainz-García, A., et al. (2022), se utilizó el microscopio electrónico de barrido HITACHI S-2400 trabajando a 18 kV. En el primer caso, se observaron muestras de mascarillas a las cuales se les había aplicado cinco ciclos de tratamiento de plasma. Tanto para los discos de mascarilla como para los fragmentos de duelas de madera, previo al estudio SEM, las muestras fueron recubiertas con una fina capa de oro y paladio para hacerlas conductivas.

Para el estudio Sainz-García, A., et al. (2024) se empleó el microscopio COXEM EM-30N trabajando a 10 kV. En este caso, las muestras de madera se recubrieron con una capa de oro con el fin de hacerlas conductivas.

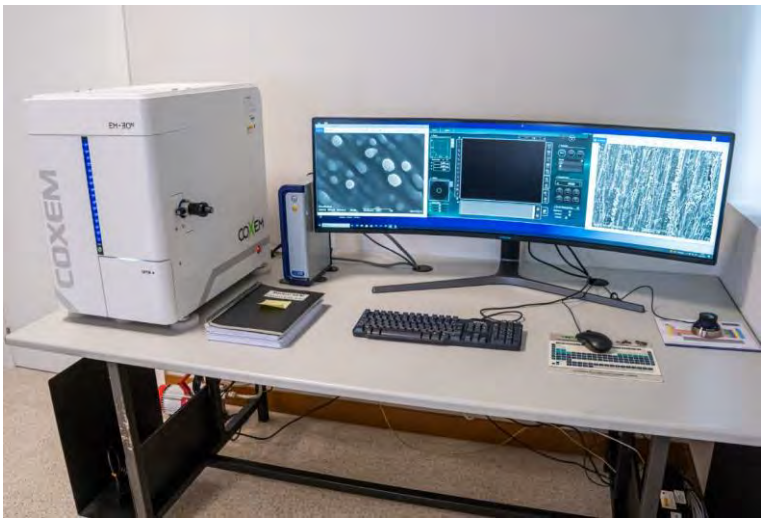

Fig. 17. Equipo de microscopía electrónica de barrido.

4. RESULTADOS: TRABAJOS PUBLICADOS

4.1. DESINFECCIÓN DE MASCARILLAS MEDIANTE PLASMA ATMOSFÉRICO FRÍO

- Mask disinfection using atmospheric pressure cold plasma. Ana Sainz-García, Paula Toledano, Ignacio Muro-Fraguas, Lydia Álvarez-Erviti, Rodolfo Múgica-Vidal, María López, Elisa Sainz-García, Beatriz Rojo-Bezares, Yolanda Sáenz, Fernando Alba-Elías. International Journal of Infectious Diseases 123 (2022) 145–156.

El uso de mascarillas faciales está muy extendido en el ámbito médico, ya que previene la propagación de enfermedades. Estos complementos ayudan a evitar contraer infecciones de microorganismos del ambiente que se respira. Además, forman parte de la estrategia de control y prevención para eliminar las contaminaciones cruzadas, por ejemplo, en hospitales.

Por otro lado, el uso de mascarillas se ha visto incrementado durante los últimos años debido, en gran parte, a la pandemia de la COVID-19 [1]. Como resultado, se ha observado que el 93,64% de las reacciones cutáneas faciales (como enrojecimiento, picor o acné) se describieron tras la exposición a mascarillas [2,65]. Es por ello que en este trabajo se ha aplicado PAF directamente sobre el interior de mascarillas (FFP2 y KN95) con el fin de eliminar bacterias patógenas y que pueden ser causantes de enfermedades faciales como el maskné (Mask + Acné).

Se analizaron doce microorganismos diferentes (de las especies *P. aeruginosa*, *E. coli* y *Staphylococcus* spp.) los cuales fueron inoculados en discos de mascarillas. Varios parámetros del tratamiento con PAF se modificaron para estudiar cómo afectaban a la inactivación; desde el gas utilizado (nitrógeno, argón y aire) y la potencia del plasma (90 – 300 W), hasta el tiempo de tratamiento (45 s – 5 min). Luego se eligió el mejor tratamiento de PAF, siendo el generado por gas N_2, 300 W, 80 slm y 1,5 min para analizar su efecto sobre mascarillas completas. Además, se llevaron a cabo pruebas de capacidad de filtración (FC) y de respiración que no mostraron efectos negativos después de 5 ciclos de mascarillas tratadas con PAF. Por último, no se identificaron modificaciones morfológicas ni deformaciones visuales en las mascarillas después de los tratamientos con plasma.

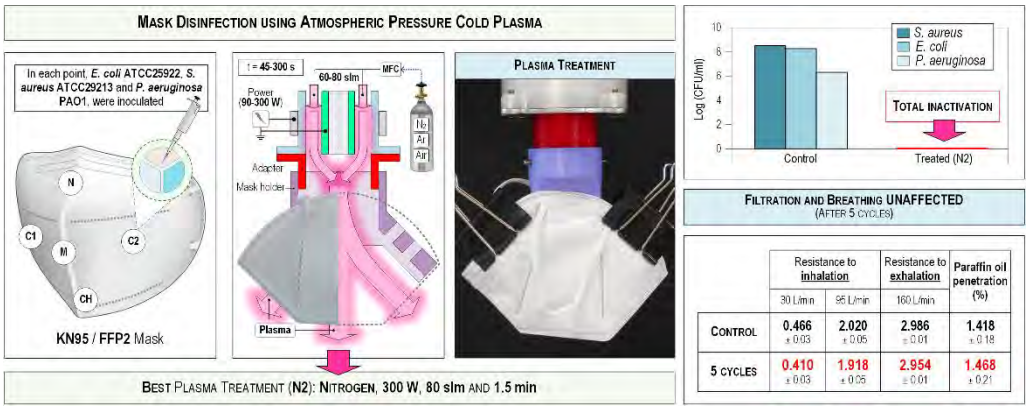

Fig. 18. Resumen gráfico del artículo I.

International Journal of Infectious Diseases 123 (2022) 145–156

Contents lists available at ScienceDirect

International Journal of Infectious Diseases

journal homepage: www.elsevier.com/locate/ijid

Mask disinfection using atmospheric pressure cold plasma

Ana Sainz-García[1], Paula Toledano[2], Ignacio Muro-Fraguas[1], Lydia Álvarez-Erviti[3], Rodolfo Múgica-Vidal[1], María López[2], Elisa Sainz-García[1], Beatriz Rojo-Bezares[2], Yolanda Sáenz[2,#,**], Fernando Alba-Elías[1,#,*]

[1] Department of Mechanical Engineering, University of La Rioja, C/ San José de Calasanz 31, 26004 Logroño, La Rioja, Spain
[2] Molecular Microbiology Area, Center for Biomedical Research of La Rioja (CIBIR), C/Piqueras 98, 26006 Logroño, La Rioja, Spain
[3] Molecular Neurobiology Area, Center for Biomedical Research of La Rioja (CIBIR), C/Piqueras 98, 26006 Logroño, La Rioja, Spain

ARTICLE INFO

Article history:
Received 29 June 2022
Revised 12 August 2022
Accepted 14 August 2022

Keywords:
Cold plasma
Plasma treatment
Mask
Antibacterial treatment
Disinfection

ABSTRACT

Objectives: Mask usage has increased over the last few years due to the COVID-19 pandemic, resulting in a mask shortage. Furthermore, their prolonged use causes skin problems related to bacterial overgrowth. To overcome these problems, atmospheric pressure cold plasma was studied as an alternative technology for mask disinfection.

Methods: Different microorganisms (*Pseudomonas aeruginosa, Escherichia coli, Staphylococcus* spp.), different gases (nitrogen, argon, and air), plasma power (90-300 W), and treatment times (45 seconds to 5 minutes) were tested.

Results: The best atmospheric pressure cold plasma treatment was the one generated by nitrogen gas at 300 W and 1.5 minutes. Testing of breathing and filtering performance and microscopic and visual analysis after one and five plasma treatment cycles, highlighted that these treatments did not affect the morphology or functional capacity of the masks.

Conclusion: Considering the above, we strongly believe that atmospheric pressure cold plasma could be an inexpensive, eco-friendly, and sustainable mask disinfection technology enabling their reusability and solving mask shortage.

Introduction

Masks that cover the nose and mouth are one of the main barriers to avoid the acquisition and transmission of microbial diseases, reducing viral transmission by 95% (Catching *et al.*, 2021; Feng *et al.*, 2020; Ng *et al.*, 2020; Suess *et al.*, 2012). During the last few years, the use of masks has increased due to the COVID-19 pandemic (Feng *et al.*, 2020). However, 93.64% of individuals hadskin reactions, like itching, stinging, dryness, and acne after mask exposure (Choi *et al.*, 2021; Damiani *et al.*, 2021). Maskne (mask+acne) is considered as the skin disease that provokes the highest number of dermatologist visits, and it could be aggravated by sebum, increase in pH, changes in CO_2 levels, and skin humidity (Choi *et al.*, 2021; Damiani *et al.*, 2021; Hua *et al.*, 2020; Kutlu *et al.*, 2020; Mutalik and Inamdar, 2020). These conditions favor the growth and proliferation of specific skin bacteria that cause respiratory diseases (Bao *et al.*, 2020; Choi *et al.*, 2021; Wei *et al.*, 2021). Daou *et al.* (2021) found that *Cutibacterium acnes* is the main bacterium responsible for maskne; however, other bacteria such as *Staphylococcus aureus, Staphylococcus epidermidis,* and *Escherichia coli* can also cause the disease (Daou *et al.*, 2021; Jusuf *et al.*, 2020; Sun and Chang, 2017). These problems are exacerbated by the prolonged use of masks during the COVID-19 pandemic because of mask shortage (Dharmaraj *et al.*, 2021; Feng *et al.*, 2020). Thus, correct and secure mask reuse is fundamental to reduce the consumption of manufacturing resources, facilitate the management of biological residues, and hence protect the environment. Masks are made of nondegradable plastic material, most of which ends up in the oceans and causes damage to the ecosystem (Dharmaraj *et al.*, 2021). However, not only recycling but also the destruction of the pathogens of the mask is important to reduce environmental pollution and the spread of microbial diseases

* Corresponding authors: Fernando Alba-Elías, Department of Mechanical Engineering, University of La Rioja, c/ San José de Calasanz 31, 26004, Logroño, La Rioja, Spain, Tel.: +34 941299276
** Corresponding authors: Yolanda Sáenz, Molecular Microbiology Area, Center for Biomedical Research of La Rioja (CIBIR), c/ Piqueras 98, 26006, Logroño, La Rioja, Spain, Tel.: +34 941278868
E-mail addresses: ysaenz@riojasalud.es (Y. Sáenz), fernando.alba@unirioja.es (F. Alba-Elías).
# These authors contributed equally to this work.

https://doi.org/10.1016/j.ijid.2022.08.012

(Dharmaraj *et al.*, 2021; Sangkham, 2020). In short, mask disinfection promotes environmental sustainability.

Researchers worldwide have studied mask disinfection systems against viruses and bacteria during the COVID-19 pandemic (Battelle, 2016; Cassorla, 2021; Heimbuch *et al.*, 2011; Kenney *et al.*, 2020; Lin *et al.*, 2018, 2017; Lore *et al.*, 2012; Mills *et al.*, 2018). A previous study investigated different mask decontamination methods (bleach, UV irradiation, autoclave, dry heating), achieving complete inactivation of *Bacillus subtilis* spores (Lin *et al.*, 2018). Another study analyzed different methods (UV radiation, dry heat, 70% ethanol, and vaporized hydrogen peroxide [VHP]) to reduce SARS-CoV-2 infection. The greatest inactivation results were obtained with VHP, which maintained the filtration characteristics even after three treatment cycles (Fischer *et al.*, 2020).

Other researchers have also pointed out the functional degradation of masks and the presence of residues after ethanol, UV irradiation, blenching, microwave heating, or VHP treatments (Battelle, 2016; Bergman *et al.*, 2010; Smith *et al.*, 2020; Viscusi *et al.*, 2009).

Low-temperature plasmas have been used for mask disinfection, with hydrogen peroxide gas plasma technology being the most widely used. Most authors have used the Sterrad 100NX plasma generator, which requires a vacuum atmosphere and long treatment times (Ibáñez-Cervantes *et al.*, 2020; Kumar *et al.*, 2020; Viscusi *et al.*, 2009; Wigginton *et al.*, 2021). Viscusi *et al.* (2009) analyzed mask deterioration after a 55 minutes of hydrogen peroxide gas plasma treatment and observed no negative impact either on filter aerosol or on filter airflow resistance. In some studies, more than one cycle of hydrogen peroxide gas plasma treatment affected the filtration and breathing capacity of masks (Bergman *et al.*, 2010; Kumar *et al.*, 2020; Wigginton *et al.*, 2021).

In this regard, atmospheric pressure cold plasma (APCP) technology has been a focus of increased research in recent years for disinfection applications. The most important investigations on the use of APCP for mask disinfection have been examined to further elaborate on the novelty of the current study, which, in conclusion, is scarce in the literature. Indeed, to our knowledge, there are only two publications. In the first publication, a dielectric barrier discharge plasma generator was used to generate ozone to treat KF94 mask portions (30 × 35 mm size) at different durations (10–300 seconds) against virus and bacteria (Lee *et al.*, 2021). The authors observed a total inactivation of *S. aureus* (10 seconds). Neither the structural characteristics of the filter layer nor the functional properties of the mask altered negatively after five 60-second treatment cycles in KF94 masks. In the second publication, plasma was generated using a dielectric barrier discharge plasma equipment to treat SARS-CoV-2 inoculated on N95/ filtering face piece 2 (FFP2) and N99/ filtering face piece 3 (FFP3) mask portions (4 × 4 cm size). No significant negative effect was detected on filtration efficiencies. Plasma was characterized by analyzing the optical emission spectrum, and it was observed that reactive oxygen and nitrogen species (RONS) such as OH^*, NO, and ozone had a viricidal effect (Kim *et al.*, 2021).

In this study, an APCP equipment known as atmospheric pressure plasma jet was used. Different combinations of plasma power, plasma gas, and treatment time were tested on the inner surface of KN95 and FFP2 masks to disinfect them. *E. coli, Pseudomonas aeruginosa,* and different *Staphylococcus* spp. were evaluated.

The original contribution of this work was the determination of the optimal plasma treatment parameters to achieve a total inactivation of all bacteria while preserving the physical and morphological properties of the masks.

For this purpose, the antimicrobial activity of both plasma-treated and thermally treated inoculated samples was analyzed. In addition, plasma-treated samples were analyzed by scanning electron microscopy (SEM), visual evaluation, as well as filtration and breathing tests.

Materials and Methods

Sample masks

Mask disks (diameter 26 mm and 10 mm) and/or complete masks were used in this study (Figures 1–3). KN95 (Chinese standard: GB/T 32610-2016) masks were used for all microbiological analyses. However, from January 2021, KN95 masks were withdrawn from the Spanish market. Therefore, FFP2 (EN 149:2001; Certificate: 20/3212/00/0161; CE-0161FFP2) masks were used for the breathing and filtration analysis.

Plasma and thermal treatments

Different plasma treatments were applied to sets of three sample masks (Table 1). The APCP equipment used was PlasmaSpot500 (MPG, Luxemburg) for mask disks and complete mask treatments (Sainz-García *et al.*, 2021). It consists of one external electrode connected to a high voltage source, one internal grounded electrode, and an aluminum oxide (Al_2O_3) dielectric tube between them. Figures 2 and 3 illustrate the APCP equipment and how mask disks and complete masks were treated, respectively.

The effect of the heat flow generated by the plasma was studied by controlling the temperature during the plasma treatment and by applying thermal treatments in complete masks. The outer surface of the mask (layer 1) subjected to the best plasma treatment (nitrogen plasma 2 [N2]) was characterized by thermography using a thermal imaging camera (TESTO 871) (Testo SE & Co. KGaA, Germany). The obtained images were analyzed with the IRSoft (version 4.3) software. The temperature of the inner surface of the mask (layer 5) was monitored during each second of the 1.5 minutes of plasma treatment by a K-type Teflon-coated thermocouple connected to a data logger (Testo 167T4) (Figure 3c). This study was performed to determine the maximum temperature reached for each treatment. Heated gas thermal treatments were applied on inoculated complete masks to analyze the antimicrobial activity of the heat flow (Figure 3d).

Antimicrobial activity of plasma treatments on mask disks

Mask disks were inoculated with 10 µl of 0.5 McFarland suspension (10^8 Colony Forming Units/ml [CFU/ml]), performed in phosphate buffer saline (PBS, Gibco), of *E. coli* ATCC25922, *P. aeruginosa* PAO1, *S. aureus* ATCC29213, *Staphylococcus hominis* W220, *Staphylococcus haemolyticus* W1493, *Staphylococcus saprophyticus* W1498, *S. epidermidis* W213, *S. epidermidis* W232, *S. epidermidis* W1346, *S. aureus* W1623, and *S. aureus* W1570. The strains W213, W232, W1570, and W1623 presented a multidrug resistance phenotype (resistant to at least three families of antibiotics). Specifically, *S. epidermidis* W213 was resistant to beta-lactams, oxazolidinones, aminoglycosides, and phenicols; *S. epidermidis* W232 was resistant to beta-lactams, oxazolidinones, lincosamides, and aminoglycosides; *S. aureus* W1570 was resistant to beta-lactams, macrolides, lincosamides, aminoglycosides, and fluoroquinolones, and *S. aureus* W1623 was resistant to beta-lactams, aminoglycosides, and fluoroquinolones.

Three bacteria were inoculated per disk for each treatment as shown in Figure 2. Three inoculated disks were used for each plasma treatment, including the CT treatment (Table 1) to control bacterial growth (positive control, CT-positive). In addition,

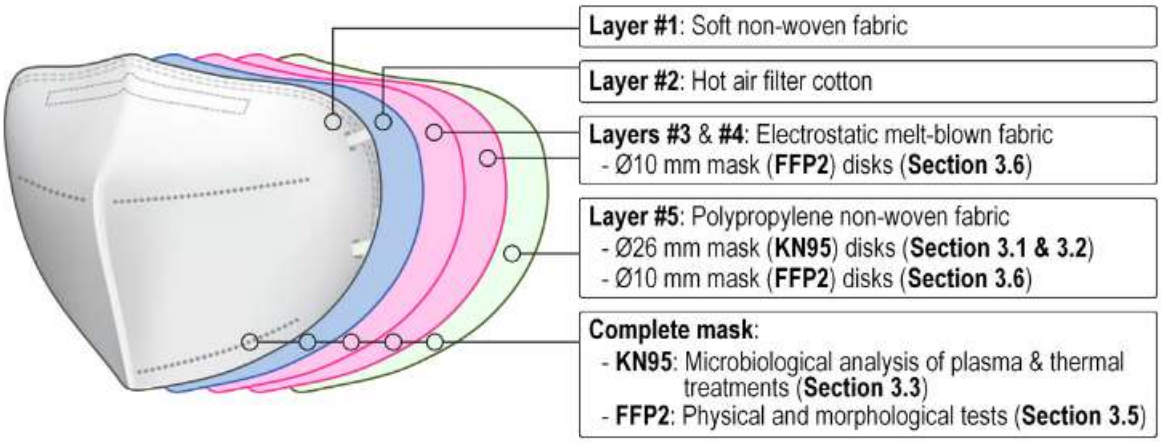

Figure 1. Scheme of the different layers of a mask (KN95 and FFP2) and description of masks used in each paper result section. FFP2 = filtering face piece 2.

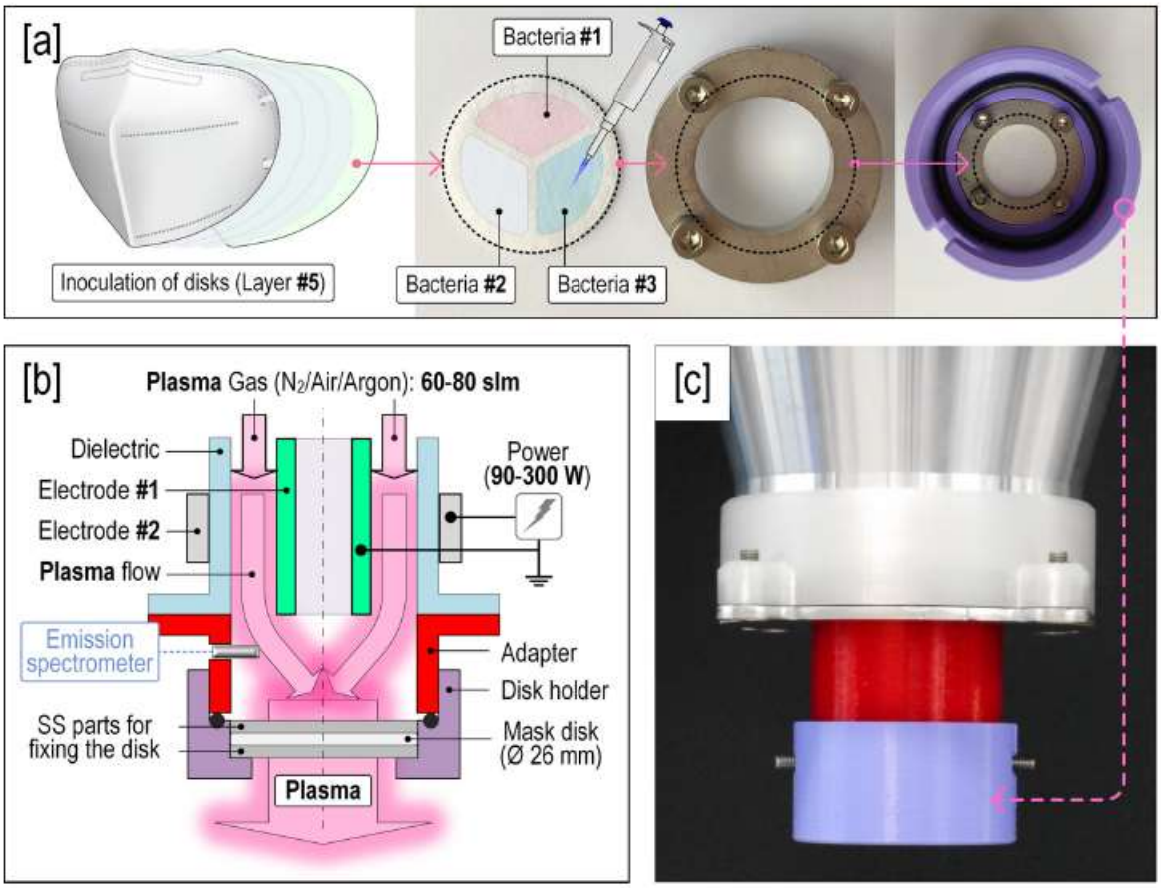

Figure 2. (a) KN95 mask from which Ø 26 mm disks were extracted. Disks and holders needed to treat the disks inoculated with *Escherichia coli* ATCC25922, *Staphylococcus aureus* ATCC29213, and *Pseudomonas aeruginosa* PAO1 suspensions; (b) Atmospheric pressure cold plasma equipment scheme; (c) Plasma equipment treating mask disks.

untreated disks without bacteria were used to analyze the presence of possible contaminants (negative control, CT-negative). No colonies were seen in the negative controls regardless of the treatment studied. Plasma treatments were applied after the inoculum was dry. Then, each inoculated area was independently washed in Eppendorf tubes with 300 µl of Mueller-Hinton broth (CondaLab) for 24 hours. After that, serial dilutions were performed and cultured in Brain Heart Infusion agar at 37° C overnight to determine the CFU/ml. Furthermore, the antimicrobial effect of the APCP treatments N2 and N3 was also analyzed by quantifying the fluorescence levels of the green fluorescent protein (GFP) in the *P. aeruginosa* strain ATCC15692GFP. For this purpose, mask disks were inoculated with 10 µl of *P. aeruginosa* ATCC15692GFP, dried, and then treated with APCP. GFP was quantified before and after the treatment by digital image analysis on a fluorescence microscope (Nikon) using the ImageJ software.

Antimicrobial activity of plasma treatments on complete masks

Five points were selected on the inner side of the masks (Nose-N; Mouth-M; Chin-CH, and both Cheeks-C1 and C2) as shown in Figure 3a. Each spot was inoculated with 10 µl of 0.5 McFar-

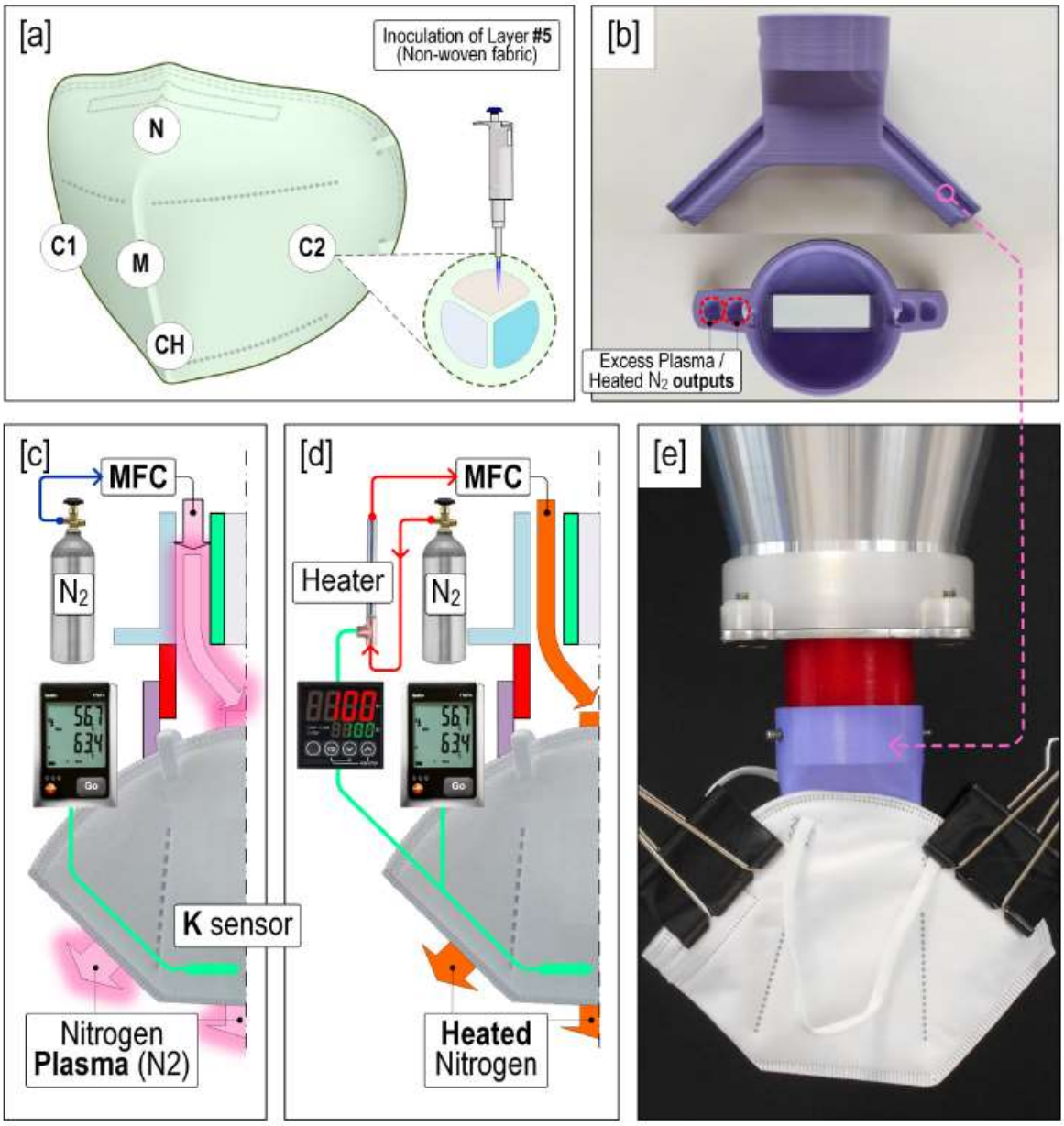

Figure 3. (a) Inoculation points on the inner layer of masks (Nose-N; Mouth-M; Chin-CH and both Cheeks-C1 and C2). Three bacteria were inoculated in each circle; (b) Mask holder; (c) and (d) Scheme of plasma and thermal treatments on masks; (e) Plasma equipment treating complete masks.

land suspension of *E. coli* ATCC25922, *S. aureus* ATCC29213, and *P. aeruginosa* PAO1. Three bacteria were inoculated per mask for each treatment. Untreated masks were used as positive controls for growth. Plasma treatment was applied after the inoculum was dried under sterile conditions. Subsequently, each area was cut and the viable bacteria CFU/ml were determined using the procedure described for mask disks.

Optical emission spectroscopy

Optical emission spectroscopy analysis was used to identify the RONS produced by N2, Ar1, and A2 plasma treatments (Table 1). The equipment used was the spectrometer F600-UVVIS-SR (StellarNet, Tampa, Florida, USA), connected to an optical fiber (QP600-2SR-Ocean Optics) with a lens that collected information of the plasma flux as shown in Figure 2b. Data were processed with the SpectraWiz software (StellarNet, Tampa, Florida, USA).

Physical and morphological characteristics of the mask after treatment

Filtration properties and breathing resistance of complete masks were measured by an external laboratory (AITEX, Spain). The filtration test was done by filter penetration with paraffin oil following the EN 149:2001+A1:2009 standard. The expanded uncertainty was ± 10% of the measured value for a 95% probability of coverage. The breathing resistance test was done following the same standard. In this case, the expanded uncertainty was ± 18% of the measured value for 95% probability of coverage. Each analysis was performed five times.

For morphological analysis, a HITACHI S-2400 SEM was used. Untreated and 5-time-plasma-treated (N2) (Table 1) mask disks from layers 4 and 5 were tested. Before SEM examination, mask disks were coated with a thin layer of gold and palladium, using a sputtering apparatus to make them conductive. In addition,

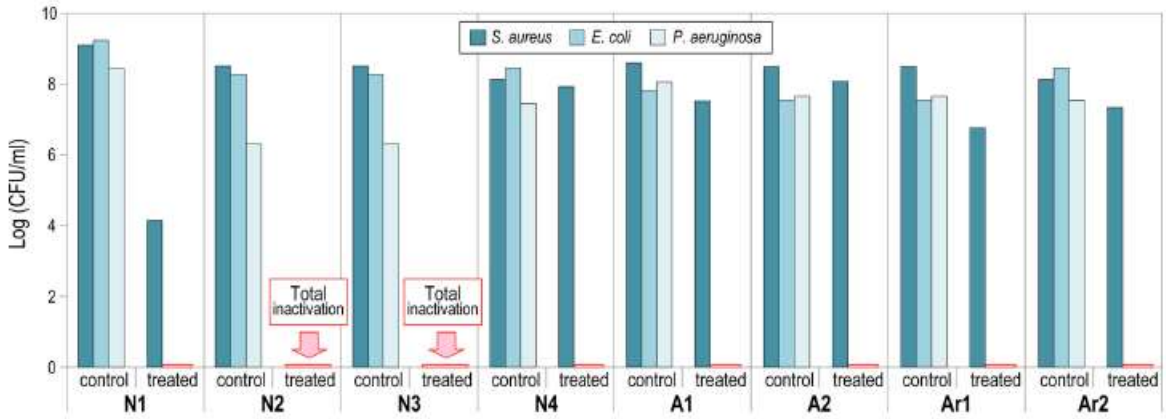

Figure 4. Comparison of antimicrobial activity of different plasma treatments and their controls in mask disksagainst *Staphylococcus aureus, Escherichia coli,* and *Pseudomonas aeruginosa.*

visual analysis was performed to detect any alterations in the treated masks.

Results and Discussion

Inactivation on mask disks by plasma treatments

The degree of bacterial inactivation was influenced by the bacterial species analyzed and the modification of the plasma treatment parameters. Figure 4 shows the antimicrobial activity of the plasma treatments against *E. coli* ATCC25922, *P. aeruginosa* PAO1, and *S. aureus* ATCC29213 on mask disks in comparison with the CT-positive.

The best treatments were the nitrogen plasma treatments (N2 and N3) as they achieved total inactivation regardless of the target bacteria. Furthermore, all studied treatments achieved complete inactivation of *E. coli* and *P. aeruginosa*, with *S. aureus* being the most resistant species, consistent with other studies (Han *et al.*, 2016; Huang *et al.*, 2020; Kayes *et al.*, 2007; Lunov *et al.*, 2016). For instance, Huang *et al.* (2020) and Han *et al.* (2016) found higher inactivation values in *Salmonella Typhimurium* and *E. coli*, respectively, than in *S. aureus* after plasma treatment of 96-well microtiter plates and Petri dishes, respectively (Han *et al.*, 2016; Huang *et al.*, 2020).

Several authors consider the morphological characteristics of bacteria as one of the factors responsible for the differences in bacterial inactivation (Huang *et al.*, 2020). Both Gram-positive and Gram-negative bacteria possess cell wall peptidoglycans, but Gram-positive bacteria have a thick peptidoglycan wall that allows them to resist plasma damage. Besides, other researchers have identified different action mechanisms depending on Gram-positive and Gram-negative bacteria. For Gram-positive bacteria, it has been suggested that RONS play the main role in provoking lipid membrane disturbances after lipid peroxidation of unsaturated fatty acids. Amino acid oxidation results in protein modification, followed by DNA damage and cell death (Arjunan *et al.*, 2015; Šimončicová *et al.*, 2018; Yong *et al.*, 2015). However, in the case of Gram-negative bacteria, with irregular surfaces, electrostatic disruption is the most effective effect (Lunov *et al.*, 2016; Mai-Prochnow *et al.*, 2016). This effect involves the rupture of the membrane when the outer membrane acquires sufficient electric charge. Regarding the bacteria analyzed in our work, *E. coli* and *P. aeruginosa* are Gram-negative bacteria, and *S. aureus* is Gram-positive, which could explain the differences in the inactivation rates.

In addition, plasma treatment time, power, or gas, influenced the bacterial inactivation results, as many authors have previously indicated (Han *et al.*, 2016; Huang *et al.*, 2020; Lunov *et al.*, 2016; Miao and Jierong, 2009; Surowsky *et al.*, 2014; Wiegand *et al.*, 2014). Han *et al.* (2016) demonstrated that the longer the exposure time, the higher the bacterial damage (Han *et al.*, 2016). This is in accordance with our results as N1 treatment (45 seconds) only achieved 4.96 log (CFU/ml) reductions, whereas N2 (1.5 minutes) or N3 (2.5 minutes), caused total inactivation. Although the treatment time for N4 plasme treatment was the longest (5 minutes), the plasma power was not enough to inactivate all bacteria (220 W). N2 treatment (300 W; 1.5 minutes) resulted in higher inactivation values than N4 (220 W; 5 minutes), indicating that treatment power plays a more important role than treatment time. In this regard, another previous study reported that when the power was increased from 75 W to 125 W, inactivation by plasma treatment against *L. monocytogenes, E. coli,* and *S. Typhimurium* also increased (Kim *et al.*, 2011). Plasma power provides energy to generate RONS. Thus, the higher the power, the larger the amount of RONS generated to inactivate the bacteria (Laroussi and Leipold, 2004; Lu *et al.*, 2016).

Finally, plasma gas played one of the main roles in terms of antimicrobial activity. Comparing the studied gases (nitrogen, air, and argon), the best was nitrogen because it achieved total inactivation regardless of the bacteria used.

The effect of N2 and N3 treatments against *P. aeruginosa* ATCC15692GFP was also studied by analyzing their antimicrobial activities and the fluorescence levels of GFP (Figure 5). This bacterium possesses a multicopy vector encoding the green fluorescent protein GFPmut3. Both plasma treatments achieved antimicrobial activity (> 7 logarithmic reductions, data not shown), and they also reduced protein concentration. GFP signals after N2 and N3 treatments were 43% and 54% respectively, in comparison with signal control (100%) with statistically significant differences ($p \leq 0.05$). Hence, it is confirmed that both treatments were effective against *P. aeruginosa* ATCC15692GFP.

Inactivation of different species of Staphylococcus

Staphylococcus species are one of the most important causes of nasopharyngeal infections and can be implicated in the most aggressive types of maskne (Daou *et al.*, 2021; Jusuf *et al.*, 2020; Revai *et al.*, 2008; Sun and Chang, 2017). For that reason, we investigated different *Staphylococcus* spp. strains (*S. hominis* W220, *S. haemolyticus* W1493, *S. saprophyticus* W1498, *S. epidermidis* W213, W232 and W1346, and *S. aureus* W1623 and W1570) from the clinical collection of Molecular Microbiology Area of the Biomedical Research Center of La Rioja (CIBIR), to determine their resistance to plasma treatment. Among them, the methicillin and linezolid-resistant

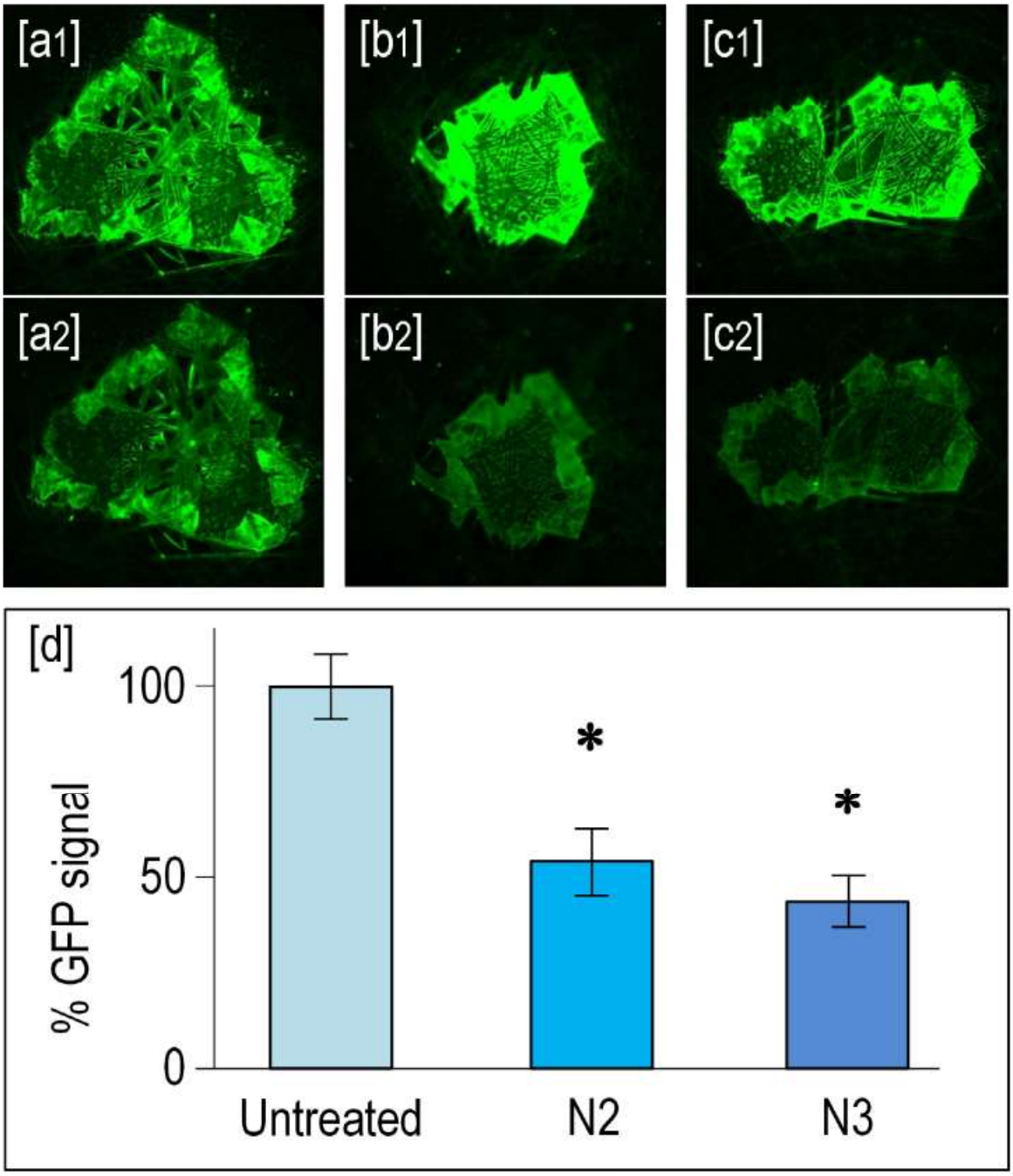

Figure 5. Fluorescence microscope digital images of GFP quantification: (a1, b1, and c1) before and (a2, b2, and c2) after CT, N2, and N3 plasma treatments, respectively; (d) GFP signal percentage of these treatments (*, $p \leq 0.05$).
GFP = green fluorescent protein.

S. epidermidis W213 and W232, and the methicillin-resistant *S. aureus* W1570 and W1623 presented multidrug-resistant phenotypes. Tests were performed applying the best plasma treatment identified in section 3.1 (N2) and following the same procedures. All strains, including the multidrug-resistant strains, were completely inactivated after 1.5 minutes of N2 treatment.

Inactivation of the complete mask by plasma and thermal treatments

N2 plasma treatment was chosen to study the antibacterial activity on complete masks as more than six logarithmic reductions were observed against *E. coli* ATCC25922, *S. aureus* ATCC29213, and *P. aeruginosa* PAO1 (Figure 4). In addition, the thermal effect was studied to determine the antimicrobial capacity associated with the flow of heat generated by the plasma.

On the one hand, the thermal images of the outer layer of the mask (layer 1) with the N2 treatment at different times showed a homogeneous thermal distribution (Figure 6), indicating a homogeneous plasma treatment. The temperatures on the outer surface of the mask at the end of the N2 treatment ranged from 80 °C to 90 °C (Figure 6d). On the other hand, the maximum temperature of the inner mouth zone of the mask during the N2 plasma treatment was 100 °C (Figure 7). This temperature was used as a guide to heat an 80 standard liter per minute -nitrogen flux using

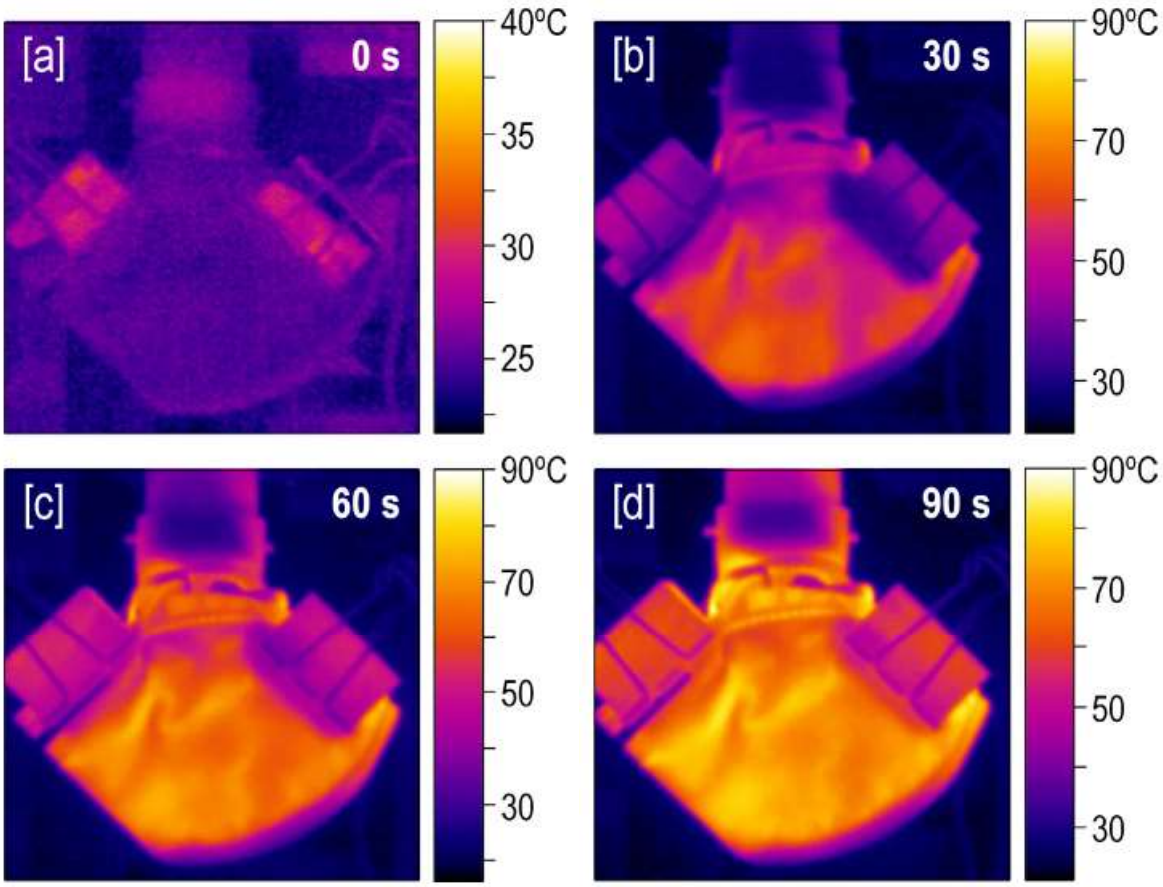

Figure 6. Mask outer surface thermography (layer 1) during N2 plasma treatment at different times: (a) 0 seconds, (b) 30 seconds, (c) 60 seconds, and (d) 90 seconds.

Table 1
Conditions of plasma treatments

Treatment code	Plasma Gas	Gas Flow (slm)	Cooling Gas	Plasma Power (W)	Treatment time
CT	-	-	-	-	-
N1	Nitrogen	80	Air	300	45 seconds
N2	Nitrogen	80	Air	300	1.5 minutes
N3	Nitrogen	80	Air	300	2.5 minutes
N4	Nitrogen	80	Air	220	5 minutes
A1	Air	80	Air	300	45 seconds
A2	Air	80	Air	300	1.5 minutes
Ar1	Argon	60	Air	90	1.5 minutes
Ar2	Argon	60	Air	60	5 minutes

slm, standard liter per minute.

Table 2
Comparison of the antimicrobial activity of plasma (N2) and thermal treatments against *S. aureus* ATCC29213, *E. coli* ATCC25922, and *P. aeruginosa* PAO1 inoculated in complete masks

Bacteria	Recuperated bacteria in control samples (control-positive)[a]		Recuperated bacteria after treatment (logarithmic reduction)[a]	
	CT	Thermal treatment	N2	Thermal treatment
Staphylococcus aureus ATCC29213	8.75	9.13	1.54 (7.21)	8.51 (0.62)
Escherichia coli ATCC25922	5.99	5.28	0 (5.99)	0 (5.28)
Pseudomonas aeruginosa PAO1	8.31	8.11	0 (8.31)	0 (8.11)

[a] The data are showed in log (CFU/ml).
CFU = colony forming units.

a thermal system controlled by a temperature regulator, and subsequently, each bacterium was subjected to that nitrogen flux for 1.5 minute. The thermal effect was the main cause of the inactivation of *P. aeruginosa* and *E. coli* as both treatments (plasma and heat flux) produced total inactivation of both bacteria (Table 2). However, heated flow was insufficient to inactivate *S. aureus*, and it could be affirmed that plasma treatment was necessary for the total inactivation of *S. aureus* in addition to heat flux treatment. To our knowledge, bacteria can be inactivated by a combination of several factors, including time and heat treatment. In this regard, some authors have studied how thermal treatment affects the inactivation of different bacteria (*P. aeruginosa* PAO1, *S. Typhimurium*,

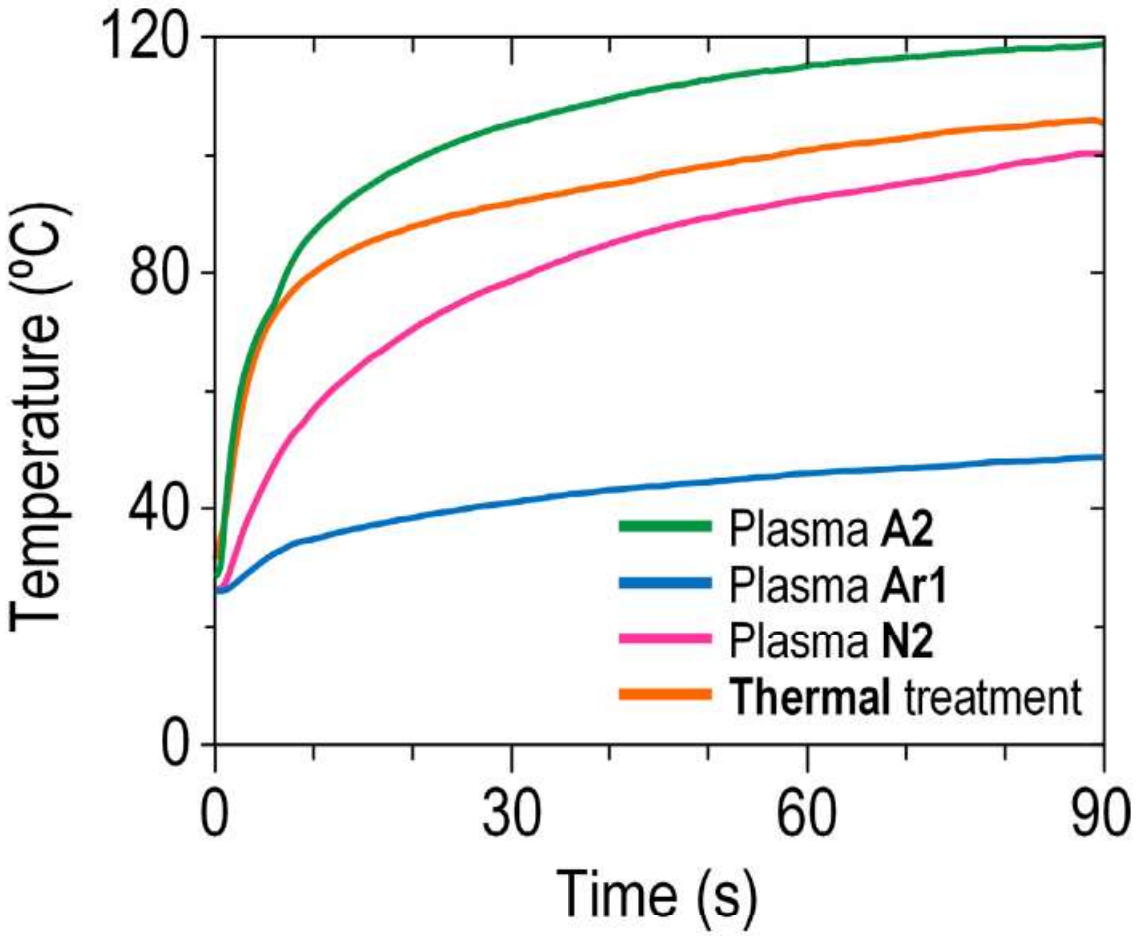

Figure 7. Temperature of the inner surface (layer 5) of a mask during plasma treatments (N2, Ar1, and A2) and thermal treatment measured by a type K thermocouple probe.

and *E. coli*) in different environments (sardinella meat, snail meat, and cells). They concluded that the higher the temperature and the time, the greater the bacteria reduction (Gabriel and Alano-Budiao, 2019; Gabriel and Ubana, 2007; Marcén *et al.*, 2017).

Optical emission spectroscopy

Figure 8 shows optical emission spectra (200-500 nm) of nitrogen, argon, and air plasma. It was possible to identify which relevant RONS appeared for each plasma gas and justify the antimicrobial activity. N2 treatment spectrum (Figure 8a) showed different species namely: (i) NO* radical (200-280 nm), (ii) Second positive system (SPS) of nitrogen (296-405 nm), and (iii) First negative system (FNS) of nitrogen (at 394 and 427 nm). SPS and FNS need to be taken into account because of their role in ozone (O_3) generation, a species with biocidal capacity and one that does not generate an excited state that emits light (Girgin Ersoy *et al.*, 2019; Marino *et al.*, 2018; Porto *et al.*, 2020; Wen *et al.*, 2020). O_3 generation is explained as follows (Kim *et al.*, 2021).

$$N_2 + e \rightarrow N_2^+ + e + e$$

$$N_2^+ + O_2 \rightarrow N_2^+ + O + O$$

$$O + O_2 + M \rightarrow O_3 + M$$

On the other hand, Ar1 (Figure 8b) showed the same species as N2, in addition to the OH* radical (309 nm). Finally, Figure 8c shows the spectrum of A2, where only the nitrogen species SPS and FNS were detected.

In this study, masks were treated using an assembly that conducts the plasma flow to the inner surface of the mask. Therefore, the combined antimicrobial effect of positive and negative ions, RONS, electrons, excited and neutral ions, heat, molecules, and UV photons can be leveraged (Scholtz *et al.*, 2015). Most authors propose that the effect of RONS is most likely responsible for the inactivation capacity of atmospheric pressure plasma jet (Iuchi *et al.*, 2018; Sainz-García *et al.*, 2021). In fact, it has been previously reported that the NO*, OH*, and O_3 species confirmed antimicrobial activity (Kaushik *et al.*, 2018; Laroussi and Leipold, 2004; Porto *et al.*, 2020; Wen *et al.*, 2020; Wu *et al.*, 2017; Zhang *et al.*, 2016).

The following conclusions might be drawn when comparing treatments: (i) N2 treatment achieved the best bacterial inactivation (Figure 4), and among all the reactive species identified, the NO* radical could be the most biocidal RONS, as it has the highest peak and intensity (Figure 8a). (ii) The antimicrobial capacity of Ar1 was similar to that of A2 despite generating a significantly lower heat flow than the other treatments (Figure 7). In this case, OH* radicals and O_3 from nitrogen species SPS and FNS seem to balance out the lower Ar1 inactivation effect due to the low temperature. (iii) Notwithstanding the lower relative intensities for all RONS (NO*, OH*, and O_3), the inactivation performed by treatment A2 could benefit from heat flux (highest temperature) (Figure 7).

Physical and morphological characteristics of the mask after treatment

Filtration capacity (FC), breathing resistance, visual modifications, and adaptability to the face were assessed after plasma

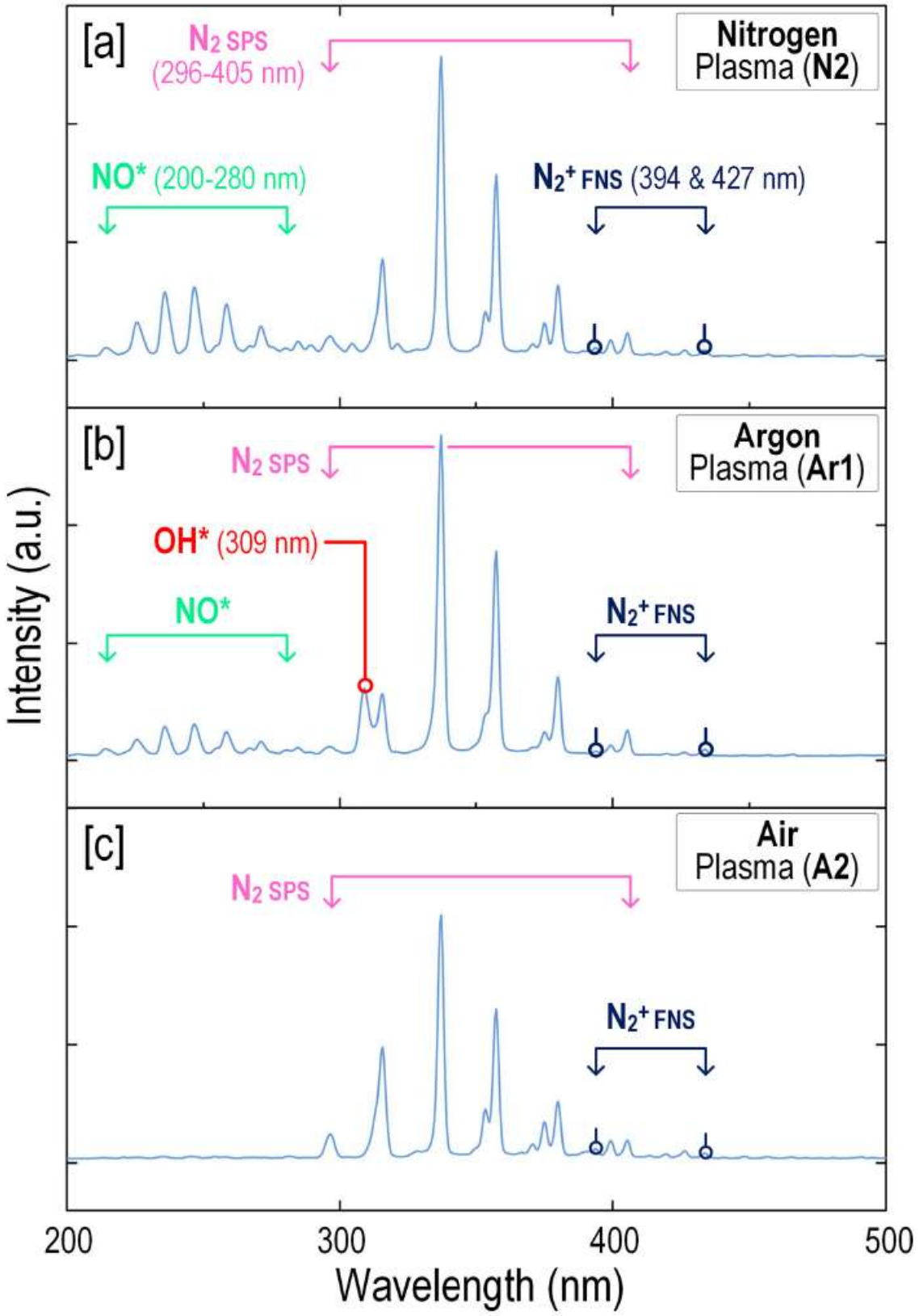

Figure 8. Optical emission spectra of plasma treatments: (a) nitrogen plasma N2, (b) argon plasma Ar1, and (c) air plasma A2.

Table 3
Filtration capacity and breathing resistance after one (KN95) and five (FFP2) treatment cycles

Type of mask		Resistance to inhalation (mbar)		Resistance to exhalation (mbar)	Paraffin oil penetration (%)
		30 l/min	95 l/min	160 l/min	
KN95	Control	0.387 ± 0.02	1.217 ± 0.05	2.160 ± 0.02	7.148 ± 0.31
	1 cycle	0.420 ± 0.01	1.350 ± 0.02	2.277 ± 0.09	7.135 ± 0.22
FFP2	Control	0.466 ± 0.03	2.020 ± 0.05	2.986 ± 0.01	1.418 ± 0.18
	5 cycles	0.410 ± 0.03	1.918 ± 0.05	2.954 ± 0.01	1.468 ± 0.21

FFP2 = filtering face piece 2.

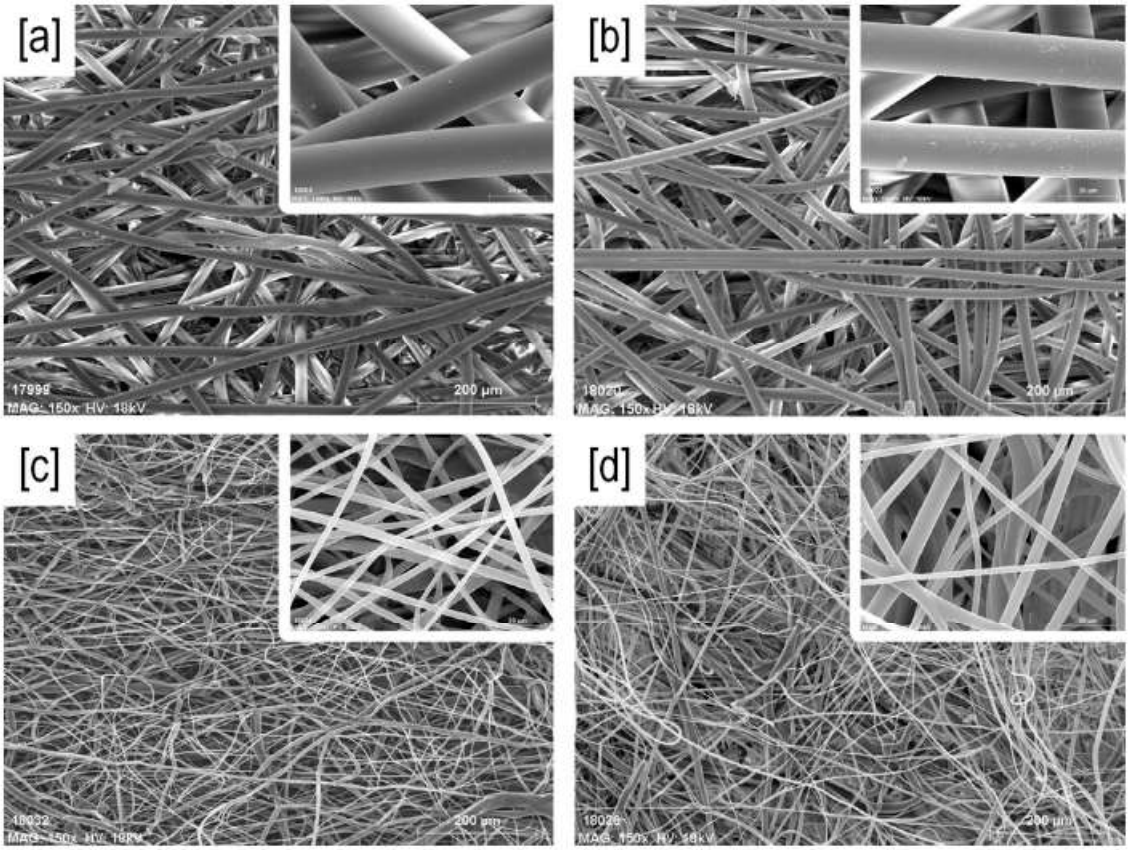

Figure 9. SEM images with a magnification of 150x and 1500x detail of samples: (a, c) Untreated layers 5 and 4, respectively, and (b, d) Layers 5 and 4 of a complete mask (FFP2) after five cycles of plasma treatment (N2).
FFP2 = filtering face piece 2; N2 = nitrogen plasma 2; SEM = scanning electron microscopy.

treatments. Table 3 shows FC and breathing resistance after one and five treatment cycles. Data obtained revealed that plasma treatment did not affect either breathing resistance or FC of masks for at least five treatment cycles. It was observed that the resistance to inhalation (30 l/minutes) increased from 0.387 mbar to 0.420 mbar after one cycle and decreased from 0.466 mbar to 0.410 mbar after five cycles, which were not significant differences. In contrast, in the study of inhalation 95 l/min and expiratory resistance, there was a slight increase in one cycle but a decrease after five cycles. Finally, the number of cycles did not affect the FC which was similar to the control masks. These results seem reasonable, and a slight increase in respiration implies a small decrease in FC. Nevertheless, this reduction could be neglected considering that FC of treated masks during five cycles only lost 3.4% of FC with regard to the control masks (FC = 1.418). Our study demonstrated that treated masks maintained a FC of 1.468, similar to FFP3 (FC = 1). These findings are in line with previous results that applied five cycles (60 seconds) of O_3 plasma treatment on masks without observing modifications in the structural characteristics, functional properties and inhalation resistance of the filter layer (Lee *et al.*, 2021). Moreover, previous studies observed no modification in the functional characteristics of masks after one cycle of plasma treatment, suggesting that after one cycle, it is possible to reuse masks in terms of FC and breathing resistance (Bergman *et al.*, 2010; Osaili *et al.*, 2020; Wigginton *et al.*, 2021). It is worth noting that we succeeded with five plasma treatment cycles, as few studies have evaluated more than one plasma treatment cycle without affecting the functional properties of the masks. Other researchers have studied the effect of more than one cycle of other decontamination technologies on the masks. Wigginton *et al.* (2021) demonstrated a maintained filtration efficacy and proper fit after 10 cycles of VHP and moist heat (Wigginton *et al.*, 2021). Bergman *et al.* (2010) showed no differences in FC with three cycles of UV, ethylene oxide or microwaves (Bergman *et al.*, 2010). Other authors applied 10 cycles of either ozone or steam and 20 cycles of microwaves without affecting filtration efficiency (Blanco *et al.*, 2021; Ou *et al.*, 2020; Zulauf *et al.*, 2020).

Furthermore, it was observed that the plasma treatment applied in this research had no impact on the mechanical and face comfort capacity as well as visual modifications. There were no

differences between control masks and treated masks: no fragmented or stretched elastic trips and no degradation in mask color (data not shown). On the contrary, Viscusi *et al.* (2009) observed that metallic nosebands were tarnished and not as shiny as in the control masks after a 55-minute plasma treatment.

SEM analysis

Layers 5 and 4 from untreated and plasma-treated samples (five cycles) were analyzed with SEM to determine the possible impact of plasma on surface morphology. SEM images of the samples with a magnification of 150x and 1500x, showed no differences (Figure 9). These results demonstrated no negative impact on the fibers of the treated masks, which is probably related to the fact that their FC was maintained. Therefore, it can be concluded that plasma treatment can be applied without provoking a noticeable damage on mask surfaces.

Conclusions

Due to the COVID-19 pandemic, mask-wearing has increased over the last few years. In this scenario, there has also been a huge increase in facial diseases caused by masks. In addition, there is a shortage of masks due to massive use. In this regard, in this study we investigated the effectiveness of an atmospheric pressure plasma jet equipment in disinfecting masks and maintaining their functional properties. It is worth mentioning that, to the best of our knowledge, this is the first study in which a complete FFP2 mask was disinfected using APCP. Our results suggested that plasma power, plasma gas, and treatment time must be considered to determine the degree of bacterial inactivation. The longer the treatment time and plasma power, the higher the inactivation. Regardless of the type of bacteria, the use of nitrogen plasma, 300 W power, and 1.5 minutes of treatment were the optimal plasma parameters for total inactivation of bacteria. Furthermore, the thermal study confirmed that both *P. aeruginosa* PAO1 and *E. coli* ATCC25922 were inactivated mainly by means of the thermal effect. In contrast, RONS generated in plasma were the main cause of *Staphylococcus* inactivation. Specifically, NO^* radical seems to be the most biocidal radical.

FC, breathing resistance analysis and SEM images confirmed that neither reduction in FC nor morphological modifications occurred in the masks even after five cycles of plasma treatment. In conclusion, disinfection of used masks with APCP could be an emergency solution to reduce facial infections and to solve mask shortages as well as the environmental problems associated with discarding masks. Moreover, this disinfecting technology could be applied to other objects and personal protective equipment used in hospitals.

Funding

This research did not receive any specific grant from funding agencies in the public, commercial, or not-for-profit sectors.

Ethical approval

Not applicable since this was a laboratory study not involving any clinical samples or human and animal subjects**.**

Author contributions

Ana Sainz-García: Study design, Data collection, Data analysis, Writing-Original Draft, Review & Editing, Visualization, Supervision. **Paula Toledano:** Study design, Data collection, Data analysis, Writing-Review & Editing. **Ignacio Muro-Fraguas:** Study design, Data collection, Data analysis, Writing-Review & Editing. **Lydia Álvarez-Erviti:** Data collection, Data analysis, Writing-Review & Editing. **Rodolfo Múgica-Vidal:** Study design, Data collection, Data analysis, Writing-Review & Editing. **María López:** Study design, Data collection, Data analysis, Writing-Review & Editing. **Elisa Sainz-García:** Study design, Data collection, Data analysis, Writing-Original Draft, Review & Editing. **Beatriz Rojo-Bezares:** Study design, Data collection, Data analysis, Writing-Review & Editing. **Yolanda Sáenz:** Study design, Data collection, Data analysis, Resources, Writing-Review & Editing, Supervision. **Fernando Alba-Elías:** Study design, Data collection, Data analysis, Resources, Writing-Review & Editing, Supervision.

Data availability statement

Data that support the findings of this study are available from the corresponding author upon reasonable request.

Declaration of competing interest

The authors have no competing interests to declare.

Acknowledgments

The authors wish to thank Dr. Francesco Tampieri (Universitat Politécnica de Catalunya) for his support in the optical emission spectra acquisition. This publication is based upon work from COST Action CA20114 PlasTHER, supported by COST (European Cooperation in Science and Technology-www.cost.eu). The author Elisa Sainz-García, as a postdoctoral researcher of the University of La Rioja, thanks the postdoctoral training program funded by the Plan Propio of the University of La Rioja. Authors Ignacio Muro-Fraguas and Ana Sainz-García are thankful to the program of pre-doctoral contracts for the training of research staff funded by the University of La Rioja and Spanish Ministry of Science and Innovation, respectively.

References

Arjunan KP, Sharma VK, Ptasinska S. Effects of atmospheric pressure plasmas on isolated and cellular DNA-a review. Int J Mol Sci 2015;16:2971–3016.
Bao L, Zhang C, Dong J, Zhao L, Li Y, Sun J. Oral microbiome and SARS-CoV-2: beware of lung co-infection. Front Microbiol 2020;11:1840.
Battelle. Bioquell hydrogen peroxide vapor (HPV) decontamination for reuse of N95 respirators. Columbus: FDA 2016:1–46.
Bergman MS, Viscusi DJ, Heimbuch BK, Wander JD, Sambol AR, Shaffer RE. Evaluation of multiple (3-Cycle) decontamination processing for filtering facepiece respirators. J Eng Fibers Fabr 2010;5:33–41.
Blanco A, Ojembarrena FB, Clavo B, Negro C. Ozone potential to fight against SAR-COV-2 pandemic: facts and research needs. Environ Sci Pollut Res Int 2021;28:16517–31.
Cassorla L. Decontamination and reuse of N95 filtering facepiece respirators: where do we stand? Anesth Analg 2021;132:2–14.
Catching A, Capponi S, Te YM, Bianco S, Andino R, Francisco S, et al. Graduate program in biophysics, University of California, San Francisco, San Francisco, CA **industrial and applied genomics, AI and cognitive software**. San Francisco: IBM Almaden Research Center; 2021.
Choi SY, Hong JY, Kim HJ, Lee GY, Cheong SH, Jung HJ, et al. Mask-induced dermatoses during the COVID-19 pandemic: a questionnaire-based study in 12 Korean hospitals. Clin Exp Dermatol 2021;46:1504–10.
Damiani G, Gironi LC, Grada A, Kridin K, Finelli R, Buja A, et al. COVID-19 related masks increase severity of both acne (maskne) and rosacea (mask rosacea): multi-center, real-life, telemedical, and observational prospective study. Dermatol Ther 2021;34:e14848.
Daou H, Paradiso M, Hennessy K, Seminario-Vidal L. Rosacea and the microbiome: a systematic seview. Dermatol Ther (Heidelb) 2021;11:1–12.
Dharmaraj S, Ashokkumar V, Hariharan S, Manibharathi A, Show PL, Chong CT, et al. The COVID-19 pandemic face mask waste: a blooming threat to the marine environment. Chemosphere 2021;272.
Feng S, Shen C, Xia N, Song W, Fan M, Cowling BJ. Rational use of face masks in the COVID-19 pandemic. Lancet Respir Med 2020;8:434–6.
Fischer RJ, Morris DH, Van Doremalen N, Sarchette S, Matson MJ, Bushmaker T, et al. Effectiveness of N95 respirator decontamination and reuse against SARS-CoV-2 Virus. Emerg Infect Dis 2020;26:2253–5.

Gabriel AA, Alano-Budiao AS. Thermal inactivation of *Pseudomonas aeruginosa* 1244 in salted *Sardinella fimbriata* meat homogenate. Agr Nat Resour 2019;53:79–83.
Gabriel AA, Ubana MA. Decimal reduction times of Salmonella Typhimurium in guinataang kuhol: an indigenous Filipino dish. LWT Food Sci Technol 2007;40:1108–11.
Girgin Ersoy Z, Barisci S, Dinc O. Mechanisms of the Escherichia coli and Enterococcus faecalis inactivation by ozone. LWT 2019;100:306–13.
Han L, Patil S, Boehm D, Milosavljević V, Cullen PJ, Bourke P. Mechanisms of inactivation by high-voltage atmospheric cold plasma differ for Escherichia coli and Staphylococcus aureus. Appl Environ Microbiol 2016;82:450–8.
Heimbuch BK, Wallace WH, Kinney K, Lumley AE, Wu CY, Woo MH, et al. A pandemic influenza preparedness study: use of energetic methods to decontaminate filtering facepiece respirators contaminated with H1N1 aerosols and droplets. Am J Infect Control 2011;39:e1–9.
Hua W, Zuo Y, Wan R, Xiong L, Tang J, Zou L, et al. Short-term skin reactions following use of N95 respirators and medical masks. Contact Dermatitis 2020;83:115–21.
Huang M, Zhuang H, Zhao J, Wang J, Yan W, Zhang J. Differences in cellular damage induced by dielectric barrier discharge plasma between Salmonella typhimurium and Staphylococcus aureus. Bioelectrochemistry 2020;132.
Ibáñez-Cervantes G, Bravata-Alcántara JC, Nájera-Cortés AS, Meneses-Cruz S, Delgado-Balbuena L, Cruz-Cruz C, et al. Disinfection of N95 masks artificially contaminated with SARS-CoV-2 and ESKAPE bacteria using hydrogen peroxide plasma: impact on the reutilization of disposable devices. Am J Infect Control 2020;48:1037–41.
Iuchi K, Morisada Y, Yoshino Y, Himuro T, Saito Y, Murakami T, et al. Cold atmospheric-pressure nitrogen plasma induces the production of reactive nitrogen species and cell death by increasing intracellular calcium in HEK293T cells. Arch Biochem Biophys 2018;654:136–45.
Jusuf NK, Putra IB, Sari L. Differences of microbiomes found in non-inflammatory and inflammatory lesions of acne vulgaris. Clin Cosmet Investig Dermatol 2020;13:773–80.
Kaushik NK, Ghimire B, Li Y, Adhikari M, Veerana M, Kaushik N, et al. Biological and medical applications of plasma-activated media, water and solutions. Biol Chem 2018;400:39–62.
Kayes MM, Critzer FJ, Kelly-Wintenberg K, Roth JR, Montie TC, Golden DA. Inactivation of foodborne pathogens using a one atmosphere uniform glow discharge plasma. Foodborne Pathog Dis 2007;4:50–9.
Kenney PA, Chan BK, Kortright KE, Cintron M, Russi M, Epright J, et al. Hydrogen peroxide vapor decontamination of N95 respirators for reuse. Infect Control Hosp Epidemiol 2020;43:45–7.
Kim B, Yun H, Jung S, Jung Y, Jung H, Choe W, et al. Effect of atmospheric pressure plasma on inactivation of pathogens inoculated onto bacon using two different gas compositions. Food Microbiol 2011;28:9–13.
Kim M, Lawson J, Hervé R, Jakob H, Ganapathisubramani B, Keevil CW. Development of a rapid plasma decontamination system for decontamination and reuse of filtering facepiece respirators. AIP Adv 2021;11.
Kumar A, Kasloff SB, Leung A, Cutts T, Strong JE, Hills K, et al. N95 mask decontamination using standard hospital sterilization technologies. MedRxiv 20 April 2020 (accessed 29 August 2022). doi:10.1101/2020.04.05.20049346.
Kutlu Ö, Güneş R, Coerdt K, Metin A, Khachemoune A. The effect of the "stay-at-home" policy on requests for dermatology outpatient clinic visits after the COVID-19 outbreak. Dermatol Ther 2020;33:e13581.
Laroussi M, Leipold F. Evaluation of the roles of reactive species, heat, and UV radiation in the inactivation of bacterial cells by air plasmas at atmospheric pressure. Int J Mass Spectrom 2004;233:81–6.
Lee J, Bong C, Lim W, Bae PK, Abafogi AT, Baek SH, et al. Fast and easy disinfection of coronavirus-contaminated face masks using ozone gas produced by a dielectric barrier discharge plasma generator. Environ Sci Technol Lett 2021;8:339–44.
Lin TH, Chen CC, Huang SH, Kuo CW, Lai CY, Lin WY. Filter quality of electret masks in filtering 14.6–594 nm aerosol particles: effects of five decontamination methods. PLoS One 2017;12.
Lin TH, Tang FC, Hung PC, Hua ZC, Lai CY. Relative survival of Bacillus subtilis spores loaded on filtering facepiece respirators after five decontamination methods. Indoor Air 2018;28:754–62.
Lore MB, Heimbuch BK, Brown TL, Wander JD, Hinrichs SH. Effectiveness of three decontamination treatments against influenza virus applied to filtering facepiece respirators. Ann Occup Hyg 2012;56:92–101.
Lu X, Naidis GV, Laroussi M, Reuter S, Graves DB, Ostrikov K. Reactive species in non-equilibrium atmospheric-pressure plasmas: generation, transport, and biological effects. Phys Rep 2016;630:1–84.
Lunov O, Zablotskii V, Churpita O, Jäger A, Polívka L, Syková E, et al. The interplay between biological and physical scenarios of bacterial death induced by non-thermal plasma. Biomaterials 2016;82:71–83.
Mai-Prochnow A, Clauson M, Hong J, Murphy AB. Gram positive and Gram negative bacteria differ in their sensitivity to cold plasma. Sci Rep 2016;6:38610.
Marcén M, Ruiz V, Serrano MJ, Condón S, Mañas P. Oxidative stress in E. coli cells upon exposure to heat treatments. Int J Food Microbiol 2017;241:198–205.
Marino M, Maifreni M, Baggio A, Innocente N. Inactivation of foodborne bacteria biofilms by aqueous and gaseous ozone. Front Microbiol 2018;9:2024.
Miao H, Jierong C. Inactivation of Escherichia coli and properties of medical poly(vinyl chloride) in remote-oxygen plasma. Appl Surf Sci 2009;255:5690–7.
Mills D, Harnish DA, Lawrence C, Sandoval-Powers M, Heimbuch BK. Ultraviolet germicidal irradiation of influenza-contaminated N95 filtering facepiece respirators. Am J Infect Control 2018;46:e49–55.
Mutalik SD, Inamdar AC. Mask-induced psoriasis lesions as Köebner phenomenon during COVID-19 pandemic. Dermatol Ther 2020;33:e14323.
Ng K, Poon BH, Kiat Puar TH, Shan Quah JL, Loh WJ, Wong YJ, et al. COVID-19 and the risk to health care workers: a case report. Ann Intern Med 2020;172:766–7.
Osaili TM, Hasan F, Dhanasekaran DK, Obaid RS, Al-Nabulsi AA, Rao S, et al. Thermal inactivation of Escherichia coli O157:H7 strains and Salmonella spp. in camel meat burgers. LWT 2020;120.
Ou Q, Pei C, Kim SC, Belani K, Faizer R, Bischof J, et al. COVID-19 pandemic—decontamination of respirators and masks for the general public, health care workers, and hospital environments. Anesthesia Patient Saf Foundation 2020;35:33–68.
Porto E, Alves Filho EG, Silva LMA, Fonteles TV, do Nascimento RBR, Fernandes FAN, et al. Ozone and plasma processing effect on green coconut water. Food Res Int 2020;131.
Revai K, Mamidi D, Chonmaitree T. Association of nasopharyngeal bacterial colonization during upper respiratory tract infection and the development of acute otitis media. Clin Infect Dis 2008;46:e34–7.
Sainz-García A, González-Marcos A, Múgica-Vidal R, Muro-Fraguas I, Escribano–Viana R, González-Arenzana L, et al. Application of atmospheric pressure cold plasma to sanitize oak wine barrels. LWT 2021;139.
Sangkham S. Face mask and medical waste disposal during the novel COVID-19 pandemic in Asia. Case Stud Chem Environ Eng 2020;2.
Scholtz V, Pazlarová J, Soušková H, Khun J, Julák J. Nonthermal plasma - a tool for decontamination and disinfection. Biotechnol Adv 2015;33:1108–19.
Šimončicová J, Kaliňáková B, Kováčik D, Medvecká V, Lakatoš B, Kryštofová S, et al. Cold plasma treatment triggers antioxidative defense system and induces changes in hyphal surface and subcellular structures of Aspergillus flavus. Appl Microbiol Biotechnol 2018;102:6647–58.
Smith JS, Hanseler H, Welle J, Rattray R, Campbell M, et al. 2020;3:7.
Suess T, Remschmidt C, Schink SB, Schweiger B, Nitsche A, Schroeder K, et al. The role of facemasks and hand hygiene in the prevention of influenza transmission in households: results from a cluster randomised trial; Berlin, Germany, 2009–2011. BMC Infect Dis 2012;12:26.
Sun KL, Chang JM. Special types of folliculitis which should be differentiated from acne. Dermatoendocrinol 2017;9.
Surowsky B, Fröhling A, Gottschalk N, Schlüter O, Knorr D. Impact of cold plasma on Citrobacter freundii in apple juice: inactivation kinetics and mechanisms. Int J Food Microbiol 2014;174:63–71.
Viscusi DJ, Bergman MS, Eimer BC, Shaffer RE. Evaluation of five decontamination methods for filtering facepiece respirators. Ann Occup Hyg 2009;53:815–27.
Wei J, Guo S, Long E, Zhang L, Shu B, Guo L. Why does the spread of COVID-19 vary greatly in different countries? Revealing the efficacy of face masks in epidemic prevention. Epidemiol Infect 2021;149:e24.
Wen G, Liang Z, Xu X, Cao R, Wan Q, Ji G, et al. Inactivation of fungal spores in water using ozone: kinetics, influencing factors and mechanisms. Water Res 2020;185.
Wiegand C, Beier O, Horn K, Pfuch A, Tölke T, Hipler UC, et al. Antimicrobial impact of cold atmospheric pressure plasma on medical critical yeasts and bacteria cultures. Skin Pharmacol Physiol 2014;27:25–35.
Wigginton KR, Arts PJ, Clack HL, Fitzsimmons WJ, Gamba M, Harrison KR, et al. Validation of N95 filtering facepiece respirator decontamination methods available at a large University Hospital. Open Forum Infect Dis 2021;8:ofaa610.
Wu S, Zhang Q, Ma R, Yu S, Wang K, Zhang J, et al. Reactive radical-driven bacterial inactivation by hydrogen-peroxide-enhanced plasma-activated-water. Eur Phys J Spec Top 2017;226:2887–99.
Yong HI, Kim HJ, Park S, Kim K, Choe W, Yoo SJ, et al. Pathogen inactivation and quality changes in sliced cheddar cheese treated using flexible thin-layer dielectric barrier discharge plasma. Food Res Int 2015;69:57–63.
Zhang Q, Ma R, Tian Y, Su B, Wang K, Yu S, et al. Sterilization efficiency of a novel electrochemical disinfectant against Staphylococcus aureus. Environ Sci Technol 2016;50:3184–92.
Zulauf KE, Green AB, Nguyen Ba ANN, Jagdish T, Reif D, Seeley R, et al. Microwave–generated steam decontamination of N95 respirators utilizing universally accessible materials. mBio 2020;11:1–9.

4.2. DESINFECCIÓN MICROBIANA Y DESCONTAMINACIÓN QUÍMICA MEDIANTE PLASMA ATMOSFÉRICO FRÍO EN LA INDUSTRIA ALIMENTARIA

- Plasma Activated Water for wine barrels disinfection. Ana Sainz-García, Ana González-Marcos, Ignacio Muro-Fraguas, Rodolfo Múgica-Vidal, Félix Gallarta-González, Lucía González-Arenzana, Isabel López-Alfaro, Pilar Santamaría, Rocío Escribano-Viana, Fernando Alba-Elías, Elisa Sainz-García. LWT - Food Science and Technology 198 (2024) 116024.

En este estudio se utilizó PAW con el fin de eliminar *B. bruxellensis* presente en duelas de madera contaminados naturalmente. El objetivo fue limpiar y desinfectar barricas de vino empleadas en la etapa del envejecimiento del mismo para poder reutilizarlas y aprovechar las características identificativas de cada vino que le aporta dicho proceso. Se generaron cuatro PAW con tiempos de generación desde los 1,5 min hasta los 30 min. El tratamiento consistió en sumergir fragmentos de duelas de madera durante 3 h en cada una de estas PAW. La PAW-5 min logró una reducción de 3,49 unidades logarítmicas de *B. bruxellensis* y las PAW de 15 min y 30 min consiguieron la inactivación total de la levadura. Se estudiaron las características físico-químicas de cada una de las PAW y se relacionaron con los resultados de la capacidad biocida de cada PAW. Así, la capacidad biocida podría verse afectada por un efecto sinérgico de las especies reactivas identificadas (OH•, NO• y NO_2•, entre otras).

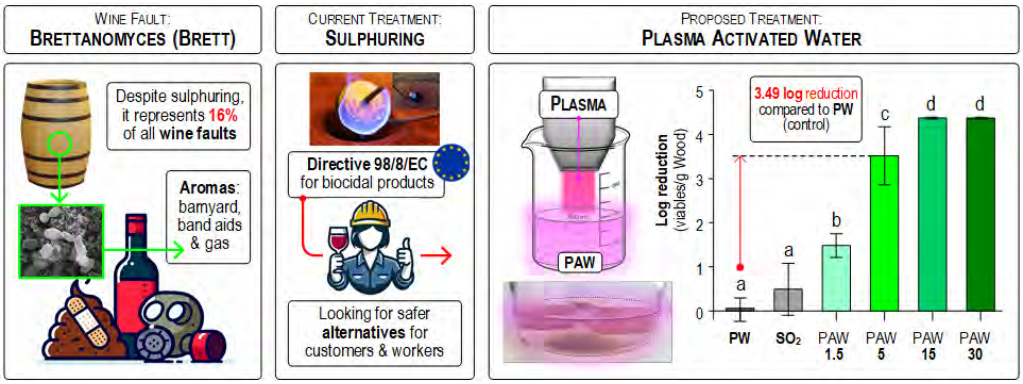

Fig. 19. Resumen gráfico del artículo III.

LWT - Food Science and Technology 198 (2024) 116024

Contents lists available at ScienceDirect

LWT

journal homepage: www.elsevier.com/locate/lwt

Plasma Activated Water for wine barrels disinfection

Ana Sainz-García [a], Ana González-Marcos [a], Ignacio Muro-Fraguas [a], Rodolfo Múgica-Vidal [a], Félix Gallarta-González [b], Lucía González-Arenzana [c], Isabel López-Alfaro [c], Pilar Santamaría [c], Rocío Escribano-Viana [c], Fernando Alba-Elías [a,*], Elisa Sainz-García [a]

[a] Department of Mechanical Engineering. University of La Rioja, C/ San José de Calasanz 31, 26004, Logroño, La Rioja, Spain
[b] Department of Chemistry. University of La Rioja, C/ Madre de Dios 51, 26006, Logroño, La Rioja, Spain
[c] Institute of Grapevine and Wine Sciences (Government of La Rioja, University of La Rioja, CSIC), Finca La Grajera, Ctra. De Burgos, LO-20, Km. 6, Salida 13, 26007, Logroño, Spain

ARTICLE INFO

Keywords:
Brettanomyces bruxellensis
Plasma activated water
Oak barrel
Wine
RONS

ABSTRACT

Barrel aging is crucial for the production of high-quality wines, with barrel reuse playing a key role in this process. Therefore, disinfecting and cleaning barrels are vital to prevent health and safety issues, being *B. bruxellensis* one of the most extended problems. In this study, naturally contaminated oak barrels with *B. bruxellensis* were immersed during 3 h in four Plasma Activated Water (PAW) generated for 1.5 min, 5 min, 15 min and 30 min. The presence of secondary radicals (OH•, NO•, NO_2•) was observed after HPLC and spectrometry analysis. The results suggested that those reactive species played an important role in the inactivation of *B. bruxellensis*. PAW_5 (generated during 5 min), which achieved a reduction of 3.49 ± 0.83 logarithmic units in *B. bruxellensis* population, was chosen as the best one in terms of economic and time consumption. Thus, an ecofriendly, sustainable and inexpensive solution was presented to inactivate *B. bruxellensis* from wine barrels.

1. Introduction

According to experts, the Spanish wine market has increased by almost 5% during the past years (Español, 2022). This fact has caused the demand for quality wines to increase, thus motivating the improvement of manufacturing conditions, food security and safety in the industry.

Aging is one of the most important steps when producing high quality wines. The use of oak wood barrels gives personality to the specific wine. Broadly speaking, during aging different processes and reactions take place giving physical and chemical stability to wines. Furthermore, since the complexity and delicacy of wines are reached, their personal aromas and taste are enriched (González-Arenzana et al., 2019). Regarding aging barrels, a differentiation between new and used ones should be done. Although, in the first case, malolactic fermentation and changes in tannins, pigments and polysaccharides are promoted, used barrels develop the volatile acidity of wines (Tomás, 2016, pp. 2013–2014). It is also worth mentioning some aspects derived from the aging of wine, such as the economic costs involved in the investment in new barrels, their limited lifespan or their cleaning (García-Alcaraz et al., 2020).

Despite the fact that barrel reusing is a recommendable practice, it is essential to be vigilant about the microbiological contamination that could arise in wooden barrels. The porous structure of wood facilitates the penetration of wine up to 8 mm, thus causing microbial contamination in crevices and cracks of the staves by different types of microorganisms such as lactic acid bacteria (LAB), acetic acid bacteria (AAB) and *Brettanomyces bruxellensis* (*B. bruxellensis*) (Bartowsky & Henschke, 2008; Costantini, Cersosimo, Del Prete, & Garcia-Moruno, 2006; Suárez, Suárez-Lepe, Morata, & Calderón, 2007). Furthermore, the latter is identified as the major cause of yeast contamination in wines and has increased in the last years because of changes in winemaking practices including the increment of sugar in wines, the decrease of sulfiting and filtering processes and the long-time aging inside barrels (Alston, Fuller, Lapsley, & Soleas, 2018; Mira de Orduña, 2010). During the International Wine Challenge of 2008, it was determined in 16% the total wine

* Corresponding author.
E-mail addresses: ana.sainz@unirioja.es (A. Sainz-García), ana.gonzalez@unirioja.es (A. González-Marcos), ignacio.muro@unirioja.es (I. Muro-Fraguas), rodolfo.mugica@unirioja.es (R. Múgica-Vidal), felix.gallarta@unirioja.es (F. Gallarta-González), lucia.gonzalez@unirioja.es (L. González-Arenzana), isabel.lopez@unirioja.es (I. López-Alfaro), psantamaria@larioja.org (P. Santamaría), roescrv@unirioja.es (R. Escribano-Viana), fernando.alba@unirioja.es (F. Alba-Elías), elisa.sainzg@unirioja.es (E. Sainz-García).

https://doi.org/10.1016/j.lwt.2024.116024
Received 23 January 2024; Received in revised form 26 March 2024; Accepted 29 March 2024
Available online 30 March 2024

faults. However, it is difficult to estimate the total litters of discarded wine due to *B. bruxellensis* spoilage (Compounds, 2008).

One of the most prominent outcomes associated with that yeast is the so-called "Brett" character, including off-aromas such as wet wool, burn plastic, horse sweat, medicinal and mousy (Licker, Acree, & Henick-Kling, 1998). This yeast is difficult to eliminate due to its ability of resisting the characteristics of wine such as low pH and oxygen, assimilable nitrogen concentrations and high ethanol concentrations (Curtin, Varela, & Borneman, 2015).

Regarding the most commonly used methods for cleaning and disinfecting wine barrels, a review carried out by Velasco (2012) encompasses some of them. They can be categorized in two groups: chemical and physical. Within the first one, sulfur dioxide (known as sulfuring) is the most widespread method and it is available in liquid, gas or solid pills. Since there is a controversy over the use of sulfuring, the European Commission proposed the prohibition of this technique (Europea, 1998); however, it is still legal. Nonetheless, in order to prevent negative sensorial characteristics in wines (residual sulfites, undesirable compounds generation or unfavorable interactions with wood barrels) and health problems among workers (allergic, skin and respiratory diseases), there is a need of looking for alternatives. They include the use of oxidizing agents (chlorinate oxidants), hydrogen peroxide, sodium percarbonate, permanganate and ozone. Among the physical treatments, hot water (80–90 °C) is the most popular technique. Additionally, water vapor at 105 °C, electromagnetic treatment by microwaves, ultrasounds, dry ice and negative oxygen are employed (Velasco, 2012). Despite the fact that these methods are widely used in wineries, they have some disadvantages: [1] potential alteration of wood composition; [2] low thermal conductivity of wood necessitating long treatment times; [3] high cost and time consumption; [4] final products that may be toxic to consumers and [5] inadequate penetration through the wood resulting in treatments that are only superficially effective for cleaning and disinfecting barrels (Costantini et al., 2006; Velasco, 2012).

Plasma Activated Water (PAW) is generated when Atmospheric Pressure Cold Plasma (APCP) transfers energy and some chemical reactivity from gas to water (Zhou et al., 2020). This technology has been recognized as one of the most sustainable and economic technologies, since PAW is generated just with water and electricity and any waste is produced. PAW has been proven to be useful, obtaining good results in several applications like the inactivation of microorganisms, the improvement of seed germination or the treatment of cancer cells, among others (Zhou et al., 2020). Despite the presence of reactive species (e.g., positive and negative electrons, molecules and ultraviolet photons or neutral and excited atoms) the potential applications of PAW are attributed to the activity of reactive oxygen species (ROS) and reactive nitrogen species (RNS) (Iuchi et al., 2018; Scholtz, Pazlarova, Souskova, Khun, & Julak, 2015).

Considering all the above, PAW could be a solution for wine barrels disinfection, enabling their reuse without sanitary problems. Therefore, the aim of the present study was to verify the effectiveness of PAW technology to inactivate *Brettanomyces bruxellensis* in naturally contaminated wine barrels and to propose this technology as a sustainable and efficient alternative to the technologies that are currently employed for cleaning and disinfecting wine barrels.

2. Materials and methods

2.1. Staves samples

Staves were obtained from oak wood barrels employed in the production of aged wine that were naturally contaminated with *B. bruxellensis*. The samples of this study consisted in portions of 5 × 5 cm that were cut from the staves. In order to determine the level of *B. bruxellensis* viable population in the wood, three portions of staves were analyzed following the protocols described in section 2.4.

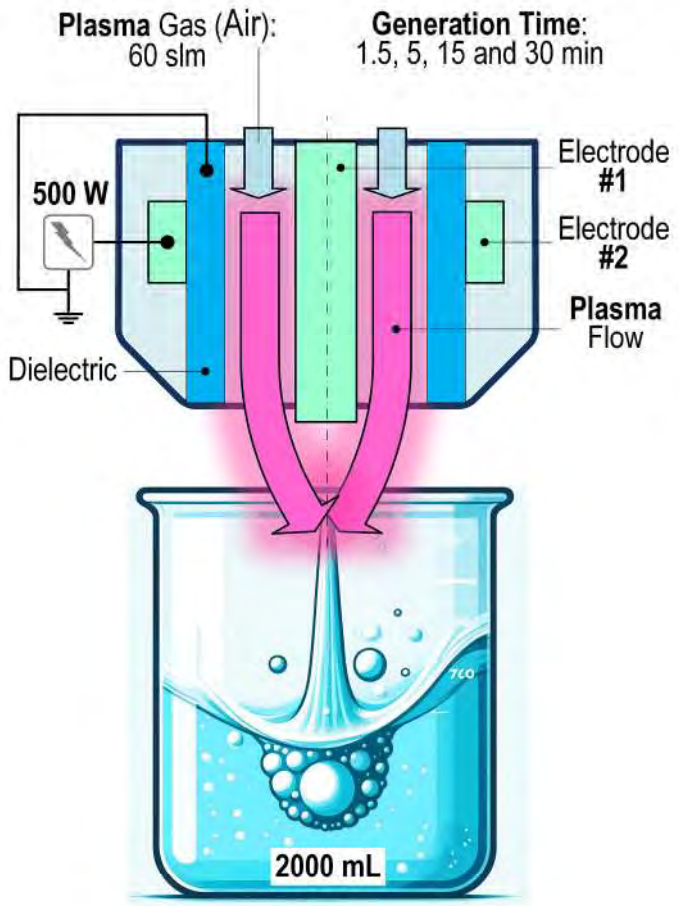

Fig. 1. PAW generation system and detail of the plasma-water interaction.

2.2. Preparation of PAW solutions

The APCP equipment employed in this study was the PlasmaSpot500 (Molecular Plasma Group, Foetz, Luxemburg). It comprises two cylindrical electrodes with an aluminum oxide dielectric tube between them. The internal electrode is grounded and the external one is connected to a high voltage source.

PAW was produced by exposing 2000 mL of purified water (PW) to the plasma jet, as shown in Fig. 1. Four different PAW were generated varying the generation time: 1.5, 5, 15 and 30 min, resulting in samples labeled as PAW_1.5, PAW_5, PAW_15 and PAW_30, respectively. For all treatments, air at 60 slm was used as plasma gas and the plasma power was set at 500 W. The distance between the PW surface and the end of the plasma nozzle remained consistently at 30 mm.

The four PAW used in this study were previously investigated in Sainz-García et al. (2023) for chemical decontamination, specifically to decompose TCA from corks. On the other hand, the present work examines the effectiveness of those PAW to decontaminate oak barrels from *B. bruxellensis*.

2.3. Characterization of physicochemical properties of PAW

The physicochemical parameters of PAW at room temperature were measured after PAW generation using different methods, as described in Sainz-García et al. (2023). A portable multimeter sensION MM150 DL with a 50 48 probe (Hach Company, United States of America) was used for oxidation-reduction potential (ORP), electrical conductivity (EC) and pH measurements. For nitrate (NO_3^-) quantification a portable Imacimus® MultiIon analyser (NTsensors S.L., Spain) was required. Nitrite (NO_2^-) concentrations were measured through colorimetric

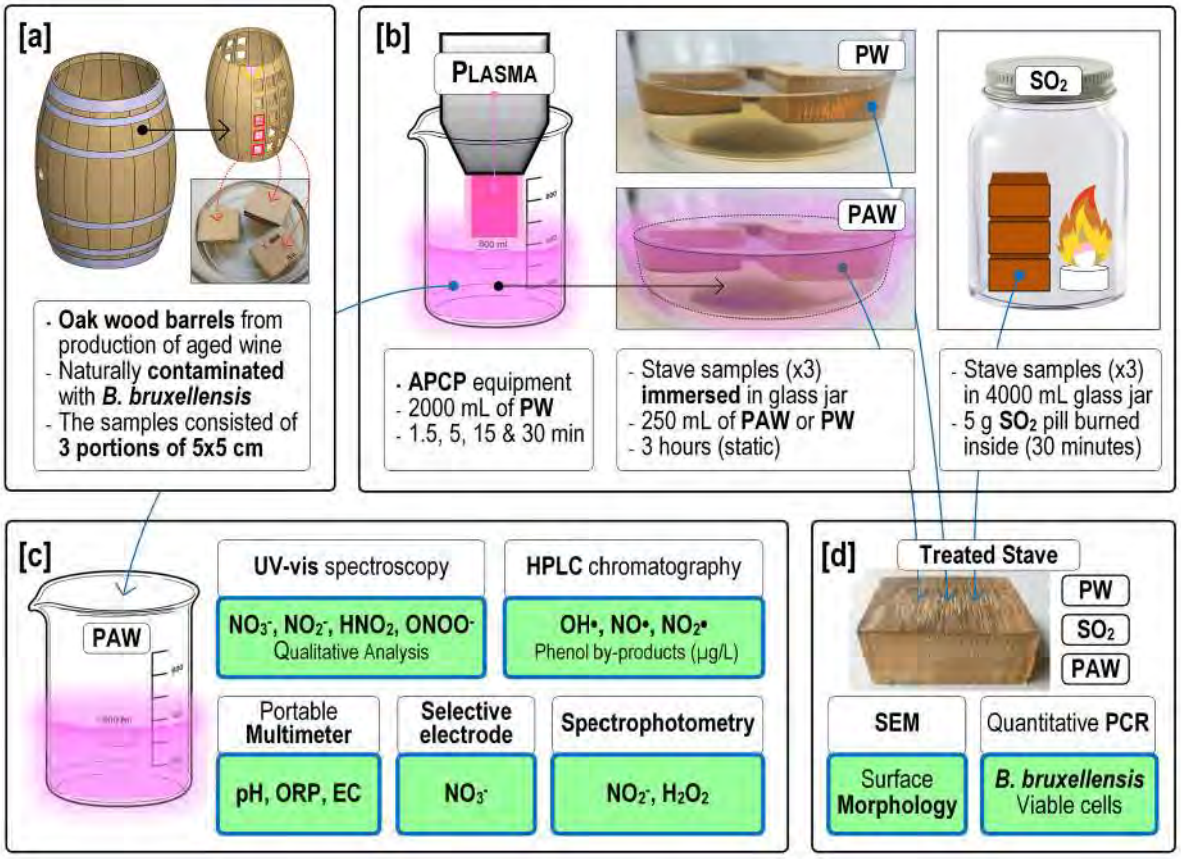

Fig. 2. Scheme of the samples treatment process: [a] Wood samples from oak barrels, [b] PAW generation and samples decontamination with PW, PAW and SO_2 and [c] and [d] PAW and sample characterization.

Griess assay by spectrophotometry. This technique is based on determining nitrites after their reaction with sulfanilic acid in low pH forming diazonium ion. This ion combines with α-naphthylamine to form a magenta dye which can be identified and quantified at 548 nm (Jablonowski & von Woedtke, 2015). Hydrogen peroxide (H_2O_2) concentration was determined by spectrophotometry at 407 nm measuring the absorbance of titanium peroxide. For all photometric measurements, an Onda V-11 SCAN spectrophotometer (Giorgio Bormac s.r.l., Italy) was used. For these tests, Titanium (IV) oxysulfate and Griess reagent were purchased from Sigma Aldrich (USA).

In order to confirm the presence of secondary reactive oxygen and nitrogen species (RONS), HPLC analyses were performed. This method was based on the reaction between OH•, NO• and NO_2• with phenol (C_6H_5-OH) (Lukes, Dolezalova, Sisrova, & Clupek, 2014). Specifically, OH• reacts with phenol to produce benzoquinone, NO• with phenol generates 4-nitrosophenol, and the reaction of NO_2• with phenol yields 2-nitrophenol. The concentrations of the phenol by-products were determined using a HPLC system with UV detection (Agilent 1100 Series, Agilent Technologies, Spain). The analysis was performed following the procedure explained in Sainz-García et al. (2023). Phenol degradation by-products were quantified using calibration curves prepared from known concentrations of benzoquinone (Sigma Aldrich, USA) ($2.05{\cdot}10^{-4}$ M), 4-nitrosophenol (TCI Chemicals, Japan) ($1.52{\cdot}10^{-3}$ M) and 2-nitrophenol (Sigma Aldrich, USA) ($2.11{\cdot}10^{-3}$ M). Typical calibration curves are: benzoquinone: A (mAU) = $0.09 + 6.99{\cdot}10^{5}$ c (M) (from $2{\cdot}10^{-6}$ to $4{\cdot}10^{-5}$ M); 2-nitrophenol: A (mAU) = $-0.24 + 1.50{\cdot}10^{5}$ c (M) (from $2{\cdot}10^{-5}$ to $4{\cdot}10^{-4}$ M); 4-nitrosophenol: A (mAU) = $-1.00 + 3.78{\cdot}10^{5}$ c (M) (from $1{\cdot}10^{-5}$ to $3{\cdot}10^{-4}$ M).

Moreover, UV–vis spectroscopy (Agilent 8453 UV–visible Spectrophotometer) was used to identify the presence of other reactive species in PAW. Particularly, the range from 280 nm to 400 nm was studied. Within this wavelength range, it is possible to identify species such as nitrates, nitrites, nitrous acid or peroxynitrites.

2.4. Plasma activated water and control treatments

For PAW and PW treatments, three contaminated samples were immersed in 500 mL of each liquid during 3 h (Fig. 2[b]). Regarding sulfur dioxide (SO_2) treatment, a 4000 mL glass jar was filled with three contaminated samples. Then, a 5 g sulfur pill was burned inside and finally, the jar was closed during 30 min (Fig. 2[b]). SO_2 and PW treatments were used as controls.

2.5. Quantification of the viable B. bruxellensis population

The initial average contamination level of *B. bruxellensis* for the naturally contaminated barrels was 4.35 ± 0.26 logarithmic units of viable cells per gram of wood.

Once the treatments with PAW, PW and SO_2 were carried out, the samples were brushed with an automatic wood planer reaching a depth of 1 cm. The chips from each treatment were collected in sterile plastic bags and their weight was recorded. Subsequently, 600 mL of sterile Trypticasein Soy Broth (TSB, Conda, Madrid, Spain) recovering medium was added and the sealed bags were incubated at 28 °C in an orbital shaker at 100 rpm for 24 h. After incubation, the liquid was recovered and centrifuged (4 °C, 30 min, 10000 g). The pellet obtained was resuspended in Ringer's solution making up to a volume of 15 ml in sterile plastic tubes.

In order to quantify the viable population of *B. bruxellensis* present in wood, the samples obtained were sent for analysis to the Excell Ibérica laboratories (Logroño, Spain). Viable *B. bruxellensis* cells were analyzed by quantitative PCR with Eva Green®. Previously, samples were treated

Table 1
Physicochemical properties of PAW and PW.

Sample	PW	PAW_1.5	PAW_5	PAW_15	PAW_30
pH	7.00 ± 0.05	4.46 ± 0.15	4.01 ± 0.17	3.58 ± 0.09	3.10 ± 0.12
Electrical Conductivity (μS/cm)	2 ± 0.5	25 ± 5	52 ± 7	103 ± 13	190 ± 15
Oxidation Reduction Potential (mV)	250 ± 10	315 ± 13	355 ± 10	383 ± 9	408 ± 21
Nitrates (mg/L)	0.00	3.67 ± 0.31	4.13 ± 0.15	9.90 ± 1.30	17.90 ± 2.05
Nitrites (mg/L)	0.00	0.74 ± 0.05	2.58 ± 0.27	3.47 ± 0.13	5.01 ± 0.87

with propidium monoazide (PMA™, Biotium, Fremont, CA) and subjected to a protocol for DNA extraction.

2.6. Morphological characterization

A COXEM EM-30N Scanning Electron Microscope (SEM) operating at 10 kV was used to analyze the surface morphology of the treated and untreated samples. For this purpose, portions of 0.5 × 0.5 cm were obtained from the 5 × 5 cm wood samples. Sample surfaces were coated with a thin layer of gold using a plasma sputtering apparatus before SEM examination to make them conductive.

2.7. Statistical analysis

Experiments were conducted in triplicate. An ANOVA was performed to determine if the reduction of *B. bruxellensis* among the various treatments and the control exhibited significant differences. If the results of this test indicated statistically significant differences, post hoc comparisons were conducted using Fisher's LSD test between each pair of groups to identify specific treatment variations. The significance level (alpha) was set at 0.05. All analyses were executed using Statgraphics Centurion software (v19, The Plains, USA).

3. Results and discussion

3.1. PAW characterization

The physicochemical attributes of the different PAW are shown in Table 1.

Regarding pH, after 1.5 min of plasma exposure, the pH of PAW_1.5 decreased from 7.00 to 4.46 ± 0.15 and further declined to 3.10 ± 0.12 after 30 min of treatment (PAW_30). On the other hand, a progressive linear rise in EC was noted when increasing the generation time. Thereby, EC rose from 5 μS/cm to 25 ± 5 μS/cm after 1.5 min of treatment and further increased to 190 ± 15 μS/cm after 30 min. The same trend was observed for ORP measurements, increasing from 315 ± 13 mV to 408 ± 21 mV for 1.5 and 30 min of PAW generation time, respectively. Regarding the chemical analysis of nitrates and nitrites, there was a significant rise in the concentration of both species with the plasma activation time. Consequently, the concentration values increased achieving 17.90 ± 2.05 mg/L (NO_3-) and 5.01 ± 0.87 mg/L (NO_2-) for PAW_30. H_2O_2 was also measured, however, it was not detected regardless the PAW studied. It is hypothesized that when an excess of NO_2- is present, H_2O_2 undergoes complete reaction to generate peroxynitrite.

The changes in the values of all of those parameters are mostly due to the formation of active ions and oxidizing species (e.g. NO_2-, H+, NO_3-) during the generation of PAW.

All of these facts are in good agreement with the work done by Rathore, Patel, Butani, & Nema (2021) where significant raises in EC and ORP, as well as a pH reduction, were observed as the plasma activation time increased (Rathore et al., 2021). Furthermore, similar findings have been reached by other researchers (El Shaer et al., 2020; Pan et al., 2017; Zhang et al., 2016).

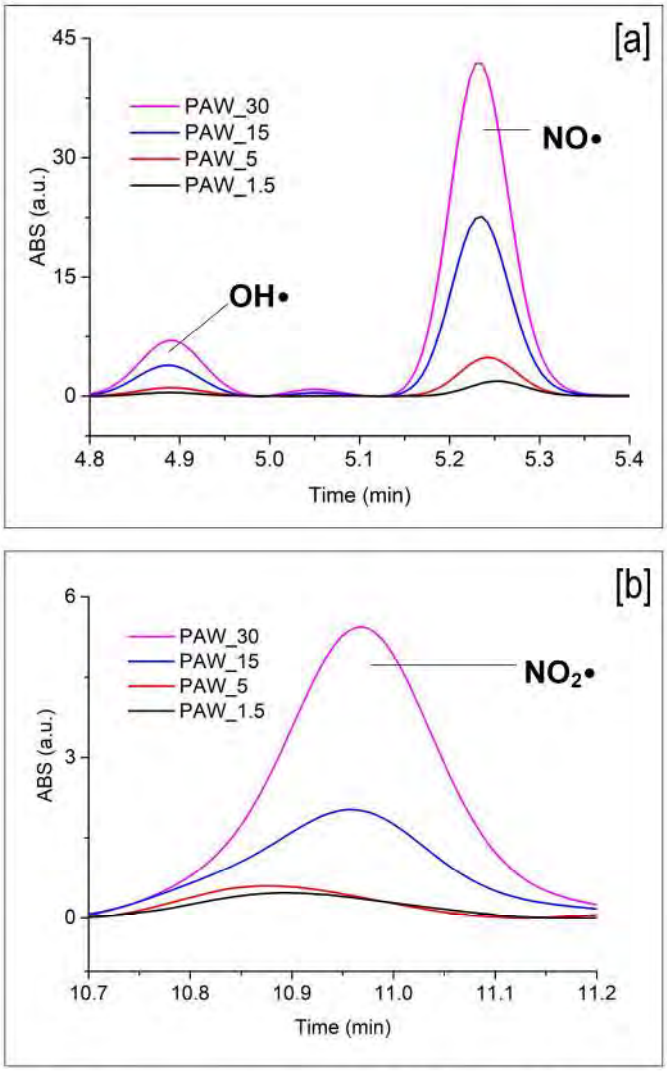

Fig. 3. HPLC chromatogram for each PAW: [a] OH• and NO• peaks; [b] NO_2• peak.

Table 2
Quantification of phenol by-products.

Phenol by-product concentration (μg/L)	PAW			
	PAW_1.5	PAW_5	PAW_15	PAW_30
OH• (benzoquinone)	8.2	23.1	91.7	168.1
NO• (4-nitrosophenol)	227.0	465.1	1873.0	3404.8
NO_2• (2-nitrophenol)	209.5	253.9	696.1	1729.6

In order to ascertain if PAW contained other secondary reactive species, HPLC analyses were conducted. The presence of OH•, NO• and NO_2• was evaluated through the detection of the phenol degradation by-products. Fig. 3 shows the HPLC chromatograms for each PAW.

Table 2 presents the phenol by-products concentrations for each PAW analyzed. These concentrations give an idea about the values of the reactive species that react with phenol to generate each phenol by-product (OH•, NO• and NO_2•). Regarding benzoquinone, it was reached 8.2 μg/L in PAW_1.5, increasing up to 168.1 μg/L in PAW_30. On the other hand, the concentration of 4-nitrosophenol was 227.0 μg/L in PAW_1.5 in comparison to the 3404.8 μg/L in PAW_30. Finally, the 2-

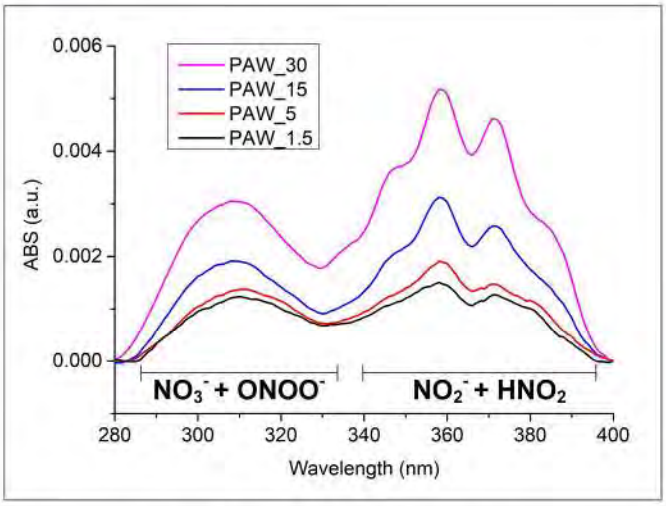

Fig. 4. UV–vis spectrum of each PAW.

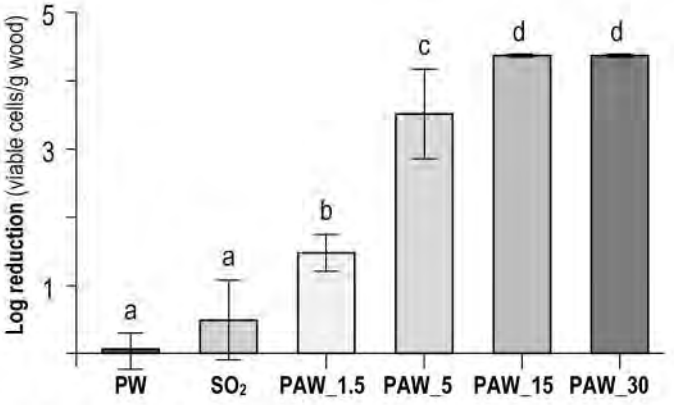

Fig. 5. Reduction of *B. bruxellensis* in wood samples after 3 h of contact with PW, SO_2 and PAW treatments. Different letters indicate statistically significant differences ($p < 0.05$).

nitrophenol concentrations ranged from 209.5 μg/L to 1729.6 μg/L when the plasma activation time increased from 1.5 to 30 min. In this respect, some authors argue that these radicals may play a key role in bacteria inactivation, but very few researchers have worked on the detection and quantification of these reactive species in PAW. For instance, Tarabová et al. (2018) found phenol by-products of these three radicals after HPLC analysis suggesting an evidence of the presence of OH•, NO• and NO_2•(Tarabová et al., 2018). Moreover, Akiyama and Heller (2017) and Lukes et al. (2014) suggested some cyclic reactions through which these three radicals are generated:

$$NO_2^- + H^+ \leftrightarrow HNO_2 \quad [a]$$

$$2\,HNO_2 \rightarrow \mathbf{NO}\bullet + \mathbf{NO_2}\bullet + H_2O \quad [b]$$

$$2\,\mathbf{NO_2}\bullet + H_2O \rightarrow NO_3^- + NO_2^- + 2\,H^+ \quad [c]$$

$$4\,\mathbf{NO}\bullet + O_2 + 2\,H_2O \rightarrow 4\,NO_2^- + 4\,H^+ \quad [d]$$

$$4\,\mathbf{NO_2}\bullet + O_2 + 2\,H_2O \rightarrow 4\,NO_3^- + 4\,H^+ \quad [e]$$

$$NO_2^- + H_2O_2 + H^+ \rightarrow O{=}NOOH + H_2O \quad [f]$$

$$O{=}NOOH \rightarrow \mathbf{OH}\bullet + \mathbf{NO_2}\bullet \quad [g]$$

Thus, NO_2- are unstable at low pH and react with HNO_2 via reaction [b] generating nitric oxide radical (NO•) and nitrogen dioxide radical (NO_2•). A hydrolysis of NO_2• takes part to produce NO_2- and NO_3- (reaction [c]). Moreover, the secondary radicals NO• and NO_2•, which are known as "acidified nitrites" (Machala et al., 2013), can react with dissolved oxygen to form NO_2^- and NO_3^-, respectively (reactions [d] and [e]). Finally, via reaction [g] peroxynitrite is transformed into OH• and NO_2•.

Moreover, UV–vis spectroscopy was used to identify the presence of other reactive species in PAW. Specifically, the range from 280 nm to 400 nm was studied. Fig. 4 shows the spectrum of each PAW analyzed. Thus, the spectrum of PAW_30 showed the highest values of absorbance, followed by PAW_15, PAW_5 and PAW_1.5. It is worth mentioning the characteristic group of five peaks between 330 nm and 395 nm that several researchers have associated with an overlapping that is caused by HNO_2 and NO_2^- (Jung et al., 2015; Ki et al., 2020; K. Liu, Liu, & Ran, 2020; Methods, 2009; Yost & Joshi, 2015). These peaks could be an indication of the presence of "acidified nitrites" as reactions [a] and [b] show. The additional overlap occurring at around 302 nm is also noteworthy and involves the presence of NO_3^- and peroxynitrite (Brisset & Pawlat, 2016; K. Liu et al., 2020).

3.2. *Brettanomyces bruxellensis* inactivation by PAW

Fig. 5 illustrates the reduction of the *B. bruxellensis* population after 3 h immersed in each PAW and control (PW and SO_2). Almost no reduction was observed in any of the controls used in this study (PW or SO_2 treatment). However, the population of *B. bruxellensis* was significantly reduced in the samples treated with PAW (statistically significant differences were found between each PAW treatment and each control). Specifically, a reduction of 1.46 ± 0.27 logarithmic units was achieved with PAW_1.5, whereas 3.49 ± 0.83 log reductions were achieved with PAW_5, and total inactivation (4.35 ± 0.00 log) was accomplished with PAW generated during 15 and 30 min. Regarding the PAW treatments, statistically significant differences were found between them, except in the case of PAW_15 and PAW_30. This fact is in good agreement with Guo et al. (2017) who observed higher *S. cerevisiae* inactivation from grapes when using PAW generated during the longest times of their study (30 and 60 min). Thus, 0.38 ± 0.17 and 0.53 ± 0.07 log CFU/mL reductions were achieved after 30 min of PAW/yeast contact. Tian et al. (2017) also obtained higher yeast reductions after their longest treatment time suggesting that the efficacy of PAW for microbial inactivation could be dependent on the PAW generation time.

Therefore, the physicochemical characteristics of each PAW played a key role to understand why the response of microorganisms was not the same with all PAW. As mentioned above, the longer the treatment time, the higher the OH•, NO• and NO_2• concentrations. Those reactive species, as well as peroxynitrite, are known to have strong antimicrobial activity (Akiyama & Heller, 2017; Bao, Lu, He, & Liu, 2016; Machala et al., 2013). They are capable of triggering oxidation and nitration reactions in biological cells such as peroxidation of lipids, proteins and DNA damage (Lukes et al., 2014; Shen et al., 2016; Thirumdas et al., 2018; Van Gils, Hofmann, Boekema, Brandenburg, & Bruggeman, 2013; Yost & Joshi, 2015). In this sense, other researchers suggested yeast death as a consequence of RONS affecting the oxidation-reduction state of antioxidants and causing membrane damage and cell structure disruption (Guo et al., 2017; Tian et al., 2017). Moreover, intrinsic ROS have been shown to increase after PAW treatment inside yeast cells provoking an over-accumulation that can cause oxidative stress and cell death (X. Liu et al., 2021; R. Zhang et al., 2020). Taken together, a possible pathway which ends up in cell death was suggested. The mechanism could be started by a lipid peroxidation in the cell membrane, followed by a rupture and damage of the cell membrane resulting in a leakage; then RONS could easily enter the cell and accumulate provoking a potential membrane shock and finally resulting in cell death (X. Liu et al., 2021).

There are other authors who studied the use of PAW for killing yeasts. Ryu et al. (2013), compared PAW with saline solution and observed their highest cell damage when treating *S. cerevisiae* with PAW

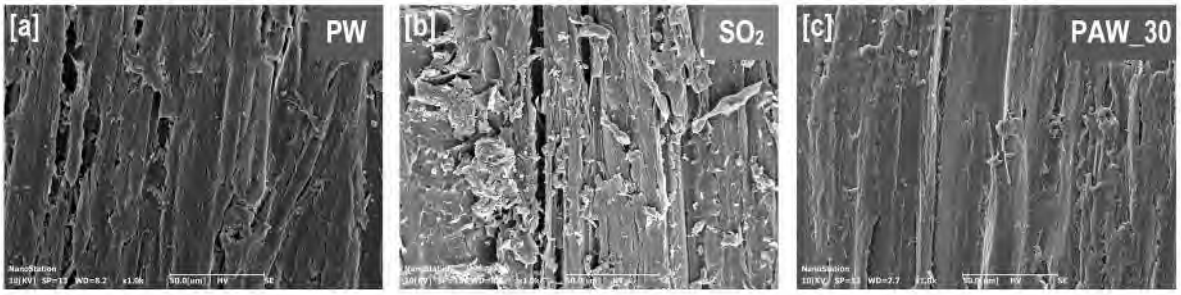

Fig. 6. SEM images of samples after: [a] PW treatment, [b] SO_2 treatment and [c] PAW_30 treatment.

during 120 s, achieving an inactivation of $2{\cdot}10^7$ cells/mL. Since PAW was the one with the top levels of reactive species, those authors suggested a crucial role of OH•. Moreover, 5.85 log CFU/g of *S. cerevisiae* inactivation in fresh grapes were reported (Xiang et al., 2020). Finally, *C. albicans* was also studied by Julák, Scholtz, Kotúčová, and Janoušková (2012) obtaining a complete inactivation ($1{\cdot}10^7$ CFU/mL) after 24 h incubation with PAW.

3.3. Morphological characterization

The morphology of the wooden surface was analyzed by SEM. Fig. 6 shows SEM images that were taken after treatment with PW, SO_2 and PAW_30.

On the one hand, comparing PAW_30 treatment and PW treatment no morphological differences were found. Thus, a smooth surface with well-defined fibers and wood vessels was observed after both treatments. On the other hand, a different structure was observed after SO_2 treatment. In this case, these features are characterized by an increase in wood roughness and by the presence of wood agglomerates, which are suggested to result from the chemical damage that sulfuring provokes in the structure of wood. Thereby, a breakage of wood occurs after SO_2 treatment, generating vessels and agglomerates of wooden debris.

To the best of our knowledge, there is no research where the wooden surface morphology has been studied after PAW treatment. However, there are several works focused on the topography of wood after direct plasma treatment. Sainz-García et al. (2021, p. 139) observed no changes in oak morphology after 12-passes treatment with 500 W and three different plasma gases (air, nitrogen and argon). Moreover, Asandulesa, Topala, and Dumitrascu (2010) showed no alterations in the appearance of either oak or beech following 5 s helium plasma treatment. Similar findings were found by Novák et al. (2015) who treated beech wood during 120 s with air plasma and observed no significant differences in size and shape of vessel, fibrils and holes between the pristine sample and the treated sample.

4. Conclusions

We have investigated PAW as a sustainable and inexpensive technology to reuse wine wooden barrels during wine aging, preventing health issues and economic waste. It was demonstrated that the longer the PAW generation time, the higher the *B. bruxellensis* inactivation achieved. Furthermore, the implication of specific reactive species when inactivating this yeast was studied. OH•, NO•, NO_2• were proposed as the reactive species that play the main role when attacking microorganisms. Then, several pathways for their formation were shown. Thus, an increase in the concentration of RONS was observed as the PAW generation time increased. Moreover, no negative morphological effects in the surface of wood samples were observed after PAW treatment, which suggested no reduction of the functional and bulk properties of the oak wood.

Finally, PAW generated during 5 min (PAW_5) and 3 h of PAW/wood contact was selected as the best treatment in terms of economic and time costs since it achieved 3.23 log reductions of *B. bruxellensis*. In conclusion, inactivating *B. bruxellensis* of oak wine barrels with PAW could be a real solution to reuse aging barrels while preventing health problems.

Within the frame of this work, the authors have found some limitations to solve in future researches. We are making effort to generate an effective RONS concentration in PAW in the shortest treatment time and to test different PAW generation configurations that improve the diffusion of RONS leading to a more effective PAW. Finally, a work regarding how this process would affect wine quality is being carried out.

Funding

This work was supported by MCIN/AEI/10.13039/501100011033 and the "European Union NextGenerationEU/PRTR" [grant numbers PID2019-105367RB-C21, PID2020-11365RB-C21 and PDC2022-133242-I00].

CRediT authorship contribution statement

Ana Sainz-García: Writing – review & editing, Writing – original draft, Visualization, Validation, Investigation, Formal analysis, Data curation, Conceptualization. **Ana González-Marcos:** Validation, Supervision, Project administration, Investigation, Funding acquisition, Data curation. **Ignacio Muro-Fraguas:** Writing – review & editing, Visualization, Investigation, Conceptualization. **Rodolfo Múgica-Vidal:** Writing – review & editing, Visualization, Investigation, Conceptualization. **Félix Gallarta-González:** Validation, Resources, Data curation. **Lucía González-Arenzana:** Writing – review & editing, Investigation, Data curation. **Isabel López-Alfaro:** Writing – review & editing, Resources, Investigation, Data curation. **Pilar Santamaría:** Resources, Data curation. **Rocío Escribano-Viana:** Writing – review & editing, Investigation, Data curation. **Fernando Alba-Elías:** Writing – review & editing, Visualization, Supervision, Project administration, Investigation, Funding acquisition, Formal analysis, Data curation, Conceptualization. **Elisa Sainz-García:** Writing – review & editing, Writing – original draft, Supervision, Investigation, Formal analysis, Data curation, Conceptualization.

Declaration of competing interest

The authors declare that they have no known competing financial interests or personal relationships that could have appeared to influence the work reported in this paper.

Data availability

Data will be made available on request.

Acknowledgements

The author Ana Sainz-García is thankful to the program of predoctoral contracts for the training of research staff funded by the

Spanish Ministry of Science and Innovation.

The author Ignacio Muro-Fraguas, thanks the program of post-doctoral orientation contracts for the training of research staff funded by the autonomous community of La Rioja.

The author Rocío Escribano-Viana as postdoctoral researcher of the University of La Rioja, thanks the postdoctoral training program funded by the Ministry of Universities.

References

Akiyama, H., & Heller, R. (2017). *Book-bioelectrics* 题目:生物电刺激.

Alston, J. M., Fuller, K. B., Lapsley, J. T., & Soleas, G. (2018). Too much of a good thing? Causes and consequences of increases in sugar content of California wine grapes. *World Scientific Handbook in Financial Economics Series, 6*(2), 135–163. https://doi.org/10.1142/9789813232747_0006

Asandulesa, M., Topala, I., & Dumitrascu, N. (2010). Effect of helium DBD plasma treatment on the surface of wood samples. *Holzforschung, 64*(2), 223–227. https://doi.org/10.1515/HF.2010.025

Bao, P., Lu, X., He, M., & Liu, D. (2016). Kinetic analysis of delivery of plasma reactive species into cells immersed in culture media. *IEEE Transactions on Plasma Science, 44*(11), 2673–2681. https://doi.org/10.1109/TPS.2016.2578955

Bartowsky, E. J., & Henschke, P. A. (2008). Acetic acid bacteria spoilage of bottled red wine-A review. *International Journal of Food Microbiology, 125*(1), 60–70. https://doi.org/10.1016/j.ijfoodmicro.2007.10.016

Brisset, J. L., & Pawlat, J. (2016). Chemical effects of air plasma species on aqueous solutes in direct and delayed exposure modes: Discharge, post-discharge and plasma activated water. *Plasma Chemistry and Plasma Processing, 36*(2), 355–381. https://doi.org/10.1007/s11090-015-9653-6

Compounds, S. (2008). *Production and sensory impact on wine*.

Costantini, A., Cersosimo, M., Del Prete, V., & Garcia-Moruno, E. (2006). Production of biogenic amines by lactic acid bacteria: Screening by PCR, thin-layer chromatography, and high-performance liquid chromatography of strains isolated from wine and must. *Journal of Food Protection, 69*(2), 391–396. https://doi.org/10.4315/0362-028X-69.2.391

Curtin, C., Varela, C., & Borneman, A. (2015). Harnessing improved understanding of Brettanomyces bruxellensis biology to mitigate the risk of wine spoilage. *Australian Journal of Grape and Wine Research, 21*, 680–692. https://doi.org/10.1111/ajgw.12200

El Shaer, M., Eldaly, M., Heikal, G., Sharaf, Y., Diab, H., Mobasher, M., et al. (2020). Antibiotics degradation and bacteria inactivation in water by cold atmospheric plasma discharges above and below water surface. *Plasma Chemistry and Plasma Processing, 40*(4), 971–983. https://doi.org/10.1007/s11090-020-10076-0

Español, O. (2022). *EXPORTACIONES españolas de VINO Y*.

Europea, U. (1998). Directiva 98/8/CE Relativa a la comercialización de biocidas. *Diario Oficial de Las Comunidades Europeas, 1–63*. Retrieved from https://www.boe.es/buscar/doc.php?id=DOUE-L-1998-80690.

García-Alcaraz, J. L., Flor Montalvo, F. J., Martínez Cámara, E., Pérez de la Parte, M. M., Jiménez-Macías, E., & Blanco-Fernández, J. (2020). Economic-environmental impact analysis of alternative systems for red wine ageing in re-used barrels. *Journal of Cleaner Production, 244*. https://doi.org/10.1016/j.jclepro.2019.118783

González-Arenzana, L., López-Alfaro, I., Gutiérrez, A. R., López, N., Santamaría, P., & López, R. (2019). Continuous pulsed electric field treatments' impact on the microbiota of red Tempranillo wines aged in oak barrels. *Food Bioscience, 27*(October 2018), 54–59. https://doi.org/10.1016/j.fbio.2018.10.012

Guo, J., Huang, K., Wang, X., Lyu, C., Yang, N., Li, Y., et al. (2017). Inactivation of yeast on grapes by plasma-activated water and its effects on quality attributes. *Journal of Food Protection, 80*(2), 225–230. https://doi.org/10.4315/0362-028X.JFP-16-116

Iuchi, K., Morisada, Y., Yoshino, Y., Himuro, T., Saito, Y., Murakami, T., et al. (2018). Cold atmospheric-pressure nitrogen plasma induces the production of reactive nitrogen species and cell death by increasing intracellular calcium in HEK293T cells. *Archives of Biochemistry and Biophysics, 654*, 136–145. https://doi.org/10.1016/j.abb.2018.07.015

Julák, J., Scholtz, V., Kotúčová, S., & Janoušková, O. (2012). The persistent microbicidal effect in water exposed to the corona discharge. *Physica Medica, 28*(3), 230–239. https://doi.org/10.1016/j.ejmp.2011.08.001

Jung, S., Kim, H. J., Park, S., Yong, H. I., Choe, J. H., Jeon, H. J., et al. (2015). Color developing capacity of plasma-treated water as a source of nitrite for meat curing. *Korean Journal for Food Science of Animal Resources, 35*(5), 703–706. https://doi.org/10.5851/kosfa.2015.35.5.703

Ki, S. H., Noh, H., Ahn, G. R., Kim, S. H., Kaushik, N. K., Choi, E. H., et al. (2020). Influence of nonthermal atmospheric plasma-activated water on the structural, optical, and biological properties of Aspergillus brasiliensis spores. *Applied Sciences, 10*(18). https://doi.org/10.3390/APP10186378

Licker, J. L., Acree, T. E., & Henick-Kling, T. (1998). What is "brett" (Brettanomyces) flavor?: A preliminary investigation. *ACS Symposium Series, 714*, 96–115. https://doi.org/10.1021/bk-1998-0714.ch008

Liu, X., Li, Y., Zhang, R., Huangfu, L., Du, G., & Xiang, Q. (2021). Inactivation effects and mechanisms of plasma-activated water combined with sodium laureth sulfate (SLES) against Saccharomyces cerevisiae. *Applied Microbiology and Biotechnology, 105*(7), 2855–2865. https://doi.org/10.1007/s00253-021-11227-9

Liu, K., Liu, S. T., & Ran, C. F. (2020). The effect of air-water-plasma-jet-activated water on penicillium: The reaction of HNO2 and H2O2 under acidic condition. *Frontiers in Physics, 8*(2), 1–12. https://doi.org/10.3389/fphy.2020.00242

Lukes, P., Dolezalova, E., Sisrova, I., & Clupek, M. (2014). Aqueous-phase chemistry and bactericidal effects from an air discharge plasma in contact with water: Evidence for the formation of peroxynitrite through a pseudo-second-order post-discharge reaction of H2O 2 and HNO2. *Plasma Sources Science and Technology, 23*(1). https://doi.org/10.1088/0963-0252/23/1/015019

Machala, Z., Tarabova, B., Hensel, K., Spetlikova, E., Sikurova, L., & Lukes, P. (2013). Formation of ROS and RNS in water electro-sprayed through transient spark discharge in air and their bactericidal effects. *Plasma Processes and Polymers, 10*(7), 649–659. https://doi.org/10.1002/ppap.201200113

Methods, E. (2009). Photochemistry of nitrous acid (HONO) and nitrous acidium ion. *Environmental Science and Technology, 43*(4), 1108–1114.

Mira de Orduña, R. (2010). Climate change associated effects on grape and wine quality and production. *Food Research International, 43*(7), 1844–1855. https://doi.org/10.1016/j.foodres.2010.05.001

Novák, I., Popelka, A., Špitalský, Z., Mičušík, M., Omastová, M., Valentin, M., et al. (2015). Investigation of beech wood modified by radio-frequency discharge plasma. *Vacuum, 119*, 88–94. https://doi.org/10.1016/j.vacuum.2015.04.038

Pan, J., Li, Y. L., Liu, C. M., Tian, Y., Yu, S., Wang, K. L., et al. (2017). Investigation of cold atmospheric plasma-activated water for the dental unit waterline system contamination and safety evaluation in vitro. *Plasma Chemistry and Plasma Processing, 37*(4), 1091–1103. https://doi.org/10.1007/s11090-017-9811-0

Rathore, V., Patel, D., Butani, S., & Nema, S. K. (2021). Investigation of physicochemical properties of plasma activated water and its bactericidal efficacy. *Plasma Chemistry and Plasma Processing, 41*. https://doi.org/10.1007/s11090-021-10161-y. Springer US.

Ryu, Y. H., Kim, Y. H., Lee, J. Y., Shim, G. B., Uhm, H. S., Park, G., et al. (2013). Effects of background fluid on the efficiency of inactivating yeast with non-thermal atmospheric pressure plasma. *PLoS One, 8*(6), 1–9. https://doi.org/10.1371/journal.pone.0066231

Sainz-García, A., González-Marcos, A., Múgica-Vidal, R., Muro-Fraguas, I., Escribano-Viana, R., González-Arenzana, L., et al. (2021). *Application of atmospheric pressure cold plasma to sanitize oak wine barrels*. Lwt. https://doi.org/10.1016/j.lwt.2020.110509 (August 2020).

Sainz-García, A., González-Marcos, A., Múgica-Vidal, R., Muro-Fraguas, I., Gallarta-González, F., González-Arenzana, L., et al. (2023). Wine corks decontamination using plasma activated water. *Current Research in Food Science, 7*(November), Article 100639. https://doi.org/10.1016/j.crfs.2023.100639

Scholtz, V., Pazlarova, J., Souskova, H., Khun, J., & Julak, J. (2015). Nonthermal plasma - a tool for decontamination and disinfection. *Biotechnology Advances, 33*(6), 1108–1119. https://doi.org/10.1016/j.biotechadv.2015.01.002

Shen, J., Tian, Y., Li, Y., Ma, R., Zhang, Q., Zhang, J., et al. (2016). Bactericidal effects against S. aureus and physicochemical properties of plasma activated water stored at different temperatures. *Scientific Reports, 6*(March). https://doi.org/10.1038/srep28505

Suárez, R., Suárez-Lepe, J. A., Morata, A., & Calderón, F. (2007). The production of ethylphenols in wine by yeasts of the genera Brettanomyces and dekkera: A review. *Food Chemistry, 102*(1), 10–21. https://doi.org/10.1016/j.foodchem.2006.03.030

Tarabová, B., Lukeš, P., Janda, M., Hensel, K., Šikurová, L., & Machala, Z. (2018). Specificity of detection methods of nitrites and ozone in aqueous solutions activated by air plasma. *Plasma Processes and Polymers, 15*(6). https://doi.org/10.1002/ppap.201800030

Thirumdas, R., Kothakota, A., Annapure, U., Siliveru, K., Blundell, R., Gatt, R., et al. (2018). Plasma activated water (PAW): Chemistry, physico-chemical properties, applications in food and agriculture. *Trends in Food Science and Technology, 77*(September 2017), 21–31. https://doi.org/10.1016/j.tifs.2018.05.007

Tian, Y., Guo, J., Wu, D., Wang, K., Zhang, J., & Fang, J. (2017). The potential regulatory effect of nitric oxide in plasma activated water on cell growth of Saccharomyces cerevisiae. *Journal of Applied Physics, 122*(12). https://doi.org/10.1063/1.4989501

Tomás, N. (2016). *Escuela Tecnica Superior de Ingeniería Agronómica y del Medio Natural*.

Van Gils, C. A. J., Hofmann, S., Boekema, B. K. H. L., Brandenburg, R., & Bruggeman, P. J. (2013). Mechanisms of bacterial inactivation in the liquid phase induced by a remote RF cold atmospheric pressure plasma jet. *Journal of Physics D: Applied Physics, 46*(17). https://doi.org/10.1088/0022-3727/46/17/175203

Velasco, A. T. (2012). *Ribera del Duero*.

Xiang, Q., Zhang, R., Fan, L., Ma, Y., Wu, D., Li, K., et al. (2020). Microbial inactivation and quality of grapes treated by plasma-activated water combined with mild heat. *Lwt, 126*(136). https://doi.org/10.1016/j.lwt.2020.109336

Yost, A. D., & Joshi, S. G. (2015). Atmospheric nonthermal plasma-treated PBS inactivates Escherichia coli by oxidative DNA damage. *PLoS One, 10*(10), 1–20. https://doi.org/10.1371/journal.pone.0139903

Zhang, Q., Ma, R., Tian, Y., Su, B., Wang, K., Yu, S., et al. (2016). Sterilization efficiency of a novel electrochemical disinfectant against Staphylococcus aureus. *Environmental Science and Technology, 50*(6), 3184–3192. https://doi.org/10.1021/acs.est.5b05108

Zhang, R., Ma, Y., Wu, D., Fan, L., Bai, Y., & Xiang, Q. (2020). Synergistic inactivation mechanism of combined plasma-activated water and mild heat against saccharomyces cerevisiae. *Journal of Food Protection, 83*(8), 1307–1314. https://doi.org/10.4315/JFP-20-065

Zhou, R., et al. (2020). *Plasma activated water (PAW): Generation, origin of reactive species and biological applications*.

- Wine corks decontamination using plasma activated water. Ana Sainz-García, Ana González-Marcos, Rodolfo Múgica-Vidal, Ignacio Muro-Fraguas, Félix Gallarta-González, Lucía González-Arenzana, Isabel López-Alfaro, Pilar Santamaría, Rocío Escribano-Viana, Elisa Sainz-García, Fernando Alba-Elías. Current Research in Food Science 7 (2023) 100639.

Los tapones de corcho con los que se cierran las botellas de vino pueden sufrir contaminaciones tanto químicas como biológicas. En relación a las primeras, el compuesto denominado 2,4,6-Tricloroanisol (TCA) es uno de los más conocidos ya que deriva en la denominada "enfermedad del corcho". Este compuesto aporta sabores desagradables al vino (olor a moho y establo) y, como consecuencia, la composición del vino es alterada [29,30]. Este defecto es tan importante que entre el 1% y el 7% de las botellas de vino son descartadas por esta razón [29].

En esta investigación se ha evaluado la capacidad de la PAW para descomponer moléculas químicas (haloanisoles y halofenoles) en tapones de corcho con el fin de disminuir la cantidad de botellas de vino eliminadas en la industria enológica.

Se empleó PAW para reducir principalmente el TCA y otras diez moléculas químicas (haloanisoles y halofenoles) de los corchos utilizados en el embotellado del vino. Se estudiaron cuatro PAW diferenciadas por el tiempo de generación de cada una de ellas (1,5; 5; 15 y 30 min). El tratamiento de PAW se aplicó mediante inmersión de corchos contaminados en un recipiente con PAW durante 3 h. Tras el estudio de capacidad de descomposición química de cada PAW, se sugirió que la especie reactiva que jugaba un papel fundamental era el radical OH. Finalmente, se eligió la PAW generada durante 5 min como la mejor, alcanzando una disminución del 75,2% de TCA en corchos artificialmente contaminados.

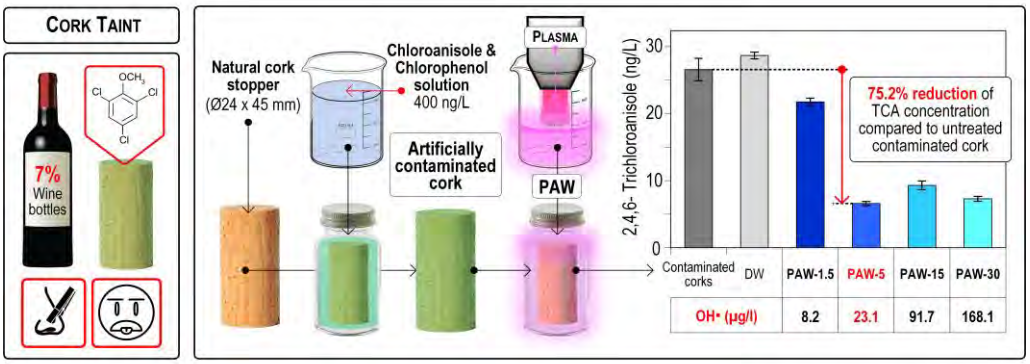

Fig. 20. Gráfico resumen del artículo IV.

Current Research in Food Science 7 (2023) 100639

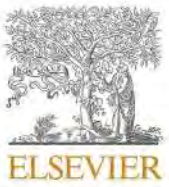

Contents lists available at ScienceDirect

Current Research in Food Science

journal homepage: www.sciencedirect.com/journal/current-research-in-food-science

Wine corks decontamination using plasma activated water

Ana Sainz-García [a], Ana González-Marcos [a], Rodolfo Múgica-Vidal [a], Ignacio Muro-Fraguas [a], Félix Gallarta-González [b], Lucía González-Arenzana [c], Isabel López-Alfaro [c], Pilar Santamaría [c], Rocío Escribano-Viana [c], Elisa Sainz-García [a,**,1], Fernando Alba-Elías [a,*,1]

[a] Department of Mechanical Engineering. University of La Rioja, Logroño, Spain
[b] Department of Chemistry. University of La Rioja, Logroño, Spain
[c] Institute of Grapevine and Wine Sciences, Logroño, Spain

ARTICLE INFO

Handling editor: Maria Corradini

Keywords:
Cork taint
2,4,6-Trichloroanisole
Plasma activated water
Wine
OH•

ABSTRACT

Cork taint provides off-odors and changes negatively wine composition. In fact, it is one of the most important causes of discarding bottled wine. 2,4,6-Trichloroanisole (TCA) is the most known molecule responsible of that problem. In this study, cork stoppers were artificially contaminated with a multi-pattern solution which contained different chloroanisoles and chlorophenols. Contaminated corks were immersed for 3 h in four Plasma Activated Water (PAW) generated during 1.5 min, 5 min, 15 min and 30 min. The products of OH•, NO• and NO_2• with phenol were determined by HPLC for each PAW. After treating contaminated corks with PAW generated during 5 min, more than 72 % of TCA was removed and it was suggested OH• as the main reactive species decomposing TCA. Finally, other chloroanisole and chlorophenol molecules were examined after PAW treatments showing successful reductions in almost every molecule. Thus, it was presented PAW treatment as an easy solution for solving cork taint problems in wine industry.

1. Introduction

Over the last year, the Spanish wine sector increased 4.7 % which makes wine one of the most important markets of the Spanish economy (Observatorio Español del Mercado del Vino, 2022). Wines are classified by parameters such as color, alcohol content, age and sweetness. However, there are some wines that need to be distinguished by more complex characteristics. In this sense, the definitions of aroma and bouquet are of great importance. The first one is related to the mixture of complex nuances that arise during its production and packaging; the latter is related to the natural taste and smell imparted by the grapes (Buja, 2022). Thus, wine is such a complex aqueous solution that involve more than 500 chemical constituents. Nevertheless, this combination could be spoiled by undesirable compounds causing wine faults (Tarasov et al., 2017).

Cork stoppers are highly effective as wine sealers, allowing wine to develop and age over time. However, they can suffer from chemical and biological contamination. This could lead to the formation of haloanisoles, being 2,4,6-Trichloroanisole (TCA) the most known molecule due to the capacity to produce the so-called cork taint, a moldy and musty off-odor and consequently affecting wine composition (about 80–85 % of total wine) (Sefton and Simpson, 2005; Silva Pereira, Figueiredo Marques and San Romão, 2000). This molecule has a very low threshold in wines, 1–2 ng/L (Sefton and Simpson, 2005; Soleas et al., 2002). The presence of TCA above these concentrations can spoil the wine organoleptic properties. It is a severe problem in wineries because between 1 and 7 % of bottled wines are discarded (Coque et al., 2006; Martín, 2018; Sefton and Simpson, 2005).

There are several publications indicating different pathways for the origin of TCA in cork bark and corks: phenol and chlorine-derived sources, chlorophenolic biocides, biosynthesis of chlorophenolic compounds in the forest, biosynthesis of chlorophenolic compounds after

* Corresponding author.
** Corresponding author.
E-mail addresses: ana.sainz@unirioja.es (A. Sainz-García), ana.gonzalez@unirioja.es (A. González-Marcos), rodolfo.mugica@unirioja.es (R. Múgica-Vidal), ignacio.muro@unirioja.es (I. Muro-Fraguas), felix.gallarta@unirioja.es (F. Gallarta-González), lucia.gonzalez@unirioja.es (L. González-Arenzana), isabel.lopez@unirioja.es (I. López-Alfaro), psantamaria@larioja.org (P. Santamaría), roescrv@unirioja.es (R. Escribano-Viana), elisa.sainzg@unirioja.es (E. Sainz-García), fernando.alba@unirioja.es (F. Alba-Elías).
[1] These authors contributed equally to this work and both are corresponding authors.

https://doi.org/10.1016/j.crfs.2023.100639
Received 7 July 2023; Received in revised form 13 November 2023; Accepted 13 November 2023
Available online 17 November 2023

harvest of the cork bark, etc. (Monteiro et al., 2022; Simpson and Sefton, 2007). However, the formation of TCA by biomethylation of 2,4,6-Trichlorophenol (TCP) is the only scientifically proven. They are produced by the reaction of chlorines and phenols commonly found in town water suppliers and drainage systems and they can be formed in the environment, at room temperature (RT) in aqueous solutions (Simpson and Sefton, 2007). Once the TCP is in trunks of trees or in corks, the microflora such as *Penicillium* spp, *Aspergillus* spp, *Actinomyces* spp and *Streptomyces* spp, among others, presented on corks transform TCP into TCA through the enzyme chlorophenol O-methyltransferase by a methylation process (Cravero, 2020). A review carried out by (Simpson and Sefton, 2007) shows a complete table with different possible origins of TCA in wine corks suggesting that most of the TCA found in corks comes from trees.

In this sense, the cork industry has tried to prevent, control or even eradicate TCA. Thus, most researches are focused on the prevention of these defects more than in its elimination, because it is a tricky action. Moreover, it is important to follow several cleaning procedures in wine cellars. For example, the sanitizers used need to be free of chlorine and the microflora has to be controlled throughout the humidity, the temperature and the room ventilation. Furthermore, the regular checking of corks, dyes, sanitizers, inks and lubricants is vital for preventing this problem.

Several studies have been carried out on the removal of TCA but they mostly focus on TCA in a liquid solution. Valdés et al. (2018) studied if some polymers (polyanilines) could reduce the TCA content in whisky. They found that 75 % of TCA was eliminated without affecting negatively the aromatic profile and phenolic content of the whisky sample. Moreover, this group used the same polymeric materials to retain TCA from wine, achieving more than 75 % of reduction of this molecule. In other work it was shown a reduction of 91 % of TCA from wine using air-depleted solvent-impregnated cork powder. However, the applied treatment affected negatively the alkyl esters and acids of wine (Cosme et al., 2022). Besides, 10 min catalytic ozonization by raw bauxite was effective in the reduction of TCA in drinking water up to 86 % (Qi et al., 2009).

Regarding TCA elimination in corks, there are some patents and articles published. Different methods and technologies were used for that purpose: a flow of ethanol and water, the supercritical fluid technology, superheated steam or chemical and electrochemical methods were some of them (Cabral, 2006; Martín, 2018; Palacios et al., 2012; Ponte et al., 2013; Guedes, Mateus, Fernandes and Ribeiro, 2019a; Recio, Álvarez-Rodríguez, Rumbero, Garzón and Coque, 2011a; Viguera et al., 2018).

Atmospheric pressure cold plasma (APCP) is an approach for different purposes such as inactivating microorganisms. It is known that reactive species produced by APCPs are brought from the gas phase through the interphase into the bulk of the water, resulting in a liquid called plasma activated water (PAW) which is being investigated (Zhou et al., 2020). Among the most important applications, sterilization, microorganisms' inactivation, either in biofilm or planktonic stage, seed germination or cancer therapy are the most investigated.

This treated liquid is commonly known to be efficient in all these applications due to the interaction and synergistic effect of different reactive species. These include reactive oxygen species (ROS), such as hydroxyl radicals (OH•), atomic oxygen, superoxide (O_2^-), ozone (O_3) and hydrogen peroxide (H_2O_2), as well as reactive nitrogen species (RNS) including atomic nitrogen, peroxynitrite, nitric oxide and nitrites (NO_2^-). Some of these reactive species are stable in the treated liquid (H_2O_2, NO_2^-) while the life-time of other ones is short. These last reactive species are supposed to be generated inside the treated liquid through secondary reactions under specific conditions (i.e. low pH).

Considering all the above, a procedure to eliminate TCA from cork stoppers is needed since the procedures and technologies evaluated up to now request high temperatures and pressures, long times, most of them cause irreversible deformations in corks and are not able to eliminate TCA spoilage. Thus, PAW could be a real solution in order to solve TCA problems in wineries and cork industry.

To the best of our knowledge, PAW was never tested for TCA removal from contaminated cork stoppers. In this study, different PAW were put into contact with cork stoppers artificially contaminated with a standard solution that included different chloroanisole and chlorophenol molecules. The aim was to demonstrate the capacity of PAW for decomposing and eliminating TCA, thus providing a new decontamination strategy to combat this known problem in wine industry.

2. Materials and methods

2.1. Cork samples, chloroanisole and chlorophenol solution

Natural cork stoppers (Ø24 × 45 mm) guaranteed free of chloroanisoles and chlorophenols were acquired in Lafitte Cork Portugal (Paços de Brandão, Portugal).

The stock solution (CPA Chem Ltd., Stara Zagora, Bulgaria) containing 0,40 ng/L of each chloroanisole and chlorophenol molecule was prepared as a standard solution in ethanol (96 % purity, Labbox Labware S.L., Premià de Dalt, Barcelona, Spain). This stock solution was diluted at 400 ng/L in deionized water for cork contamination. The chloroanisole molecules found in stock solution were: 2,4,6-Trichloroanisole; 2,4,5-Trichloroanisole; 2,3,4,5-Tetrachloroanisole; 2,3,4,6-Tetrachloroanisole; 2,3,5,6Tetrachloroanisole and Pentachloroanisole. The chlorophenol molecules: 2,4,6-Trichlophenol; 2,3,4-Trichlophenol; 2,3,4,5-Tetrachlorophenol; 2,3,4,6-Tetrachlorophenol and 2,3,5,6-Tetrachlorophenol.

Purified water (PW) for PAW generation and for preparing the 400 ng/L solution of chloroanisoles and chlorophenols was obtained from a water purification system (Elix® Essential, Merck Millipore, Burlington, Massachusetts, United States) with an electrical conductivity of <0.2 μS/cm and natural pH of >7.00 at 25 °C.

2.2. Chloroanisole and chlorophenol contamination procedure of cork stoppers and quantification method

Natural cork stoppers were individually immersed in glass jars (Ø44 × 94.8 mm) containing 80 mL of the 400 ng/L solution of chloroanisoles and chlorophenols. During 4 h the glass jars were in a rotating stirrer at 50 rpm (Multi Bio RS-24, Biosan, Riga, Latvian) (Fig. 1). Then, each cork stopper was dried at RT during 24 h. After that, the twelve different chloroanisoles and chlorophenols were analyzed following two chemical methods: OIV-MA-AS315-16 (determination of 2,4,6-Trichloroanisole in wine given from the cork stoppers; Resolution OIV/OENO 296/2009) and OIV-MA-AS315-17 (determination of polychlorophenols and polychloroanisoles in wines, cork stoppers, wood and bentonites used as adsorbent of those compounds in the atmosphere; Resolution OIV/OENO 374/2009) (International Organization of Vine and Wine -OIV-) (OIV, 2009). These methods simulate the migration of 2,4,6-Trichloroanisole, 2,4,6-Trichlorophenol, 2,3,4,6-Tetrachloroanisole, 2,3,4,6-Tetrachlorophenol, Pentachloroanisole and Pentachlorophenol susceptible of being produced between bottled wine and cork stoppers. Firstly, an alcoholic extraction with a by solid-phase microextraction system (SPME Fibras ARROW: 50/30μm DVB/CAR/PDMS) with a "liner" (SPME Injection Sleeve 0,75 mmID) was carried out. Then, samples were analyzed by gas chromatography (AGILENT TECHNOLOGIES. Model 8890; Injector: Agilent Technologies. PAL-System Model PAL III Series 2) with detection by mass spectrometer (Agilent Technologies. Model 7000C).

2.3. Preparation of PAW solutions

The APCP equipment used in this study was PlasmaSpot500 (Molecular Plasma Group, Foetz, Luxemburg). It consists of an internal grounded electrode, an external electrode linked to a high voltage

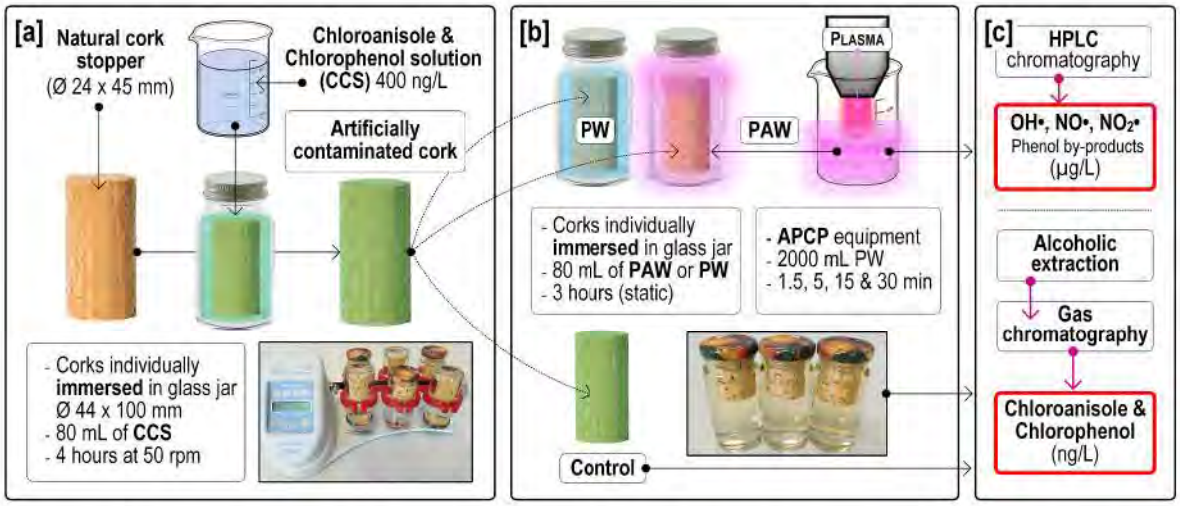

Fig. 1. Scheme of the cork treatment process: [a] cork contamination, [b] PAW generation and cork decontamination and [c] PAW and cork characterization.

source and an aluminum oxide dielectric tube between both electrodes.

PAW was generated by exposing PW to the plasma jet as shown in Fig. 2. After filling a 3000 mL beaker with 2000 mL of PW, plasma was turned on during four different times (1.5, 5, 15 and 30 min; samples referred to as PAW-1.5, PAW-5, PAW-15 and PAW-30, respectively). For all PAW generation treatments, air was used as plasma gas at 60 standard liter per minute (slm) and plasma power was 500 W. The distance between the end of the plasma nozzle and the PW surface was constant at 30 mm to optimize the transport of RONS from the plasma jet to the water volume while lowering the water losses.

2.4. Characterization of physicochemical properties of PAW

Physicochemical parameters of PAW were measured by different methods.

For pH, oxidation-reduction potential (ORP) and electrical conductivity (EC) a portable multimeter sensION MM150 DL with a 50 48 probe (Hach Company, United States of America) was used. Nitrates (NO_3^-) in PAW were quantified with a portable Imacimus® MultiIon analyser (NTsensors S.L., Spain). Nitrites (NO_2^-) were measured following the colorimetric Griess assay by spectrophotometry. Through this procedure nitrites were determined by reaction with sulfanilic acid under acidic conditions to form a diazonium ion, which couples to α-naphthylamine, forming a magenta colored dye that can be spectrophotometrically quantified based on its absorbance at 548 nm (Jablonowski and von Woedtke, 2015). The concentration of hydrogen peroxide (H_2O_2) was determined by measuring the absorbance of titanium peroxide at 407 nm. This method was based on the reaction of titanyl sulfate to yellow-colored peroxotitanyl sulfate. For all photometric measurements a Onda V-11 SCAN spectrophotometer (Giorgio Bormac s.r.l., Italy) was

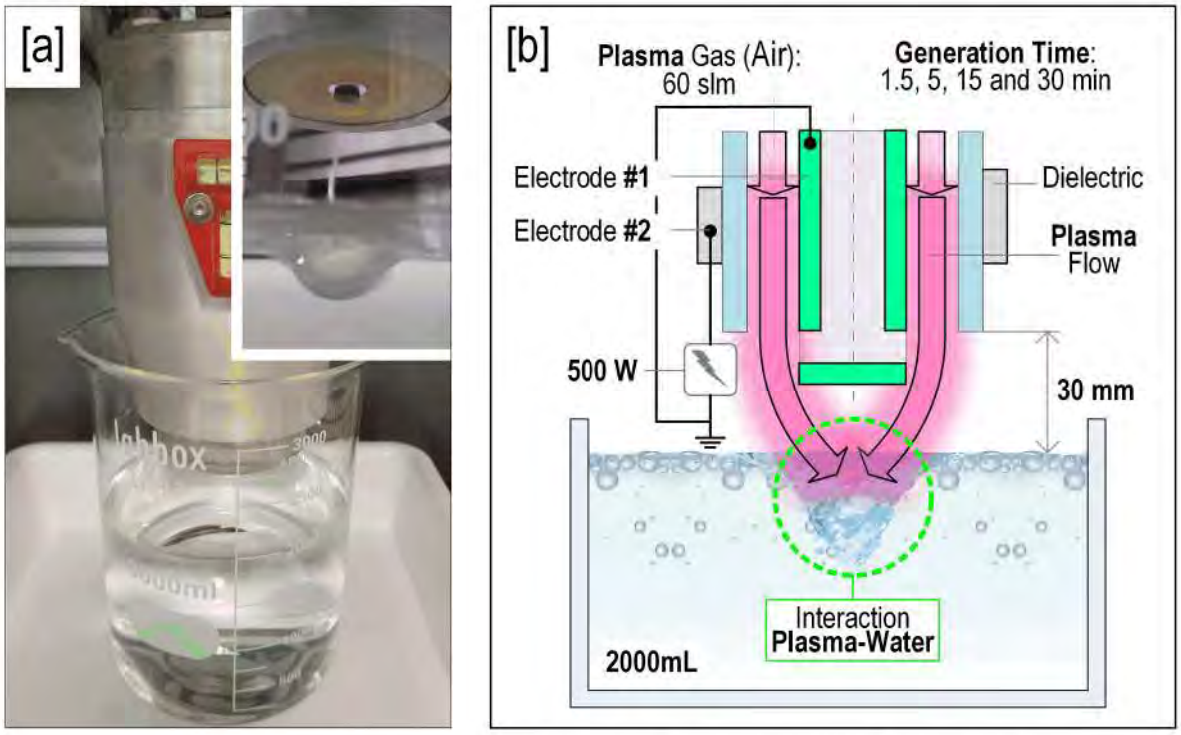

Fig. 2. [a] PAW generation system and detail of the interaction plasma-water and [b] PAW generation scheme.

used. Griess reagent and Titanium (IV) oxysulfate were purchased from Sigma Aldrich (USA). All these parameters were measured at RT after PAW generation.

Finally, in order to detect secondary RONS, a method based on the reaction between phenol (C_6H_5-OH) and radicals OH•, NO• or NO_2• was used (P. Lukes et al., 2014). The concentrations of phenol and its primary degradation by-products (benzoquinone (phenol + OH•), 4-nitrosophenol (phenol + NO•) and 2-nitrophenol (phenol + NO_2•)) were analyzed using HPLC system with UV detection (Agilent 1100 Series, Agilent Technologies, Spain). Analyses were made using a 5 μm reversed phase Supelcosil C-18 column (25 cm × 2.4 mm; Supelco Inc. USA). The detection limit for the HPLC analysis was 0.01–0.1 μM (depending on the compound and the detection used). A solution of $2{\cdot}10^{-2}$ M of phenol (Monplet & Esteban S.A., Spain) was prepared in water; 5.0 mL of this solution were mixed with 95 mL of PAW and incubated at 50 °C for 24 h. Then, the solution was filtered (0.45 μm) and measured by HPLC analysis using a gradient elution (Table 1) and the following conditions: injection volume of 20 μL, flow rate at 1.0 mL/min mobile phase; total time 16 min; *P*: ≈90 bar at 90-10, ≈60 bar at 60-40; and a detector at 260 nm (reference: 699 nm). The retention times were as follows: benzoquinone 5.0 min, 4-nitrosophenol 5.4 min, phenol 8.2 min, and 2-nitrophenol 11.2 min (Table 2).

In order to quantify the degradation by-products, different calibration curves were prepared with solutions of known concentration of benzoquinone (Sigma Aldrich, USA) ($1.35{\cdot}10^{-5}$ M), 4-nitrosophenol (TCI Chemicals, Japan) ($2.54{\cdot}10^{-4}$ M) and 2-nitrophenol (Sigma Aldrich, USA) ($2.54{\cdot}10^{-4}$ M).

2.5. Chloroanisole and chlorophenol decontamination procedure from cork stoppers

Contaminated cork stoppers were individually immersed during 3 h in glass jars containing 80 mL of each type of PAW or PW (Fig. 1). After that, each cork stopper was dried at RT during 24 h and sent to the laboratory to analyze the concentration of the different chloroanisoles and chlorophenols following the procedure of section 2.2.

2.6. Statistical analysis

All experiments were conducted in triplicate. Statistical analysis of the data was performed using Statgraphics Centurion software (v19, The Plains, USA). p value < 0.05 was used to analyze statistically significant differences.

3. Results and discussion

3.1. Characterization of PAW

The physicochemical parameters of PAW (pH, EC, ORP, NO_3^- and NO_2^-) were characterized as a function of plasma activation time (Table 3).

The pH of PW dropped from 7.00 to 4.46 after exposure to plasma for 1.5 min and lowered to 3.10 after 30 min, showing plasma treatment acidified the water. A linear increase of EC over plasma activation time was observed, which raised from 5 μS/cm to 25 μS/cm after 1.5 min of treatment and increased to 190 μS/cm after 30 min. The ORP value increased from 299 mV to 315 mV after plasma activation for 1.5 min and reached 408 mV after 30 min. Related to the chemical analysis of PAW for NO3- and NO2-, there was a significant increase in the NO3- and NO2- concentrations during plasma activation time. Thus, the highest concentrations were reached for PAW-30 being 17.90 mg/L (NO3-) and 5.01 mg/L (NO2-), respectively. Finally, H_2O_2 was not detected in any of the PAW analyzed. It is supposed that in case of NO2- excess, H_2O_2 was completely reacted.

Table 1
Gradient elution for HPLC analysis.

t (min)	Acetic acid:1 % (*V/V*)	Acetonitrile
0	90	10
7	60	40
13	90	10

Table 2
Calibration curves for phenol by-products quantification.

Degradation by-product	Calibration curve	R^2
benzoquinone	A (mAU) = 0.09 + 6.99 × 10^5 c (M)	0.9996
4-nitrosophenol	A (mAU) = −0.24 + 1.50 × 10^5 c (M)	0.9997
2-nitrophenol	A (mAU) = −1.00 + 3.78 × 10^5 c (M)	0.9997

Table 3
Physicochemical parameters of each PAW at RT.

PAW	pH	EC (μS/cm)	ORP (mV)	NO_3^- (mg/L)	NO_2^- (mg/L)
PAW-1.5	4.46 ± 0.15	25 ± 5	315 ± 13	3.67 ± 0.31	0.74 ± 0.05
PAW-5	4.01 ± 0.17	52 ± 7	355 ± 10	4.13 ± 0.15	2.58 ± 0.27
PAW-15	3.58 ± 0.09	103 ± 13	383 ± 9	9.90 ± 1.30	3.47 ± 0.13
PAW-30	3.10 ± 0.12	190 ± 15	408 ± 21	17.90 ± 2.05	5.01 ± 0.87

It is in accordance with the investigation carried out by (Rathore and Nema, 2021) who said that while the plasma activation time increased, a significant raise in EC and ORP and a pH reduction was observed. This trend is mainly due to the oxidizing species and active ions (such as H+, NO2-, NO3-) generated during PAW generation time. Moreover, other researchers have come to the same conclusion (El Shaer et al., 2020; Pan et al., 2017; Q. N. Zhang et al., 2016).

In order to further analyze other reactive species that could be present in PAW, HPLC chromatography was performed. Thus, the detection of phenol and its degradation by-products was used as an indirect analytical method to evaluate the presence of OH•, NO• and NO2•. The chromatograms showed the identified by-products after the reaction of OH•, NO• and NO2• with phenol (benzoquinone, 4-nitrosophenol and 2 nitrophenol, respectively) (Fig. 3).

Table 4 indicates the concentration of the phenol by-products for each analyzed PAW. It was observed a common trend, since the three by products showed an increase with longer plasma activation times. Talking about benzoquinone, PAW-1.5 generated 8.2 μg/L in comparison to the 168.1 μg/L of PAW-30. Besides, the concentration of 4-nitrosophenol ranged from 227.0 μ/L to 3404.8 μg/L. Finally, 2-nitrophenol, varied from 209.5 μg/L to 1729.6 μg/L when the treatment time increased from 1.5 to 30 min. These products give evidence about the formation OH·, NO· and NO_2·. There are few articles where those reactive species were found and quantified in PAW (P. Lukes et al., 2014; Tarabová et al., 2018).

Two possible theories about the origin of the reactive species identified by chromatography have been identified: (1) instability of acidified nitrites at acid pH and (2) photochemical reactions induced by UV radiation from plasma with ozone, nitrates and nitrites. On the other hand, it is known the short lifetime (nanoseconds) of these reactive species; however, they are implicated in cyclic reactions which could justify their presence in PAW several hours after the generation (Liu et al., 2020; Ptr Lukes et al., 2017).

3.2. TCA degradation in corks by PAW

Different methods and technologies have been tested trying to eliminate TCA from cork. For example, the use of an ethanol and water flow at 0.1 mbar and 100 °C during 10 h showed a reduction of 76 % of

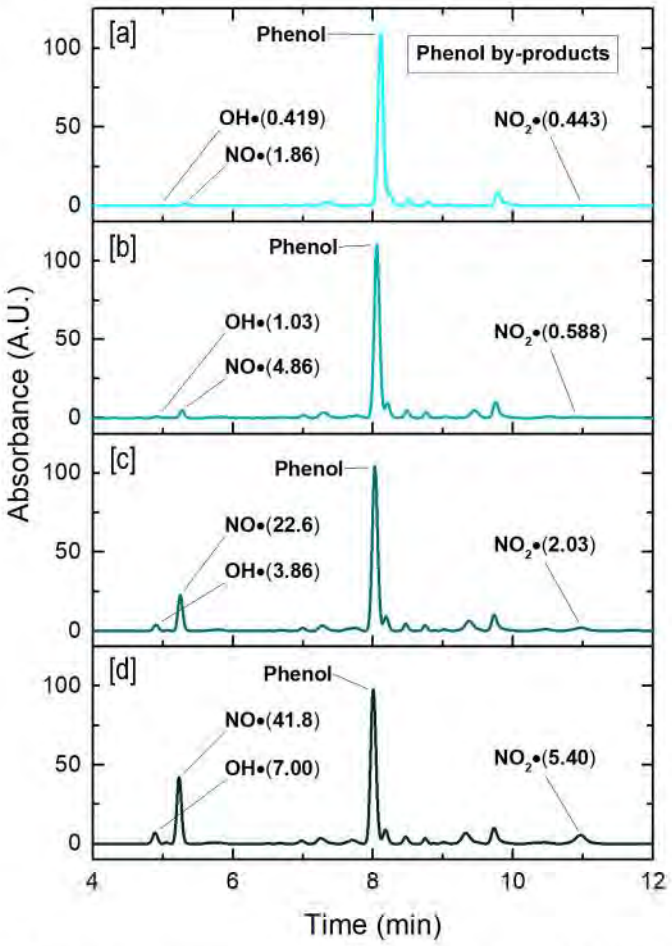

Fig. 3. HPLC chromatograms of each PAW: [a] PAW-1.5; [b] PAW-5; [c] PAW-15 and [d] PAW-30.

Table 4
Phenol by-products quantification.

PAW	Phenol by-product concentration (μg/L)		
	Benzoquinone (OH•)	4-nitrosophenol (NO•)	2-nitrophenol (NO_2•)
PAW-1.5	8.2	227.0	209.5
PAW-5	23.1	465.1	253.9
PAW-15	91.7	1873.0	696.1
PAW-30	168.1	3404.8	1729.6

TCA (Palacios et al., 2012). When using a steam distillation system in rotative mode (100-125 °C, 0.2–0.8 bar, 6–65 min and 1–10 rpm) a similar percentage of TCA reduction (70 %) was achieved (Cabral, 2006). In this line, a device that use superheated steam at 125-135 °C and 4–8 bar was patented to reduce TCA from cork (Martín, 2018). Moreover, chemical methods like hydrogen peroxide as an oxidant were test removing 86 % of TCA from the surface of natural cork stoppers (Recio, Álvarez-Rodríguez, Rumbero, Garzón and Coque, 2011b). Guedes et al. (2019a, b) investigated different electrochemical reactors achieving 41 % decrease of TCA in cork disks after 24 h immersion in saline solution. Finally, supercritical fluids technology has been applied with results below the TCA detection limit (Ponte et al., 2013; Viguera et al., 2018). However, for most technologies, very expensive and complex equipment operating at elevated pressures and temperatures are needed.

Considering that the chemical compound 2,4,6-Trichloroanisole was identified as the main cause of cork taint in wine, first experiments were focused on its removal. For this purpose, four different PAW were tested against artificially contaminated corks. PW was applied to assess possible washing effects and three artificially contaminated corks were used as control sample.

Fig. 4 shows the average TCA concentration in cork samples after 3 h of contact with PAW and PW and the TCA concentration of dried contaminated corks (as control). For the shortest PAW generation time (PAW-1.5) only 18.1 % of TCA was removed. For PAW-5 and PAW-30 there were no statistically significant differences reaching 75.2 % and 72.6 % of removal, respectively; for PAW-15 the degradation was a little lower, 65.0 %. Finally, corks treated with PW did not show significative changes in TCA content with respect to the control which means that a washing effect did not take place.

There are no researchers who have investigated PAW technology in order to decompose or degrade TCA chemical molecule. However, some authors have studied how to decompose TCA molecules by other technologies, mainly ozonation. Those researchers have suggested OH• as the main reactive species decomposing TCA. Peter and Von Gunten (2007) observed higher TCA decomposition when increasing TCA exposure in water during off-flavors elimination by ozonation. In other work, (Qi et al., 2009) found 86 % of TCA decomposition in drinking water after 10 min ozonation with raw bauxite as catalyst. They indicated that the high percentage of reduction when using this catalyst could be attributed to the generation of more OH•. They carried out a scavenging experiment that confirmed the higher OH• generation accounted for the enhancement of the degradation of TCA. The same authors achieved almost 100 % of TCA degradation using iron modified bauxite and being attributed to the promotion of the OH• formation (Qi et al., 2012). Besides, (Xu and Qi, 2016) studied the elimination of TCA in catalytic ozonation by g-AlOOH in water obtaining 79.3 % of reduction and suggesting that OH• was the main reactive species which attacks TCA.

Considering the abovementioned, OH• was the reactive species proposed to play the main role in TCA decomposition. Moreover, (X. Zhang et al., 2018) quantified the products of reaction of OH• with salicylic acid. They indicated the measurement of 2,3-DHBA and 2,5-DHBA should provide an accurate estimation of the amount of OH• and they found highest concentrations when using air and oxygen as plasma gas and longer treatment times.

Thus, it is suggested that the main cause for TCA removal could be a result of the OH• found in each PAW. The lower values of TCA decomposition were obtained with PAW-1.5 because the OH• level was the minimum (Table 4). On the other hand, the highest decomposition could be expected for PAW-30 treatment, however, it seems that a huge amount of OH• did not produce the maximum decomposition. In this regard, (Qi et al., 2012) indicated that an excess in OH• generation resulted in OH• quenching. This is what probably occurs for PAW generated during the highest activation times, 15 and 30 min. Thereby, PAW-5 achieved the best TCA decomposition.

Furthermore, it is important to investigate how OH• attacks TCA molecules. In this context, OH• has a high oxidative potential and is known to oxidize molecules that other radicals cannot even react. Taking notice of what (Benitez et al., 2000) said, the first attack of OH• to TCA molecule is in the sites where chlorine is not bonded. Thus, the -OCH_3 group is proposed to be the target. This is in line with (N. Q. Zhang et al., 2016), who showed the reaction between OH• and -OCH_3 group by H abstraction, followed by a reaction with O_2 forming peroxyl radicals and finally a disproportionation maybe through Russell mechanism. Besides, (Trewick et al., 2005) suggested a demethylation by hydroxylation; thus, OH• could be capable of eliminating methyl group from TCA. Once -OCH_3 group is attacked, OH• goes for chlorine bonds (Kavitha and Palanivelu, 2016; Trewick et al., 2005). As far as we are concerned, there are two possible mechanisms to attack Cl atoms. The first one is when the three Cl atoms are replaced with OH• (L. L. Zhang et al., 2011). The second one is characterized by a dissociation of Cl

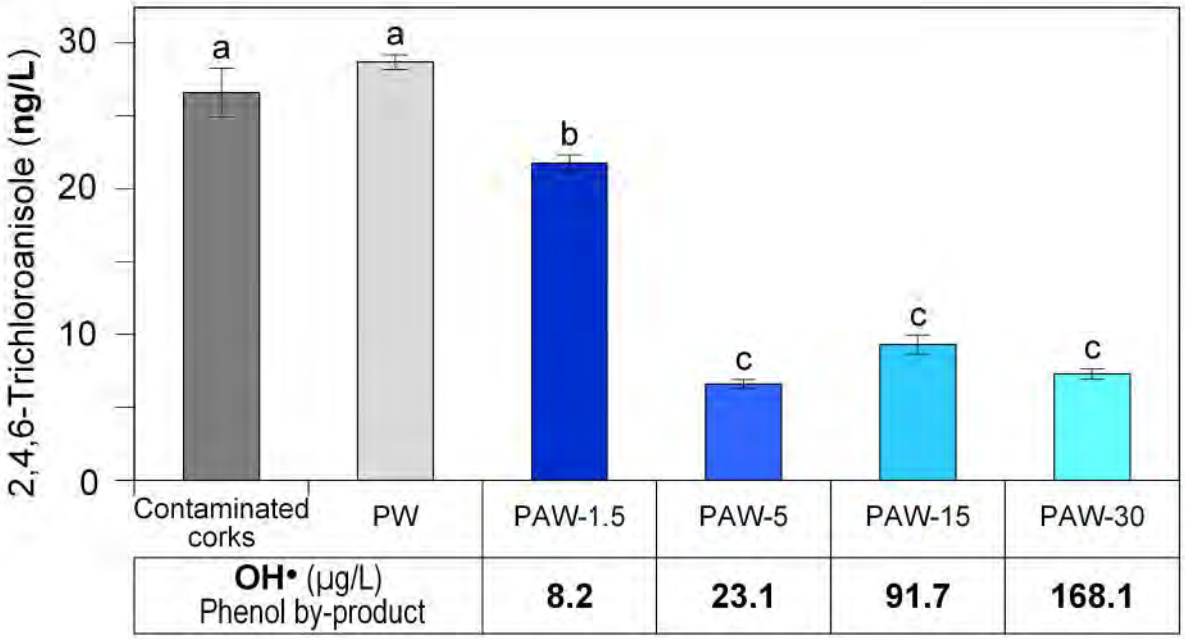

Fig. 4. Average TCA concentration (ng/L) of cork samples after 3 h in contact with different PAW and PW and contaminated corks (control). Different letters indicate statistically significant differences ($p < 0.05$).

atoms (Benitez et al., 2000).

3.3. Other chlorine molecules degradation in corks by PAW

After successfully proving the power of PAW to remove TCA from corks, we tried to know if other chloroanisole and chlorophenol molecules could also be decomposed by PAW. Since it was confirmed that PW has no effect in eliminating this type of chemical molecules, PW was not tested within this part of the study. In this case, ten molecules of chloroanisole and chlorophenol were analyzed after PAW treatment in corks.

Fig. 5 illustrates the average concentration of chloroanisole molecules after 3 h in contact with PAW and dried contaminated cork control. In general, it was observed high levels of decomposition regardless the chloroanisole analyzed or the PAW used.

Fig. 6 shows the average concentration of chlorophenol molecules after 3 h in contact with PAW and dried contaminated corks (control). It could be confirmed, similarly to the results for chloroanisoles, that PAW treatments were successful in decomposing almost the total chlorophenol molecules analyzed. Comparing Figs. 5 and 6, it can be observed a higher degree of decomposition for chlorophenols than chloroanisoles. This fact could be explained because –OH group of phenol molecule is more reactive towards polar molecules, such as OH•, than $–OCH_3$ group of anisole (Revolution, 2021). Among all the chlorophenol molecules studied, the most known and important one is TCP since it is the precursor of TCA formation. Thus, we found two articles that investigate its removing. Saritha et al. (2009) compared four advanced oxidation processes for TCP removal (UV, UV/H2O2, Fenton, UV/Fenton and UV/TiO2). UV/Fenton was the best oxidation process since it achieved 90 % of TCP eliminated. In the same way, (Kavitha and Palanivelu, 2016) observed TCP decomposition after photo-Fenton process of almost 100 % suggesting a critical role of OH•.

Finally, it is worth mentioning that the percentage of chloroanisole and chlorophenol molecules reduction were quite similar when applying

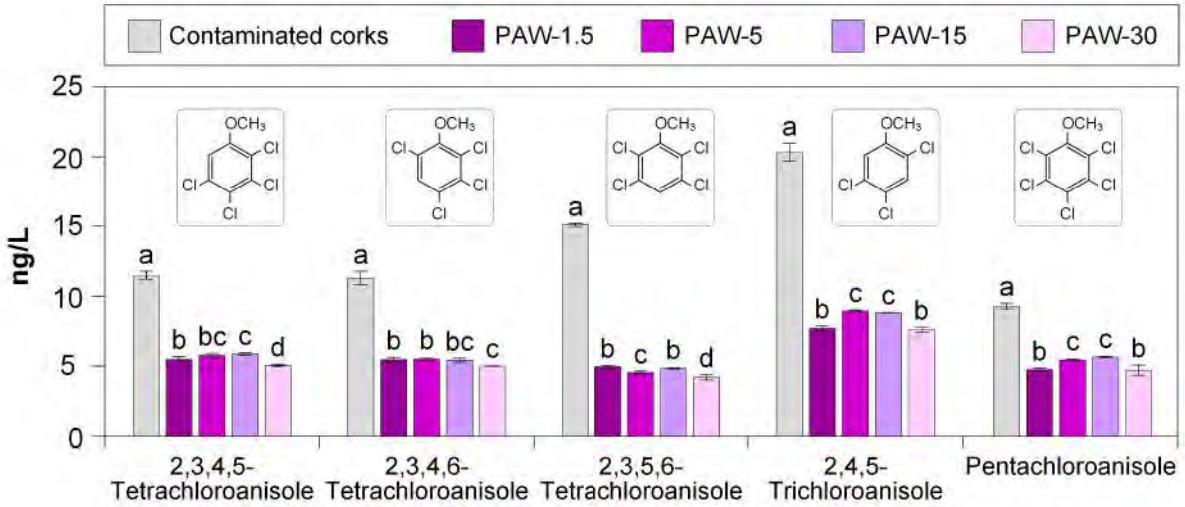

Fig. 5. Average concentration (ng/L) of different chloroanisole molecules of cork samples after 3 h in contact with different PAW and dried contaminated corks (control). Different letters indicate statistically significant differences ($p < 0.05$).

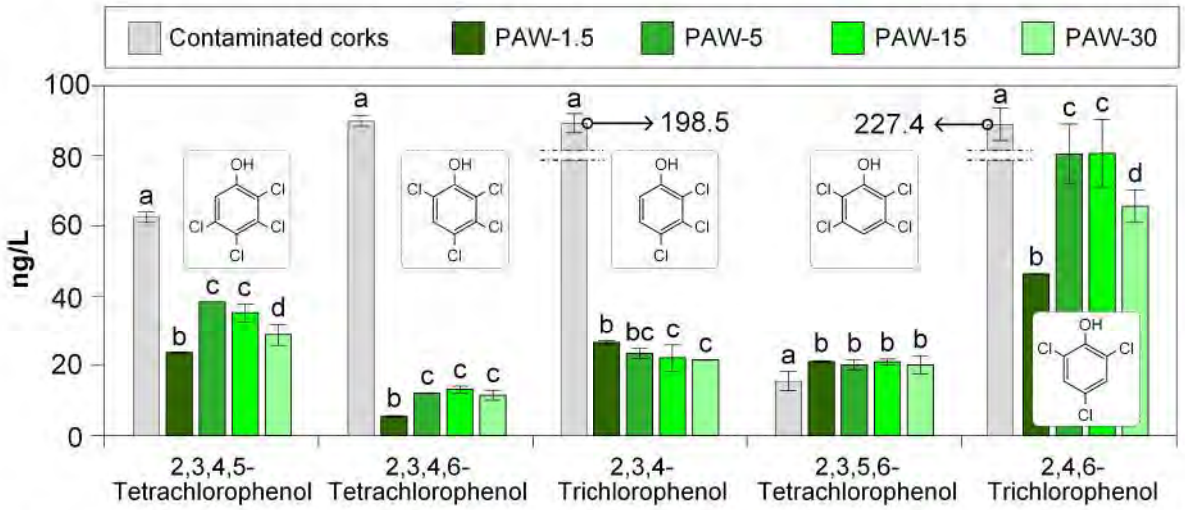

Fig. 6. Average concentration (ng/L) of different chlorophenol molecules of cork samples after 3 h in contact with different PAW and dried contaminated corks (control). Different letters indicate statistically significant differences ($p < 0.05$).

a treatment with PAW generated during a plasma activation time equal or higher than 5 min (PAW-5, PAW-15 and PAW-30). Considering that the energy and time consumed when generating each PAW were different, PAW-5 was chosen as the best PAW from the economical and the ecofriendly points of view.

4. Conclusions

The huge percentage of wine bottles discarded each year due to the so-called cork taint is an important issue for wineries. Different chloroanisole and chlorophenol molecules seem to be responsible of such a big problem, specially the known 2,4,6-Trichloroanisole molecule.

In this research, it was confirmed PAW treatment as an effective method to eliminate TCA from artificially contaminated corks. It was also showed the activity of PAW to decompose other chloroanisole and chlorophenol molecules. The best treatment was the one using PAW generated during 5 min of plasma activation time (PAW-5) in which contaminated corks were individually immersed for 3 h.

Moreover, it was determined that the reactive species which plays the main role decomposing TCA and probably other chloroanisole and chlorophenol molecules, was OH•. It was suggested the mechanisms by the one OH• degrades TCA molecule; first a demethylation by hydroxylation reaction is produced, then OH• attacks Cl atoms.

In conclusion, decomposing chloroanisole and chlorophenol molecules with PAW could be an emerging solution to reduce the number of wine bottles discarded in wineries due to this major problem.

Funding

This work has been funded by MCIN/AEI/10.13039/501100011033 and the "European Union NextGenerationEU/PRTR" through grants PID2019-105367RB, PID2020-11365RB-C21 and PDC2022-133242-I00.

CRediT authorship contribution statement

Ana Sainz-García: Conceptualization, Data curation, Formal analysis, Investigation, Validation, Visualization, Writing – original draft, Writing – review & editing. **Ana González-Marcos:** Data curation, Funding acquisition, Supervision, Validation, Writing – review & editing. **Rodolfo Múgica-Vidal:** Conceptualization, Data curation, Formal analysis, Investigation, Visualization, Writing – review & editing. **Ignacio Muro-Fraguas:** Conceptualization, Data curation, Formal analysis, Investigation, Writing – review & editing. **Félix Gallarta-González:** Data curation, Resources, Validation, Writing – review & editing. **Lucía González-Arenzana:** Data curation, Investigation, Writing – review & editing. **Isabel López-Alfaro:** Conceptualization, Resources, Writing – review & editing. **Pilar Santamaría:** Conceptualization, Resources, Writing – review & editing. **Rocío Escribano-Viana:** Data curation, Investigation, Writing – review & editing. **Elisa Sainz-García:** Conceptualization, Data curation, Formal analysis, Investigation, Supervision, Writing – original draft, Writing – review & editing. **Fernando Alba-Elías:** Conceptualization, Data curation, Formal analysis, Funding acquisition, Investigation, Supervision, Visualization, Writing – review & editing.

Declaration of competing interest

The authors declare that they have no known competing financial interests or personal relationships that could have appeared to influence the work reported in this paper.

Data availability

Data will be made available on request.

Acknowledgements

The author Ana Sainz-García is thankful to the program of predoctoral contracts for the training of research staff funded by the Spanish Ministry of Science and Innovation.

The author Ignacio Muro-Fraguas, thanks the program of postdoctoral orientation contracts for the training of research staff funded by the autonomous community of La Rioja.

The author Rocío Escribano-Viana as postdoctoral researcher of the University of La Rioja, thanks the postdoctoral training program funded by the Ministry of Universities.

References

Benitez, F.J., Beltran-Heredia, J., Acero, J.L., Rubio, F.J., 2000. Contribution of free radicals to chlorophenols decomposition by several advanced oxidation processes. Chemosphere 41 (8), 1271–1277. https://doi.org/10.1016/S0045-6535(99)00536-6.

Buja, L.M., 2022. The history, science, and art of wine and the case for health benefits: perspectives of an oenophilic cardiovascular pathologist. Cardiovasc. Pathol. 60, 107446 https://doi.org/10.1016/j.carpath.2022.107446.

Cabral, M. (2006). 2 268 459.

Coque, J.J.R., Pérez, E.R., Goswami, M., Martínez, R.F., García, S.C., Rodríguez, M.L.A., Martín, J.F.M., 2006. Wine Contamination by Haloanisoles: towards the

development of biotechnological strategies to remove chloroanisoles from cork stoppers. Inbiotec 3–51. Retrieved from. https://www.apcor.pt/wp-content/uploads/2015/08/Inbiotec-index.pdf.

Cosme, F., Gomes, S., Vilela, A., Filipe-Ribeiro, L., Nunes, F.M., 2022. Air-depleted and solvent-impregnated cork powder as a new natural and sustainable fining agent for removal of 2,4,6-trichloroanisole (TCA) from red wines. Molecules 27 (14). https://doi.org/10.3390/molecules27144614.

Cravero, M.C., 2020. Musty and moldy taint in wines: a review. Beverages 6 (2), 1–13. https://doi.org/10.3390/beverages6020041.

El Shaer, M., Eldaly, M., Heikal, G., Sharaf, Y., Diab, H., Mobasher, M., Rousseau, A., 2020. Antibiotics degradation and bacteria inactivation in water by cold atmospheric plasma discharges above and below water surface. Plasma Chem. Plasma Process. 40 (4), 971–983. https://doi.org/10.1007/s11090-020-10076-0.

Español del Mercado del Vino, Observatorio, 2022. Exportaciones españolas de vino y productos vitivinícolas.

Guedes, P., Mateus, E.P., Fernandes, J.P., Ribeiro, A.B., 2019a. Electro-technologies for the removal of 2,4,6-trichloroanisole from naturally contaminated cork discs: reactor design and proof of concept. Chem. Eng. J. 361 (December 2018), 80–88. https://doi.org/10.1016/j.cej.2018.12.040.

Guedes, P., Mateus, E.P., Fernandes, J.P., Ribeiro, A.B., 2019b. Electro-technologies for the removal of 2,4,6-trichloroanisole from naturally contaminated cork discs: reactor design and proof of concept. Chem. Eng. J. 361, 80–88. https://doi.org/10.1016/j.cej.2018.12.040. August 2018.

Jablonowski, H., von Woedtke, T., 2015. Research on plasma medicine-relevant plasma-liquid interaction: what happened in the past five years? Clinical Plasma Medicine 3 (2), 42–52. https://doi.org/10.1016/j.cpme.2015.11.003.

Kavitha, V., Palanivelu, K., 2016. Degradation of phenol and trichlorophenol by heterogeneous photo-Fenton process using Granular Ferric Hydroxide®: comparison with homogeneous system. Int. J. Environ. Sci. Technol. 13 (3), 927–936. https://doi.org/10.1007/s13762-015-0922-y.

Liu, K., Liu, S.T., Ran, C.F., 2020. The effect of air-water-plasma-jet-activated water on Penicillium: the reaction of HNO2 and H2O2 under acidic condition. Frontiers in Physics 8 (2), 1–12. https://doi.org/10.3389/fphy.2020.00242.

Lukes, P., Dolezalova, E., Sisrova, I., Clupek, M., 2014. Aqueous-phase chemistry and bactericidal effects from an air discharge plasma in contact with water: evidence for the formation of peroxynitrite through a pseudo-second-order post-discharge reaction of H2O 2 and HNO2. Plasma Sources Sci. Technol. 23 (1) https://doi.org/10.1088/0963-0252/23/1/015019.

Lukes, Ptr, Akiyama, H., Jiang, C., Doria, A., Gallerano, G.P., Ramundo-Orlando, A., et al., 2017. Special electromagnetic agents: from cold plasma to pulsed electromagnetic radiation. In: Bioelectrics. https://doi.org/10.1007/978-4-431-56095-1.

Martín, R. B. (2018). 2 726 598.

Monteiro, S., Bundaleski, N., Malheiro, A., Cabral, M., Teodoro, O.M.N.D., 2022. Cross contamination of 2,4,6-trichloroanisole in cork stoppers. J. Agric. Food Chem. 70 (22), 6747–6754. https://doi.org/10.1021/acs.jafc.2c02493.

OIV, 2009. Compendium of International Methods of Analysis-OIV Alkalinity of Ash, vol. 2. International Organisation of Vine and Wine.

Palacios, F. S., Misiego, C. I., Montero, M. J. S., García, J. M., & Sánchez, N. M. (2012). 2 423 255.

Pan, J., Li, Y.L., Liu, C.M., Tian, Y., Yu, S., Wang, K.L., et al., 2017. Investigation of cold atmospheric plasma-activated water for the dental unit waterline system contamination and safety evaluation in vitro. Plasma Chem. Plasma Process. 37 (4), 1091–1103. https://doi.org/10.1007/s11090-017-9811-0.

Peter, A., Von Gunten, U., 2007. Oxidation kinetics of selected taste and odor compounds during ozonation of drinking water. Environ. Sci. Technol. 41 (2), 626–631. https://doi.org/10.1021/es061687b.

Ponte, M. L. D. M. N. Da, Lopes, J. A. D. S., Vesna, N.-V., Manic, M., Mesquita, A. C. D. A. L. C., Silva, R. P. M. Da, & Montenegro, I. M. D. Q. (2013). 2 402 890.

Qi, F., Xu, B., Chen, Z., Ma, J., Sun, D., Zhang, L., Wu, F., 2009. Ozonation catalyzed by the raw bauxite for the degradation of 2,4,6-trichloroanisole in drinking water. J. Hazard Mater. 168 (1), 246–252. https://doi.org/10.1016/j.jhazmat.2009.02.037.

Qi, F., Xu, B., Zhao, L., Chen, Z., Zhang, L., Sun, D., Ma, J., 2012. Comparison of the efficiency and mechanism of catalytic ozonation of 2,4,6-trichloroanisole by iron and manganese modified bauxite. Appl. Catal. B Environ. 121–122, 171–181. https://doi.org/10.1016/j.apcatb.2012.04.003.

Rathore, V., Nema, S.K., 2021. Optimization of process parameters to generate plasma activated water and study of physicochemical properties of plasma activated solutions at optimum condition. J. Appl. Phys. 129 (8) https://doi.org/10.1063/5.0033848.

Recio, E., Álvarez-Rodríguez, M.L., Rumbero, A., Garzón, E., Coque, J.J.R., 2011a. Destruction of chloroanisoles by using a hydrogen peroxide activated method and its application to remove chloroanisoles from cork stoppers. J. Agric. Food Chem. 59 (23), 12589–12597. https://doi.org/10.1021/jf2035753.

Recio, E., Álvarez-Rodríguez, M.L., Rumbero, A., Garzón, E., Coque, J.J.R., 2011b. Destruction of chloroanisoles by using a hydrogen peroxide activated method and its application to remove chloroanisoles from cork stoppers. J. Agric. Food Chem. 59 (23), 12589–12597. https://doi.org/10.1021/jf2035753.

Revolution, E., 2021. Why OH group shows MORE +R than OCH3. Retrieved June 1, 2023, from. https://edurev.in/question/264878/Why-OH-group-shows-MORE-R-than-OCH3#:~:text=The OH group is more acidic%2C nucleophilic%2C and can form, versatile than the OCH3 group.

Saritha, P., Raj, D.S.S., Aparna, C., Laxmi, P.N.V., Himabindu, V., Anjaneyulu, Y., 2009. Degradative oxidation of 2,4,6 trichlorophenol using advanced oxidation processes - a comparative study. Water Air Soil Pollut. 200 (1–4), 169–179. https://doi.org/10.1007/s11270-008-9901-y.

Sefton, M.A., Simpson, R.F., 2005. Compounds causing cork taint and the factors affecting their transfer from natural cork closures to wine - a review. Aust. J. Grape Wine Res. 11 (2), 226–240. https://doi.org/10.1111/j.1755-0238.2005.tb00290.x.

Silva Pereira, C., Figueiredo Marques, J.J., San Romão, M.V., 2000. Cork taint in wine: scientific knowledge and public perception - a critical review. Crit. Rev. Microbiol. 26 (3), 147–162. https://doi.org/10.1080/10408410008984174.

Simpson, R.F., Sefton, M., 2007. Origin and fate of 2,4,6-trichloroanisole in cork bark and wine corks. Aust. J. Grape Wine Res. 13 (2), 106–116. https://doi.org/10.1111/j.1755-0238.2007.tb00241.x.

Soleas, G.J., Yan, J., Seaver, T., Goldberg, D.M., 2002. Method for the gas chromatographic assay with mass selective detection of trichloro compounds in corks and wines applied to elucidate the potential cause of cork taint. J. Agric. Food Chem. 50 (5), 1032–1039. https://doi.org/10.1021/jf011149c.

Tarabová, B., Lukeš, P., Janda, M., Hensel, K., Šikurová, L., Machala, Z., 2018. Specificity of detection methods of nitrites and ozone in aqueous solutions activated by air plasma. Plasma Process. Polym. 15 (6) https://doi.org/10.1002/ppap.201800030.

Tarasov, A., Rauhut, D., Jung, R., 2017. "Cork taint" responsible compounds. Determination of haloanisoles and halophenols in cork matrix: a review. Talanta 175 (March), 82–92. https://doi.org/10.1016/j.talanta.2017.07.029.

Trewick, S.C., McLaughlin, P.J., Allshire, R.C., 2005. Methylation: lost in hydroxylation? EMBO Rep. 6 (4), 315–320. https://doi.org/10.1038/sj.embor.7400379.

Valdés, O., Marican, A., Avila-Salas, F., Castro, R.I., Amalraj, J., Laurie, V.F., Santos, L.S., 2018. Polyaniline based materials as a method to eliminate haloanisoles in spirits beverages. Ind. Eng. Chem. Res. 57 (24), 8308–8318. https://doi.org/10.1021/acs.iecr.8b01139.

Viguera, M., Prieto, C., Casas, J., Casas, E., Cabañas, A., Calvo, L., 2018. The parameters that affect the supercritical extraction OF 2,4,6-trichloroanisol from cork. J. Supercrit. Fluids 141 (March), 137–142. https://doi.org/10.1016/j.supflu.2018.03.017.

Xu, B., Qi, F., 2016. Reaction mechanism of 2-methylisoborneol and 2,4,6-trichloroanisole in catalytic ozonation by γ-AlOOH: role of adsorption. Clean 44 (9), 1099–1105. https://doi.org/10.1002/clen.201500749.

Zhang, L.L., Leng, S.Q., Zhu, R.Y., Chen, J.M., 2011. Degradation of chlorobenzene by strain Ralstonia pickettii L2 isolated from a biotrickling filter treating a chlorobenzene-contaminated gas stream. Appl. Microbiol. Biotechnol. 91 (2), 407–415. https://doi.org/10.1007/s00253-011-3255-x.

Zhang, N., Geronimo, I., Paneth, P., Schindelka, J., Schaefer, T., Herrmann, H., et al., 2016. Analyzing sites of OH radical attack (ring vs. side chain) in oxidation of substituted benzenes via dual stable isotope analysis (δ13C and δ2H). Sci. Total Environ. 542, 484–494. https://doi.org/10.1016/j.scitotenv.2015.10.075.

Zhang, Q., Ma, R., Tian, Y., Su, B., Wang, K., Yu, S., et al., 2016. Sterilization efficiency of a novel electrochemical disinfectant against Staphylococcus aureus. Environ. Sci. Technol. 50 (6), 3184–3192. https://doi.org/10.1021/acs.est.5b05108.

Zhang, X., Zhou, R., Bazaka, K., Liu, Y., Zhou, R., Chen, G., et al., 2018. Quantification of plasma produced OH radical density for water sterilization. Plasma Process. Polym. 15 (6), 1–12. https://doi.org/10.1002/ppap.201700241.

Zhou, R., Zhou, R., Wang, P., Xian, Y., Mai-Prochnow, A., Lu, X., et al., 2020. Plasma-activated water: generation, origin of reactive species and biological applications. J. Phys. Appl. Phys. 53 (30) https://doi.org/10.1088/1361-6463/ab81cf.

5. RESULTADOS Y DISCUSIÓN CONJUNTA

En este capítulo se detallan y discuten los resultados de cada uno de los artículos incluidos en esta tesis en función de los cuatro objetivos específicos planteados. Cada apartado se ha dividido a su vez en subapartados con el fin de describir cada una de las publicaciones individualmente.

5.1. EFECTO ANTIMICROBIANO DEL TRATAMIENTO DEL PLASMA ATMOSFÉRICO FRÍO SOBRE MICROORGANISMOS DE INTERÉS CLÍNICO Y ALIMENTARIO

Se describen los resultados de inhibición del crecimiento o inactivación de cada microorganismo según la publicación en la que se ha estudiado.

5.1.1. MASCARILLAS

Se evaluó la capacidad antimicrobiana de tratamientos directos de PAF generados con nitrógeno, aire y argón durante tiempos y potencias diferentes (Tabla 3) sobre las bacterias *E. coli* ATCC25922, *P. aeruginosa* PAO1 y *S. aureus* ATCC29213 inoculadas sobre los discos de mascarillas KN95. La Fig. 21 muestra los resultados obtenidos en comparación con sus respectivos controles-positivos.

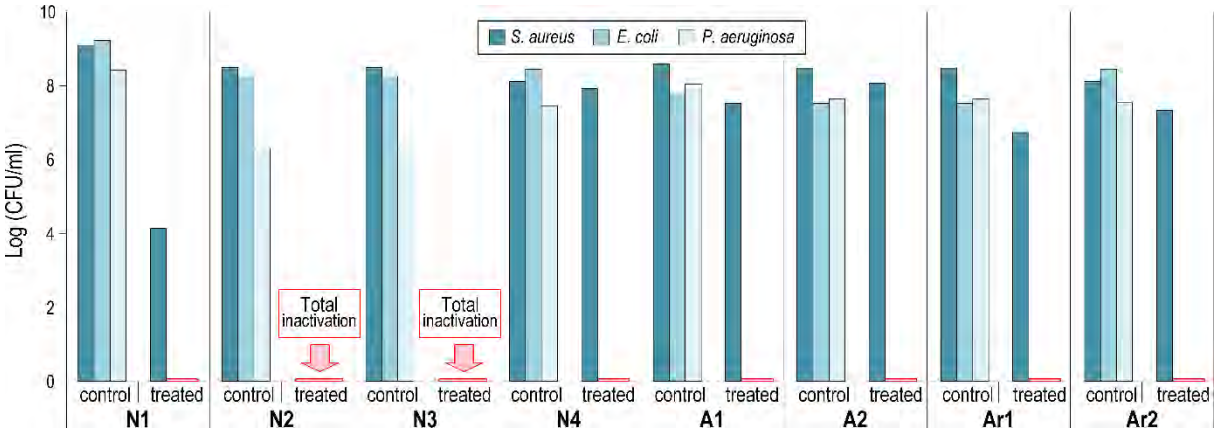

Fig. 21. Actividad antimicrobiana de los tratamientos de plasma en discos de mascarillas frente a *S. aureus* ATCC29213, *E. coli* ATCC25922 y *P. aeruginosa* PAO1.

Se observó que el grado de inactivación bacteriana estuvo influido por las especies bacterianas analizadas y a su vez por los parámetros del tratamiento de plasma. Así, los tratamientos con N_2 (N2 y N3) fueron los mejores ya que consiguieron la inactivación total de todas las bacterias (*E. coli* ATCC25922, *P. aeruginosa* PAO1 y *S. aureus* ATCC29213). Además, las bacterias *E. coli* y *P. aeruginosa* llegaron a una letalidad total con cualquiera de los tratamientos de plasma aplicados, mientras que *S. aureus* fue la especie bacteriana más resistente al tratamiento de PAF, como también describieron estudios previos [67–70]. Varios autores consideran las características morfológicas de los microorganismos como uno de los factores

[67–70]. Varios autores consideran las características morfológicas de los microorganismos como uno de los factores responsables de las diferencias en inactivación [68]. En este sentido, tanto las bacterias Gram-positivas como las Gram-negativas poseen peptidoglicanos en la pared celular; sin embargo, las bacterias Gram-positivas tienen una pared gruesa de peptidoglicanos que les permite resistir mejor el daño del plasma. Se han identificado diferentes mecanismos de acción para su inactivación dependiendo de que se trate de bacterias Gram-positivas o Gram-negativas [71,72]. Así, en el caso de las bacterias Gram-positivas, se ha sugerido que los RONS desempeñan el papel principal en la provocación de alteraciones de la membrana lipídica tras la peroxidación lipídica de los ácidos grasos insaturados. La oxidación de aminoácidos provoca la modificación de proteínas, seguida de daños en el ADN y muerte celular [73–75]. En el caso de las bacterias Gram-negativas, cuya superficie es irregular, se ha descrito la disrupción electrostática como el efecto más eficaz [61,70]. Este mecanismo implica la ruptura de la membrana cuando ésta adquiere suficiente carga eléctrica. En cuanto a las bacterias analizadas en este trabajo, *E. coli* y *P. aeruginosa* son bacterias Gram-negativas, y *S. aureus* es Gram-positiva, lo que podría explicar las diferencias en las tasas de inactivación.

Por otro lado, el tiempo de tratamiento con plasma, la potencia o el gas, influyeron en los resultados de inactivación bacteriana, como otros autores han indicado [67,68,70,76–78]. Algunos demostraron que cuanto mayor era el tiempo de exposición, mayor era el daño bacteriano [67]. Esto concuerda con los resultados de este trabajo, pues el tratamiento N1 (45 seg, 300 W) consiguió una reducción de 4,96 log UFC/mL mientras que el N2 (1,5 min, 300 W) o el N3 (2,5 min, 300 W), provocaron una inactivación total. Sin embargo, aunque el tiempo de tratamiento con plasma N4 fue el más largo (5 min, 220 W), la potencia del plasma no fue suficiente para inactivar todas las bacterias. El tratamiento con N2 (300 W; 1,5 minutos) produjo valores de inactivación superiores a los de N4 (220 W; 5 min), indicando que la potencia del tratamiento desempeña un papel más importante que el tiempo de tratamiento. En esta línea, un estudio anterior observó que al aumentar la potencia de 75 W a 125 W del tratamiento de plasma, también aumenta la inactivación frente a *L. monocytogenes, E. coli* y *S. Typhimurium* [79]. Por tanto, como la potencia del plasma proporciona energía para generar RONS, cuanto mayor sea la potencia, mayor será la cantidad de RONS generados para inactivar las bacterias [80,81].

Por último, el gas de plasma desempeñó uno de los papeles principales en términos de actividad antimicrobiana. Comparando los gases estudiados (nitrógeno, aire y argón), el mejor fue el nitrógeno ya que consiguió una inactivación total independientemente de las bacterias utilizadas. También se estudió el efecto de los tratamientos con N2 y N3 contra *P. aeruginosa* ATCC15692GFP analizando sus actividades antimicrobianas y los niveles de fluorescencia de la GFP (Fig. 22). Ambos tratamientos con plasma consiguieron alta actividad antimicrobiana (>7 log UFC/mL) y también redujeron la concentración de proteína. Las señales de GFP tras los tratamientos N2 y N3 fueron del 43% y 54% respectivamente, en comparación con la señal control (100%) con diferencias estadísticamente significativas ($p \leq 0,05$). Por lo tanto, se confirmó que ambos tratamientos fueron eficaces contra *P. aeruginosa* ATCC15692GFP.

Teniendo en cuenta que especies de *Staphylococcus* son causantes de infecciones cutáneas y nasofaríngeas, que además pueden estar implicadas en los tipos más agresivos de maskné, se eligieron diferentes cepas de *Staphylococcus* spp. para evaluar el efecto del mejor tratamiento de PAF que fue N2. Se trataron discos de mascarillas inoculados con *S. hominis* W220, *S. haemolyticus* W1493, *S. saprophyticus* W1498, *S. epidermidis* W213, *S. epidermidis* W232, *S. epidermidis* W1346, *S. aureus* W1623 y *S. aureus* W1570 y todas ellas, incluyendo las bacterias multirresistentes a los antibióticos, mostraron crecimiento cero tras la aplicación de PAF.

Además, se utilizaron mascarillas enteras inoculadas con *E. coli* ATCC25922, *P. aeruginosa* PAO1 y *S. aureus* ATCC29213 consiguiendo más de 6 $\log_{10}$ de reducción. Con el fin de discernir entre el efecto térmico del plasma y el efecto directo del mismo (RONS, luz UV, etc.), se caracterizó la temperatura máxima a la que llegaba el tratamiento N2.

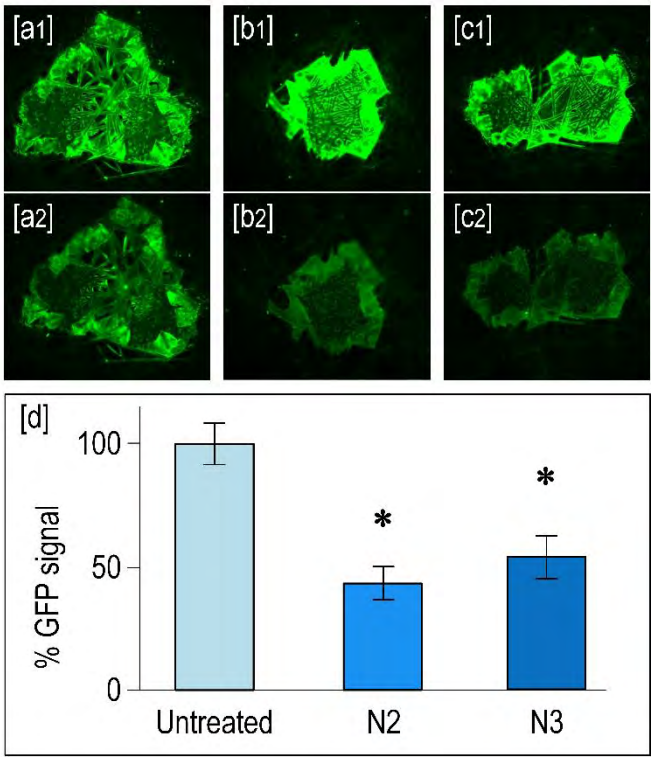

Fig. 22. Imágenes digitales de microscopio de fluorescencia de la cuantificación de GFP: antes (a1, b1 y c1) y después (a2, b2 y c2) de los tratamientos con plasma CT, N2 y N3, respectivamente y (d) Porcentaje de señal de GFP de estos tratamientos (∗, $p \leq 0,05$).

La Fig. 23 muestra las imágenes térmicas de la capa exterior de la mascarilla con el tratamiento de N2 a diferentes tiempos donde se observa una distribución térmica homogénea, indicando un tratamiento de plasma homogéneo. Las temperaturas en la superficie exterior de la mascarilla al final del tratamiento con N2 oscilaron entre 80 °C y 90 °C. Por otra parte, la temperatura máxima alcanzada en la capa interior de la mascarilla fue de 100 ºC y dicha temperatura se aplicó al flujo de nitrógeno durante 1,5 min sobre las mascarillas inoculadas.

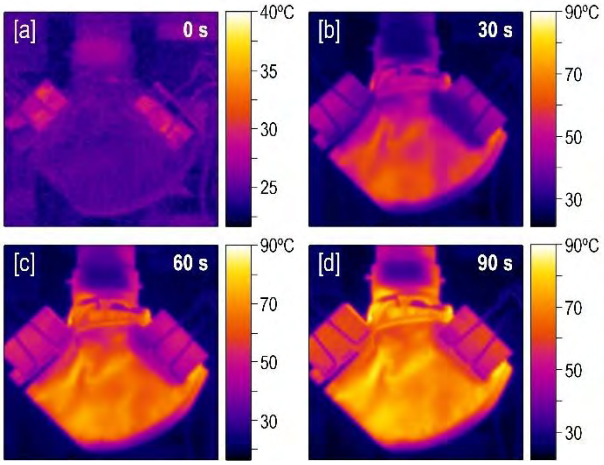

Fig. 23. Termografía de la capa externa durante el tratamiento de plasma N2 a diferentes tiempos: (a) 0 segundos, (b) 30 segundos, (c) 60 segundos y (d) 90 segundos.

Con los datos obtenidos en la Tabla 8 se puede sugerir que el efecto térmico fue la causa principal de la inactivación de *P. aeruginosa* y *E. coli*, ya que ambos tratamientos (plasma y flujo térmico) produjeron la eliminación total de ambas bacterias.

Sin embargo, el flujo térmico fue insuficiente para inactivar *S. aureus*, pudiendo afirmar que el tratamiento con plasma fue necesario para la eliminación total de esta bacteria además del tratamiento con flujo térmico. Hasta donde se sabe, las bacterias pueden inactivarse mediante una combinación de varios factores, entre ellos el tiempo y el tratamiento térmico. En este sentido, algunos autores han estudiado cómo afecta el tratamiento térmico en la inactivación de diferentes bacterias y han concluido que cuanto mayor sea la temperatura y el tiempo de tratamiento, mayor será la inactivación bacteriana [82–84].

Tabla 8. Comparación de los resultados de actividad antimicrobiana de N2 y del tratamiento térmico frente a *S. aureus* ATCC29213, *E. coli* ATCC25922, y *P. aeruginosa* PAO1 inoculadas en mascarillas completas. Los datos están mostrados en UFC/mL.

Bacteria	Bacteria recuperada en las muestras control		Bacteria recuperada tras cada tratamiento de plasma (reducción logarítmica)	
	Control	Tratamiento térmico	N2	Tratamiento térmico
S. aureus ATCC29213	8,75	9,13	1,54 (7,21)	8,51 (0,62)
E. coli ATCC25922	5,99	5,28	0 (5,99)	0 (5,28)
P. aeruginosa PAO1	8,31	8,11	0 (8,31)	0 (8,11)

5.1.2. DUELAS TRATADAS CON PAW

En esta publicación se aplicaron cuatro PAW con diferentes tiempos de generación contra la levadura *B. bruxellensis*.

En la Fig. 24 se muestran los resultados obtenidos tras la aplicación de PAW en comparación con el tratamiento de SO_2 y una muestra control en AP. Tras aplicar la PAW generada durante 1,5 min (PAW-1,5), la población de *B. bruxellensis* se redujo 1,46 ± 0,27 unidades logarítmicas. Sin embargo, la reducción fue enorme con PAW-5, PAW-15 o PAW-30. Así, se consiguieron reducciones de 3,49 ± 0,83 log_{10} con PAW-5 y una inactivación total (4,35 ± 0,00 log_{10}) con la PAW generada durante 15 y 30 min (no se mostraron diferencias estadísticamente significativas entre ambas).

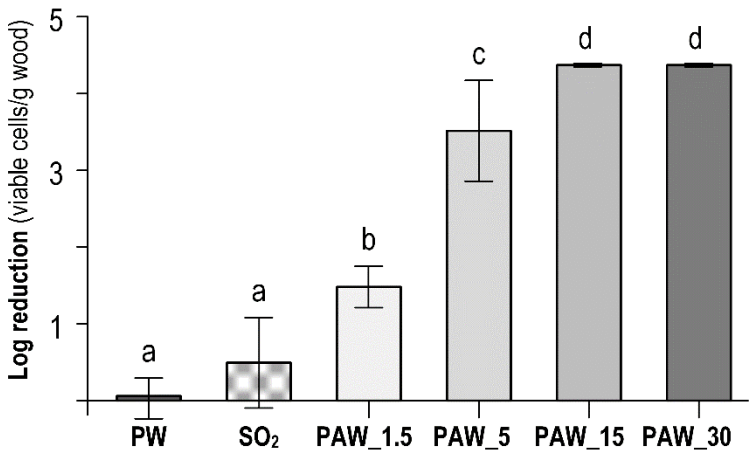

Fig. 24. Reducción microbiana de *B. bruxellensis* en duelas de madera tras 3 h en contacto con: AP (PW), SO_2 y tratamientos de PAW. Las letras a, b, c y d indican las diferencias significativas entre los tratamientos ($p \leq 0,05$).

En este trabajo se explica que las características físico-químicas de cada PAW desempeñaron un papel clave para entender por qué la respuesta de los microorganismos no fue la misma con todas las PAW.

A mayor tiempo de tratamiento, mayores las concentraciones de OH•, NO• y NO_2•. Se sabe que esas especies reactivas, así como el peroxinitrito, tienen una fuerte actividad antimicrobiana [56,58,85]. Son capaces de desencadenar tanto reacciones de oxidación y nitración en las células biológicas, como la peroxidación de lípidos, proteínas y daños en el ADN [48,57,86–88]. En este sentido, se sugirió la muerte de la levadura como consecuencia de las RONS al afectar al estado de oxidación-

reducción de los antioxidantes, el daño de la membrana y la alteración de la estructura celular [89,90]. Además, se demostró que las ROS intrínsecas aumentan tras el tratamiento con PAW dentro de las células de levadura provocando una sobreacumulación que puede causar estrés oxidativo y muerte celular [68,91]. Así, en este trabajo se sugirió un mecanismo por el cual muere la levadura estudiada. El mecanismo podría iniciarse por una peroxidación lipídica en la membrana celular, seguida de una ruptura y daño de la membrana celular que da lugar a una fuga; entonces los RONS podrían entrar fácilmente en la célula y acumularse provocando un choque de potencial de membrana y finalmente produciendo la muerte celular [91].

5.2. EFECTO DE DESCOMPOSICIÓN DEL TRATAMIENTO DEL PLASMA ATMOSFÉRICO FRÍO SOBRE MOLÉCULAS QUÍMICAS DE INTERÉS ALIMENTARIO, EN CONCRETO DE LA INDUSTRIA ENOLÓGICA.

En este apartado se describen los resultados obtenidos tras la aplicación de PAW a corchos de botellas de vino con el fin de descomponer haloanisoles (Sainz-García, A., et al. 2023).

Se probaron cuatro PAW diferentes contra corchos contaminados artificialmente; estas PAW son las mismas que las utilizadas en el artículo Sainz-García, A., et al. (2024). Como controles se utilizaron tres corchos contaminados artificialmente y se empleó AP para evaluar los posibles efectos del lavado. La Fig. 25 muestra la concentración media de TCA en muestras de corcho después de 3 h de contacto con PAW y AP y la concentración de TCA en corchos contaminados (como control). El compuesto principal que se analizó fue el TCA ya que es el más importante en la industria enológica. Para el tiempo de generación de PAW más corto (PAW-1,5) únicamente se eliminó el 18,1% del TCA, mientras que para PAW-5, PAW-15 y PAW-30 no hubo diferencias estadísticamente significativas, alcanzándose un 75,2%, un 65,0 % y un 72,6% de eliminación del TCA, respectivamente. Por último, los tapones tratados con AP no mostraron cambios en el contenido de TCA con respecto al control, lo que significa que no se produjo un efecto de lavado.

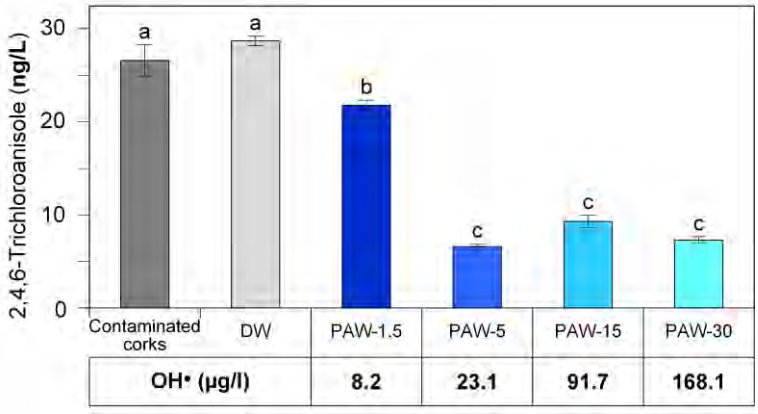

Fig. 25. Concentración media de TCA (ng/L) en corchos tras 3 h de inmersión en PAW y AP (DW) y concentración de OH• de cada PAW. Las letras a, b y c indican las diferencias significativas entre los tratamientos ($p \leq 0,05$).

Algunos autores cuantificaron los productos de reacción de OH• con ácido salicílico [92], indicando que la medición de 2,3-DHBA y 2, 5-DHBA debería proporcionar una estimación precisa de la cantidad de OH•, con lo que encontraron concentraciones más altas cuando se utilizaba aire y oxígeno como gases de plasma y tiempos de tratamiento más largos. En este trabajo de la tesis se propuso el radical OH• como la especie reactiva que juega el papel principal en la descomposición del TCA. Como consecuencia, los valores más bajos de TCA se obtuvieron con PAW-1,5 porque el nivel de OH• era el mínimo (Fig. 25). Por otro lado, la mayor descomposición podría esperarse para el tratamiento con PAW-30; sin embargo, parece que una alta concentración de OH• no produjo la máxima descomposición. Diferentes autores indicaron que un exceso en la generación de OH• provocaba el apagado del OH• [93]. Esto es lo que probablemente ocurre en el caso de la PAW generada durante los tiempos de activación más altos, 15 y 30 min. Por lo tanto, PAW-5 logró la mayor descomposición del TCA.

Asimismo, en este trabajo se sugirió un mecanismo por el cual el radical OH• ataca a las moléculas de TCA. El OH• tiene un alto potencial oxidativo y es conocido por oxidar moléculas que otros radicales ni siquiera pueden hacer reaccionar. Teniendo en cuenta lo dicho por algunos autores, el primer ataque del OH• a la molécula de TCA sería en los sitios donde el cloro no está enlazado [94]. Por lo tanto, se propuso que el grupo -OCH_3 podría ser el objetivo. Esto concuerda con lo sugerido por otros investigadores, quienes mostraron la reacción entre OH• y el grupo -OCH_3 por abstracción de H, seguida de una reacción con O_2 formando radicales peroxilo y finalmente una desprotonización, quizás a través del mecanismo de Russell [95]. También, se sugirió una desmetilación por hidroxilación; así, el OH• podría ser capaz de eliminar el grupo metilo del TCA [96]. Una vez atacado el grupo -OCH_3, el OH• se dirigiría a los enlaces de cloro [96,97]. Además, existen dos mecanismos posibles para atacar a los átomos de cloro. El primero tiene lugar cuando los tres átomos de cloro se sustituyen por OH• [98]. El segundo se caracteriza por una disociación de átomos de cloro [94].

Asimismo, en este artículo se analizaron otras moléculas químicas importantes de la industria enológica alcanzando su descomposición como se muestra en las Fig. 26 y Fig. 27.

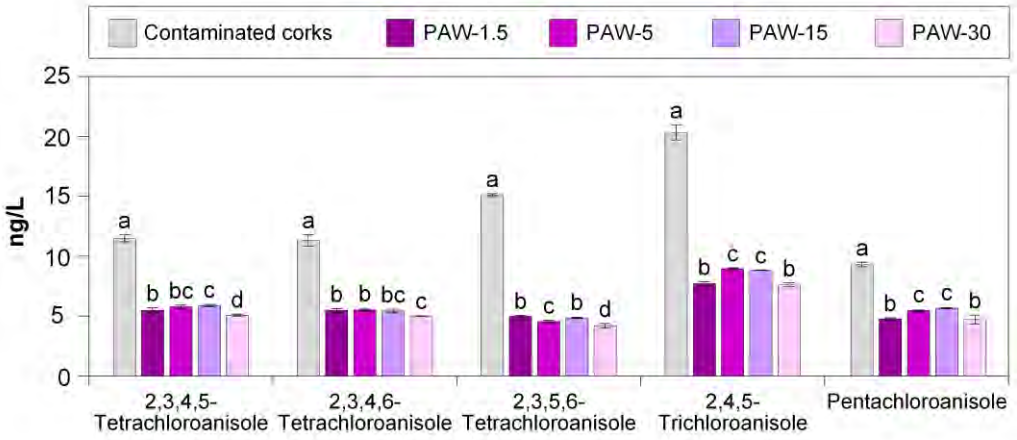

Fig. 26. Concentración media de cloroanisoles (ng/L) en corchos tras 3 h de inmersión en PAW y AP.

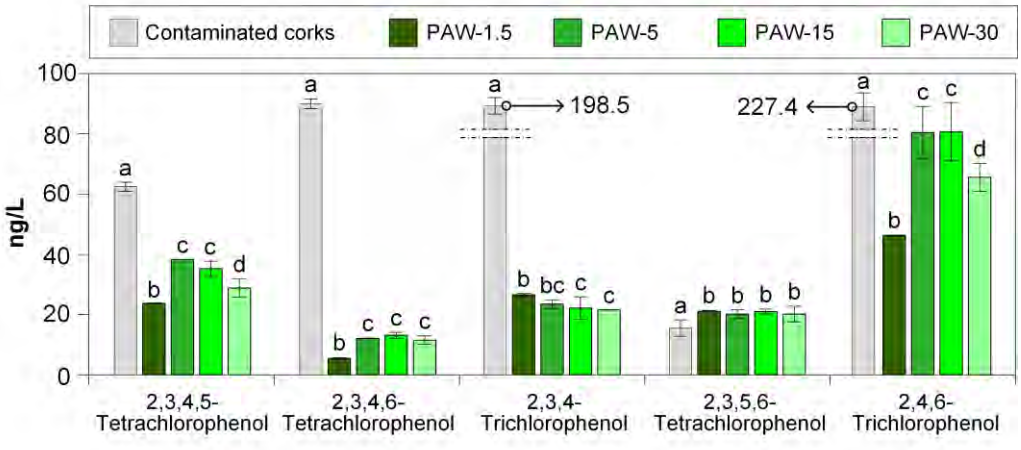

Fig. 27. Concentración media de clorofenoles (ng/L) en corchos tras 3 h de inmersión en PAW y AP.

5.3. EFECTO DEL TRATAMIENTO CON PAF EN LAS CARACTERÍSTICAS MORFOLÓGICAS Y FUNCIONALES DE LAS SUPERFICIES TRATADAS

En este subapartado se procede a describir las características morfológicas y funcionales de las superficies tratadas con PAF, bien directo o indirecto en comparación con ellas mismas sin tratar. Como se ha comentado anteriormente, en la presente tesis se han estudiado estas características en mascarillas y fragmentos de duelas de madera.

5.3.1. MASCARILLAS

En la publicación Sainz-García, A., (2022) se realizaron ensayos para comprobar las características físicas, morfológicas y funcionales de las mascarillas aplicando 5 ciclos del tratamiento de PAF N2 caracterizado por ser plasma de N_2 durante 1,5 min a 300 W.

El análisis SEM mostró que el tratamiento con plasma no impactó negativamente en la morfología de la superficie de las capas 4 y 5 de las mascarillas (Fig. 28). No se observaron diferencias entre las fibras de las mascarillas a las que se aplicaron los 5 ciclos de tratamiento de plasma en comparación con la mascarilla control, es decir una mascarilla sin tratamiento.

En esta misma línea, se hicieron pruebas con el fin de comprobar si el tratamiento con plasma aplicado en esta investigación reducía la capacidad de confort mecánico y facial y si aparecían modificaciones visuales. No se observaron diferencias entre las mascarillas control y las tratadas; es decir, no se produjeron fragmentos ni estiramientos de las tiras elásticas ni degradación del color de la mascarilla.

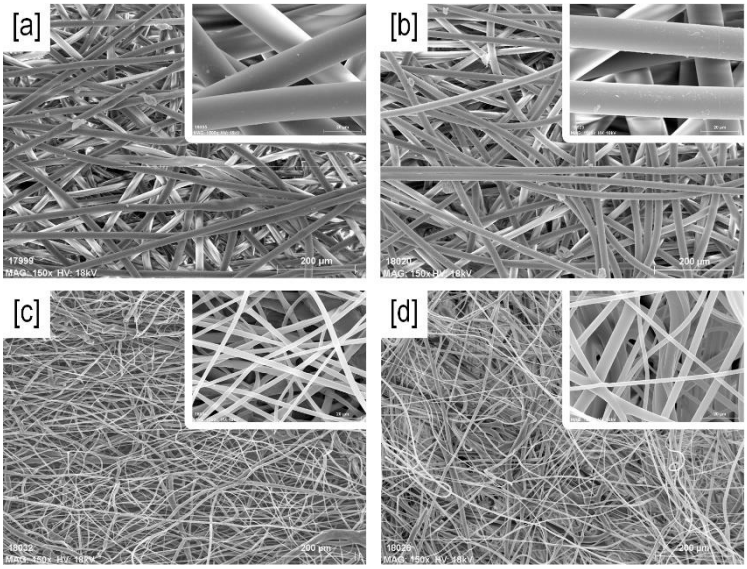

Fig. 28. Imágenes SEM con magnificación 150x y 1500x de: [a,c] Capas 5 y 4 sin tratar y [b,d] capas 5 y 4 de mascarillas completas tras 5 ciclos de tratamiento directo con PAF N2.

En cuanto a las características funcionales, las mascarillas se sometieron a un test de capacidad de filtración (CF) y de resistencia a la respiración. La Tabla 9 indica los valores obtenidos en estos análisis tras uno y cinco ciclos de tratamiento y de ellos se revela que ninguno de los tratamientos aplicados afecta a la CF o a la resistencia a la respiración. Así se comprueba que la resistencia a la inhalación (30 L/min) aumentó de 0,387 mbar a 0,420 mbar después de un ciclo y disminuyó de 0,466 mbar a 0,410 mbar después de cinco ciclos, diferencias que no fueron significativas ($p \leq 0,05$). Por el contrario, en el estudio de la inhalación 95 L/min y la resistencia a la respiración, se produjo un ligero aumento tras un ciclo, pero una disminución después de cinco ciclos. Por último, el número de ciclos no afectó a la CF, que fue similar a la de las mascarillas de control.

Un ligero aumento de la respiración implica una pequeña disminución de la CF. No obstante, esta reducción podría despreciarse teniendo en cuenta que la CF de las mascarillas tratadas durante cinco ciclos sólo perdió un 3,4% de CF con respecto a las mascarillas de control (CF = 1,418). El estudio demostró que las mascarillas tratadas mantuvieron una CF de 1,468; similar a la de FFP3 (CF = 1).

Tabla 9. Capacidad de filtración y respirabilidad tras 1 (KN95) y 5 (FFP2) ciclos de tratamiento con plasma.

Tipo de mascarilla y tratamiento		Resistencia a la inhalación		Resistencia a la exhalación	Porcentaje de penetración de parafina
		30 L/min	95 L/min	160 L/min	
KN95	Control	0,387 ± 0,02	1,217 ± 0,05	2,160 ± 0,02	7,148 ± 0,31
	1 ciclo	0,420 ± 0,01	1,350 ± 0,02	2,277 ± 0,09	7,135 ± 0,22
FFP2	Control	0,466 ± 0,03	2,020 ± 0,05	2,986 ± 0,01	1,418 ± 0,18
	5 ciclos	0,410 ± 0,03	1,918 ± 0,05	2,954 ± 0,01	1,468 ± 0,21

5.3.2. DUELAS DE MADERA

Fragmentos de duelas de madera de barrica de roble fueron las superficies de estudio para dos de las publicaciones incluidas en la presente tesis. Asimismo, en ambos estudios se analizaron las muestras mediante la técnica SEM para comprobar si el tratamiento con plasma aplicado afectaba negativamente a las características morfológicas de las mismas.

En Sainz-García, A., et al. (2024) se sumergieron las muestras en cuatro PAW durante 3 h. El análisis SEM se realizó para la PAW más potente, es decir, la generada durante 30 min (PAW-30) en comparación con la muestra control (AP) y la muestra tras aplicarle el mechado de sulfuroso (SO_2) (Fig. 29).

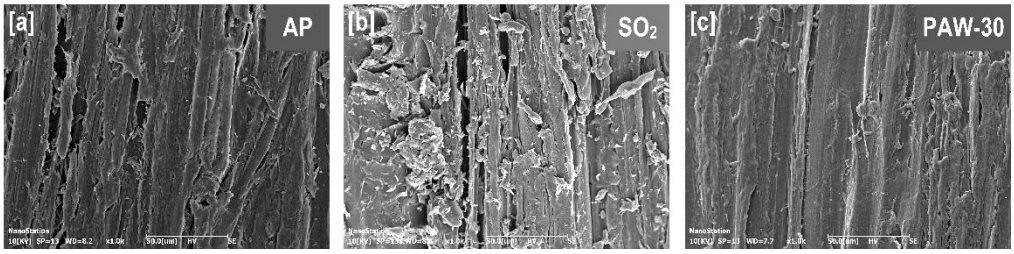

Fig. 29. Imágenes SEM con magnitud 1000x de las muestras tratadas con [a] agua purificada; [b] sulfuroso y [c] PAW-30.

Por un lado, comparando el tratamiento PAW-30 y el tratamiento AP no se encontraron diferencias morfológicas. Así, después de ambos tratamientos se observó una superficie lisa con fibras y vasos de madera bien definidos. Por otro lado, se observó una estructura diferente tras el tratamiento con SO_2. En este caso, estos rasgos se caracterizaron por un aumento de la rugosidad de la madera, así como por la presencia de aglomerados de madera. Se sugirió que estas formas se crean debido al daño químico que el mechado de sulfuroso provoca en la estructura de la madera. De este modo, se produce una rotura de la madera tras el SO_2 que genera enormes vasos y grupos de madera desprendida.

5.4. CARACTERÍSTICAS FÍSICO-QUÍMICAS DEL PLASMA ATMOSFÉRICO FRÍO EN CADA TRATAMIENTO

Otro de los objetivos de esta tesis fue entender los resultados de inactivación microbiana y descomposición química obtenidos. Para ello, se estudiaron las características de cada tipo de plasma (directo y PAW).

En relación al PAF directo (Sainz-García, A., et al. 2022), se empleó espectrometría de emisión óptica (OES) para conocer las especies reactivas que se formaban durante la fase gas. La Fig. 30 muestra los espectros de emisión óptica (200-500 nm) del plasma de nitrógeno, argón y aire. Se identificaron las RONS más relevantes para cada gas de plasma y que podían justificar la actividad antimicrobiana. El espectro del tratamiento con nitrógeno mostró diferentes especies: a) NO• (200-280 nm), b) Segundo sistema positivo (SPS) del nitrógeno (296-405 nm) y c) Primer sistema negativo (FNS) del nitrógeno (a 394 y 427 nm). El SPS y el FNS juegan un destacado papel en la generación de ozono (O_3), una especie con capacidad biocida y que no genera un estado excitado que emita luz.

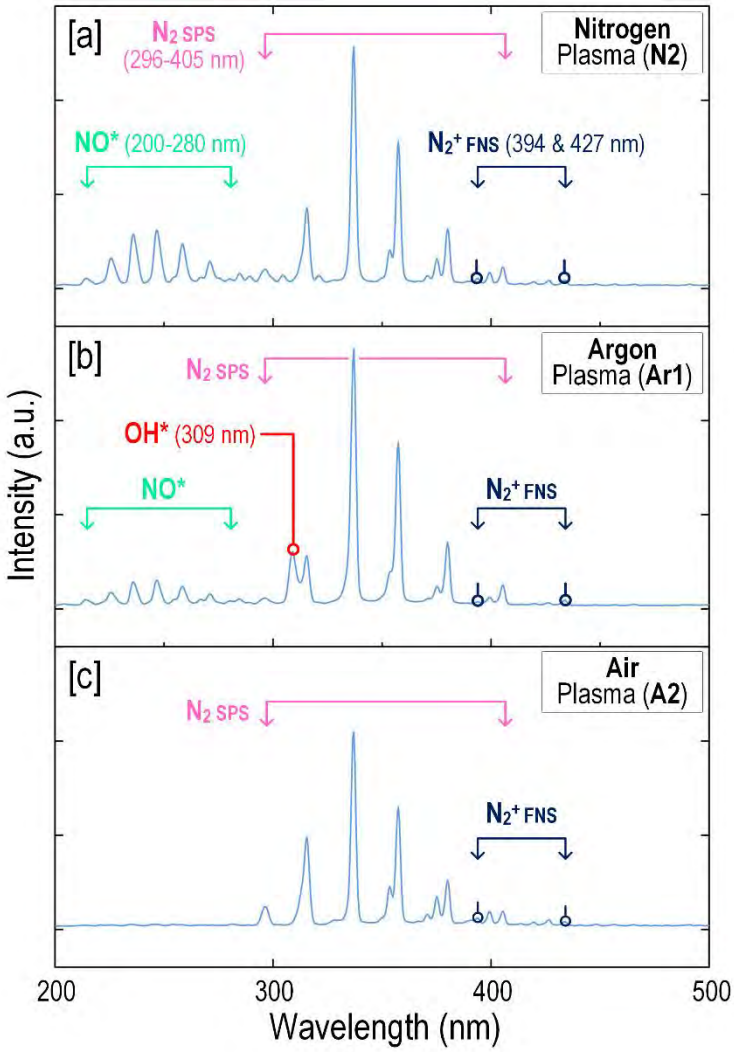

Fig. 30. Espectro de emisión óptica de los tratamientos de plasma: [a] plasma de nitrógeno; [b] plasma de argón y [c] plasma de aire.

El plasma de argón mostró las mismas especies que el de N_2, además del OH• (309 nm). Por último, la Fig. 30c muestra el espectro del PAF de aire, donde sólo se detectaron las especies nitrogenadas SPS y FNS.

Por otro lado, en los estudios Sainz-García, A., et al. (2024) y Sainz-García, A., et al. (2023) se realizó un análisis profundo de las características físico-químicas de cada una de las PAW aplicadas. En la Tabla 10 se muestran los datos de pH, EC, ORP, nitratos y nitritos de cada una de ellas.

Tabla 10. Parámetros fisicoquímicos de cada PAW a temperatura ambiente.

PAW	pH	EC (µS/cm)	ORP (mV)	NO_3^- (mg/L)	NO_2^- (mg/L)
PAW-1,5	4,46 ± 0,15	25 ± 5	315 ± 13	3,67 ± 0,31	0.74 ± 0,05
PAW-5	4,01 ± 0,17	52 ± 7	355 ± 10	4,13 ± 0,15	2,58 ± 0,27
PAW-15	3,58 ± 0,09	103 ± 13	383 ± 9	9,90 ± 1,30	3,47 ± 0,13
PAW-30	3,10 ± 0,12	190 ± 15	408 ± 21	17,90 ± 2,05	5,01 ± 0,87

El pH del AP descendió de 7,00 a 4,46 tras la exposición al plasma durante 1,5 min y bajó a 3,10 tras 30 min, lo que demostró que el tratamiento con plasma acidificó el agua. Se observó un aumento lineal de la EC con el tiempo de activación del plasma, que pasó de 5 µS/cm a 25 µS/cm después de 1,5 min de tratamiento y aumentó a 190 µS/cm después de 30 min. El valor ORP aumentó de 299 mV a 315 mV tras la activación del plasma durante 1,5 min y alcanzó 408 mV después de 30 min. Los cambios en los valores de todos esos parámetros se deben principalmente a la formación de iones activos y especies oxidantes (NO_2^-, H^+, NO_3^-) durante la generación de PAW.

En relación con el análisis químico de la PAW para NO_3^- y NO_2^-, se produjo un aumento significativo de ambas concentraciones durante el tiempo de activación del plasma. Así, las concentraciones más altas se alcanzaron para PAW-30 siendo 17,90 mg/L (NO_3-) y 5,01 mg/L (NO_2^-). Por último, no se detectó H_2O_2 en ninguna de las PAW analizadas. Se sugirió que en caso de exceso de NO_2^-, el H_2O_2 podría haber reaccionado por completo para generar peroxinitrito.

Con el fin de analizar otras especies reactivas secundarias, se siguió un procedimiento de HPLC. Así, la detección de fenol y sus subproductos de degradación se utilizó como método analítico indirecto para evaluar la presencia de OH•, NO• y NO_2• (Fig. 31).

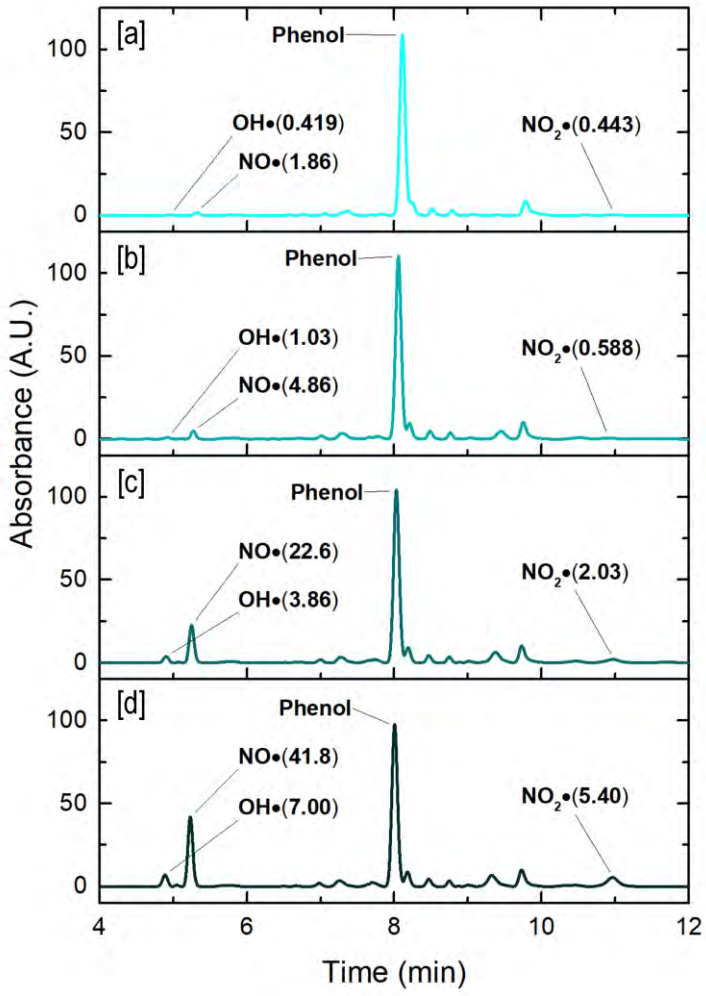

Fig. 31. Cromatogramas HPLC de cada PAW: [a] PAW-1,5; [b] PAW-5; [c] PAW-15 y [d] PAW-30.

La Tabla 11 indica la concentración de los subproductos del fenol para cada PAW analizada. Se observó una tendencia común, ya que los tres subproductos mostraron un aumento conforme al incremento del tiempo de generación de la PAW. En cuanto a la benzoquinona, la PAW-1,5 generó 8,2 µg/L en comparación con los 91,7 µg/L de la PAW-15 y con los 168,1 µg/L de PAW-30. Además, el rango de concentración de 4-nitrosofenol fue entre 227,0 µ/L y 3404,8 µg/L. Por último, el 2-nitrofenol, varió de 209,5 µg/L a 1729,6 µg/L cuando el tiempo de generación de PAW aumentó de 1,5 a 30 min. Estos productos confirmaron la formación de OH•, NO• y NO_2•.

Tabla 11. Cuantificación de los subproductos del fenol para cada PAW.

PAW	Concentración de cada subproducto del fenol (µg/L)		
	Benzoquinona (OH•)	4-nitrosofenol (NO•)	2-nitrofenol (NO_2•)
PAW-1,5	8,2	227,0	209,5
PAW-5	23,1	465,1	253,9
PAW-15	91,7	1873,0	696,1
PAW-30	168,1	3404,8	1729,6

Se han identificado dos posibles teorías sobre el origen de las especies reactivas identificadas mediante cromatografía: a) la inestabilidad de los nitritos acidificados a pH ácido y b) reacciones fotoquímicas inducidas por la radiación UV del plasma con ozono, nitratos y nitritos.

Por otro lado, es conocida la corta vida (nanosegundos) de estas especies reactivas; sin embargo, están implicadas en reacciones cíclicas que podrían justificar su presencia en la PAW durante varias horas y días [56]. Las reacciones cíclicas por las que se cree que estas especies secundarias están presentes en la PAW pese a su corta vida se presentaron en el apartado de la "Introducción" (Reacciones [u-ag]).

Los NO_2^- son inestables a pH bajo y reaccionan con el HNO_2 mediante la reacción $2HNO_2 \rightarrow NO\bullet + NO_2\bullet + H_2O$ [v] generando un radical de óxido nítrico ($NO\bullet$) y un radical de dióxido de nitrógeno ($NO_2\bullet$). Se produce una hidrólisis de $NO_2\bullet$ para producir NO_2^- y NO_3^- (reacción $2NO_2\bullet + H_2O \rightarrow NO_3^- + NO_2^- + 2H^+$ [x]). Además, los radicales secundarios $NO\bullet$ y $NO_2\bullet$, que se conocen como "nitritos acidificados", pueden reaccionar con el oxígeno disuelto y formar $NO_2\bullet$ y NO_3^-, respectivamente (reacciones $4NO\bullet + O_2 + 2H_2O \rightarrow 4NO_2^- + 4H^+$ [y] y $4NO_2^- + O_2 + 2H_2O \rightarrow 4NO_3^- + 4H^+$ [z]) [58]. Por último, mediante la reacción $O_2^{\bullet-} + NO\bullet \leftrightarrow O{=}NOO^- \leftrightarrow O{=}NOOH \leftrightarrow OH\bullet + NO_2\bullet$ [ag], el peroxinitrito se transforma en $OH\bullet$ y $NO_2\bullet$.

Finalmente, se sometieron las PAW a espectroscopía UV-vis para identificar la presencia de otras especies reactivas, concretamente en el rango de 280-400 nm. Fig. 32 muestra el espectro de cada PAW analizada. Así, el espectro de la PAW-30 mostró los mayores valores de absorbancia, seguido de la PAW-15, PAW-5 y PAW-1,5. Cabe destacar el característico grupo de cinco picos entre 330 nm y 395 nm que varios investigadores han asociado a la presencia de un solapamiento de HNO_2 y NO_2^- ([88,99–101]. Estos picos podrían ser una indicación de la presencia de "nitritos acidificados", como muestran las reacciones [u] y [v]. Cabe destacar un solapamiento adicional que se produce en torno a 302 nm, en el que intervienen NO_3^- y peroxinitrito ([100,102].

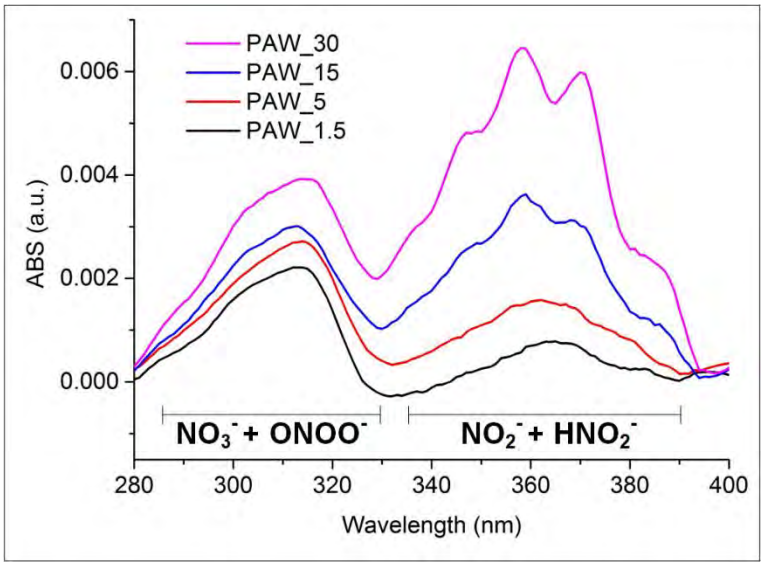

Fig. 32. Espectro UV-vis de cada PAW.

6. CONCLUSIONES/CONCLUSIONS

6.1. CONCLUSIONES

En esta tesis se ha investigado la tecnología del plasma atmosférico frío (PAF) directamente aplicado sobre superficies e indirectamente aplicado mediante agua activada por plasma (PAW). Se ha analizado el grado de inactivación microbiana que esta tecnología es capaz de alcanzar frente a microorganismos de interés clínico y de la industria alimentaria. Asimismo, se ha evaluado la capacidad de la PAW para descomponer moléculas de haloanisoles relacionados con la industria enológica.

Se han realizado análisis de filtración y respirabilidad en las mascarillas estudiadas y ensayos SEM tanto en las mascarillas como en las duelas de madera con el objeto de comprobar si el tratamiento de PAF directo afecta negativamente a las propiedades morfológicas y funcionales de las superficies tratadas.

Se ha caracterizado tanto la fase gas como la fase líquida de los tratamientos de plasma mediante OES, HPLC y espectrometría UV-vis, identificando las especies reactivas (RONS) más importantes y su papel frente al objetivo perseguido.

Tras todo lo anteriormente comentado, las conclusiones de esta tesis son:

1. La tecnología del PAF es capaz de inactivar tanto bacterias como levaduras en distintas superficies como mascarillas o duelas de madera.
2. El grado de inactivación de los microorganismos depende de factores como el gas utilizado en la generación del plasma, la potencia o el tiempo de tratamiento. Así, el argón es el gas menos efectivo en comparación con el aire y el nitrógeno; mientras que con mayores potencias y tiempos de generación de PAF, mayor es la actividad antimicrobiana alcanzada.
3. Cada microorganismo tiene una respuesta diferente al tratamiento con PAF, demostrándose que la inactivación de las especies *E. coli* o *P. aeruginosa* se debe principalmente al efecto térmico de la aplicación directa de PAF; mientras que la inhibición de *S. aureus* se consigue con la suma del efecto térmico y las RONS producidas por el PAF.
4. Se ha demostrado que la tecnología del PAF es capaz de descomponer moléculas químicas como el 2,4,6-Tricloroanisol de tapones de corcho y se ha sugerido que el radical OH• es el responsable de dicha descomposición mediante una vía que posiblemente implica una primera desmetilación del TCA y un ataque posterior del OH• a los átomos de cloro.
5. Se ha observado un aumento de RONS generadas conforme se incrementa el tiempo de producción de PAW. En este sentido, también se han sugerido los mecanismos por los cuales estas RONS reaccionan y se encuentran presentes en la PAW tras varios días. Asimismo, se ha detallado el papel que desempañan cada una de ellas en la inactivación de microorganismos y descomposición de moléculas químicas.
6. Se mantiene la morfología y la capacidad funcional de las superficies tras los tratamientos con la tecnología PAF.

Como conclusión general, teniendo en cuenta todo lo anterior, se puede decir que la tecnología del PAF aplicada directamente o mediante PAW podría ser una solución sostenible y económica para problemas microbianos y químicos de salud global y de la industria alimentaria.

En concreto, la desinfección con PAF de mascarillas usadas podría ser una solución de emergencia para reducir las infecciones faciales y solucionar la escasez de mascarillas, así como los problemas ambientales asociados al descarte de las mismas. Además, esta tecnología desinfectante podría aplicarse a otros objetos y equipos de protección personal utilizados en los hospitales.

En el ámbito de la industria alimentaria, según los resultados anteriores, el PAF directo y la PAW son una solución prometedora para desinfectar biológicamente barricas y químicamente corchos de botellas de vino. Con ello se resolverían en gran medida algunos problemas descritos en enología relacionados con la reutilización de barricas de vino en la etapa del envejecimiento y el descarte de vinos embotellados como consecuencia de malos olores aportados por los corchos de dichas botellas.

6.2. CONCLUSIONS

This thesis investigated atmospheric cold plasma (PAF) directly applied over surfaces or indirectly applied through plasma activated water (PAW). The antimicrobial activity of the PAF treatments has been determined against food and clinical microorganisms. Furthermore, the PAW activity was evaluated to discompose haloanisole molecules related to the wine industry.

Filtration and breathing analysis for face masks, and SEM analysis for masks and staves were performed to determine the effect of PAW versus the morphological and functional properties of treated surfaces.

OES, HPLC and spectrometry UV-vis were used to characterize liquid and gas phases of plasma treatments. Thus, the most important reactive species (RONS) and their role to achieve the objectives were identified.

The conclusions of this doctoral thesis are:

1. The PAF capacity to inactivate bacteria and yeasts on varied surfaces, such as face masks or wood staves, was demonstrated.
2. The microbial inactivation degree was dependent on the plasma parameters: plasma gas, power or treatment time. Argon was the less effective PAF gas in comparison with air and nitrogen, and higher PAF powers and generation times resulted in higher antimicrobial activity.
3. Each microorganism responds different to PAF treatments. *E. coli* or *P. aeruginosa* inactivation was caused by the PAF thermal effect, whereas *S. aureus* inactivation was caused by addition of the thermal effect and RONS produced by PAF.
4. PAF has the capacity to discompose chemical molecules such as 2,4,6-Trichloroanisole (TCA) from corks, and the radical OH• was proposed as the responsible agent of TCA decomposition using a firstly TCA demethylation step and a subsequent OH• attack to TCA chloro atoms.
5. The RONS quantity increased according to the increasing PAW generation time. To this extent, the mechanisms of RONS reaction were suggested; as well as their presence in the PAW during several days. The role of each RONS in the microbial inactivation and chemical decomposition was also detailed.
6. The morphology and functional capacity of all the treated surfaces were maintained after PAF treatments.

In conclusion, taking into account all the above mentioned, the PAF technology directly applied or the use of PAW could be a sustainable and economic solution to microbial and chemical problems related to global health and food industry.

The disinfection of used masks using PAF could be an emergency solution to reduce facial skin diseases and deal with mask shortage and environmental problems associated with mask discard. Moreover, this technology could be applicable to other devices and personal protection equipment manipulated in hospitals.

Regarding the food industry, direct plasma and PAW are a promising solution to disinfect wood barrels and wine corks. Therefore, oenological problems related to barrel reusing during wine aging and bottled wine exclusion due to undesirable odor will be avoided.

7. FUTURAS INVESTIGACIONES

7.1. ESTUDIO Y SIMULACIÓN DE NUEVOS MÉTODOS DE GENERACIÓN DE PAW Y SU CAPACIDAD DE INACTIVACIÓN

Se ha investigado un nuevo método de generación de PAW mediante el uso de una pieza impresa en 3D con orificios por los cuales pasa el gas de plasma formando burbujas en el interior del volumen de agua a tratar. Se ha realizado un estudio con diferentes configuraciones de agujeros, tanto en número como en disposición.

La elección de la mejor configuración se hace con estudios de capacidad de inactivación bacteriana, de manera que la mejor configuración de orificios es aquella con la cual se genera la PAW con mayor poder bactericida. Así, se está observando que la mejor pieza contiene el máximo número de orificios y con la configuración equidistante de los mismos.

Por otro lado, también se está realizando un estudio de flujos. Es decir, se modifica el flujo de gas de plasma con el cual se genera cada PAW (60, 80, 100 y 120 slm) con el fin de observar si el flujo es un parámetro clave a la hora de generar PAW con alto poder bactericida.

De la misma manera, se ha realizado la simulación numérica de la generación de las PAW con diferentes flujos de plasma. En estos momentos se está investigando el tamaño de burbuja, la forma de las mismas al entrar en el tubo central así como el sistema dinámico donde las burbujas se forman, se desprenden, ascienden, y colapsan en la superficie libre y el área total de la interfaz aire-agua.

7.2. BÚSQUEDA DE ESPECIES REACTIVAS EN LA PAW

Con el fin de entender y poder explicar la capacidad antibacteriana de cada PAW se están realizando pruebas para demostrar cuáles son las diferentes especies reactivas que se cree juegan un papel fundamental en la capacidad para inactivar microorganismos de cada PAW.

Para ello se utilizan scavengers específicos capaces de atrapar una especie reactiva específica y se analiza la capacidad antimicrobiana de ambas PAW.

En este sentido, también se están haciendo pruebas de capacidad inactivadora de microorganismos con determinadas PAW y soluciones artificiales. Con estos ensayos se quiere comprobar que un agua artificial con las mismas concentraciones de nitratos, nitritos y pH no es tan efectiva, en términos de inactividad bacteriana, como la PAW generada, ya que esta última contiene otras muchas especies reactivas, las cuales son las principales responsables de su capacidad antimicrobiana

.

BIBLIOGRAFÍA

[1] S. Feng, C. Shen, N. Xia, W. Song, M. Fan, B.J. Cowling, Rational use of face masks in the COVID-19 pandemic, Lancet Respir. Med. 8 (2020) 434–436. https://doi.org/10.1016/S2213-2600(20)30134-X.

[2] S.Y. Choi, J.Y. Hong, H.J. Kim, G.Y. Lee, S.H. Cheong, H.J. Jung, C.H. Bang, D.H. Lee, M.S. Jue, H.O. Kim, E.J. Park, J.Y. Ko, S.W. Son, Mask-induced dermatoses during the COVID-19 pandemic: a questionnaire-based study in 12 Korean hospitals, Clin. Exp. Dermatol. 46 (2021) 1504–1510. https://doi.org/10.1111/ced.14776.

[3] J. Wei, S. Guo, E. Long, L. Zhang, B. Shu, L. Guo, Why does the spread of COVID-19 vary greatly in different countries? Revealing the efficacy of face masks in epidemic prevention, Epidemiol. Infect. (2021). https://doi.org/10.1017/S0950268821000108.

[4] L. Bao, C. Zhang, J. Dong, L. Zhao, Y. Li, J. Sun, Oral Microbiome and SARS-CoV-2: Beware of Lung Co-infection, Front. Microbiol. 11 (2020). https://doi.org/10.3389/fmicb.2020.01840.

[5] S. Dharmaraj, V. Ashokkumar, S. Hariharan, A. Manibharathi, P.L. Show, C.T. Chong, C. Ngamcharussrivichai, The COVID-19 pandemic face mask waste: A blooming threat to the marine environment, Chemosphere. 272 (2021) 129601. https://doi.org/10.1016/j.chemosphere.2021.129601.

[6] S. Sangkham, Face mask and medical waste disposal during the novel COVID-19 pandemic in Asia, Case Stud. Chem. Environ. Eng. 2 (2020) 100052. https://doi.org/10.1016/j.cscee.2020.100052.

[7] N. Allocati, M. Masulli, M.F. Alexeyev, C. Di Ilio, Escherichia coli in Europe: An overview, Int. J. Environ. Res. Public Health. 10 (2013) 6235–6254. https://doi.org/10.3390/ijerph10126235.

[8] A. Andreu, J. Cacho, A. Coira, J.A. Lepe, Diagnóstico microbiológico de las infecciones del tracto urinario, Enferm. Infecc. Microbiol. Clin. 29 (2011) 52–57. https://doi.org/10.1016/j.eimc.2010.06.008.

[9] A. Callejas-Díaz, C. Fernández-Pérez, A. Ramos-Martínez, E. Múñez-Rubio, I. Sánchez-Romero, J.A. Vargas Núñez, Impact of Pseudomonas aeruginosa bacteraemia in a tertiary hospital: Mortality and prognostic factors, Med. Clin. (Barc). 152 (2019) 83–89. https://doi.org/10.1016/j.medcli.2018.04.020.

[10] D. Chessa, G. Ganau, V. Mazzarello, An overview of staphylococcus epidermidis and staphylococcus aureus with a focus on developing countries, J. Infect. Dev. Ctries. 9 (2015) 547–550. https://doi.org/10.3855/jidc.6923.

[11] M.S. Bergman, D.J. Viscusi, B.K. Heimbuch, J.D. Wander, A.R. Sambol, R.E. Shaffer, Evaluation of multiple (3-Cycle) decontamination processing for filtering facepiece respirators, J. Eng. Fiber. Fabr. 5 (2010) 33–41. https://doi.org/10.1177/155892501000500405.

[12] J.S. Smith, D. Ph, H. Hanseler, J. Welle, R. Rattray, M. Campbell, T. Moudgil, T.F. Pack, D. Ph, K. Wegmann, D. Ph, S. Jensen, D. Ph, J. Jin, C.B. Bifulco, S.A. Prahl, D. Ph, B.A. Fox, D. Ph, L. Stucky, D. Ph, 3, 7 , (2020).

[13] D.J. Viscusi, M.S. Bergman, B.C. Eimer, R.E. Shaffer, Evaluation of five decontamination methods for filtering facepiece respirators, Ann. Occup. Hyg. 53 (2009) 815–827. https://doi.org/10.1093/annhyg/mep070.

[14] Battelle, Final Report for the Bioquell Hydrogen Peroxide Vapor (HPV) Decontamination for Reuse of N95 Respirators, J. Phys. Chem. A. 4 (2016) 10863–10872. http://dx.doi.org/10.1016/j.watres.2012.03.036.

[15] N. Tomás-Hernandez, Efecto del tipo de madera y su envejecimiento sobre la fracción volátil del vino, (2016) 2015–2016.

[16] E.J. Bartowsky, P.A. Henschke, Acetic acid bacteria spoilage of bottled red wine-A review, Int. J. Food Microbiol. 125 (2008) 60–70. https://doi.org/10.1016/j.ijfoodmicro.2007.10.016.

[17] A. Costantini, E. Vaudano, M.C. Cravero, M. Petrozziello, F. Piano, A. Bernasconi, E. Garcia-Moruno, Dry ice blasting, a new tool for barrel regeneration treatment, Eur. Food Res. Technol. 242 (2016) 1673–1683. https://doi.org/10.1007/s00217-016-2667-3.

[18] R. Suárez, J.A. Suárez-Lepe, A. Morata, F. Calderón, The production of ethylphenols in wine by yeasts of the genera Brettanomyces and Dekkera: A review, Food Chem. 102 (2007) 10–21. https://doi.org/10.1016/j.foodchem.2006.03.030.

[19] V. Falguera, M. Forns, A. Ibarz, UV-vis irradiation: An alternative to reduce SO2 in white wines?, Lwt. 51 (2013) 59–64. https://doi.org/10.1016/j.lwt.2012.11.006.

[20] L. González-Arenzana, P. Santamaría, R. López, P. Garijo, A.R. Gutiérrez, T. Garde-Cerdán, I. López-Alfaro, Microwave technology as a new tool to improve microbiological control of oak barrels: A preliminary study, Food Control. 30 (2013) 536–539. https://doi.org/10.1016/j.foodcont.2012.08.008.

[21] F. Schmid, P. Grbin, A. Yap, V. Jiranek, Relative efficacy of high-pressure hot water and high-power ultrasonics for wine oak barrel sanitization, Am. J. Enol. Vitic. 62 (2011) 519–526. https://doi.org/10.5344/ajev.2011.11014.

[22] J.M. Alston, K.B. Fuller, J.T. Lapsley, G. Soleas, Too much of a good thing? Causes and consequences of increases in sugar content of california wine grapes, World Sci. Handb. Financ. Econ. Ser. 6 (2018) 135–163. https://doi.org/10.1142/9789813232747_0006.

[23] R. Mira de Orduña, Climate change associated effects on grape and wine quality and production, Food Res. Int. 43 (2010) 1844–1855. https://doi.org/10.1016/j.foodres.2010.05.001.

[24] J. Harrouard, C. Eberlein, P. Ballestra, M. Dols-Lafargue, I. Masneuf-Pomarede, C. Miot-Sertier, J. Schacherer, W. Albertin, Brettanomyces bruxellensis: Overview of the genetic and phenotypic diversity of an anthropized yeast, Mol. Ecol. 32 (2023) 2374–2395. https://doi.org/10.1111/mec.16439.

[25] M.E. Wade, M.T. Strickland, J.P. Osborne, C.G. Edwards, Role of Pediococcus in winemaking, Aust. J. Grape Wine Res. 25 (2019) 7–24. https://doi.org/10.1111/ajgw.12366.

[26] D. Zgardan, I. Mitina, R. Sturza, V. Mitin, S. Rubtov, C. Grajdieru, E. Behta, F. Inci, N. Haciosmanoglu, A Survey on Acetic Acid Bacteria Levels and Volatile Acidity in Several Wines of the Republic of Moldova, (2023) 79. https://doi.org/10.3390/foods2023-15153.

[27] U. Europea, Directiva 98/8/CE Relativa a la comercialización de biocidas, D. Of. Las Comunidades Eur. (1998) 1–63. https://www.boe.es/buscar/doc.php?id=DOUE-L-1998-80690.

[28] Palacios García, A.T, Estudio comaprativo de sistemas de desinfección de barricas de vino como alternativas al empleo de sulfuroso., 2012.

[29] M.A. Sefton, R.F. Simpson, Compounds causing cork taint and the factors affecting their transfer from natural cork closures to wine - A review, Aust. J. Grape Wine Res. 11 (2005) 226–240. https://doi.org/10.1111/j.1755-0238.2005.tb00290.x.

[30] C. Silva Pereira, J.J. Figueiredo Marques, M. V. San Romão, Cork taint in wine: Scientific knowledge and public perception - A critical review, Crit. Rev. Microbiol. 26 (2000) 147–162. https://doi.org/10.1080/10408410008984174.

[31] J.F. Coque, Juan-José R; Recio Pérez, Eliseo; Goswami, Mandira; Feltrer Martínez, Raúl; Campoy García, Sonia; Álvarez Rodríguez Mª Luisa; Martín Martín, Wine Contamination by Haloanisoles, (2006).

[32] R.B. Martín, DISPOSITIVO Y PROCEDIMIENTO PARA LA REDUCCIÓN DEL TCA EN PRODUCTOS DE CORCHO, (2018).

[33] R.F. Simpson, M. Sefton, Origin and fate of 2,4,6-trichloroanisole in cork bark and wine corks, Aust. J. Grape Wine Res. 13 (2007) 106–116. https://doi.org/10.1111/j.1755-0238.2007.tb00241.x.

[34] M.C. Cravero, Musty and moldy taint in wines: A review, Beverages. 6 (2020) 1–13. https://doi.org/10.3390/beverages6020041.

[35] M. Cabral, Proceso de tratamiento de productos de corcho mediante extracción de compuestos arrastrados en vapor de agua., (2006) 1–20.

[36] F. Patente, Solicitud D ESALVADOR PALACIOS, C. IZQUIERDO MISIEGO, M.J. SÁNCHEZ MONTERO, J. y MONTERO GARCÍA, N. MARTÍN SÁNCHEZ, Procedimiento para la eliminación de haloanisoles y halofenoles presentes en el corcho e instalación para llevar a cabo dicha eliminación, (2012).

[37] M. DE MAGALHÃES NUNES DA PONTE, LUIS;, J.A. DA SILVA LOPES, N.-V. VESNA, M. MANIC, A. DE AVELAR LOPES CARDOSO MESQUITA, CRISTINA;, R.P. y MOREIRA DA SILVA, D.Q.M. SOLLARI, I.M. ALLEGRO, Procedimiento para el tratamiento directo de tapones de corcho, utilizando fluidos supercríticos, (2013) 1–12.

[38] P. Guedes, E.P. Mateus, J.P. Fernandes, A.B. Ribeiro, Electro-technologies for the removal of 2,4,6-trichloroanisole from naturally contaminated cork discs: Reactor design and proof of concept, Chem. Eng. J. 361 (2019) 80–88. https://doi.org/10.1016/j.cej.2018.12.040.

[39] E. Recio, M.L. Álvarez-Rodríguez, A. Rumbero, E. Garzón, J.J.R. Coque, Destruction of chloroanisoles by using a hydrogen peroxide activated method and its application to remove chloroanisoles from cork stoppers, J. Agric. Food Chem. 59 (2011) 12589–12597. https://doi.org/10.1021/jf2035753.

[40] M. Viguera, C. Prieto, J. Casas, E. Casas, A. Cabañas, L. Calvo, The parameters that affect the supercritical extraction OF 2,4,6-trichloroanisol from cork, J. Supercrit. Fluids. 141 (2018) 137–142. https://doi.org/10.1016/j.supflu.2018.03.017.

[41] C. Tendero, C. Tixier, P. Tristant, J. Desmaison, P. Leprince, Atmospheric pressure plasmas: A review, Spectrochim. Acta - Part B At. Spectrosc. 61 (2006) 2–30. https://doi.org/10.1016/j.sab.2005.10.003.

[42] V. Scholtz, J. Pazlarova, H. Souskova, J. Khun, J. Julak, Nonthermal plasma - A tool for decontamination and disinfection, Biotechnol. Adv. 33 (2015) 1108–1119. https://doi.org/10.1016/j.biotechadv.2015.01.002.

[43] K. Iuchi, Y. Morisada, Y. Yoshino, T. Himuro, Y. Saito, T. Murakami, H. Hisatomi, Cold atmospheric-pressure nitrogen plasma induces the production of reactive nitrogen species and cell death by increasing intracellular calcium in HEK293T cells, Arch. Biochem. Biophys. 654 (2018) 136–145. https://doi.org/10.1016/j.abb.2018.07.015.

[44] W. Siemens, Ueber die elektrostatische Induction und die Verzögerung des Stroms in Flaschendrähten[As to the electrostatic induction and the delay of the current Bottled wires], Ann. Der Phys. Und Chemie. 178 (1857) 66–122. http://doi.wiley.com/10.1002/andp.18571780905.

[45] T. Ding, P.J. Cullen, W. Yan, Applications of Cold Plasma in Food Safety, 2021. https://doi.org/10.1007/978-981-16-1827-7.

[46] A. Schütze, J.Y. Jeong, S.E. Babayan, J. Park, G.S. Selwyn, R.F. Hicks, The atmospheric-pressure plasma jet: A review and comparison to other plasma sources, IEEE Trans. Plasma Sci. 26 (1998) 1685–1694. https://doi.org/10.1109/27.747887.

[47] R. Zhou, R. Zhou, K. Prasad, Z. Fang, R. Speight, K. Bazaka, K. Ostrikov, Cold atmospheric plasma activated water as a prospective disinfectant: The crucial role of peroxynitrite, Green Chem. 20 (2018) 5276–5284. https://doi.org/10.1039/c8gc02800a.

[48] R. Thirumdas, A. Kothakota, U. Annapure, K. Siliveru, R. Blundell, R. Gatt, V.P. Valdramidis, Plasma activated water (PAW): Chemistry, physico-chemical properties, applications in food and agriculture, Trends Food Sci. Technol. 77 (2018) 21–31. https://doi.org/10.1016/j.tifs.2018.05.007.

[49] K. Oehmigen, M. Hähnel, R. Brandenburg, C. Wilke, K.D. Weltmann, T. Von Woedtke, The role of acidification for antimicrobial activity of atmospheric pressure plasma in liquids, Plasma Process. Polym. 7 (2010) 250–257. https://doi.org/10.1002/ppap.200900077.

[50] B. Xu, F. Qi, Reaction Mechanism of 2-Methylisoborneol and 2,4,6-Trichloroanisole in Catalytic Ozonation by γ-AlOOH: Role of Adsorption, Clean - Soil, Air, Water. 44 (2016) 1099–1105. https://doi.org/10.1002/clen.201500749.

[51] R. Ma, S. Yu, Y. Tian, K. Wang, C. Sun, X. Li, J. Zhang, K. Chen, J. Fang, Effect of Non-Thermal Plasma-Activated Water on Fruit Decay and Quality in Postharvest Chinese Bayberries, Food Bioprocess Technol. 9 (2016) 1825–1834. https://doi.org/10.1007/s11947-016-1761-7.

[52] N. Shainsky, D. Dobrynin, U. Ercan, S.G. Joshi, H. Ji, A. Brooks, G. Fridman, Y. Cho, A. Fridman, G. Friedman, Retraction: Plasma Acid: Water Treated by Dielectric Barrier Discharge, Plasma Process. Polym. 9 (2012) 1–6. https://doi.org/10.1002/ppap.201100084.

[53] X. Yang, C. Zhang, Q. Li, J.H. Cheng, Physicochemical Properties of Plasma-Activated Water and Its Control Effects on the Quality of Strawberries, Molecules. 28 (2023). https://doi.org/10.3390/molecules28062677.

[54] J.L. Brisset, B. Benstaali, D. Moussa, J. Fanmoe, E. Njoyim-Tamungang, Acidity control of plasma-chemical oxidation: Applications to dye removal, urban waste abatement and microbial inactivation, Plasma Sources Sci. Technol. 20 (2011). https://doi.org/10.1088/0963-0252/20/3/034021.

[55] V. Rathore, D. Patel, S. Butani, S.K. Nema, Investigation of Physicochemical Properties of Plasma Activated Water and its Bactericidal Efficacy, Springer US, 2021. https://doi.org/10.1007/s11090-021-10161-y.

[56] H. Akiyama, R. Heller, Book-Bioelectrics 题目：生物电刺激, 2017.

[57] P. Lukes, E. Dolezalova, I. Sisrova, M. Clupek, Aqueous-phase chemistry and bactericidal effects from an air discharge plasma in contact with water: Evidence for the formation of peroxynitrite through a pseudo-second-order post-discharge reaction of H2O 2 and HNO2, Plasma Sources Sci. Technol. 23 (2014). https://doi.org/10.1088/0963-0252/23/1/015019.

[58] Z. Machala, B. Tarabova, K. Hensel, E. Spetlikova, L. Sikurova, P. Lukes, Formation of ROS and RNS in water electro-sprayed through transient spark discharge in air and their bactericidal effects, Plasma Process. Polym. 10 (2013) 649–659. https://doi.org/10.1002/ppap.201200113.

[59] E. Tsoukou, P. Bourke, D. Boehm, Temperature stability and effectiveness of plasma-activated liquids over an 18 months period, Water (Switzerland). 12 (2020) 1–18. https://doi.org/10.3390/w12113021.

[60] M. Domonkos, P. Tichá, J. Trejbal, P. Demo, Applications of cold atmospheric pressure plasma technology in medicine, agriculture and food industry, Appl. Sci. 11 (2021). https://doi.org/10.3390/app11114809.

[61] A.M.-P. Renwu Zhou1, 2, Rusen Zhou1, Peiyu Wang1, Yubin Xian3, 15, 4 Xinpei Lu3, P. J. Cullen2, Kostya (Ken) Ostrikov1 and Kateryna Bazaka1, Plasma activated water (PAW): generation, origin of reactive species and biological applications, (2018).

[62] N.H. Survey, M Pl E M Pl E Ly, Perform. Stand. Antimicrob. Susceptibility Test. (2022). https://clsi.org/standards/products/microbiology/documents/m100/.

[63] H. Jablonowski, T. von Woedtke, Research on plasma medicine-relevant plasma-liquid interaction: What happened in the past five years?, Clin. Plasma Med. 3 (2015) 42–52. https://doi.org/10.1016/j.cpme.2015.11.003.

[64] OIV, Compendium of international methods of analysis-OIV Alkalinity of ash, 2009.

[65] G. Damiani, L.C. Gironi, A. Grada, K. Kridin, R. Finelli, A. Buja, N.L. Bragazzi, P.D.M. Pigatto, P. Savoia, COVID-19 related masks increase severity of both acne (maskne) and rosacea (mask rosacea): Multi-center, real-life, telemedical, and observational prospective study, Dermatol. Ther. 34 (2021) 2–6. https://doi.org/10.1111/dth.14848.

[66] L. González-Arenzana, I. López-Alfaro, A.R. Gutiérrez, N. López, P. Santamaría, R. López, Continuous pulsed electric field treatments' impact on the microbiota of red Tempranillo wines aged in oak barrels, Food Biosci. 27 (2019) 54–59. https://doi.org/10.1016/j.fbio.2018.10.012.

[67] L. Han, S. Patil, D. Boehm, V. Milosavljević, P.J. Cullen, P. Bourke, Mechanisms of inactivation by high-voltage atmospheric cold plasma differ for Escherichia coli and Staphylococcus aureus, Appl. Environ. Microbiol. 82 (2016) 450–458. https://doi.org/10.1128/AEM.02660-15.

[68] Z.J. Huang Mingming, Zhuang Hong, Zhao Jianying, Wang Jiamei, Yan Wenjing, Differences in cellular damage induced by dielectric barrier discharge plasma between Salmonella Typhimurium and Staphylococcus aureus, Bioelectrochemistry. 132 (2020).

[69] M.M. Kayes, Inactivation of Foodborne Pathogens Using a One Atmosphere Uniform Glow Discharge Plasma, 4 (2016) 1–23.

[70] K.S. Lunov Oleg, Zablotskii Vitalii, Churpita Olexander, Jäger Ales, Leôs Polívka, Syková Eva, Dejneka Alexandr, The interplay between biological and physical scenarios of bacterial death induced by non-thermal plasma, 0 (n.d.).

[71] J.H. Choi, I. Han, H.K. Baik, M.H. Lee, D.-W. Han, J.-C. Park, I.-S. Lee, K.M. Song, Y.S. Lim, Analysis of sterilization effect by pulsed dielectric barrier discharge, J. Electrostat. 64 (2006) 17–22. https://doi.org/10.1016/j.elstat.2005.04.001.

[72] T.M.C. Nishime, A.C. Borges, C.Y. Koga-Ito, M. Machida, L.R.O. Hein, K.G. Kostov, Non-thermal atmospheric pressure plasma jet applied to inactivation of different microorganisms, Surf. Coatings Technol. 312 (2017) 19–24. https://doi.org/10.1016/j.surfcoat.2016.07.076.

[73] P.S. Arjunan Krishna Priya, Sharma Virender K, Effects of Atmospheric Pressure Plasmas on Isolated and Cellular DNA-A review, Int. J. Mol. Sci. 16 (2015) 2971–3016.

[74] A. Šimončicová, Juliana; Kaliňáková, Barbora; Kovácik, Dusan; Medvecká, Veronika; Lakatos, Boris; Krystofová, Svetlana; Hoppanová, Lucia; Palusková, Veronika; Hudeková, Daniela; Durina, Pavol; Zahoranová, Cold plasma

treatment triggers antioxidative defense system and induces changes in hyphal surface and subcellular structures of Aspergillus flavus, (2018).

[75] C. Yong, Hae In; Kim, Hyun-Joo; Park, Sanghoo; Kim, Kijung; Choe, Wonho; Yoo, Suk Jae; Jo, Pathogen Inactivation and Quality Changes in Sliced Cheddar Cheese Treated Using Flexible Thin-Layer Dielectric Barrier Discharge Plasma, Food Res. Int. (2014).

[76] C. Miao, Hu; Jierong, Inactivation of Escherichia coli and properties of medical poly(vinyl chloride) in remote-oxygen plasma, Appl. Surf. Sci. 255 (2009) 5690–5697.

[77] D. Surowsky, Björn; Fröhling, Antje; Gottschalk, Nathalie; Schlüter, Oliver; Knorr, Impact of cold plasma on Citrobacter freudii in apple juice: Inactivation kinetics and mechanisms, Int. J. Food Microbiol. 174 (2014) 63–71.

[78] A. Wiegand, C., Beier, O., Horn, H., Pfuch, A., Tölke, T., Hipler, U.C., Schimanski, Antimicrobial Impact of Cold Atmospheric Pressure Plasma on Medical Critical Yeasts and Bacteria Cultures, Skin Pharmacol. Physiol. 27 (2014) 25–35. https://doi.org/10.7868/s0044451017120100.

[79] C. Kim, Binna; Yun, Hyejeong; Jung, Samooel; Jung, Yeonkook; Jung, Heesoo; Choe, Wonho; Jo, Effect of atmospheric pressure plasma on inactivation of pathogens inoculated onto bacon using two different gas compositions, Food Microbiol. 28 (2011) 9–13.

[80] M. Laroussi, F. Leipold, Evaluation of the roles of reactive species, heat, and UV radiation in the inactivation of bacterial cells by air plasmas at atmospheric pressure, Int. J. Mass Spectrom. 233 (2004) 81–86. https://doi.org/10.1016/j.ijms.2003.11.016.

[81] K. Lu, X., Naidis, G.V., Laroussi, M., Reuter, S., Graves, D.B., Ostrikov, Reactive species in non-equilibrium atmospheric-pressure plasmas: Generation, transport and biological effects, Phys. Rep. 630 (2016) 1–84.

[82] S. Gabriel, Alonzo .A., Alano-budiano, Alexie, Thermal inactivation of Pseudomonas aeruginosa 1244 in salted Sardinella fimbriata meat homogenate, 2019.

[83] M. Gabriel, Alonzo A., Aranza-Ubana, Decimal reduction times of Salmonella Typhimurium in guinataang kuhul: An indigenous Filipino dish, Lwt. 40 (2007) 1108–1111.

[84] P. Marcén, María., Ruiz, Virginia., Serrano, Mª Jesús., Condón, Santiago., Mañas, Oxidative stress in E. coli cells upon exposure to heat treatments, Int. J. Food Microbiol. 241 (2017) 198–205.

[85] P. Bao, X. Lu, M. He, D. Liu, Kinetic Analysis of Delivery of Plasma Reactive Species into Cells Immersed in Culture Media, IEEE Trans. Plasma Sci. 44 (2016) 2673–2681. https://doi.org/10.1109/TPS.2016.2578955.

[86] J. Shen, Y. Tian, Y. Li, R. Ma, Q. Zhang, J. Zhang, J. Fang, Bactericidal Effects against S. aureus and Physicochemical Properties of Plasma Activated Water stored at different temperatures, Sci. Rep. 6 (2016). https://doi.org/10.1038/srep28505.

[87] C.A.J. Van Gils, S. Hofmann, B.K.H.L. Boekema, R. Brandenburg, P.J. Bruggeman, Mechanisms of bacterial inactivation in the liquid phase induced by a remote RF cold atmospheric pressure plasma jet, J. Phys. D. Appl. Phys. 46 (2013). https://doi.org/10.1088/0022-3727/46/17/175203.

[88] A.D. Yost, S.G. Joshi, Atmospheric nonthermal plasma-treated PBS inactivates Escherichia coli by oxidative DNA damage, PLoS One. 10 (2015) 1–20. https://doi.org/10.1371/journal.pone.0139903.

[89] J. Guo, K. Huang, X. Wang, C. Lyu, N. Yang, Y. Li, J. Wang, Inactivation of yeast on grapes by plasma-activated water and its effects on quality attributes, J. Food Prot. 80 (2017) 225–230. https://doi.org/10.4315/0362-028X.JFP-16-116.

[90] Y. Tian, J. Guo, D. Wu, K. Wang, J. Zhang, J. Fang, The potential regulatory effect of nitric oxide in plasma activated water on cell growth of Saccharomyces cerevisiae, J. Appl. Phys. 122 (2017). https://doi.org/10.1063/1.4989501.

[91] X. Liu, Y. Li, R. Zhang, L. Huangfu, G. Du, Q. Xiang, Inactivation effects and mechanisms of plasma-activated water combined with sodium laureth sulfate (SLES) against Saccharomyces cerevisiae, Appl. Microbiol. Biotechnol. 105 (2021) 2855–2865. https://doi.org/10.1007/s00253-021-11227-9.

[92] X. Zhang, R. Zhou, K. Bazaka, Y. Liu, R. Zhou, G. Chen, Z. Chen, Q. Liu, S. Yang, K. (Ken) Ostrikov, Quantification of plasma produced OH radical density for water sterilization, Plasma Process. Polym. 15 (2018) 1–12. https://doi.org/10.1002/ppap.201700241.

[93] F. Qi, B. Xu, L. Zhao, Z. Chen, L. Zhang, D. Sun, J. Ma, Comparison of the efficiency and mechanism of catalytic

ozonation of 2,4,6-trichloroanisole by iron and manganese modified bauxite, Appl. Catal. B Environ. 121–122 (2012) 171–181. https://doi.org/10.1016/j.apcatb.2012.04.003.

[94] F.J. Benitez, J. Beltran-Heredia, J.L. Acero, F.J. Rubio, Contribution of free radicals to chlorophenols decomposition by several advanced oxidation processes, Chemosphere. 41 (2000) 1271–1277. https://doi.org/10.1016/S0045-6535(99)00536-6.

[95] N. Zhang, I. Geronimo, P. Paneth, J. Schindelka, T. Schaefer, H. Herrmann, C. Vogt, H.H. Richnow, Analyzing sites of OH radical attack (ring vs. side chain) in oxidation of substituted benzenes via dual stable isotope analysis (δ13C and δ2H), Sci. Total Environ. 542 (2016) 484–494. https://doi.org/10.1016/j.scitotenv.2015.10.075.

[96] S.C. Trewick, P.J. McLaughlin, R.C. Allshire, Methylation: Lost in hydroxylation?, EMBO Rep. 6 (2005) 315–320. https://doi.org/10.1038/sj.embor.7400379.

[97] V. Kavitha, K. Palanivelu, Degradation of phenol and trichlorophenol by heterogeneous photo-Fenton process using Granular Ferric Hydroxide®: comparison with homogeneous system, Int. J. Environ. Sci. Technol. 13 (2016) 927–936. https://doi.org/10.1007/s13762-015-0922-y.

[98] L.L. Zhang, S.Q. Leng, R.Y. Zhu, J.M. Chen, Degradation of chlorobenzene by strain Ralstonia pickettii L2 isolated from a biotrickling filter treating a chlorobenzene-contaminated gas stream, Appl. Microbiol. Biotechnol. 91 (2011) 407–415. https://doi.org/10.1007/s00253-011-3255-x.

[99] S. Jung, H.J. Kim, S. Park, H.I. Yong, J.H. Choe, H.J. Jeon, W. Choe, C. Jo, Color developing capacity of plasma-treated water as a source of nitrite for meat curing, Korean J. Food Sci. Anim. Resour. 35 (2015) 703–706. https://doi.org/10.5851/kosfa.2015.35.5.703.

[100] K. Liu, S.T. Liu, C.F. Ran, The Effect of Air-Water-Plasma-Jet-Activated Water on Penicillium: The Reaction of HNO2 and H2O2 Under Acidic Condition, Front. Phys. 8 (2020) 1–12. https://doi.org/10.3389/fphy.2020.00242.

[101] S.H. Ki, H. Noh, G.R. Ahn, S.H. Kim, N.K. Kaushik, E.H. Choi, G.J. Lee, Influence of nonthermal atmospheric plasma-activated water on the structural, optical, and biological properties of Aspergillus brasiliensis spores, Appl. Sci. 10 (2020). https://doi.org/10.3390/APP10186378.

[102] J.L. Brisset, J. Pawlat, Chemical Effects of Air Plasma Species on Aqueous Solutes in Direct and Delayed Exposure Modes: Discharge, Post-discharge and Plasma Activated Water, Plasma Chem. Plasma Process. 36 (2016) 355–381. https://doi.org/10.1007/s11090-015-9653-6.

ANEXOS

ANEXO I: PUBLICACIÓN V

Este anexo adjunta la publicación V. Ésta fue escrita con los resultados obtenidos de las investigaciones realizadas durante la estancia de la doctoranda en la Università di Bologna, Italia.

Plasma Chemistry and Plasma Processing
https://doi.org/10.1007/s11090-023-10410-2

ORIGINAL PAPER

Evaluation of the Antimicrobial Efficacy of a Large-Area Surface Dielectric Barrier Discharge on Food Contact Surfaces

Caterina Maccaferri[1] · Ana Sainz-García[2] · Filippo Capelli[1] · Matteo Gherardi[1,3] · Fernando Alba-Elías[2] · Romolo Laurita[1,4]

Received: 28 June 2023 / Accepted: 4 October 2023

Abstract
The food industry, as a consequence of globalization and in particular with the outbreak of the COVID-19 pandemic, is calling for additional measures to reduce the risks of contamination throughout the steps of the food chain. Several methods are used to avoid this problem, such as hot water or chemical procedures. However, they have some disadvantages like high economic costs or the fact that they are not eco-friendly technologies. For those reasons, novel strategies are being sought in order to substitute or work in synergy with conventional decontamination systems. Cold atmospheric pressure plasma (CAP) can be produced by many various sources for a wide range of different applications, including decontamination. In this study, a Large-Area Surface Dielectric Barrier Discharge plasma source has been used with the aim of inactivating *Staphylococcus epidermidis* inoculated on polypropylene food packaging samples inside a treatment chamber. Moreover, electrical and chemical analysis of the plasma source has been carried out, as well as temperature measurements. A homogenous distribution of the reactive species inside the treatment chamber was suggested, achieving almost 2 log of bacteria reduction for every plasma treatment. Finally, it was suggested that the inactivation rates reached were not caused by the thermal effect. Thus, it is strongly believed that CAP could be an eco-friendly, cheap, and sustainable technology for food packaging and food tools decontamination.

Keywords Surface dielectric barrier discharge · Food industry · Nuclear technology · Plasma technology · Atmospheric pressure cold plasma · Decontamination

Introduction

Food safety is which has begun to call for additional actions aimed at circumscribing as far as possible the risk introduced by the presence of potentially contaminated individuals in food production and marketing environments [1]. In that way, food packaging

Caterina Maccaferri and Ana Sainz-García are contributed equally to this work.

Extended author information available on the last page of the article

Published online: 20 October 2023

plays a crucial role during the final steps of the food chain preserving food from undesirable microorganisms and maintaining the original taste and odor.

Moreover, there is a globalization trend in the food market, which is beneficial for the supply and availability of food [2]. However, this fact has some disadvantages, such as economic or biological issues. Regarding the latter situation, contamination of food packaging and processing materials by microorganisms is an upsurging problem that could cause foodborne diseases. Taking into account the global market, contaminated packaging is known to be a means of transport for spreading diseases. According to the World Health Organization, 23 million people become ill each year in Europe due to foodborne diseases, and 5000 die [3]. Regarding the most frequent microorganisms seen in the food industry, *Staphylococcus* spp., *Listeria* spp., *E. coli*, *S. cerevisiae*, norovirus or anisakis are some of them [4, 5].

Traditional methods for the removal and inactivation of surface-attached pathogens from food contact surfaces are based on thermal, chemical, or mechanical mechanisms, which are generally time-consuming and energy-consuming [6].

Regarding thermal treatments, dry heat (> 180 °C), hot water and steam (130–150 °C) are the most commonly applied. Although thermal methods do not present residues of environmental hazards, some spores are resistant to heat [6]. Moreover, they require a lot of energy and long treatment times, being only possible to employ materials with high thermal resistance.

Chemical treatments such as hydrogen peroxide, ozone, peracetic acid or ethylene oxides could be toxic for people when used wrongly. Besides, they are known to leave residues on the treated surfaces causing resistances to bacteria and increasing their economic cost [6–8]. Additionally, there are some chemicals used in the food industry which could react with organic matter present on the surface reducing the efficacy (i.e. chlorine-based sanitizers) [9].

Therefore, there is a need to identify and develop new strategies, based on non-thermal physical mechanisms. Among these, ultraviolet, high hydrostatic pressure, ionizing or electron beam radiation and pulsed light have been effectively proven [10]. These technologies work at high efficiency requiring less energy input compared to the above technologies, and almost no residue or process waste is produced.

Cold Atmospheric Pressure Plasma (CAP) treatments may be a viable option for microbial inactivation, as they have antimicrobial active components, such as reactive oxygen and nitrogen species (RONS), ultraviolet radiation, electrons, radicals, ions, excited molecules and electromagnetic fields [11]. Several of these components have been found to be effective, thus it is reasonable to assume that their synergistic action could be highly beneficial. Moreover, these types of treatments represent an economical, green, and safe technology, which can allow the avoidance or reduction of traditional chemical sanitizers [12].

By virtue of the above considerations, it is of great interest to investigate the potential use of cold plasmas for the decontamination of products, instruments, and packaging in the food industry. Besides, some authors studied this technology for food-packaging decontamination [13–15].

In particular, many authors investigated the potential use of DBD (Dielectric Barrier Discharge) and SDBD (Surface Dielectric Barrier Discharge) for the decontamination of food packaging and food-processing surfaces [1, 16, 17].

Among the characteristics of DBD, they have two electrodes and at least one dielectric layer between them. They provide a huge homogenous plasma area, being easy to use, stable, and affordable, making them suitable for surface treatment [18]. Moreover, thin films

can easily fit in the gap (0.1 mm to several centimeters) between the DBD electrodes, thus being especially appropriate to be treated by DBD sources.

Additionally, the features of these devices rely on the electrode geometries and dimensions, materials selected, gas characteristics, and the applied electric field. Many different setups are possible, varying these parameters.

SDBD is one of the several setups possible for DBD. There, both electrodes are in contact with the dielectric material, and plasma is generated on the ground electrode surface. The main advantage of SDBD configuration, as opposed to DBD presenting a gap between electrodes, is the fact that the treated surface is kept outside of the electrical circuit, and, therefore, the working of the plasma source is almost independent of the treated material. Another benefit of both DBD and SDBD is that they can easily work using air as process gas. Specifically, the use of ambient air rather than expensive technical gases makes the difference from an industrial perspective [18].

The present work has characterized an SDBD plasma source from an electrical, chemical, and physical point of view. Moreover, its anti-bacterial efficacy has been evaluated against *Staphylococcus epidermidis* inoculated on polypropylene samples.

Materials and Methods

Plasma System

A Large Area Surface Dielectric Barrier Discharge (LA-SDBD, AlmaPlasma s.r.l., Bologna, Italy) was used to achieve indirect treatments [19].

The main components of the source are illustrated in Fig. 1. Four rectangular high-voltage electrodes (115 cm^2 each) were embedded in resin, and they were cooled by a glycol flux provided by a commercial cooling system (EXT-440, Koolance, USA). A dielectric layer made of mica (2 mm thick) was in contact with both the high-voltage electrodes and

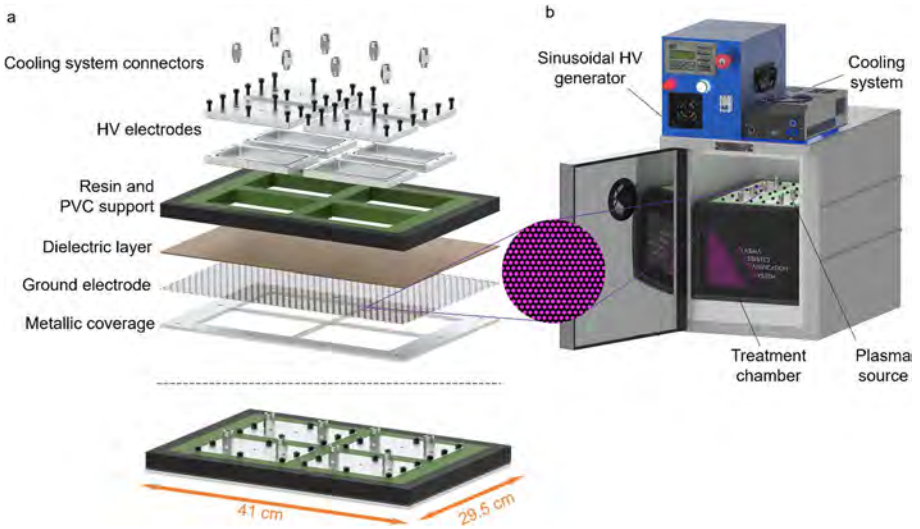

Fig. 1 **a** Plasma source components: exploded and assembly view; **b** plasma system components

ground electrodes. The latter, consisting of a perforated plate, was kept in place thanks to a metallic coverage. Plasma was generated in correspondence with the holes of the ground electrode, as depicted in Fig. 1. The plasma source was fed by a sinusoidal high-voltage generator (AlmaPlasma s.r.l., Bologna, Italy) working with a peak-to-peak voltage of 14 kV and a frequency of 23 kHz.

The plasma source constituted the lid of a PVC treatment chamber with a volume of 17.5 L. During treatments, the plasma source closed the treatment chamber, in order to create a confined atmosphere.

The source was designed to produce reactive species at atmospheric pressure, within the temperature and relative humidity ranges of 5–40 °C and 0–90%, respectively.

Microbial Strain and Sample Inoculation/Recovery

Circular polypropylene (PP) samples (Ø 2.5 cm) were contaminated.

Staphylococcus epidermidis ATCC12228 was selected as the target microorganism. Bacteria inoculum was cultured in tryptic soy agar (TSA, VWR International, Belgium) for 24 h at 37 °C. After that, the master suspension was adjusted at OD600 nm = 0.2 (10^7–10^8 CFU/mL) and assessed with a spectrophotometer (FullTech Instruments, Italy) [20].

Before treatments, PP samples were sterilized with ethanol 70% (Sigma-Aldrich, USA) before 5 min under UV light (Bio II Advance, Telstar, Japan). The master suspension was used in order to inoculate the PP samples with 20 drops of 1 µL (treatment samples and control samples). For bacteria recovery, treated and control samples were submerged for 2 min in PBS (Corning, USA) + 1% Tween 80 solution (Sigma-Aldrich, USA) and dilutions and spreading on agar plates were done. Then, the samples were kept for 24 h at 37 °C and recounted. Control samples followed the same procedure as plasma-treated samples but with plasma OFF.

The next formula was used to evaluate the antibacterial activity of plasma treatments after recovery steps:

$$Log\ reduction = \log N0 - \log Nt$$

where $N0$ and Nt are the number of colony-forming units of control and plasma treated, respectively.

Analytical Determinations

Electrical Characterization

In order to calculate the mean electrical power, voltage, and current waveforms were acquired. A voltage probe (P6015A, 1000×, Rp = 100 MΩ, Tektronix, USA) and a current probe (Current Monitor 6585, Pearson Electronics, USA) were placed respectively on the high voltage and the ground cable, and they were both connected to a fast oscilloscope (MSO46, Tektronix, USA) for the detection (Fig. 2).

Waveforms were acquired at the beginning and every five minutes of treatment, with a total of seven acquisitions for each 30-min test. Every acquisition had a record length of 180 ms, equal to four periods. Three tests were performed.

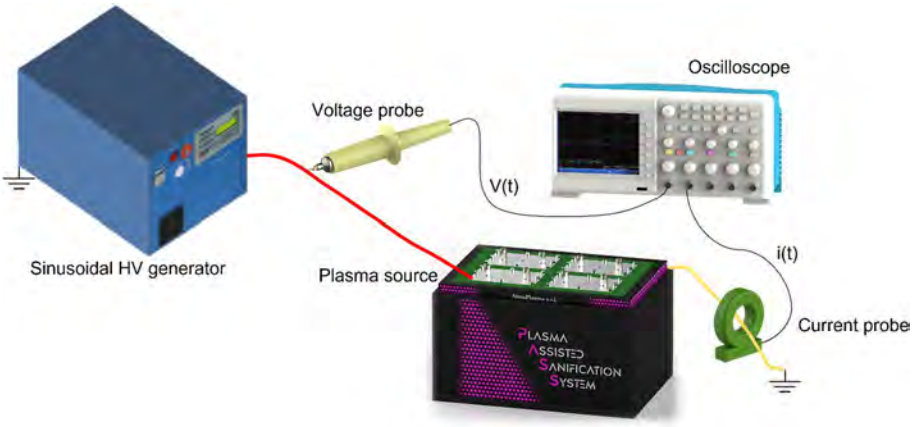

Fig. 2 Setup for voltage and current waveforms acquisition

Voltage and current values were used to calculate the electrical power at each time step on the basis of Ohm's law:

$$P(t) = V(t) * I(t)$$

where P is the electrical power, V is the voltage, and I the current.

The average power was calculated over the whole record length for each acquisition, as follows:

$$P_{average} = \frac{1}{T} \int_0^T P(t)dt$$

where the average power ($P_{average}$) is equal to the time integral of the power at each time step ($\int_0^T P(t)dt$), divided by the total amount of time (T, record length).

The calculation of the average power consumption is useful in order to calculate the specific power density (SPD) characteristic of the two duty cycles, by dividing the average power ($P_{average}$) by the plasma generation area (A):

$$SPD = \frac{P_{average}}{A}$$

where A should be calculated as the multiplication of the total surface of the high voltage electrodes (S) and the empty coefficient of the ground electrode ($e = 0.33$), since plasma is generated only in the holes of the perforated plate, as already mentioned.

$$A = S * e$$

For the plasma source used in this study, the plasma generation area resulted equal to 151.8 cm^2.

Optical Absorption Spectroscopy (OAS) and Data Processing

An Optical Absorption Analysis has been performed in order to understand the reactive species kinetics inside the treatment chamber. Two reactive species were chosen: ozone (O_3) and nitrogen dioxide (NO_2). Their kinetics were detected during 30-min treatments with different plasma conditions.

Two different optical paths were selected, in order to acquire the kinetics at two different distances from the plasma generation region, corresponding to the two positions later illustrated.

Optical Absorption Spectroscopy (OAS) is based on the Lambert–Beer law, which states that it is possible to quantify the number of a specific type of molecule by measuring the absorption of certain specific wavelengths. The light intensity of a beam passing through a region where there are molecules that absorb the characteristic wavelength of the beam is attenuated proportionally to the amount of molecules present in that region.

A similar setup for OAS was previously described by Simoncelli et al. [21] (Fig. 3). The light source used for ozone detection was a deep-UV led lamp (LEDMOD255.001.V2, Omicron Laserage, Germany), set at a wavelength of 255 nm. For nitrogen dioxide detection, a commercial led with an emission wavelength of 400 nm has been used. The light beam was focused in both cases with a lens in order to obtain a parallel beam under the mesh and to be able to collect it into a 500 mm spectrometer (Acton SP2500i, Princeton Instruments).

OAS acquisitions were performed using a grating with a resolution of 150 mm^{-1} or 1800 mm^{-1}, respectively, when detecting ozone or nitrogen dioxide, and setting a width of 10 μm for the inlet slit of the spectrometer. With the aim of achieving fast acquisition with a time resolution of 40 ms, a photomultiplier tube (PMT—PD439, Princeton Instruments) connected to a fast oscilloscope (MSO46, Tektronix, USA) was used as a detector. The PMT amplification factor was fixed at 585 and kept constant for all measurements. Each measurement was repeated three times.

The concentration of RONS in the closed chamber can be calculated spectrally by resolving the collected beam and taking the Lambert–Beer Law into account:

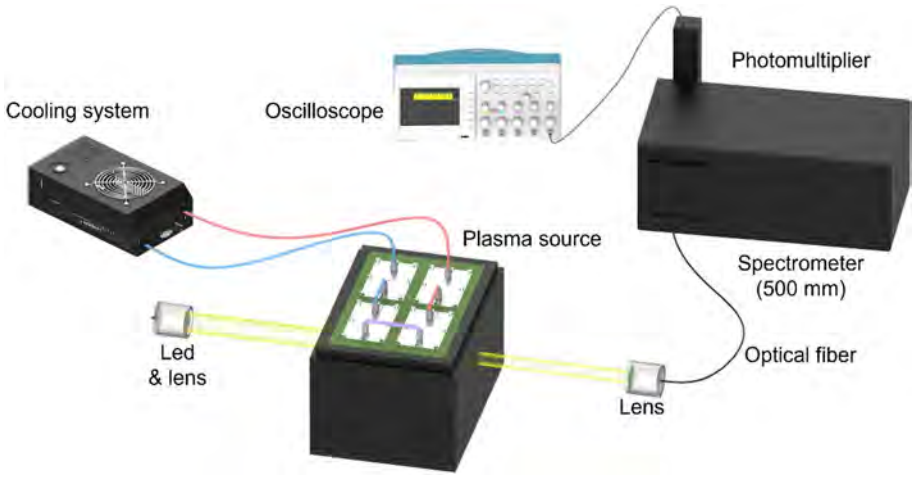

Fig. 3 Schematic of the experimental setup for optical absorption spectroscopy

Table 1 Selected wavelengths and absorption cross-sections of the O_3 and NO_2 (cm^2)

Selected wavelength (nm)	O_3 cross-section	NO_2 cross-section
253 ± 1.2	(1.12 ± 0.02)E–17	(1.1 ± 0.3)E–20
400 ± 1.2	(1.12 ± 0.08)E–23	(6.4 ± 0.2)E–19

Table 2 Plasma treatments conditions

Treatment number	1	2	3	4	5	6	7	8
Duty cycle 10–100%	10%	10%	100%	100%	10%	10%	100%	100%
Gap (cm)	20	4	20	4	20	4	20	4
Treatment time (min)	30	30	30	30	30	30	30	30
Fan ON–OFF	OFF	OFF	OFF	OFF	ON	ON	ON	ON

Each treatment consisted of a group of three samples and was performed three times

$$\frac{I}{I_0} = e^{(-L\sigma n)}$$

where the concentration of the absorbers (n), which has to be quantitatively evaluated, is correlated with the light absorbed after an optical path length (L) and expressed as the ratio between the initial light intensity (I_0) and the residual light intensity (I) after passing through the absorbers region. The absorption cross-section (σ) is a function of the light wavelength ($\sigma = \sigma(\lambda)$). In the experiments, the optical path was 25 cm long.

The wavelengths selected to perform the acquisitions and the relative absorption cross-sections for the absorbers (O_3 and NO_2) are reported in Table 1. These wavelengths were defined, in accordance with Moiseev [22], to maximise the absorption of the molecules relevant to our study while minimising the contribution, and thus the disturbance, of other absorbing molecules. The contribution of background radiation is subtracted from the measured values of light intensity.

Temperature Measurements

The temperature inside the treatment chamber during the treatment was measured. Two commercial fibre-optic sensors (MultiSens, OpSens, Canada) were placed inside the treatment chamber in the same positions chosen for the sample placement. The temperature was monitored for 30 min of plasma treatment under all the different operating conditions. Each measurement was repeated three times. The probes were connected to a detection device (MultiSens, OpSens, Canada) for data acquisition.

Plasma Treatments

The contaminated samples were located inside the treatment chamber and laid on plastic plates. Eight different treatments were carried out depending on the duty cycle (DC), fan mode, and gap (i.e., the distance between samples and plasma generation region) selected (Table 2). Two different sample positions were chosen, the first one centred on

the bottom of the treatment chamber (gap equal to 20 cm) and the second one in proximity to the plasma discharge (4 cm under the ground electrode). They will be hereafter called "Position 1" and "Position 2", respectively, as shown in Fig. 4.

The duty cycle (i.e., the ratio between the on-time of the discharge and the sum of on and off time) was either 10% or 100%.

A fan has been placed inside the treatment chamber in order to evaluate the effect of a turbulent atmosphere. All the tests were performed, either with the fan working or not. The fan was located near a short side of the chamber, parallel to it, and facing the other short side, as shown in Fig. 4.

Statistical Analysis

All experiments were repeated three times. Results are presented as mean value and standard error. In order to assess statistically significant differences among different results, a Student's test was performed (p-value < 0.001). Statistical analysis of microbiological data was performed using Statgraphics Centurion software (v19, The Plains, United States).

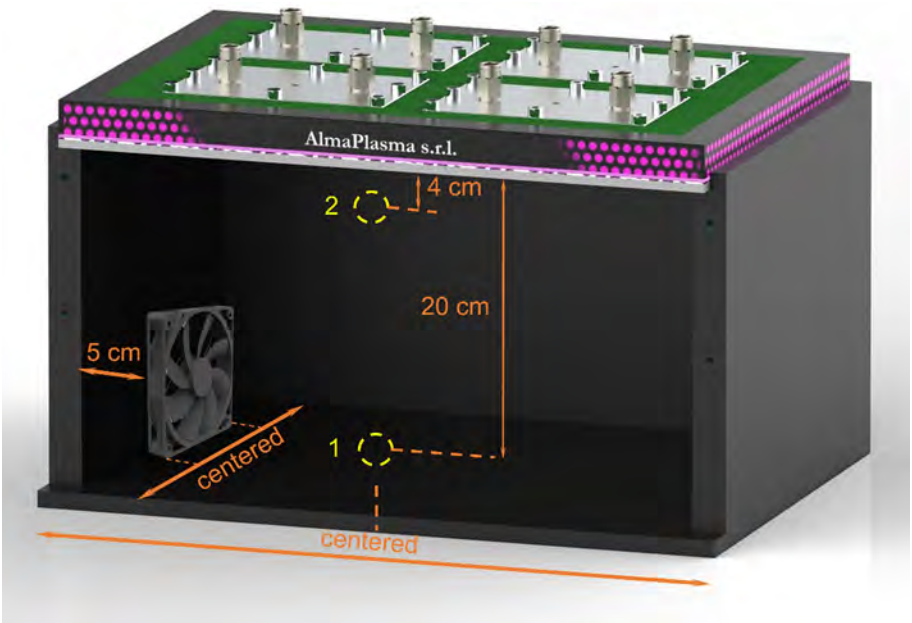

Fig. 4 Views of the plasma system showing the two chosen positions for the tests, indicated by the circles, and the position of the fan inside the treatment chamber (placed 5 cm apart from one of the short sides of the chamber, centred with respect to it, moving the air toward the other short side)

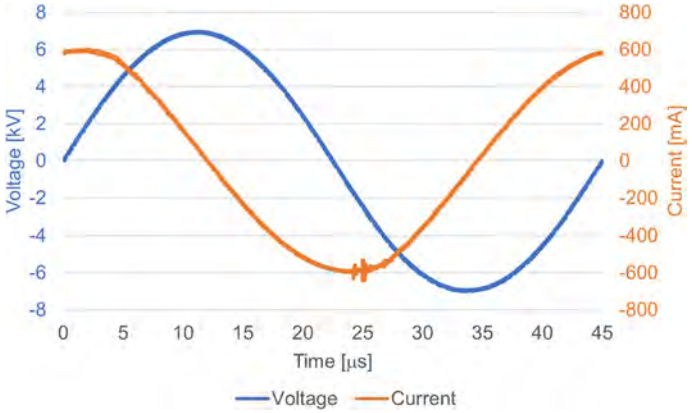

Fig. 5 Voltage (blue) and current (orange) waveforms acquired during 45 µs of discharge with DC 100% (Color figure online)

Table 3 Average power and SPD results

DC (%)	Average power [W]	SPD [W cm^{-2}]	Regime
10	19 ± 1.6	0.13	Ozone
100	190 ± 16.6	1.25	Nitrogen oxides

Results and Discussion

Electrical Characterization

Figure 5 shows voltage and current waveforms recorded for each duty cycle (10 and 100%). From those results the mean electric power was calculated as previously explained, resulting in values of 19 ± 16.6 W and 190 ± 1.6 W for DC 10 and DC 100% respectively.

Table 3 shows the SPD values. With DC 10%, the SPD was about 0.1 W cm^{-2}, which is the value identified by the literature [21, 22] as the threshold between the ozone regime (SPD < 0.1 W cm^{-2}) and the nitrogen oxides regime. When DC was set at 100%, the source was working in a nitrogen oxides regime.

Bacteria Inactivation

This section shows the results of bacteria inactivation after each plasma treatment.

Figure 6 illustrates the inactivation rates achieved with plasma treatments in the ozone regime. When comparing fan ON and OFF, for position 1 plasma treatments achieved bacteria reductions of 1.59 ± 0.42 log and 0.92 ± 0.34 log, with fan ON and OFF respectively. While the inactivation obtained for position 2 was 1.6 ± 0.53 log with fan ON and 1.38 ± 0.23 log with fan OFF. They showed no statistically significant differences when comparing fan ON and OFF for each gap, which suggested a homogeneous distribution of the reactive species within the treatment chamber. On the other hand, when doing an evaluation about the two positions where the samples

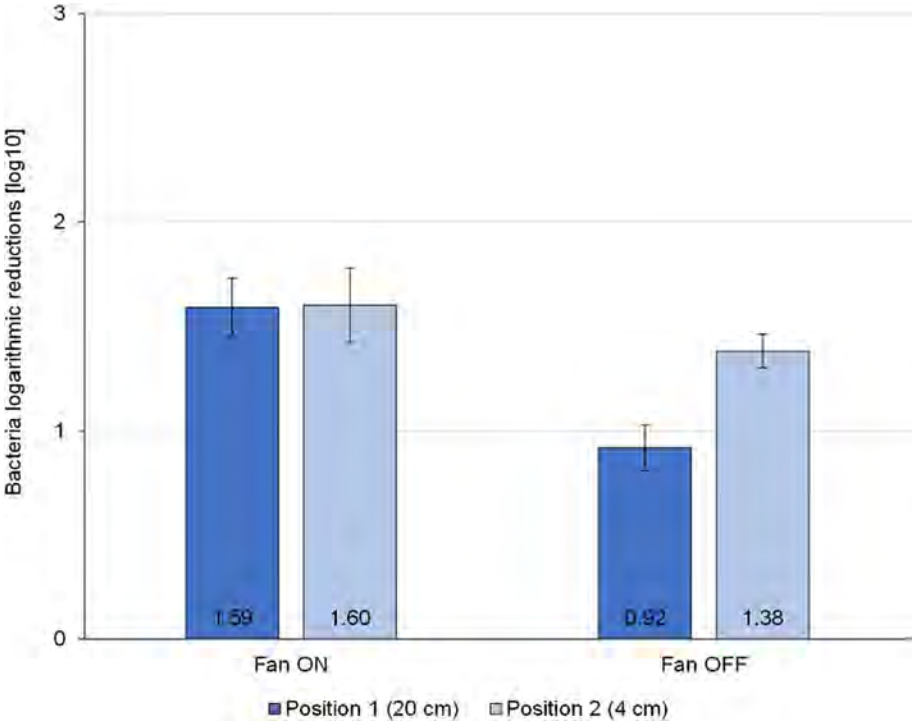

Fig. 6 *Staphylococcus epidermidis* inactivation rates with fan ON and fan OFF and sample position 1 and 2 for DC 10%; no statistically significant differences were observed among the different conditions

were laid, without changing the fan mode, no statistically significant differences were shown, which is in line with the last suggestion. Since the position of the sample did not affect the final inactivation rates, it was proposed the idea of an equal mixture of RONS inside the chamber. Furthermore, Fig. 7 shows *S. epidermidis* inactivation relative to each plasma treatment condition, when operating in NOx regimen. For instance, when the fan was ON and the samples were in position 1, 1.51 ± 0.59 log reduction was reached and 1.24 ± 0.96 log reduction with the fan OFF. No statistically significant differences were observed among any plasma treatment, neither comparing sample position nor comparing fan mode.

Those results are in accordance with the ones of other authors such as Min [23], who observed 0.9 log CFU/tomato of *Salmonella* wherever the tomatoes samples were inside the plasma treatment chamber, either the bottom layer or the top layer. Nevertheless, a study carried out by Miao [24], using a DBD plasma system without a treatment chamber, investigated how the gap affected the inactivation rate. They showed that the higher the gap (cm) the lower the inactivation values which is not in agreement with the results of this paper. These differences may be due to the fact that in this work, a plasma treatment chamber was used and RONS could be kept inside the chamber. However, without a chamber, RONS could be dispersed throughout the ambient atmosphere, not directly contacting the bacteria sample.

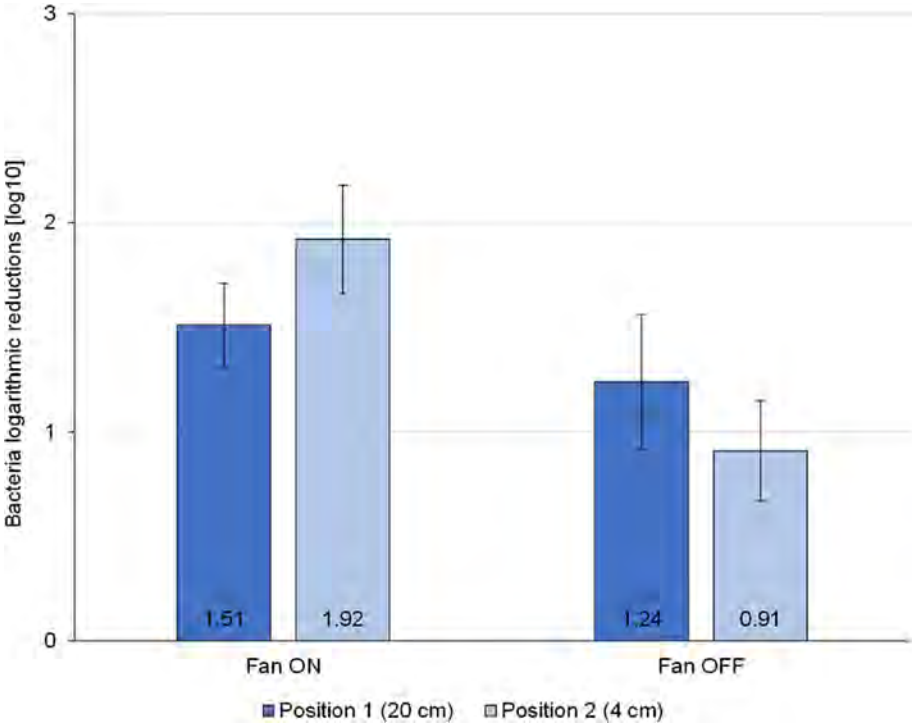

Fig. 7 *Staphylococcus epidermidis* inactivation rates with fan ON and fan OFF and sample position 1 and 2) for DC 100%; no statistically significant differences were observed among the different conditions

Reactive Species Concentrations

OAS measurements of reactive species kinetics in the different conditions were elaborated in order to calculate the mean concentrations in correspondence of each optical path during the whole treatment time. Results of calculations with DC 10 and 100% are respectively shown in Figs. 8 and 9.

Ozone concentration in the nitrogen regime was also measured by OAS resulting in not significant values (data not shown). Regarding nitrogen dioxide in the ozone regime, the measured concentrations were considered irrelevant. The presented results suggest that the reactive species concentration inside the treatment chamber is homogeneous, since no statistically significant difference was observed among the results relative to different positions, even without the gas mixing provided by the fan. Indeed, the results obtained in the two different positions were equal from a statistical point of view even in the "fan OFF" condition.

Temperature Profiles

In order to evaluate the plasma treatment influence on the temperature of the atmosphere inside the chamber, thermal measurements with the two fan modes were carried out. As

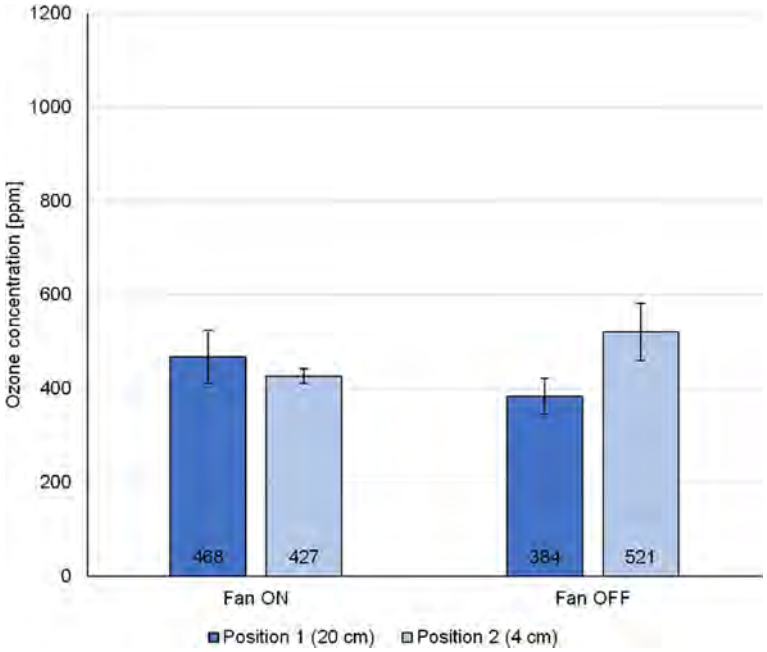

Fig. 8 Mean ozone concentration in the two selected positions over 30-min treatments (each result is the average of three replicates) with DC 10%; no statistically significant differences were observed among the different conditions

Figs. 10 and 11 show, the temperature increase was higher in the case of NOx regime, for both the investigate positions and the fan modes. This fact is an expected result, since the higher DC has the effect of a higher power consumption, and thus Joule heating of the plasma source. Furthermore, it was also expected to observe a greater temperature increase in correspondence with position 2, due to the reduced distance from the ground electrode. However, the greatest increase observed was equal to about 10 °C with respect to the ambient temperature (Fig. 11b, DC 100%).

The results suggested that the temperature reached inside the treatment chamber, cannot significantly influence the microbial cells viability, since its value was holding below 40 °C. That temperature is much higher than the temperature range of growth of *Staphylococci* strains, which is 6.5–46 °C [25]. Thus, it is suggested that the inactivation rate achieved after plasma treatments was not caused by a thermal effect.

Furthermore, the temperature results indicate that the process could be suitable for heat-sensitive materials, such as polymeric packaging.

Conclusions

In the present work, the effectiveness of an LA-SDBD was studied for decontaminating food packaging surfaces. Different parameters, such as the gap (20 and 4 cm) or the fan mode (ON and OFF), were investigated during the plasma treatment. Biological results showed bacterial inactivations of 1–2 logarithmic reductions, which can be considered

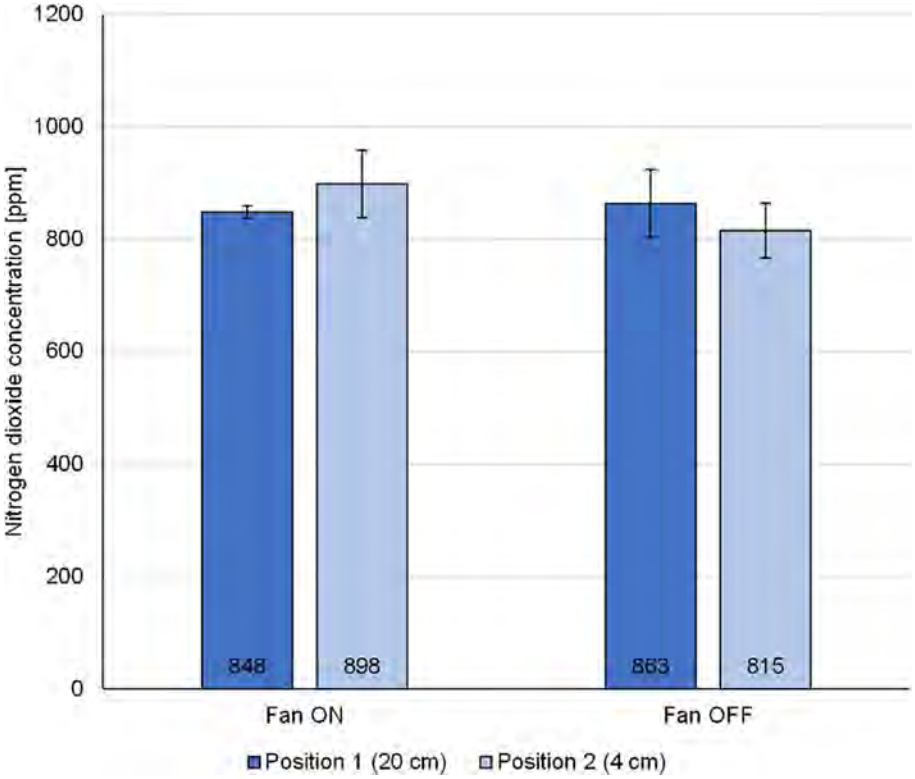

Fig. 9 Mean nitrogen dioxide concentration in the two selected positions over 30-min treatments (each result is the average of three replicates) with DC 100%; no statistically significant differences were observed among the different conditions

as a preliminary result for further process optimization. It was also suggested a homogenous RONS diffusion inside the treatment chamber since there were no statistically significant differences in terms of bacteria inactivation for each plasma treatment condition. This fact was also corroborated by OAS analysis which illustrated no statistically significant differences for O_3 and NO_2 regardless of the operating condition applied. It is thus possible to conclude that the device can effectively work in both operating conditions. Moreover, it has been verified that the anti-bacterial action is unvaried in different positions inside the 17.5 L treatment chamber. This statement suggests that three-dimensional objects could be sanitized with high efficacy.

Furthermore, since the samples were not in direct contact with plasma and there was a slight temperature increase, it could be assumed that reactive oxygen and nitrogen species play a key role in the antimicrobial efficacy of the plasma source used. Finally, it is remarkable that the presented homogeneous results were obtained inside a treatment chamber with a volume of 17.5 L and with a plasma source characterized by a large electrode area. According to the authors´ knowledge, this is the plasma system intended for food packaging decontamination with the largest discharge area and one of the largest volumes in the literature.

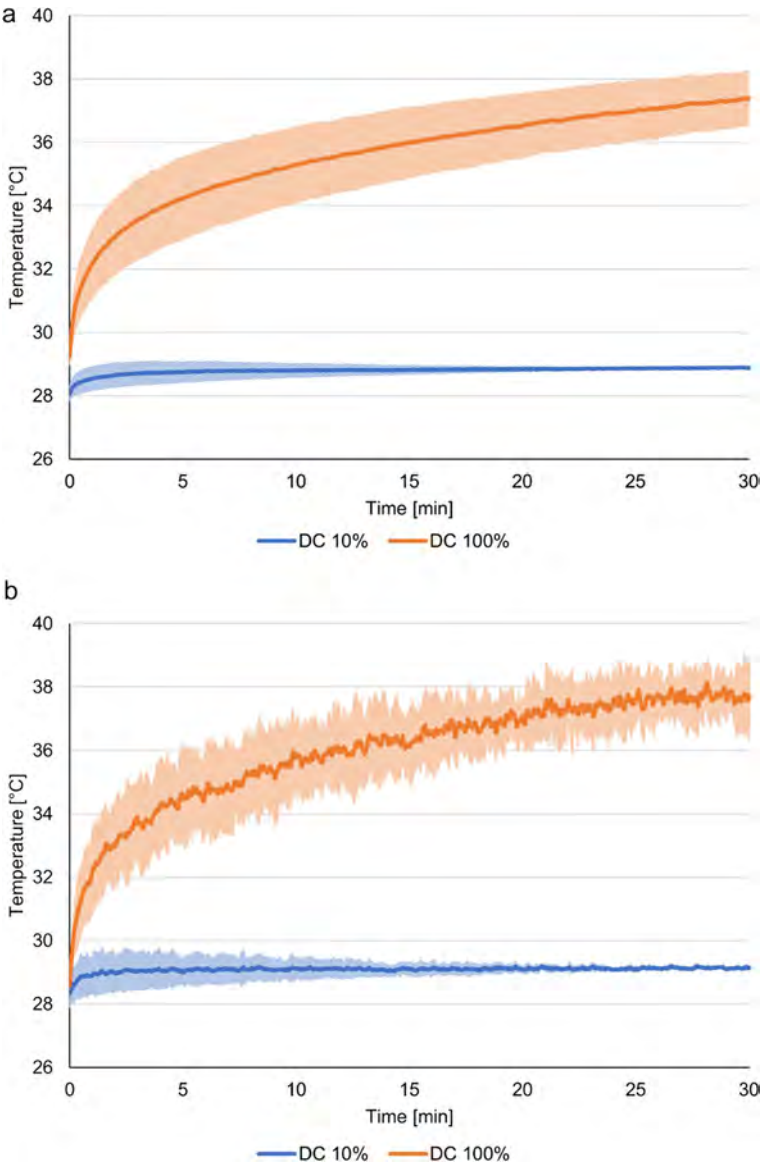

Fig. 10 Temperature profiles inside the treatment chamber with fan OFF at distances of 20 cm (position 1, **a**) and 4 cm (position 2, **b**) from the ground electrode

Future research may include the optimization of the plasma system and the process in general, the antimicrobial efficacy evaluation on different types of microorganisms and the evaluation of potential modification of PP matrix induced by CAP treatment.

In conclusion, disinfecting food packaging and tools by LA-SDBD could be a sustainable and cost-efficient electricity-based solution for food chain contamination and thus for avoiding and reducing foodborne diseases.

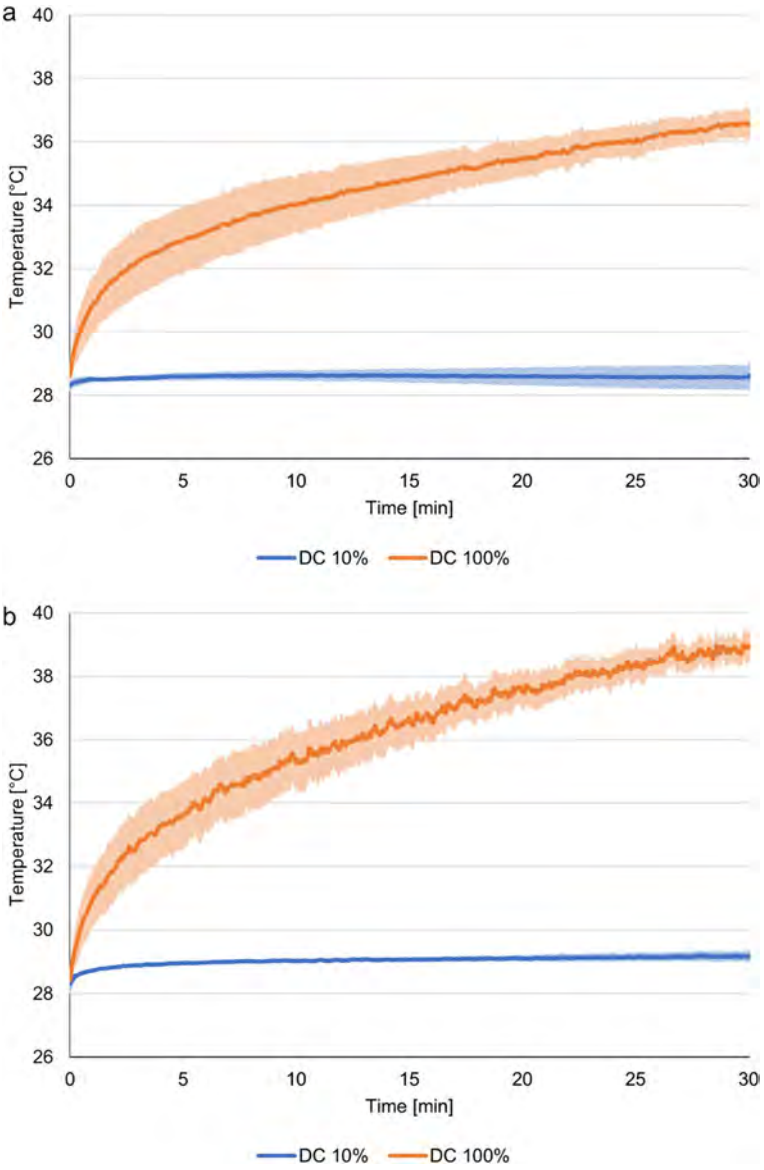

Fig. 11 Temperature profiles inside the treatment chamber with fan ON at distances of 20 cm (position 1, **a**) and 4 cm (position 2, **b**) from the ground electrode

Acknowledgements The author Sainz-García, A. is thankful to the program of pre-doctoral contracts for the training of research staff that is funded by the Spanish Ministry of Science and Innovation and the COST Action CA20114 PlasTHER, supported by COST (European Cooperation in Science and Technology—https://www.cost.eu). The PhD scholarship of the author Maccaferri, C. was funded by the European Union—NextGenerationEU through the Italian Ministry of University and Research under PNRR—Mission 4 Component 2, Investment 3.3 "Partnerships extended to universities, research centres, companies and funding of basic research projects" D.M. 352/2021-CUP J33C22001330009.

Author Contribution C.M.: Conceptualization, Methodology, Validation, Formal analysis, Investigation, Data curation, Writing—original draft preparation, Writing—review and editing, Visualization. A.S.G.: Methodology, Validation, Formal analysis, Investigation, Data curation, Writing—original draft preparation, Writing—review and editing, Visualization. F.C.: Methodology, Validation, Formal analysis, Investigation, Writing—review and editing. M.G.: Writing—review and editing, Supervision, Funding acquisition. F.A.E: Writing—review and editing, Supervision, Funding acquisition. R.L.: Conceptualization, Methodology, Resources, Writing—review and editing, Supervision, Project administration, Funding acquisition.

Funding Open access funding provided by Alma Mater Studiorum - Università di Bologna within the CRUI-CARE Agreement. This work has been funded by MCIN/AEI/https://doi.org/10.13039/501100011033 and the "European Union NextGenerationEU/PRTR" through Grants PID2019-105367RB, PID2020-11365RB-C21 and PDC2022-133242-I00.

Declarations

Conflict of Interest None.

References

1. Capelli F, Tappi S, Gritti T, et al (2021) Decontamination of food packages from SARS-COV-2 RNA with a cold plasma-assisted system. Appl Sci (Switzerland). https://doi.org/10.3390/app11094177
2. Godfray HCJ, Crute IR, Haddad L et al (2010) The future of the global food system. Philos Trans R Soc B: Biol Sci 365:2769–2777. https://doi.org/10.1098/rstb.2010.0180
3. World Health Organization—23 million people falling ill from unsafe food each year in Europe is just the tip of the iceberg (2019). https://www.who.int/news/item/05-06-2019-23-million-people-falling-ill-from-unsafe-food-each-year-in-europe-is-just-the-tip-of-the-iceberg. Accessed 23 Mar 2023
4. Farias A da S, Akutsu R de CC de A, Botelho RBA, Zandonadi RP (2019) Good practices in home kitchens: construction and validation of an instrument for household food-borne disease assessment and prevention. Int J Environ Res Public Health. https://doi.org/10.3390/ijerph16061005
5. Lorenzo JM, Munekata PE, Dominguez R, et al (2018) Main groups of microorganisms of relevance for food safety and stability: general aspects and overall description. Innov Technol Food Preser 53–107. https://doi.org/10.1016/B978-0-12-811031-7.00003-0
6. Ansari IA, Datta AK (2003) An overview of sterilization methods for packaging materials used in aseptic packaging systems. Food Bioprod Process 81:57–65. https://doi.org/10.1205/096030803765208670
7. Khadre MA, Yousef AE (2001) Decontamination of a multilaminated aseptic food packaging material and stainless steel by ozone. J Food Saf 21:1–13. https://doi.org/10.1111/j.1745-4565.2001.tb00304.x
8. Office of the Federal Register National Archives and Records Administration (1939; Revised April 2021). Food and Drug Administration, Department of Health and Human Services. 21 CFR 170.3
9. Virto R, Mañas P, Álvarez I et al (2005) Membrane damage and microbial inactivation by chlorine in the absence and presence of a chlorine-demanding substrate. Appl Environ Microbiol 71:5022–5028. https://doi.org/10.1128/AEM.71.9.5022-5028.2005
10. Prakasam M, Largeteau A (2017) Flexible packaging for nonthermal decontamination by high hydrostatic pressure. Elsevier
11. Liao X, Liu D, Xiang Q et al (2017) Inactivation mechanisms of non-thermal plasma on microbes: a review. Food Control 75:83–91. https://doi.org/10.1016/j.foodcont.2016.12.021

12. Puligundla P, Lee T, Mok C (2016) Inactivation effect of dielectric barrier discharge plasma against foodborne pathogens on the surfaces of different packaging materials. Innov Food Sci Emerg Technol 36:221–227. https://doi.org/10.1016/J.IFSET.2016.06.027
13. Ucar Y, Ceylan Z, Durmus M et al (2021) Application of cold plasma technology in the food industry and its combination with other emerging technologies. Trends Food Sci Technol 114:355–371. https://doi.org/10.1016/j.tifs.2021.06.004
14. Sani IK, Aminoleslami L, Mirtalebi SS et al (2023) Cold plasma technology: applications in improving edible films and food packaging. Food Packag Shelf Life 37:101087. https://doi.org/10.1016/j.fpsl.2023.101087
15. Kordová T, Scholtz V, Khun J, et al (2018) Inactivation of microbial food contamination of plastic cups using nonthermal plasma and hydrogen peroxide. J Food Qual. https://doi.org/10.1155/2018/5616437
16. Pina-Perez MC, Martinet D, Palacios-Gorba C, et al (2020) Low-energy short-term cold atmospheric plasma: controlling the inactivation efficacy of bacterial spores in powders. Food Res Int. https://doi.org/10.1016/j.foodres.2019.108921
17. Timmons C, Pai K, Jacob J et al (2018) Inactivation of *Salmonella enterica*, Shiga toxin-producing *Escherichia coli*, and Listeria monocytogenes by a novel surface discharge cold plasma design. Food Control 84:455–462. https://doi.org/10.1016/j.foodcont.2017.09.007
18. Katsigiannis AS, Bayliss DL, Walsh JL (2022) Cold plasma for the disinfection of industrial food-contact surfaces: an overview of current status and opportunities. Compr Rev Food Sci Food Saf 21:1086–1124
19. Molina-Hernandez JB, Capelli F, Laurita R, et al (2022) A comparative study on the antifungal efficacy of cold atmospheric plasma at low and high surface density on Aspergillus chevalieri and mechanisms of action. Innov Food Sci Emerging Technol. https://doi.org/10.1016/j.ifset.2022.103194
20. Yang C, Mamouni J, Tang Y, Yang L (2010) Antimicrobial activity of single-walled carbon nanotubes: length effect. Langmuir 26:16013–16019. https://doi.org/10.1021/la103110g
21. Simoncelli E, Schulpen J, Barletta F, et al (2019) UV-VIS optical spectroscopy investigation on the kinetics of long-lived RONS produced by a surface DBD plasma source. Plasma Sour Sci Technol. https://doi.org/10.1088/1361-6595/ab3c36
22. Moiseev T, Misra NN, Patil S, et al (2014) Post-discharge gas composition of a large-gap DBD in humid air by UV-Vis absorption spectroscopy. Plasma Sour Sci Technol. https://doi.org/10.1088/0963-0252/23/6/065033
23. Min SC, Roh SH, Niemira BA et al (2018) In-package atmospheric cold plasma treatment of bulk grape tomatoes for microbiological safety and preservation. Food Res Int 108:378–386. https://doi.org/10.1016/j.foodres.2018.03.033

24. Miao H, Yun G (2011) The sterilization of Escherichia coli by dielectric-barrier discharge plasma at atmospheric pressure. Appl Surf Sci 257:7065–7070. https://doi.org/10.1016/j.apsusc.2011.03.014
25. Onyango LA, Dunstan RH, Gottfries J et al (2012) Effect of low temperature on growth and ultrastructure of *Staphylococcus* spp. PLoS ONE 7:1–10. https://doi.org/10.1371/journal.pone.0029031

Authors and Affiliations

Caterina Maccaferri[1] · Ana Sainz-García[2] · Filippo Capelli[1] · Matteo Gherardi[1,3] · Fernando Alba-Elías[2] · Romolo Laurita[1,4]

✉ Romolo Laurita
romolo.laurita@unibo.it

Caterina Maccaferri
caterina.maccaferri3@unibo.it

Ana Sainz-García
ana.sainz@unirioja.es

Filippo Capelli
Filippo.capelli@unibo.it

Matteo Gherardi
matteo.gherardi4@unibo.it

Fernando Alba-Elías
fernando.alba@unirioja.es

[1] Department of Industrial Engineering, Alma Mater Studiorum, Università di Bologna, Bologna, Italy

[2] Department of Mechanical Engineering, Universidad de La Rioja, Logroño, Spain

[3] Advanced Mechanics and Materials, Interdepartmental Center for Industrial Research (AMM-ICIR), Alma Mater Studiorum, Università di Bologna, Bologna, Italy

[4] Interdepartmental Centre for Industrial Research Health Sciences and Technologies, Alma Mater Studiorum, Università di Bologna, Ozzano Dell'Emilia, Italy